

Developing Affimers for the detection of biomarkers in cancer

Danah A A A Q AL-Qallaf

Submitted in accordance with the requirements for the
degree of Doctor of Philosophy

University of Leeds

Faculty of Biological Sciences

School of Molecular and Cellular Biology

December 2018

The candidate confirms that the work submitted is her own and that appropriate credit has been given where reference has been made to the work of others.

A full list of publications arising from work within this thesis is provided in Appendix B. Copy of publication is provided as separate document.

This copy has been supplied on the understanding that it is copyright material and that no quotation from the thesis may be published without proper acknowledgement

© 2018 The University of Leeds and Danah A A A Q Al-Qallaf

The right of Danah A A A Q Al-Qallaf to be identified as Author of her work has been asserted by her in accordance with the copyright, Designs and Patents Act 1988

Acknowledgments

First and foremost, my deepest gratitude goes to Almighty God “Allah” for providing me with his generous blessing, continuous support and guidance throughout my life. Thank you, God, for answering my prayers and empowering me with the passion for persisting and thriving till reaching the end line of all new phases I started and will start.

Second, I would like to express my sincere gratitude to my supervisors Dr. Darren Tomlinson, Dr. Sandra Bell and Professor Michael McPherson for their continuous support, patience, motivation and immense knowledge. Thank you for not giving up on me even on the times when I did give up on myself. Dr. Sandra Bell, allow me here to address your help and valuable advice with regards to cell work. Moreover, your motivating words have really brightened me in my dark times and provided me the strength I needed to stand-up on my foot and walk through the journey.

Further, my sincere thanks goes to Dr. Filomena Esteves who always believed in me and took care of me as a mother. Besides helping me personally, I would like to acknowledge all the work you did, the advice you gave me with regards to IHC application and the images of stained sections of cells and tissues we captured.

Now, this journey wouldn't have been so joyful and possible without the great scientists I have started my journey with (Sophie H, Lia, and Rob). I cannot forget all the helpful advice and comfort I had received when I reached a dead end of my experiment. A big thanks goes to Dr. Christian Tiede, Dr. Heather Martin, Dr. Temp, Dr. Modupe and all other BSTG members. To Tom, although you left the group, your valuable support will always be felt and appreciated. To Dr. Sandra's group members, thank you for teaching me all the related cell culturing work and how to get brilliant pictures of my stained cells.

Dr. James Ault, thank you for performing the MS analysis, and Dr. Michael szymonik, thank you for helping me in generating the ALP-Affimer fusion. Michael Hall, thank you for scanning my TMA slides. Thank you to professor Michelle Peckham and her group for their advice with regard to cytokeratin staining and providing me with some related antibodies. To Avacta company, thank you for providing me with the Fc-Affimer fusions, and to all other people who contributed to get this thesis done, especially to those who gave me part of their time and helped me edit my written work.

The whole PhD journey would not be possible without the funding of the Kuwait University and the opportunity given by the University of Leeds. Thank you for making my dream come true.

To my parents, sisters, my best friend, Farah, my husband and my children (Zainab, Ali and Bibi), thank you for all your limitless love and support. My children, I know that being away from your cousins was difficult, but I hope that, in future, you will know that nothing is impossible. Just set your mind at your goal and go for it, you will reach it even if you don't currently know when, where and how.

Finally, I would like to thank and cherish the memory of my friend Khadija (Um Hassan) who died from breast cancer in my second year of PhD. I was lucky to meet her in Leeds and build memories with her, which I will cherish forever. Khadija, your presence is always felt, and I will hold to my promise to you and will dedicate my life to find the answer of your question: "Why my cancer is not responding to treatment like others?"

Abstract

Biomarkers are molecules present in the patients' samples. They are used to detect the presence of a disease or an infection. An array of laboratory tools is used to monitor changes in the biomarker levels for diagnostic and prognostic purposes. Affimers are relatively new tools, which can be used in similar ways to commonly used antibodies with many advantages over the later. The work described in this PhD thesis has focused on a number of methodologies for the generation of Affimers against purified proteins and cell-surface molecules, with the intention of using these to detect biomarkers in cancer.

To ensure the development of functional Affimer reagents against different membrane target molecules, EGFR, HER2, and HER3 were used as models to optimise the process of Affimers isolation and selection using phage display technology. *In vitro* production of Affimers using bacterial cells was assessed and optimised. Following optimisation, a range of Affimers that bound to EGFR, HER2, and HER3 were generated and partially characterised by different molecular applications, including immunofluorescence, immunohistochemistry, and pull-down assay. Upon characterisation, the developed reagents were not only able to identify their targets on cells and to precipitate them down from cell lysates, but also exhibited a complete inhibition of the downstream signalling activation of both EGFR and HER3.

In addition, this thesis provides clear evidence of the potential of Affimers in biomarker discovery studies. After multiple rounds on non-tumourigenic (HB2) and cancerous (MDA-MB-453) breast-cell lines, eight novel anti-breast-cancer Affimers were successfully isolated and characterised. Following pull-down assay and mass spectrometry analysis, the target proteins to which these Affimers were found to bind was identified as CK18 and 19. Upon identification, the specificity of Affimers was further validated on a panel of breast cells, tissues, and on multiple breast-tissue microarrays (TMAs).

There is a need to develop the knowledge to utilise this new Affimers-based technology to encourage adoption of this useful tool. With the aid of such technology, several novel detection reagents were generated, partially validated and proved to be promising tools for biomarker detection in different conventional assays.

Table of Content

ACKNOWLEDGMENTS	III
ABSTRACT	V
TABLE OF CONTENT	VI
LIST OF TABLES	XI
LIST OF FIGURES	XII
ABBREVIATIONS	XV
CHAPTER 1 INTRODUCTION	1
1.1 CANCER	1
1.1.1 CANCER DEVELOPMENT	1
1.1.2 PROTEINS AND CANCER PROGRESSION	2
1.1.3 CANCER SCREENING AND DIAGNOSIS	5
1.1.3.1 Analytical assays for the detection of protein-based biomarkers in cancer	5
1.1.4 CANCER THERAPY	7
1.2 THE HER FAMILY OF RECEPTORS AND CANCER	8
1.2.1 HERs ACTIVATION, DIMERIZATION, AND CELL SIGNALLING	9
1.2.2 THE ROLE OF HER PROTEINS IN CANCER DEVELOPMENT	12
1.2.3 TARGETING HERs: MECHANISM OF ACTION AND RESISTANCE	15
1.2.3.1 Currently used therapeutic agents and their inhibitory mechanism	15
1.3 THE NEED FOR CANCER BIOMARKERS	16
1.3.1 Challenges and limitations in biomarker discovery and validation	16
1.3.2 BIOMARKERS CURRENTLY USED IN BREAST CANCER	18
1.3.3 IDENTIFICATION OF NEW BIOMARKERS: WHY?	20
1.4 BINDING MOLECULES FOR BIOMARKER RECOGNITION IN HEALTH AND DISEASE	21
1.4.1 ANTIBODY AND ITS DERIVATIVES	21
1.4.1.1 Monoclonal antibody production: the endless supply	22
1.4.1.2 Drawbacks of antibodies pushing towards the development of other engineered antibody-based formats	23
1.4.2 APTAMERS	24
1.4.2.1 Drawbacks of aptamers	25
1.4.3 ENGINEERED PROTEIN BINDING TOOLS	25
1.4.3.1 The diversity of the non-antibody based protein scaffolds	26
1.4.3.2 Generation of non-antibody binding proteins	29
1.4.3.3 Are some scaffolds better than others?	33
1.4.3.4 Current status of antibody alternatives in disease diagnosis and treatment	34
1.5 RESEARCH AIMS AND OBJECTIVES	35

CHAPTER 2 MATERIALS AND METHODS	41
2.1 MATERIALS	41
2.1.1 GENERAL REAGENTS	41
2.1.2 MAMMALIAN CELL LINES AND THEIR CHARACTERISTICS	41
2.1.3 WHOLE TISSUE SAMPLES AND TISSUE MICROARRAYS (TMAs).....	41
2.2 METHODS	44
2.2.1 MAMMALIAN CELL CULTURING.....	45
2.2.1.1 Cell culture	45
2.2.1.2 Cell recovery, feeding, and passaging	47
2.2.1.3 Cell counting	47
2.2.1.4 Cryopreservation	48
2.2.2 AFFIMERS ISOLATION BY PHAGE DISPLAY	48
2.2.2.1 Target preparation	49
2.2.2.2 Bio-panning: selection rounds.....	50
2.2.2.3 Phage ELISA.....	58
2.2.3 <i>IN VITRO</i> PRODUCTION OF SOLUBLE HIS ₈ -TAGGED AFFIMER PROTEINS	60
2.2.3.1 Molecular subcloning of Affimers	60
2.2.3.2 Production and purification of His ₈ -tagged Affimers	63
2.2.4 <i>IN VITRO</i> PRODUCTION OF VEGFR2 AFFIMER-ALKALINE PHOSPHATASE (AP) FUSION PROTEIN	65
2.2.4.1 Molecular construction of the fusion protein	65
2.2.4.2 Production and purification of the fusion protein	65
2.2.5 <i>IN VITRO</i> CHEMICAL MODIFICATION OF AFFIMERS.....	66
2.2.5.1 Bio-conjugation of horseradish peroxidase (HRP) enzyme to Affimers	66
2.2.5.2 Biotinylation of Affimer proteins.....	68
2.2.6 FUNCTIONAL CHARACTERISATION OF AFFIMERS	69
2.2.6.1 Affinity/immunofluorescence (AF/IF) microscopy on fixed-cells	69
2.2.6.2 AF/IF microscopy on live cells	70
2.2.6.3 Immunohistochemistry staining (IHC) staining.....	70
2.2.6.4 Pull-down assay and western blot (WB) analysis	72
2.2.7 CELLULAR STUDIES: TREATING CELLS WITH AFFIMERS	74
2.2.8 PROTEIN IDENTIFICATION BY PULL-DOWN ASSAY AND MASS SPECTROMETRY (MS) ANALYSIS	74
2.2.9 DATA ANALYSIS AND IMAGE CONSTRUCTION	74
 CHAPTER 3 PHAGE DISPLAY-BASED SELECTION STRATEGIES TO ISOLATE AFFIMER REAGENTS AGAINST HER2	 76
3.1 INTRODUCTION.....	76
3.2 RESULTS.....	80
3.2.1 ISOLATING AFFIMERS AGAINST THE RECOMBINANT PROTEIN OF THE ECD OF HER2	80
3.2.2 SELECTION OF AFFIMERS ON WHOLE-FIXED CELLS ENGINEERED TO OVEREXPRESS HER2.....	81

3.2.3 A COMBINED PHAGE SELECTION STRATEGY	83
3.2.4 SELECTING ENRICHED POOL OF HER2-BINDING AFFIMERS ON CELLS ENHANCED THE DIVERSITY OF ISOLATED BINDERS.....	89
3.2.5 MOLECULAR CLONING, BACTERIAL PRODUCTION, AND PURIFICATION OF EIGHT ISOLATED HER2-BINDING AFFIMERS	92
3.2.5.1 Optimisation of temperature, shaking speed and time for production of Affimers	92
3.2.5.2 Optimisation of induction of Affimer production.....	95
3.2.6 CHARACTERISING THE BINDING ABILITY OF ANTI-HER2 AFFIMERS ON A PANEL OF BREAST CANCER CELLS	99
3.2.6.1 Immunofluorescence staining of HER2 using Affimers.....	99
3.2.6.2 Testing anti-HER2 Affimer reagents on live cells.....	101
3.2.6.3 Anti-HER2 Affimers pull down endogenous HER2 from cell lysates	101
3.3 DISCUSSION.....	104

CHAPTER 4 ISOLATION AND CHARACTERISATION OF ANTI-EGFR AND ANTI-HER3 AFFIMERS 109

4.1 INTRODUCTION.....	109
4.2 RESULTS.....	110
4.2.1 SELECTION OF HER3-BINDING AFFIMERS	110
4.2.2 ISOLATING AFFIMERS AGAINST THE EXTRACELLULAR DOMAIN OF EGFR USING A RECOMBINANT PROTEIN	117
4.2.3 MOLECULAR CLONING, PRODUCTION AND PURIFICATION OF ANTI-HER3 AND ANTI-EGFR AFFIMER PROTEINS	118
4.2.4 ANTI-HER3 AFFIMERS CAN RECOGNISE THE RECEPTOR ON CELLS AND IN CELL LYSATE.....	120
4.2.4.1 Binding characterisation by immunofluorescence microscopy	120
4.2.4.2 Anti-HER3 Affimers pulled-down the endogenous HER3 protein from different cell lysates	123
4.2.4.3 Anti-HER3 Affimers as biotin-conjugated reagents for use in IHC	124
4.2.5 INHIBITION OF DOWNSTREAM CELL SIGNALLING BY ANTI-HER3 AFFIMERS	127
4.2.6 ABILITY OF EGFR BINDING AFFIMERS TO RECOGNISE THE RECEPTOR IN DIFFERENT APPLICATIONS	129
4.2.6.1 Anti-EGFR Affimers bind to cells	129
4.2.6.2 All anti-EGFR Affimers pulled down the endogenous receptor from cell lysate	132
4.2.7 ANTI-EGFR AFFIMERS DOWNREGULATED THE MAPK-ERK1/2 SIGNALLING ACTIVATION IN HER2 OVEREXPRESSION CELLS	133
4.3 DISCUSSION.....	135

CHAPTER 5 MODIFIED AFFIMER REAGENTS FOR IMPROVED BIOMARKER DETECTION IN IHC 139

5.1 INTRODUCTION.....	139
5.2 RESULTS.....	141

5.2.1 AFFIMER-ALKALINE PHOSPHATASE FUSION PROTEIN AS A RAPID, SINGLE-STEP DETECTION TOOL FOR IHC	141
5.2.1.1 Construction of a monomeric alkaline phosphatase (mAP)-fused Affimer.....	142
5.2.1.2 Monomeric alkaline phosphatase-fused Affimer production, its catalytic activity and stability	142
5.2.1.3 Direct affinity staining of the VEGFR2 protein on tissue using the mAp-Affimer fusion.....	143
5.2.2 DEVELOPMENT OF THE OPTIMAL BIO-CONJUGATE VIA CHEMICAL MODIFICATION OF AFFIMERS.....	145
.....	147
5.2.2.1 Optimisation of biotinylation incubation time, biotin concentration and temperature.....	150
5.2.2.2 Testing different biotin linker lengths.....	151
5.2.2.3 Testing different reduction techniques for biotin labelling.....	156
5.2.3 APPLICABILITY OF THE BIOTINYLATED, SINGLE CYSTEINE AFFIMER AS A DETECTION REAGENT IN IHC	156
5.2.4 SIGNAL AMPLIFICATION ACHIEVED BY THE INTRODUCTION OF TWO CYSTEINE RESIDUES INTO THE AFFIMER SCAFFOLD	160
5.2.5 CHARACTERISATION OF AFFIMER-FC CHIMERAS IN IHC DIAGNOSTIC APPLICATION	162
5.3 DISCUSSION.....	164

CHAPTER 6 IDENTIFICATION OF CANCER-SPECIFIC AFFIMERS USING PHAGE DISPLAY

6.1 INTRODUCTION.....	169
6.2 RESULTS.....	170
6.2.1 SELECTION AND SCREENING FOR CANCER-SPECIFIC AFFIMERS.....	170
6.2.2 <i>IN VITRO</i> PRODUCTION OF CANCER-SPECIFIC BINDING AFFIMERS	175
6.2.3 VALIDATION OF AFFIMER BINDING SPECIFICITY TOWARDS CANCER CELLS	176
6.2.3.1 Immunofluorescence microscopy	176
6.2.3.2 Staining on formalin-fixed paraffin embedded cell pellets.....	176
6.2.4 A2 AND C1 AFFIMERS STAINING IS INCREASED IN BREAST CANCER	180
6.2.5 BOTH A2 AND C1 AFFIMERS BIND TO CYTOKERATIN 19 AND 18/8 PROTEINS.....	182
6.2.6 BINDING OF A2 AND C1 TO CYTOKERATIN 19 AND 18 WAS CONFIRMED BY FLUORESCENCE MICROSCOPY AND WESTERN BLOTTING.....	183
6.2.7 CYTOKERATIN 18 AND 19 ARE EXPRESSED ON THE CELL SURFACE OF CANCER CELLS	184
6.2.8 CYTOKERATIN 19 EXPRESSION UPREGULATION IS NOT SOLELY DEPENDENT ON HER2 OVEREXPRESSION IN BREAST CANCER	186
6.3 DISCUSSION.....	190

CHAPTER 7 GENERAL DISCUSSION AND FUTURE DIRECTIONS

7.1 FIXED-CELLS PHAGE DISPLAY AS STRATEGY FOR AFFIMERS DEVELOPMENT	193
7.1.1 FIXED-CELL PHAGE DISPLAY FOR THE DISCOVERY OF NEW BIOMARKERS	195

7.1.2 CELL-BASED VS PROTEIN-BASED PHAGE SELECTION STRATEGIES FOR THE ISOLATION OF IHC-BINDING REAGENTS	197
7.2 EFFICIENT AFFIMERS FUNCTIONALISATION AND MICROSCOPIC APPLICATIONS.....	197
7.2.1 AFFIMERS AS PRIMARY REAGENTS IN IHC.....	198
7.2.2 AFFIMERS AS PRIMARY REAGENTS IN FLUORESCENCE VISUALISATION MICROSCOPY	199
7.3 FUTURE DIRECTIONS OF AFFIMERS AS THERAPEUTIC AGENTS	201
7.4 RECOMMENDATION FOR FUTURE WORK	202
7.4.1. DESIGN AND CONSTRUCTION OF A HIGH-COMPLEXITY LIBRARY	202
7.4.2. HER2-BINDING AFFIMERS	204
7.4.3. HER3-BINDING AFFIMERS	205
7.4.5. APPLICATION OF AFFIMER TECHNOLOGY TO BIOMARKER DISCOVERY	208
7.5 CONCLUSION	210
REFERENCES	212
APPENDIX A	240
APPENDIX B	241
PUBLICATIONS & CONFERENCE PROCEEDING	241
B.1. ACCEPTED MANUSCRIPTS	241
B.2. POSTER PRESENTATIONS	241
B.3 ORAL PRESENTATIONS	241

List of Tables

CHAPTER 1

Table 1.1 HER ligand-binding specificity.....	10
Table 1.2 Types of biomarkers and their applications.....	17
Table 1.3 Molecular classification of breast carcinomas.....	20
Table 1.4. Examples of protein-display scaffolds, and their similarities and differences in relation to display strategy, pharmacokinetic properties and binding kinetics.....	36
Table 1.5. Summary of the advantages and limitations of Affimers and other antibody alternatives in comparison with those of antibodies and aptamers.....	38

CHAPTER 2

Table 2.1 Primary antibodies.....	42
Table 2.2 Secondary antibodies	43
Table 2.3 Affimer reagents.....	44
Table 2.4 Mammalian cell lines characteristics and growth conditions.....	45
Table 2.5 Purchased tissue microarrays (TMAs).. ..	46
Table 2.6 PCR condition for the amplification of Affimer sequence in the phagemid vector. ..	62
Table 2.7 PCR Components of 25 µl reaction volume required to clone the Affimer sequence into a digested pET11a expressing vector.....	62
Table 2.8 Primers used in molecular subcloning of Affimers.....	62
Table 2.9 Lysis, wash and elution buffers used in Affimer production and purification protocol.	64
Table 2.10 HRP- conjugation approaches.....	67
Table 2.11 Thiol-reducing reagents.....	68
Table 2.12 Biotin-Maleimide linkers.	69

CHAPTER 3

Table 3.1. Analysis of constructed Affimer (Ella2) library.....	78
Table 3.2 Amino acid sequence of the binding loops of eight different HER2 binding Affimer.....	80

CHAPTER 4

Table 4.1 Amino acid sequences of the binding loops of 6 different EGFR binding Affimers.	118
---	-----

List of Figures

CHAPTER 1

Figure 1.1 Schematic overview showing the development of cancerous mass and its metastasis to different regions in the body.	3
Figure 1.2 Hallmarks of cancer.	4
Figure 1.3 Currently used diagnostics approaches in cancer.	6
Figure 1.4 Current therapeutic strategies for cancer treatment.	8
Figure 1.5 A schematic presentation of the structural arrangement of HER2..	9
Figure 1.6 The role of HER proteins in cell signalling.	13
Figure 1.7 Antibody molecule and its derivatives.	22
Figure 1.8 Production of monoclonal antibody using ascites and in vitro culturing method.	23
Figure 1.9 Selection of aptamers (SELEX).	25
Figure 1.10 Structural features of some newly developed non-antibody based scaffolds.	27
Figure 1.11 Three-dimensional structure of the Affimer scaffold.	28
Figure 1.12 Schematic presentation of an M13 filamentous phage..	31
Figure 1.13 Phage display technology..	32

CHAPTER 2

Figure 2.1 Isolation of Affimers by phage selection on immobilized-recombinant target protein.	52
Figure 2.2 Cell-based phage screening strategy using FFPE cell sections on a glass-slide and enriched Affimer phage library.	54
Figure 2.3 Isolation of Affimers on fixed-monolayer of cells using phage display.	57
Figure 2.4 Schematic overview of the subcloning process of Affimer cDNA sequences from pDHis phagemid vectors into different expression vectors.	61
Figure 2.5 Workflow of pull-down assay coupled with either western blot (WB) or Mass-spectrometry (MS) analyses.	75

CHAPTER 3

Figure 3.1 Demonstrating the unsuccessful isolation of Affimers using cell-based screen against HER2-HB2 transfected cells.	82
Figure 3.2 Phage screen on fixed monolayer of engineered (HER2-transfected) HB2 cells to isolate binders against HER2 using the naïve Affimer phage library.	82
Figure 3.3 Phage screen on fixed monolayer of engineered (HER2-transfected) HB2 cells to isolate binders against HER2 using the naïve Affimer phage library.	86
Figure 3.4 Showing the phage ELISA results from isolating Affimers using alternate proteins and cell based screening.	87
Figure 3.5 Selection outcome of the combined-phage screen to isolate HER2 binder..	88
Figure 3.6 Affimer phage screen on HER2-overexpressing cells (MDA-MB-453) after multiple enrichment rounds on biotinylated HER2-ECD recombinant protein.	90
Figure 3.7 Showing the phage ELISA from clones isolated after three panning rounds against recombinant protein and three against cells.	91
Figure 3.8 The effect of different shaking speeds on the production of Affimer proteins.	94
Figure 3.9 SDS-PAGE analysis of Affimer protein produced at different temperatures.	95
Figure 3.10 The effect of using different IPTG concentrations on both cell density and Affimer production.	97
Figure 3.11 Optimising the induction of Affimer production at different OD of cultures.	98

Figure 3.12 SDS-PAGE showing the purification of anti-HER2 Affimers.....	98
Figure 3.13 Affinity/Immunofluorescence (AF/IF) staining of HER2 receptor on fixed cells.	100
Figure 3.14 Affinity/Immunofluorescence staining of HER2 binding Affimers on live BT474 breast cancer cells.	102
Figure 3.15 Anti-HER2 Affimers showed ability to pull-down HER2 complexes.....	103
Figure 3.16 Mechanism of stabilising the HER2 receptor on the cancer cell surface.	107

CHAPTER 4

Figure 4.1 Evaluating the efficiency of HER3 (ECD) recombinant protein biotinylation for use in phage display screen.	111
Figure 4.2 Phage-display screen against biotinylated recombinant HER3-ECD protein to isolate binders against the ECD of the receptor... ..	112
Figure 4.3 Phage ELISA of 48 picked clones after 3 panning rounds against the HER3 recombinant protein	113
Figure 4.4 Schematic presentation of the three phage screens performed against HER3-overexpressing cells after three rounds of library enrichment on HER3-ECD recombinant protein.. ..	115
Figure 4.5 The phage output of the three different phage screens on cells that overexpressed HER3 using an enriched-HER3 phage library.	116
Figure 4.6 Cell-based phage ELISA to examine the ability of 11 isolated HER3 Affimers to bind the native receptor on fixed cells.....	117
Figure 4.7 SDS-PAGE gel showing production and purification of Affimer proteins.. ..	119
Figure 4.8 Immunofluorescence microscopy confirming the ability of anti-HER3 Affimers to bind the HER3 on fixed cells.....	121
Figure 4.9 Immunofluorescence microscopy showing the capability of anti-HER3 Affimer reagents to bind native receptor on live cells and causing it to internalise.....	122
Figure 4.10 Anti-HER3 Affimers showed ability to pull-down endogenous HER3 overexpressed in MDA-MB-453 and MCF7 cancer cells.....	124
Figure 4.11 ELISA confirming the efficiency of biotinylated anti-HER3 Affimers.....	125
Figure 4.12 Staining of anti-HER3 Affimers on a panel of FFPE cancerous and non-cancerous breast cells.....	126
Figure 4.13 Western blots indicating the inhibitory effect of HER3-binding Affimers on downstream signalling pathway (MAPK/ERK1/2) after NRG stimulation in various HER3-overexpressing cells... ..	128
Figure 4.14 Immunofluorescence microscopy showing the ability of anti-EGFR Affimers to bind the native EGFR.....	130
Figure 4.15 Anti-EGFR Affimers bind to MDA-MB-468 cells in live cell culture.....	131
Figure 4.16 Anti-EGFR Affimers pulled-down EGFR from cell lysate prepared form MDA-MB-468 cancer cells.....	133
Figure 4.17 EGFR binding Affimers inhibit EGF-stimulated signal transduction in BT474 cells.....	134
Figure 4.18 The suggested mechanism of anti-HER3 Affimers modulating the stimulatory effect on NRG-stimulated signal transduction in cells with different HER2 expression level..	126

CHAPTER 5

Figure 5.1 Schematic overview of the different methods used in IHC to detect the biomarker of interest.....	140
--	-----

Figure 5.2 Production and characterisation of a monomeric alkaline phosphatase (mAP)-fused VEGFR2 binding Affimer.	144
Figure 5.3 Fused mAP-Affimer protein for staining VEGFR2 in human placenta tissue.	146
Figure 5.4 Cloning and producing of an Affimer containing a single cysteine residue.	147
Figure 5.5 HRP-conjugated Affimer showed low specificity in IHC.	149
Figure 5.6 ELISA showing the efficiency of biotin labelling of Affimers at different temperatures.	150
Figure 5.7 Mass spectrometry analysis of biotinylated reagents.	152
Figure 5.8 Graphs showing optimisation of Affimer:biotin ratio.	153
Figure 5.9 The length of the spacer-arm between the biotin molecule and the maleimide reactive group affected the biotinylation.	155
Figure 5.10 Comparing the efficacy of different reducing approaches.	157
Figure 5.11 Applicability of the biotin-labelled-VEGFR2 binding Affimer as a detection reagent in IHC.	159
Figure 5.12 Affimer Plus _{2C} reagent enhanced the signal intensity but did not improve the sensitivity of the IHC.	161
Figure 5.13 Characterisation of the developed Affimer-Fc chimeras in IHC.	163

CHAPTER 6

Figure 6.1 Isolation of eight cancer-specific binders after 4 rounds of panning on MDA-MB-453 breast cancer cells.	172
Figure 6.2 Schematic overview of the panning rounds to isolate Affimers against unidentified protein biomarkers.	173
Figure 6.3 Binding of selected phage clones by ELISA and immunofluorescence.	174
Figure 6.4 Coomassie stained SDS-PAGE gel showing production of Affimers.	147
Figure 6.5 Immunofluorescence staining of cells using Affimer reagents.	177
Figure 6.6 ELISA showing successful site-specific biotinylation of Affimers confirmed by ELISA assay.	178
Figure 6.7 IHC-like staining on a panel of tumorigenic and non-tumorigenic cells confirming the binding selectivity of some soluble Affimers towards cancer cells.	179
Figure 6.8 The cognate antigen to which both Affimer A2 and C1 bind is overexpressed in breast cancer.	181
Figure 6.9 Isolated Affimers pulled down endogenous protein overexpressed in cancer cell lysates.	182
Figure 6.10 Immunofluorescence using Affimers and antibodies.	185
Figure 6.11 Affimer C1 and A2 pulled bind to cytokeratin in cancer cell lysates.	186
Figure 6.12 Cytokeratin proteins are expressed on cell surface.	187
Figure 6.13 CK18 and 19 expression is not dependent on HER2 upregulation.	188
Figure 6.14 Affimer C1 confirms the heterogeneous localisation pattern of cytokeratins in the different molecular subtypes of breast cancer.	189
Figure 6.15 CK19 upregulation caused by HER2/ERK pathway is responsible for HER2 stability on cell membrane.	192

CHAPTER 7

Figure 7.1 Schematic representation of the newly constructed and generated Affimer (single loop) library.	203
Figure 7.2 Schematic representation of the EGFR structure and its mutated variant.	207

Abbreviations

A	Absorbance
AA	Amino acid
AF	Affinity fluorescence
AH	Affinity histochemistry
Akt	v-Akt Murine Thymoma viral Oncogene
AP	Alkaline phosphatase enzyme
Ap-1	Activator protein 1
AR	Ampiregulin
AR	Antigen retrieval
Bad	Bcl2-associated death promotor
BCA	Bicinchoninic acid
BM	Biotin-Maleimide
BRCA1/2	Breast cancer type 1/2 susceptibility protein
BSTG	Bioscreening technology group
BTC	Betacellulin
Ca ²⁺	Calcium ion
CA-125	Cancer antigen 125
CARD	Catalysed reporter deposition technique
CDK-2	Cyclin dependent kinase 2
cDNA	Complementary DNA
CDRs	Complementary determining regions
CK	Cytokeratin
CLIA	Chemiluminescence immunoassay

Da	Dalton
DAB	3,3'-diaminobenzidine
DAG	Diacylglycerol
DARPin	Designed ankyrin repeat protein
DAPI	4',6-diamidino-2-phenylindole
DMEM	Dulbecco's modified eagle media
DMSO	Dimethyl sulfoxide
DNA	Deoxyribonucleic acid
DTT	Dithiothreitol
ECD	Extracellular domain
EDTA	Ethylenediaminetetraacetic acid
EGF	Epidermal growth factor
EGFR	Epidermal growth factor receptor
ELISA	Enzyme linked immunosorbent assay
EPN	Epigen
EPR	Epiregulin
EPOS	Enhanced polymer one-step stain
ER	Oestrogen receptor
ERK1/2	Extracellular signal regulated kinase 1/2
EU	European union
Fab	Fragment of antigen binding domain
FACS	Fluorescence-activated cell sorting
FBS	Foetal bovine serum
FDA	Food and drug administration
FFPE	Formalin fixed paraffin embedded

FN3	Fibronectin type III
FoxO1	Forkhead family transcription factor 1
GDP	Guanosine-5'-diphosphate
Grb2	Growth factor receptor-bound protein 2
GPC3	Glypican-3
GTP	Guanosine-5'-triphosphate
HB-EGFR	Heparin-binding EGFR like growth factor
HER1/2/3/4	Human epidermal growth factor receptor 1/2/3/4
HPV	Human Papilloma virus
HRG	Heregulin
HRP	Horseradish peroxidase
IB	Immunoblot
ICD	Intracellular domain
IF	Intermediate filament
IF	Immunofluorescence
Ig	Immunoglobulin
IHC	Immunohistochemistry
IP ₃	Inositol-1,4,5-triphosphate
IPTG	Isopropyl β -D-1-thiogalactopyranoside
Jnk	c-Jun-N-terminal kinase
kDa	kilodalton
LB	Luria Bertani media
LRR	Leucine rich repeat
LN2	Liquid nitrogen
mAb	Monoclonal antibody

mAP	Monomeric alkaline phosphatase
MAPK	Mitogen activated protein kinase
MEK	Mitogen activated protein kinase kinase
mg	Milligram
ml	Milliliter
mM	Millimolar
mRNA	Messenger Ribose nucleic acid
mTOR	Mammalian target of rapamycin
NDF	Neuregulating factor
NRGs	Neuregulins
nm	nanometer
OD	Optical density
pAb	Polyclonal antibody
Pak	p21-activated protein kinase
PBS	Phosphate buffered saline
PCR	Polymerase chain reaction
PDB	Protein data bank
PK1	Pyruvate dehydrogenase kinase 1
PEG	Polyethylene glycol
PFA	Paraformaldehyde
PIP3	Phosphatidylinositol-(3,4,5)-triphosphate
PI3K	Phosphoinositide-3-kinase
PKC	Protein kinase C
PLC γ	Phospholipase C γ 1
pNPP	para-Nitrophenylphosphate

PR	Progesterone receptor
PSA	Prostate specific antigen
PTEN	Phosphatase and tensin homolog
PTKIP51	Protein tyrosine kinase interacting protein 51
Rac	Rho family of GTPases
RNA	Ribnonucleic acid
Rpm	Revolution per minute
RPMI	Roswell Park Memorial Institute medium
SB	Super broth media
ScFv	Single chain fragments of variable domains
SDS-PAGE	Sodium dodecyl sulfate polyacrylamide gel electrophoresis
SELEX	Sequential evolution of ligands by exponential enrichment
Shc	Shc-transforming protein
siRNA	Small interfering RNA
SOS	Son of sevenless
SP-1	Specific protein 1/ active transcription factor 1
SteA	Stefin A
STR	Short tandem repeats
ssDNA	single strand DNA
SUMO	Small ubiquitin modifier
TB	Terrific broth media
TBS	Tris buffered saline
TCEP	Tris(2-carboxyethyl) phosphine hydrochloride
TE	Triethylene amine
TGF	Transforming growth factor

TGFR	Transforming growth factor receptor
TKs	Tyrosine kinases
TKI	Tyrosine kinase inhibitor
TMA	Tissue microarray
TMB	3,3',5,5'-Tetramethylbenzidine
TN-C	Tenascin-C
TRPV1	Transient receptor potential cation channel subfamily V member1
TrxA	Thioredoxin
TSA	Tyramide signal amplification
V	Volt
Vav2	Guanine nucleotide exchange factor vav2
VEGFR2	Vascular endothelial growth factor receptor 2
WB	Western blot
WGA	Wheat germ agglutinin
WHO	World health organisation

CHAPTER 1

Introduction

1.1 Cancer

Cancer is a major health problem worldwide. Every year, the European union experiences about 9.6 million deaths and 18.1 million newly diagnosed cases of cancer (WHO, 2018). The World Health Organisation report the prevalence of cancer to be about 2.7%, which means that almost 14 million people in the EU are currently suffering from cancer. It was estimated that approximately two million of the people currently residing in UK were previously diagnosed with cancer (Maddams et al., 2012). In descending order, people are commonly diagnosed with breast, prostate, lung, colon, skin and other lymphatic cancers (WHO, 2013;Maddams et al., 2012).

Despite its low prevalence compared to other infections and heart diseases, cancer has a crucial impact on the healthcare system and economic interests (Ferlay et al., 2010). High healthcare cost is not the complete reason why governments, researchers and pharmaceutical companies are making efforts to develop better treatment and diagnostic procedures, but it certainly acts as the trigger. The motivation of cancer research comes from the desire to alleviate the effect cancer has on people's lives.

1.1.1 Cancer development

In order to define cancer, it is important to know that cancer is not a single disease but a complex system of mechanisms resulting in a group of diseases subject to research studies. The human genome comprises about 6 billion base pairs (Lander et al., 2001) that are replicated within 10 hours (Rew and Wilson, 2000). With this speed of replication, mistakes can occur at a rate of 1 in 100,000 base pairs (Popanda et al., 2000). Therefore, for every single division of a healthy cell, approximately 60,000 single mutations accumulate. However, this number of accumulated mutations drops to 0.5 mutations after DNA proofreading (Bebenek and Ziuzia-Graczyk, 2018;Roberts and Kunkel, 1988). Despite the low number of mutations, their accumulation increases throughout lifetime, causing what is known as somatic mutations (Martincorena and Campbell, 2015). In addition to the somatic mutations, other factors can contribute towards increasing the risk

of developing additional abnormalities, such as radiation (Gilbert and Marks, 1979; Graves et al., 2017), cellular stress (Chircop and Speidel, 2014) and various other factors (Badr et al., 2018).

Many of the mutations occur in different parts of a genome that either does not encode for a protein or does not affect its function; contrarily, in other parts of genome, the produced proteins can be functionally or structurally affected. The problem really starts when the accumulated genomic instability or mutations in a cell affect its cellular functions, causing an uncontrolled cell growth and suppressing normal cells' own control mechanisms (figure 1.1). Currently, about 609 human genes (almost 3%) have been identified as key players in cancer developments (Futreal et al., 2004), such as the well-known BRCA1 and 2 genes involved in breast and ovarian cancer (Neff et al., 2017; Smith and Isaacs, 2011). Alteration in these genes with other accumulated mutations result in the formation of tumorous cells that can grow to form new cell masses. These masses live without being detected by the immune system and thus keep growing, consequently leading to cancer, with an ability to spread from their primary site to other organs of the body (figure 1.1).

Each cancer is categorised based on the type of cells from which the tumour has originally been derived and can further be sub-classified into subtypes (Seemayer and Cavenee, 1989; Hanahan and Weinberg, 2000). However, there are some common functional changes in cancer, known as the hallmarks of cancer (Hanahan and Weinberg, 2000) (figure 1.2). These hallmarks are: (1) reduced dependence on exogenous growth signals; (2) capability to avoid apoptotic cell death; (3) insensitivity to anti-proliferative signals; (4) unlimited cell replication; (5) persistent angiogenesis; and (6) invasiveness towards adjacent tissues to start metastasis. Later, in 2011, the authors added two emerging hallmarks to their previous model of multistep process of cancer development, including genomic instability and inflammation (Hanahan and Weinberg, 2011) (figure 1.2). This molecular understanding has already been applied to clinical practice through the development of targeted therapies that interfere with various proteins within each hallmark (Jungic et al., 2012).

1.1.2 Proteins and cancer progression

Every cell in our body is functioning with the help of proteins. These proteins serve a remarkable range of different purposes, including maintaining cell's structure, molecules

transportation, cell signalling, gene regulation and catalysis processes (Stevenson et al., 2012;Reggi and Diviani, 2017). In the human genome, there are about 20,000 protein - encoding genes carrying the inheritable information coding for the structure and function of each protein (Consortium, 2012). As each protein provides a normal level of cell

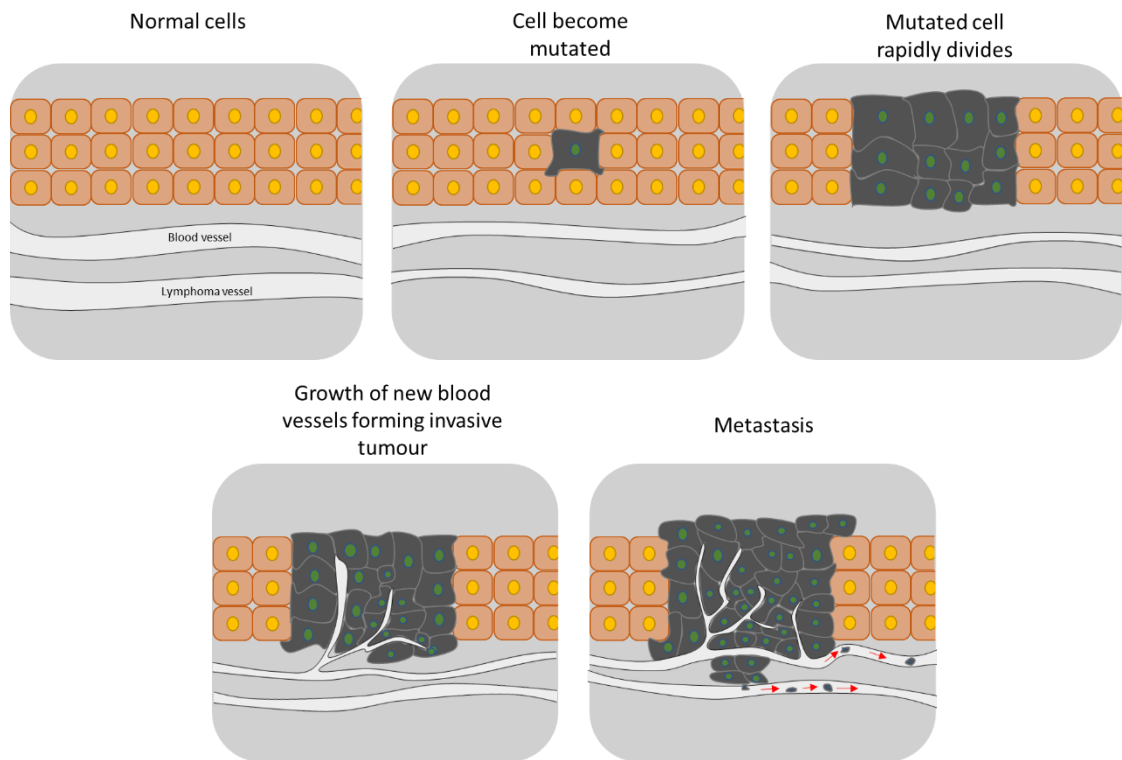


Figure 1.1 Schematic overview showing the development of cancerous mass and its metastasis to different regions in the body.

functionality through its own specific structure and function, this functional normality can be altered when the protein is being mutated, misfolded, truncated, dysregulated and expressed in abundance or not being expressed at all in cells. This change in cell functions due to altered protein has led to the development of the hallmarks of cancer.

In recent years, these cancer hallmarks have represented a challenging opportunity for biomarker research in order to further explore and gain insight into the healthy and diseased functioning of cells.

A biomarker is defined as a biological molecule found in blood, tissues or other body fluids and can be measured and evaluated to differentiate normal and abnormal biological

processes (Henry and Hayes, 2012;Goossens et al., 2015). However, over the past decade, World Health Organization (WHO) came up with a broad definition of a biomarker as any substance, structure, or process that can be measured in the body or its products and impact or predict the frequency of an outcome or disease (WHO, 2001;Lassere, 2008).

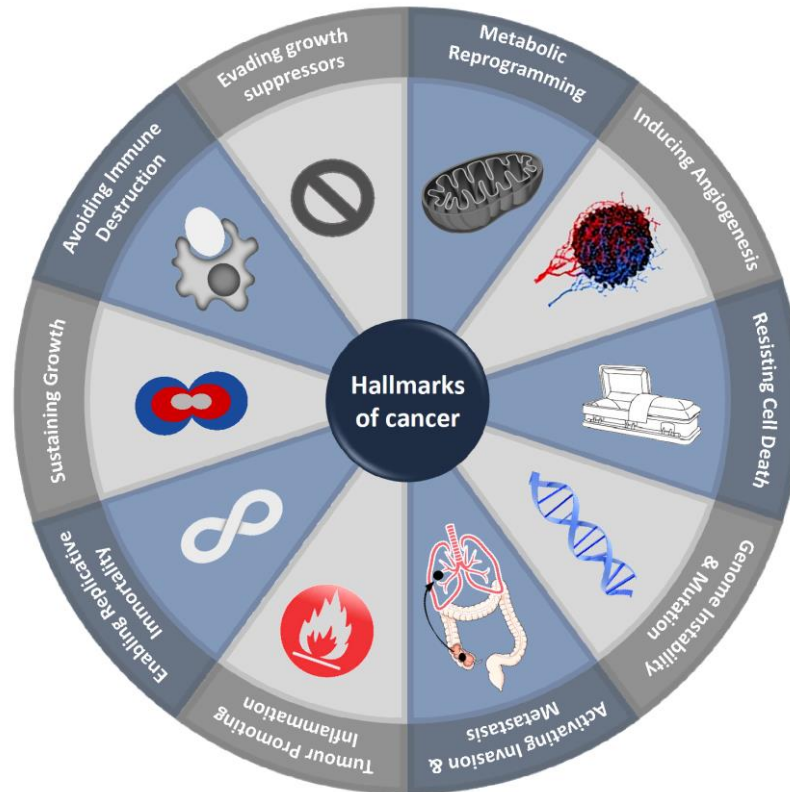


Figure 1.2 Hallmarks of cancer.

Cancer biomarkers can be classified into four categories: predictive, prognostic, diagnostic and screening. Predictive biomarkers aid in predicting the response to specific treatment interventions such as the overexpression or amplification of the human epidermal growth factor 2 (HER2) that predicts the response to trastuzumab in breast cancer (Perez et al., 2014b;Romond et al., 2005), and the KRAS mutations that predict the resistance to EGFR targeting using cetuximab in colorectal cancer (Kim et al., 2017;Reynolds and Wagstaff, 2004). On other hand, prognostic markers inform about the risk of clinical outcomes, including cancer recurrence or disease progression in future. Currently used prognostic biomarkers are the prostate-specific antigen (PSA) in prostate cancers (Heidenreich and Nitschmann, 2010;Olsen and Michalski, 2013), calcitonin for thyroid tumours (Calmettes et al., 1979;Ramos-Vara et al., 2016), and cancer antigen-125 (CA-125) in ovarian cancer (Al-Ogaidi et al., 2014;Bast, 2010). Most of the prognostic

and predictive biomarkers act as diagnostic and screening biomarkers as well because they can also contribute in identifying people with a specific condition or may be at the risk of developing it.

1.1.3 Cancer screening and diagnosis

Looking at the history of cancer, it seems to accompany the evolutionary life of a human. A fossil of an early human ancestor dating back to over 1.7 million years discovered in South Africa has been recently found to have osteosarcoma, which is a lethal bone cancer (Odes et al., 2016). The awareness of the existence of a disease threatening human life has led to the first progress in cancer diagnosis in the nineteenth century, where the post-mortem pathological examination were seem to be correlated to the pre-mortem symptoms (Silver, 1987). Today, various techniques for cancer diagnosis and screening has been developed and are often used in combination (figure 1.3) (Smith et al., 2018).

The approach of diagnostic screening involved testing healthy individuals who did not show symptoms of cancer using multiple techniques including serum antigen testing, sonograms, and endoscopies. When a positive result is suspected during cancer screening, a final diagnosis is reached with further tests involving biopsies examination, x-ray imaging, sigmoidoscopies, and magnetic resonance imaging (Crowell et al., 2009). Currently, a combined use of sonograms and biopsies is the most commonly adapted approach for reaching a conclusive diagnosis of cancer. The visual histological evaluation of biopsy samples is often supplemented with biomarker testing, such as the HerceptTest for the assessment of HER2 expression in breast cancer and EGFR-PharmDX kit for evaluating the expression level of EGFR (Jacobs et al., 1999; Ensinger and Sterlacci, 2008). Several new strategies providing faster and precise diagnosis that have recently evolved include genome sequencing, cancer transcriptomics and the identification of circulating tumour cells (Stahl et al., 2016; Alix-Panabieres and Pantel, 2014).

1.1.3.1 Analytical assays for the detection of protein-based biomarkers in cancer

Whereas different cancer screens utilise molecular analysis to detect and characterise the disease, protein examination is needed for greater accuracy since transcription at the gene level does not necessarily correspond to expression at the protein level (Hudelist et al.,

2004). For instance, in cervical cancer screening, molecular testing of human papilloma virus (HPV) can detect its presence, but protein applications are required to determine whether the virus is active or latent (Gutierrez-Xicotencatl et al., 2009).

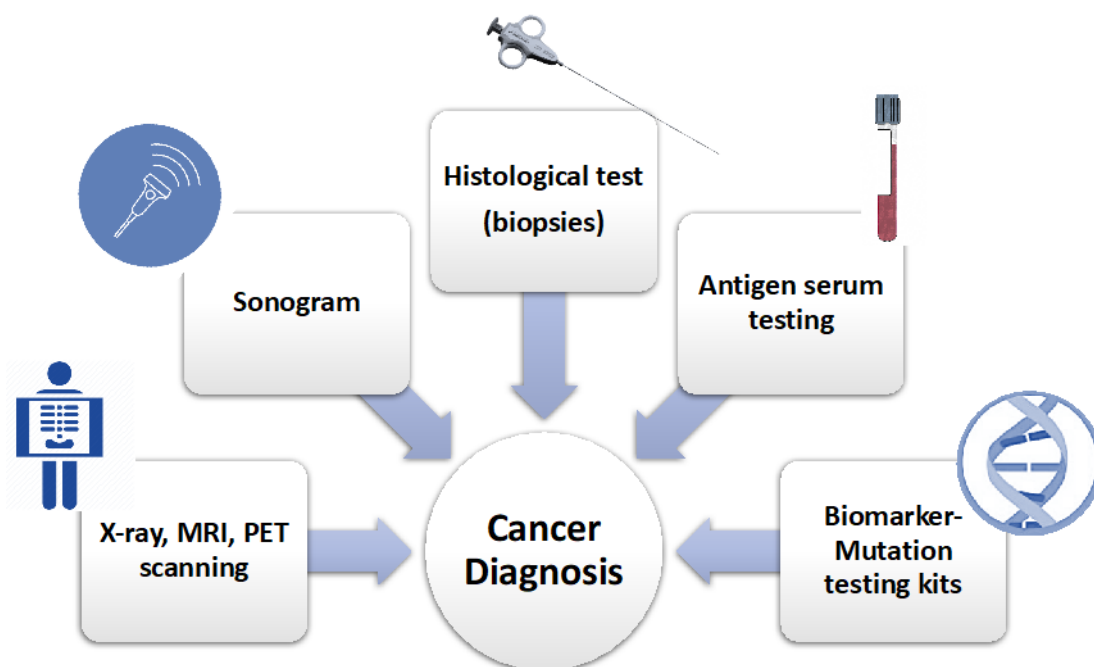


Figure 1.3 Currently used diagnostics approaches in cancer. MRI: Magnetic resonance imaging, **PET:** Positron emission tomography.

Proteins are vital biomolecules in living organisms and their role ranges from storage, metabolism of energy to regulation of cellular functions (Berezovsky and Bastolla, 2017).

Abnormal expression of some proteins often associates with certain diseases and cancer. Thus, protein analysis offers further opportunities for disease diagnosis, stratifying and progression (Ingvarsson et al., 2008). However, protein-based assays must fulfil certain requirements in order to be clinically useful. First, the assay must be sensitive and specific enough to detect the protein of interest. In ovarian cancer, which occurs in 40 out of 100,000 individuals, an assay requires 99.6% specificity (Visintin et al., 2008). In addition to specificity, some cancer biomarkers found at very low concentration (pg/ml) and to be detected, highly sensitive diagnostic assay is needed (Darmanis et al., 2010). Upon providing high sensitivity and specificity for protein detection, both false positive and false negative results, which may significantly affect patients' physical and emotional health, can be prevented. Second, assays must function with a minimal size of samples

being obtained from patients. Finally, protein-applications should be cost-effective and robust enough to result in comparable results between different laboratories and different personnel (Yaziji et al., 2008).

Many protein-based analytical cancer diagnostic and prognostic assays have been developed and widely utilised in clinical settings and research (Powers and Palecek, 2012). This research provides an overview of the most commonly used techniques including immunohistochemistry (IHC), immunofluorescence (IF), enzyme-linked immunosorbent assay (ELISA), and western blotting (WB) applications that were discussed in more details in chapter 2. Other emerging analytical applications, such as mass-spectrometry analysis, proximity assays, miniaturised techniques, and functional activity assays are reviewed elsewhere (Badawi, 2017; Nimse et al., 2016).

1.1.4 Cancer therapy

Once the diagnosis of cancer is confirmed, a treatment regimen, from the different available palliative and curative approaches, can be assigned (figure 1.4). The oldest approach for cancer treatment is surgery, which was discovered in 3,000 BCE by the ancient Egyptians (Atta, 1999). Despite being successful approach for treating solid tumours, surgery is not the optimal solution for treating small tumours, blood cancers, and other metastasised lesions (Kubota, 2011). Other treatment approaches, such as chemotherapy and radiation, can be used alone or in combination with the surgery. However, all the current curative methods are not specific to cancer cells. A combined treatment strategy involving both surgery and radiation can cause a removal of healthy tissues surrounding the cancerous mass, while chemotherapeutic agents are killing cells by halting their cell division, thus impacting the growth of not only the cancerous cells but also other normal cells, including the skin, hair follicles and intestinal epithelium (Kohn et al., 1994).

In the past 30 years, more targeted therapies termed as immunotherapy and targeted therapy have been emerged (Nissim and Chernajovsky, 2008; Weiner, 2015; Weiner, 2007). Some examples of these specific therapeutic approaches are the monoclonal antibodies (Weiner, 2015; Weiner, 2007), immune checkpoint inhibitors (Dine et al., 2017), tyrosine kinase inhibitors (Arora and Scholar, 2005), cancer vaccines (Guo et al., 2013) and chimeric T cells (Curran et al., 2012). Among them, monoclonal antibodies (mAb) were the oldest and most commonly used in targeting membrane receptors to elicit

an inhibitory effect by blocking the function of the biomarker and thus triggering immune response. The effect of such directed mAb is determined by the abundance of the biomarker on cancerous cells (Weiner, 2015). Recently, there are 22 FDA-approved monoclonal antibodies for treating cancer with another 20 being in the late stage of clinical trials (Reichert, 2017). Among the FDA-approved mAbs are the ones used for targeting HER2 and EGFR proteins, both of which are biomarkers of interest in this research.

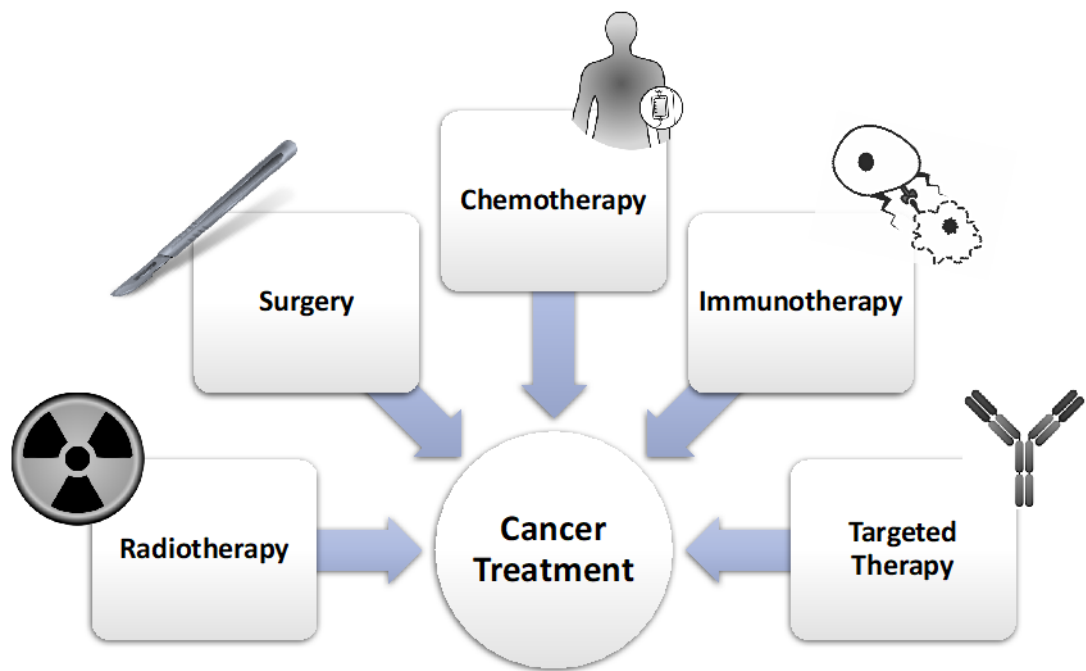


Figure 1.4 Current therapeutic strategies for cancer treatment.
These methods are often used in combination.

1.2 The HER family of receptors and cancer

Among the established protein biomarkers involved in cancer targeting is the family of human epidermal growth factor receptors (HER). This family consists of four closely related type I transmembrane tyrosine kinase receptors; EGFR (also known as HER1 or ErbB1), HER2 (ErbB2), HER3 (ErbB3), and HER4 (ErbB4). They were given the gene symbol Ebb as they are homologous to Erythroblast leukaemia viral oncogene (Roskoski, 2014). These four receptors regulate vital functional activities, include cell growth, differentiation, migration, adhesion and apoptosis. Structurally, the HER family of

receptors consists of an extracellular region (ECD), a transmembrane, a juxta-membrane and intracellular region (ICD) (figure1.5). The extracellular region is divided into four subdomains; I and III subdomains have leucine rich repeats and assist ligand binding, while subdomain II and IV are cysteine rich and their interaction prevents subdomains I and III from binding to ligand through disrupting the ligand binding pocket (Linggi and Carpenter, 2006;Lafky et al., 2008). Signalling carried out by these receptors is initiated by binding of ligand to the extracellular domain I and III.

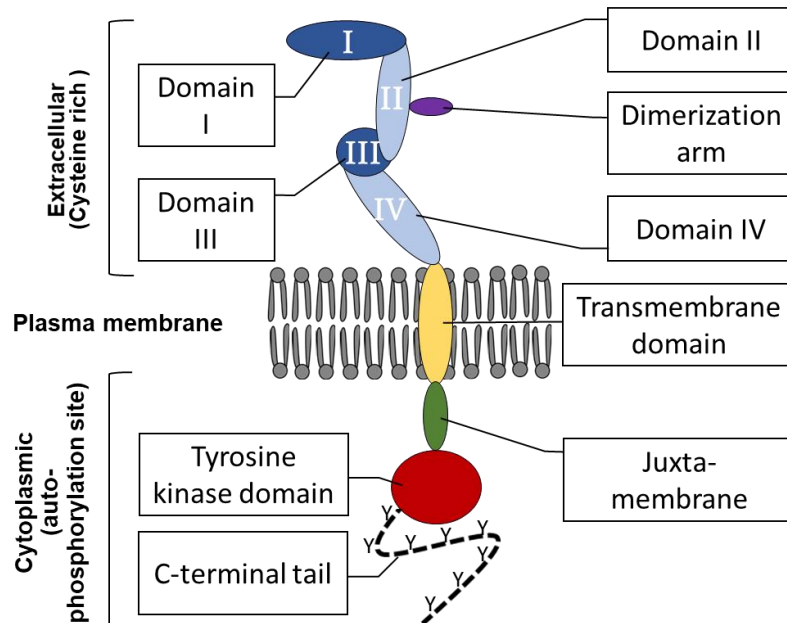


Figure 1.5 A schematic presentation of the structural arrangement of HER2. The extracellular part of the receptor is comprised of four domains: I and III are ligand binding domain (dark blue); II and IV are cysteine-rich domains (light blue). The dimerization arm (purple) is contained in the second domain. The receptor consists of extracellular region, a single transmembrane domain (yellow), a juxta-membrane region (green), the tyrosine kinase (red) and the C-terminal tail that consists of numerous tyrosine, which are phosphorylated upon activation (dotted line).

1.2.1 HERs activation, dimerization, and cell signalling

Around 11 ligands have been identified of which some are specific to one receptor while others are more promiscuous (Yarden, 2001;Yarden and Sliwkowski, 2001). Ligands can be categorised into three groups based on their receptor-binding specificities. The first group consists of epidermal growth factor (EGF), transforming growth factor alpha (TGF α), epigen (EPN) and amphiregulin (AR), which bind selectively to EGFR (Cohen et al., 1981). The second group comprises betacellulin (BTC), heparin-binding EGF (HB-

EGF) and epiregulin (EPR), which also bind to EGFR (Riese and Stern, 1998) but can also bind to HER4 (Koutras et al., 2010). The third group, the neuregulins (NRGs), show different binding specificities towards HER3 and HER4 but not to EGFR (Falls, 2003). NRGs are further categorised into two subgroups: NRG-1 and NRG-2 bind to HER3 and HER4, while NRG-3 and NRG-4 bind exclusively to HER4 (Koutras et al., 2010). Among all four receptors, HER2 is the only one that does not bind directly to any ligand (Rubin and Yarden, 2001).

Receptor	Ligands
EGFR	EGF, TGF- α , Amphiregulin, HB-EGF, Betacellulin, Epigen, Epiregulin
HER2	No ligands identified
HER3	Neuregulin 1 and 2, Neureg1yc-C
HER4	Betacellulin, Epigen, Epiregulin, Neuregulin 1, 2, 3 and 4, Tomoregulin

Table 1.1 HER ligand-binding specificity. This table is adopted from (Wieduwilt and Moasser, 2008).

EGFR binding ligands are synthesised as transmembrane protein precursors with a single membrane spanning segment (Singh et al., 2016). The mature peptide is cleaved from the extracellular domain of the precursor by the action of proteases, resulting in the release of a soluble growth factor. Different enzymes have been shown to be involved in the cleavage processes of different ligand precursors. For example, in the case of TGF α , the converting enzymes (TACE) known as metalloprotease and the tumour necrosis factor alpha (TNF α) are known to be responsible for such cleavage processes (Browne, 1991; Singh et al., 2016). The mature, soluble, EGF-like growth factors are distinguished by the presence of six conserved cysteine residues in the consensus (CX7, CX4-5, CX10-13, and CXCX8 C). These residues form three disulphide bonds significant for function: Cys1 forms a bond with Cys3, Cys2 with Cys4 and Cys5 with Cys6 (Browne, 1991). The disulphide-bonded regions in the growth factors are known as the EGF-like motifs. Among all EGF-like factors, the TGF α and heparin-binding EGF are the ligands most involved in cancer pathogenesis (Hobor et al., 2014; Schrevel et al., 2017).

Neuregulins represent the most complex family of growth factors. NRG-1 is the only well-characterised factor (Falls, 2003; Yarden and Pines, 2012). NRG-1 is encoded by a 1.4-megabase gene that produces more than 15 distinct protein products by alternative splicing in addition to the use of more than one promoter (Falls, 2003). Structurally, NRGs are classified into two groups based on the presence of an immunoglobulin-like domain in addition to the EGF-like domain (Ig-NRG), or the presence of an additional cysteine-rich domain (CRD-NRGs) (Bao et al., 2003).

Ligand binding leads to structural rearrangement of the ECD of the receptor from inactive closed conformation to an open form where the dimerization arm on domain II is exposed to facilitate the interaction with another receptor nearby to form a homo or heterodimer (Ogiso et al., 2002; Ferguson et al., 2003). Dimerization results in the activation of the intracellular tyrosine kinase domain in an asymmetric manner, where one receptor provokes a structural change of its binding partner's catalytic domain, activating it by phosphorylation of tyrosine in the C-terminal tail (Zhang et al., 2006). The phosphorylation provides docking sites for adaptor proteins stimulating signalling cascades, such as the mitogen-activated protein kinase (MAPK) and phosphatidylinositol-3 kinase (PI-3K) pathway that promote phenotypic changes such as proliferation, survival, and migration (Lu et al., 2017; Yarden and Sliwkowski, 2001) (figure 1.6).

Mitogen-activated protein kinase (MAPK)

There are at least four different MAPK cascades; the extracellular signal-regulated kinases (ERK) 1 and 2, Jun amino-terminal kinases (Jnk) 1/2/3, p38-MAPK and Erk5 (Marmor et al., 2004). The MAPK signalling pathway is three levels signalling route in which one kinase phosphorylates the other (MAPKKK-MAPKK-MAPK). The Erk1/2 MAPK pathway begins with the recruitment of the Grb-2 to the phosphorylated receptor, leading to a linear kinase cascade that finally results in the phosphorylation of ERK1 and 2 (figure 1.6). Consequently, the activated ERK 1 and 2 phosphorylates various cytoplasmic proteins and also translocated to the nucleus for further activation of transcription factors involved in cell cycle progression (Zhang and Liu, 2002). One key upstream regulator of the ERK1/2 MAPK pathway is the Ras protein, and approximately 30% of human tumours that harbour mutations in the Ras protein show constitutively activated MAPK pathway (Roberts and Der, 2007).

Phosphatidylinositol 3-kinase (PI3-K)/Akt

PI3K activation occurs via binding of the regulatory p85 subunit to a phosphorylated tyrosine on the receptor (figure 1.6) (Downward, 2004). As a result of binding, several signalling effectors are recruited to the plasma membrane such as the serine/threonine protein kinase (Akt; also, known as protein kinase B). When Akt is activated, it will translocate to the cell nucleus targeting proteins involved in regulating apoptosis and cell survival, such as Bad and caspase 9 (Downward, 2004). The PI3K pathway can also be activated by Ras (Franke et al., 1997). The Akt pathway is negatively regulated by phosphatase and tensin homologue deleted on chromosome ten (PTEN), and several mutations reported in this molecule have led to a constitutively active Akt signalling contributing to the observed resistance of the EGFR-targeted therapy (Li and Ross, 2007; Kruser and Wheeler, 2010).

Phospholipase C-gamma (PLC γ)

Activated EGFR and HER2 recruit PLC γ to the cell membrane (Marmor et al., 2004; Kassis et al., 1999), to hydrolyse lipids promoting the release of secondary messengers such as calcium, which in turn activate the calcium/calmodulin-dependant kinases (figure 1.3) (Wells and Grandis, 2003). In cancer, PLC γ is responsible for promoting tumour invasion and cell motility. Furthermore, PLC γ also contributes to the reported resistance of both radiation and chemotherapy treatments (Yang et al., 2001).

1.2.2 The role of HER proteins in cancer development

Due to the growth and survival stimulatory signalling by the EGFR receptors, abnormal signal transduction of this family is contributed to cancer progression, particularly, EGFR and HER2 that have been extensively studied in this context. Overexpression, gene amplification, activating point mutations, autocrine signalling, or partial gene deletions of any member of this EGFR family were reported as the driving force behind the aggressiveness of many cancer types (Hynes and MacDonald, 2009).

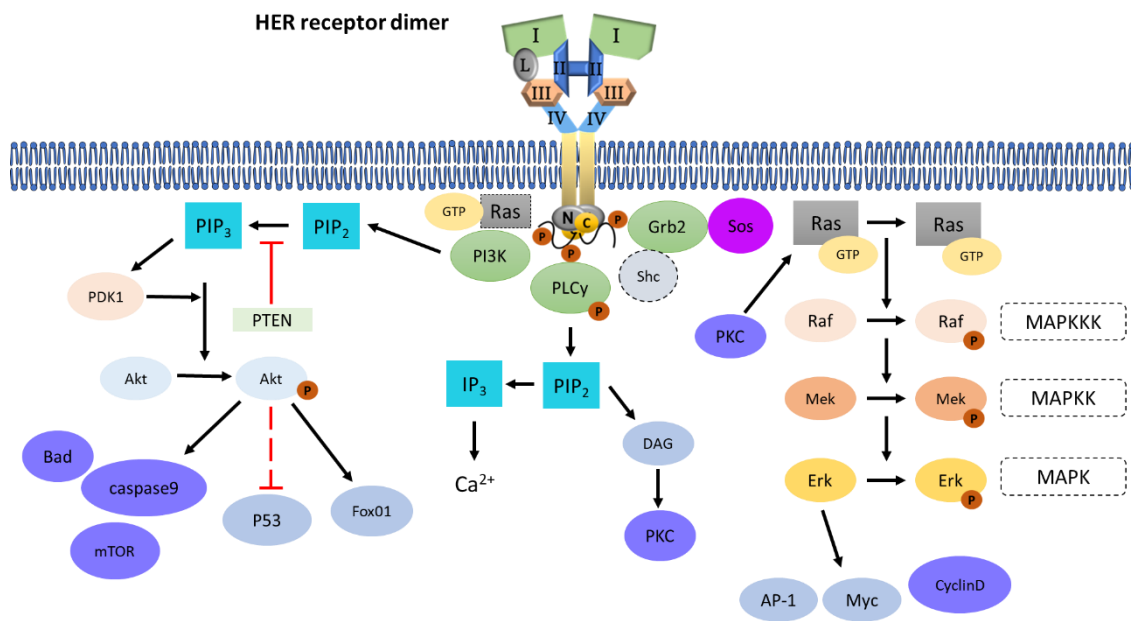


Figure 1.6 The role of HER proteins in cell signalling. Upon activation of HERs they dimerise causing activation of three signalling pathways: MAPK/ERK1/2, PLC γ and PI-3K/Akt1/2. Promoting these pathways lead to increase in cell proliferation, metastasis and survival. See list of Abbreviations for more details about the mentioned proteins.

EGFR/HER1

HER1 was the first identified receptor and the most studied member within the family. Furthermore, it was often acted as a model to reveal how the EGFR family of receptors functions. In 1980, Stanley Cohen and his co-workers discovered HER1 as a receptor for epidermal growth factor (EGF) (Cohen et al., 1981). HER1 can bind to different ligands, including the EGF, transforming growth factor- α (TGF- α), betacellulin (BTC), heparin-binding EGF-like growth factor (HB-EGFR), epiregulin (EPR), epigen (EPN), and ampiregulin (AR), but not to any neuregulins (NRGs) (Riese and Stern, 1998).

Deregulation of the HER1 has been associated with poor prognosis in different cancers, such as head and neck, colorectal, breast, and ovarian cancers (Nicholson et al., 2001). The best-known example of EGFR overexpression is found in colorectal tumours (Cunningham et al., 2005). In addition to its overexpression, EGFR can mediate cancer initiation and progression through oncogenic mutations, such as the EGFRvIII, or by the autocrine signalling of the ligands, resulting in a constitutively active receptor (Kuan et al., 2000).

HER2

HER2, which is also known as p185^{ErbB2/neu}, ErbB2, or *neu*, is considered as an oncogene because it can lead to cell transformation even in the absence of a ligand (Di Fiore, 1987). In cancer, HER2 was first discovered as an amplified gene, and as a product of the *neu* oncogene in rat neuroblastomas (King et al., 1985). HER2 has been of the most studied cancer related biomarker for drug discovery. HER2 overexpression due to gene amplification or transcriptional deregulation was seen in 20-30% of breast cancer (Slamon et al., 1987;Baselga and Swain, 2009), as well as other cancer types, such as ovarian (Koopman et al., 2018), colorectal (Kavanagh et al., 2009), and gastric cancers (Gravalos and Jimeno, 2008), and is associated with poor prognosis, and increased risk of disease metastasis and recurrence (Zahnow, 2006). Furthermore, in a subset of lung cancer, a mutated version of the receptor has been found (Falchook et al., 2013;Pillai et al., 2017).

HER3

HER3 has an inactive intracellular tyrosine kinase domain and requires another receptor to mediate signalling (Citri et al., 2003;Sierke et al., 1997). In fact, the heterodimer formed by HER2 and HER3 has been shown to be the most potent signalling pair within the HER family of receptors (Pinkas-Kramarski et al., 1996). In comparison with both EGFR and HER2, HER3 has six binding sites for PI3K which making it a potent activator of the PI3K/Akt pathway affecting the overall survival of cancer cells (Soltoff et al., 1994). The receptor has two known ligands that have several splicing variants (Riese and Stern, 1998). These ligands are neuregulin 1 (NRG-1), also known as heregulin (HRG) and neuregulating factor (NDF), and neuregulin 2 (NRG-2). When co-expressed in tumours that overexpress HER2, HER3 plays a crucial role in increasing cell growth and acting as an escape route for cancer cells to resist the HER2-targeted tyrosine kinase inhibitors (TKIs) (Holbro et al., 2003;Lee-Hoeflich et al., 2008). Therefore, HER3 is an interesting target when considering combinatorial therapies for targeting tumours with HER2 overexpression.

HER4

HER4 is the least studied member within the HER family. It has many different activator molecules, including HB-EGF, BTC, EPR (shared by the EGFR), NRG1 and NRG2 (shared by the HER3), NRG3 and others that are exclusive for HER4 (Koutras et al., 2010). Furthermore, HER4 has four dissimilar isoforms (4ICD) produced by alternative splicing of the mRNA (Rudloff and Samuels, 2010; Jones, 2008). In cancer, the HER4 role is still ambiguous and numerous studies suggest that this receptor may have bifacial, conveying both pro- and anti-tumour effects depending on the cancer subtype and the HER4 isoform being expressed (Guo et al., 2018; Machleidt et al., 2013).

1.2.3 Targeting HERs: mechanism of action and resistance

1.2.3.1 Currently used therapeutic agents and their inhibitory mechanism

Many therapeutic agents, including monoclonal antibodies and tyrosine kinase inhibitors (TKIs), have been used to target both EGFR and HER2. Currently, two mAbs targeting EGFR are approved for clinical use, cetuximab and panitumumab (Adams and Weiner, 2005). Both antibodies bind to domain III in the extracellular region of the receptor preventing ligand binding (Duffy et al., 2011). Cetuximab seems to sensitize head and neck patients to irradiation (Bonner et al., 2010), while no effect of both antibodies have been reported on patients with mutations in the *ras* gene (Guo et al., 2016; Guren et al., 2017). The major drawback of such EGFR-targeted drugs is the skin toxicity (Potthoff et al., 2011).

With regards to targeting HER2, both trastuzumab and pertuzumab are effective treatments of cancer. Trastuzumab binds to the extracellular domain IV to block the downstream PI3K/Akt signalling by mediating downregulation of HER2 as well as activating the human complement cascade (Albanell et al., 2003; Baselga et al., 2001). Trastuzumab increases the survival rate of the HER2 positive metastatic breast cancer patients, particularly, when given as a combination with chemotherapy (von Minckwitz et al., 2017; Baselga et al., 2012). In addition to trastuzumab, another antibody known as pertuzumab has been developed and proved its capability to bind to domain II in the ECD of HER2 inhibiting the formation of receptor dimers (Franklin et al., 2004). However, this antibody is still under clinical trials.

Tyrosine kinase inhibitors (TKIs) are small molecule inhibitors that bind to the intracellular region of the receptors blocking the transduction of signals. EGFR has been targeted by two TKIs, such as gefitinib and erlotinib that have been approved for clinical use (Gazdar et al., 2004). Patients that have mutated EGFR kinase were the only ones who responded to the gefitinib treatment (Gazdar et al., 2004). Another molecule that is known as lapatinib was used to target the tyrosine kinase domain of both EGFR and HER2 proteins causing an inhibition of the ATP-binding site (Untch and Luck, 2010). It was proposed that lapatinib TKI inhibitor may be used to overcome the resistance shown with the trastuzumab treatment (Untch and Luck, 2010).

1.3 The need for cancer biomarkers

Biomarkers are classified into seven groups based on their applicability (Currid and Gallagher, 2008;Jungic et al., 2012;Kraus, 2018;Weigel and Dowsett, 2010). In clinics, biomarkers are used as predictors, and as diagnostic, prognostic, mechanistic, pharmacodynamic, surrogate end-point, and safety markers (Table 1.2). Biomarkers can take the form of human genes, RNA measurements, genetic variations, proteins and metabolites (Currid and Gallagher, 2008;Kulasingham and Diamandis, 2007). Therefore, many methodologies for the discovery of new biomarkers are constantly emerging and existing technologies are continuously evolving (Ahram and Petricoin, 2008;Sandow et al., 2018;Theodorescu et al., 2006). Omics methodologies including genomics, proteomics and metabolomics, in addition to other imaging techniques, hold promise for discovery of biomarkers.

1.3.1 Challenges and limitations in biomarker discovery and validation

Despite progress in biomarker discovery, the number of currently used biomarkers that are known to be clinically useful is pitifully small (McDermott et al., 2013;Ileana Dumbrava et al., 2018). This is mainly due to a lack of consistency between initial study reports that show great potential of certain molecules as biomarkers, and subsequent studies that often fail to repeat the findings or that even show contrasting results. It is imperative that researchers attempt to understand the reasons for such lack of consistency between studies on the same biomarkers. Multiple problems, including general

Type of biomarker	Description	Example
Predictor	Disease-associated biomarkers that indicate whether there is a threat of disease and measure patient responsiveness to treatment	Serum level of VEGF and fibronectin can predict clinical response to interleukin-2 therapy in metastatic melanoma and renal carcinoma (Singh and Rose, 2009;Sabatino et al., 2009)
Diagnostic	Biomarkers that aid in diagnosis of an existing disease and staging it	ER, PR and HER2 expression level in breast cancer (BC) used to stratify BC to subtypes and determine the therapeutic regimen (Onitilo et al., 2009;Wesseling et al., 2016)
Prognostic	Biomarkers that predict the future outcome in an individual, as well as to predict the overall survival rate and clinical benefit offered by a therapeutic intervention	The presence of correlated with improved prognosis in advanced ovarian carcinoma (Zhang et al., 2003) Overexpression of EGFR in colorectal carcinoma indicates poor prognosis (Pabla et al., 2015)
Mechanistic	Biomarkers that inform and validate the mechanism of action of a particular treatment	Acute immune response developed after the tissue injection of a drug agent (Salamanca et al., 2014)
Pharmacodynamic	Biomarkers that are signatures of a certain pharmacological response to an active compound. They are used to monitor the clinical response	Haemoglobin A1C for treatment of diabetes is used to optimise doses and in drug development (Lyons and Basu, 2012)
Surrogate end-point	Biomarkers that yield information regarding the clinical benefit/survival rates at early stages	HIV viral load as a measure of probable clinical benefit with later confirmation of mortality benefit (Mermin et al., 2011)
Safety	Biomarkers that predict the potential toxicity of a specific treatment	Albumin, total protein, B2-microglobulin, cystatin C have been selected as biomarkers of drug-induced kidney injuries (van Meer et al., 2014)

Table 1.2 Types of biomarkers and their applications. EGFR: Epidermal growth factor; HER2: Human epidermal growth factor receptor 2; ER: oestrogen receptor; PR: progesterone receptor. This table is adopted from (Seyhan, 2010).

differences in methodology, non-standardised assays, lack of reproducibility of conditions, poor study designs and misleading statistical analyses that are often based on Small sample sizes, have been cited as reasons for such discrepancies (McDermott et al., 2013;Ileana Dumbrava et al., 2018;Erler and Linding, 2010).

Successful delivery of fit-for-purpose biomarkers relies on the solution of these experimental problems, as well as the understanding of the advantages and limitations of the different multi-omics platforms, and ways in which these technologies can be utilised (Erler and Linding, 2010). For example, a DNA microarray technology has led to significant advances in the study of gene profiling. However, its use can be limited due to the physiological mechanism of mRNA splicing, which results in the presence of different splice variants in individual cell populations (Bayele et al., 2010). Furthermore, not all mRNAs are translated into proteins, despite their active state.

In line with DNA microarray and mRNA quantitative analysis, proteomic approaches suffer from certain limitations including the low analytical sensitivity of some techniques and the scarcity of high-quality detection reagents (Sallam, 2015;Chan et al., 2016).

1.3.2 Biomarkers currently used in breast cancer

Certain characteristics of biomarkers are required for their clinical use. Biomarkers must be robust, measurable and accessible, and their results must be reproducible (Holland, 2016). Furthermore, a biomarker should be specific and sensitive to distinguish true positives from false negatives (Holland, 2016). Examples of clinically valuable biomarkers are those for which routine tests are applied to tissue biopsy samples of breast cancer patients (Hanna et al., 2007;Ahn et al., 2018).

Based on the molecular expression of four biomarkers: oestrogen receptor (ER), progesterone receptor (PR), human epidermal growth factor receptor 2 (HER2) and the antigen Ki-67, tumours of the breast are classified into the luminal A, luminal B, basal and HER2 subtypes. The expression of these biomarkers results in the production of tumours that display different phenotypic signatures (Table 1.3) (Holliday and Speirs, 2011;Ahn et al., 2018). Breast-cancer classification is often used as a key reference to estimate the disease prognosis and to choose the appropriate therapeutic approach, as each subtype differs from the others in its disease progression, pattern of metastatic spread, clinical prognosis and response to therapy (Weigelt et al., 2005). Tumours of the type

ER+ luminal account for 70 per cent of breast cancer cases and this group has been further subdivided into two types (Cancer Genome Atlas, 2012). ER+ luminal type A has a favourable prognosis and can be treated with hormone therapy, while ER+ luminal type B is more aggressive and exhibits poor disease prognosis compared with the luminal subtype A. This is due to the presence of high expression levels of HER2 (Sledge et al., 2014).

The HER2+ subtype accounts for 10 per cent to 15 per cent of cancer cases and is dominated by HER2-gene amplification, which results in high HER2 expression levels (Prat et al., 2014;Prat et al., 2017). This phenotype is considered an aggressive type of breast cancer. However, personalised anti-HER2 therapy using monoclonal antibodies such as trastuzumab (discussed further in section 1.3) has prolonged the lives of patients through the control of extracranial metastasised lesions; however it does not treat metastasised cells localised in the brain (Drebin et al., 1985;Vogel et al., 2002;Paik et al., 2008;Shen et al., 2019).

The basal-like tumours, which are negative for all three markers (HER2, ER and PR), form the most aggressive group of all tumour subtypes. They account for between 15 per cent and 20 per cent of breast-cancer cases (Schmadeka et al., 2014;Kumar and Aggarwal, 2016). These triple-negative tumours are marked with TP53 mutations (up to 80 per cent) with a subset found to be enriched with BRCA1 mutations (Komatsu et al., 2013;Ma et al., 2010). Patients who present with this type are managed with cytotoxic chemotherapy, unless a BRCA1 mutation is detected (Lebert et al., 2018). Recently, mutations in BRCA1/2 have shown sensitivity to poly (ADP-ribose) polymerase (PARP) inhibitors (Lee et al., 2014) and this sensitivity represents a form of treatment that can improve survival rates.

Classification	Expression profile	Other characteristics	Examples of breast-cell lines
Luminal A	ER ⁺ , PR ^{+/-} , HER2 ⁻	Low Ki-67, endocrine treatment responsive, often chemotherapy responsive	MCF-7, T47D, SUM185
Luminal B	ER ⁺ , PR ^{+/-} , HER2 ⁺	High Ki-67, usually endocrine responsive, variable chemotherapy responsiveness, HER2 ⁺ are trastuzumab responsive	BT474, ZR-75
Basal	ER ⁻ , PR ⁻ , HER2 ⁻	EGFR ⁺ and/or cytokeratin 5/6 ⁺ , high Ki-67, endocrine responsive, often chemotherapy responsive	MDA-MB-468, SUM190
Claudin-low	ER ⁻ , PR ⁻ , HER2 ⁻	Low in all Ki-67, E-cadherin, claudin-3, claudin 4 and claudin 7, intermediate response to chemotherapy	BT549, MDA-MB-231, Hs578T, SUM1315
HER2	ER ⁻ , PR ⁻ , HER2 ⁺	High Ki-67, trastuzumab responsive, chemotherapy responsive	SKBR3, MDA-MB-453

Table 1.3 Molecular classification of breast carcinomas. ER: oestrogen receptor; PR: progesterone receptor; HER2: human epidermal growth factor receptor 2. The table is adopted from (Holliday and Speirs, 2011).

1.3.3 Identification of new biomarkers: Why?

Despite the efficacy of current monoclonal antibodies, some tumours exhibit resistance to them. This is thought to occur either within the tumours (*de novo* non-responding tumours) or to have been acquired during the treatment (Facchinetti et al., 2018; Creighton et al., 2008). In both cases, one possible explanation for resistance to treatment with antibodies such as trastuzumab (HER2-targeting monoclonal antibody) is broad cross-links and signal plasticity within the homologous HER family or other closely related families of receptors. These characteristics lead to the possibility that if signalling by one receptor is blocked, another activated receptor may fill in. Such networking in cancer cells indicates the level of complexity of the disease and the involvement of many entities in cancer development and progression (Croce et al., 2016). The identification and validation of various cancer players, as well as progress in drug discoveries and in the development of point-of-care diagnostic assays, have the potential to improve patients' response rates and overall management of the disease (Geeleher et al., 2016; Collins et al., 2017).

1.4 Binding molecules for biomarker recognition in health and disease

1.4.1 Antibody and its derivatives

Antibodies, also known as immunoglobulins (Ig), are a large group of proteins capable of binding antigens as part of an immune response. They bind to epitopes on an antigen to promote phagocytosis and removal by other biological processes. Epitopes that are recognised by antibodies are usually short amino acid sequences present within the foreign protein (Kipriyanov and Le Gall, 2004). There are five mammalian classes of the antibody: IgA, IgD, IgM, IgE, and IgG. Antibodies that belong to the IgG class are the most predominant in human serum, as well as, the most commonly used antibody in research. Structurally, they exhibit a Y-shape comprising two heavy and two light chains (figure 1.7). The shorter light chains interrelate with the N-terminus of the other heavy chains to form two arms or as they called the antigen-binding (Fab) domains, which are further constituted of both constant and variable regions (Singh et al., 2018). Six variable amino acid loops at the ends of the Fab domains, also known as complementarity determining regions (CDRs), are responsible for binding events between the antibody molecule and the antigen. The tail of the Y-shape (Fc-domain) facilitates the antibody interaction with macrophages and other cells expressing the Fc receptors (Singh et al., 2018).

Antibodies can bind to their target antigen with high specificity, and high affinity typically in the nano- or pico-molar range (Kohler and Milstein, 2005). According to their origin, antibodies can be classified as monoclonal (mAbs) or polyclonal (pAbs). The monoclonal antibody is a single antibody variant originating from a single cell line (hybridoma) and binds only to one epitope on a single antigen, which makes it more specific than the pAb. In contrast, the polyclonal antibodies are purified from serum of an immunized mammal and considered as a set of antibody variants that binds to different epitopes (Chiarella and Fazio, 2008). Because of their high affinity and specificity, monoclonal antibodies are commonly used tool for diagnostic, research and therapeutics (Nelson et al., 2010;Reichert, 2008).

1.4.1.1 Monoclonal antibody production: the endless supply

Since the discovery of hybridoma technology by Köhler and Milstein in 1975, several advances in the methods of generating mAbs have been made (Kohler and Milstein, 2005; Kohler et al., 1975). They described the hybridisation of antibody-producing B cells from the spleens of immunised mice with an immortal mouse myeloma tumour cell line facilitated the production of an investigational mAb. There are two general ways to produce monoclonal antibodies in animals, which are the ascites and the *in vitro* methods.

At first, the animal (usually a mouse) is immunised with the target antigen multiple times over several weeks before it is finally killed and the spleen extracted. The spleen, which is rich in immunocompetent B cells that have a limited life span, is then fused with an immortalised myeloma tumour cells *in vitro* to produce the hybridoma. This hybridoma can be further extended in two ways: (1) by injection into the peritoneal cavity of a second animal (known as the *in vivo* ascites technology) or (2) by *in vitro* culturing of the hybridoma cells (known as *in vitro* technology) (figure 1.8) (Hendriksen and de Leeuw, 1998a; Hendriksen and de Leeuw, 1998b; Leenaars and Hendriksen, 2005).

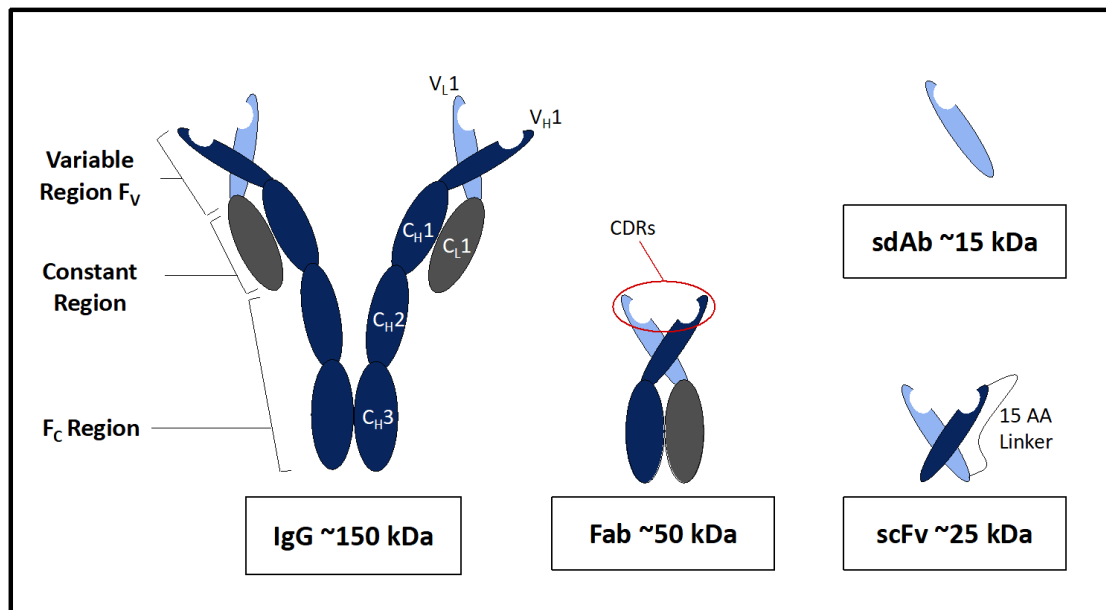


Figure 1.7 Antibody molecule and its derivatives.

In the ascites antibody production method, the abdominal lining of the animal is injected with a priming solution to induce inflammation and interfere with drainage of peritoneal fluid. After priming, the hybridoma cell suspension is injected to the animal to cause more multiplication of cells. The produced antibodies accumulate in the abdominal cavities

causing a distended abdomen as the tumour grows and ultimately results in an animal with pain and distress symptoms (Peterson, 2000). The accumulated fluid is then extracted one to three times before killing the animal causes more complications to the animal's health (Love, 2010). Despite their seemingly endless supply, antibody production faces multiple scientific issues besides the concerns of animal welfare (Glassy and Gupta, 2014).

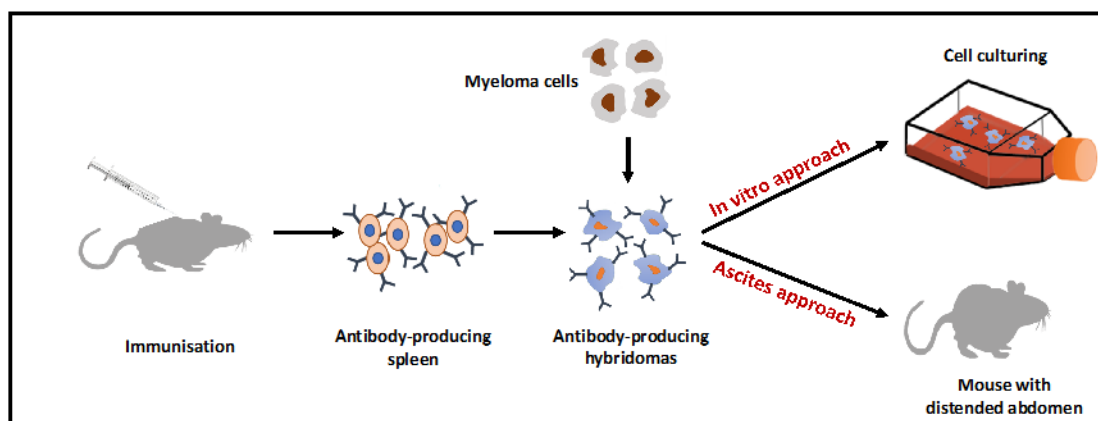


Figure 1.8 Production of monoclonal antibody using ascites and *in vitro* culturing method. Antibody production starts with immunising the animal with the target of interest followed by the isolation of the antibodies from the spleen and fuse them to immortal myeloma cells. This fusion results in the generation of hybridoma cells that continuously produce antibodies. To improve the production, hybridoma cells will either re-injected to a second animal (ascites approach) or re-cultured *in vitro*.

1.4.1.2 Drawbacks of antibodies pushing towards the development of other engineered antibody-based formats

Among the scientific problems encountered during the production of the antibodies (Geyer et al., 2012; Frenzel et al., 2014), their large size has limited their potentials in some application, such as affinity chromatography and imaging applications (Ruigrok et al., 2011). To alleviate the size-related problems of antibodies, specific fragments of it, such as the fragments of antigen binding (Fab) regions or the single chain fragments of variable domains (ScFv) (figure 1.7), have been developed. ScFv are well suited for molecular biology as the antigen binding sites of the heavy and light chains can be connected by a 15-amino acid linker (figure 1.7) and then tagged at their C-termini with both a c-myc epitope and a six histidine, permitting their detection and purification steps.

Despite the small size of the ScFv variant, they can still exhibit high binding affinity similar to the full-length antibody (Hanes et al., 1998;Hanes et al., 2000).

In contrast, Fab fragments are approximately about 50 kDa in size and consists of two polypeptides with constant regions linked through disulfide bonds. Fabs are monovalent and they can resist aggregation compared to the ScFv variants (Rader, 2009). An alternative to Fab and ScFv fragments is heavy chain antibodies (figure 1.7). These heavy chain antibodies are natural variants derived from the V_{HH} immunoglobulins present in camelid species (Hamers-Casterman et al., 1993) and cartilaginous fish (Stanfield et al., 2004). Heavy chain antibodies are termed as nanobodies, and they are much smaller (approximately around 15 kDa in size) than both conventional antibodies and other IgG engineered fragments. Nanobodies can be produce in a microbial host and can be isolated for certain specificities using a phage display technology (Allegra et al., 2018;Schumacher et al., 2018).

In parallel to the advance in the generation of different antibody-based binding formats, many researchers have focused on modifying non-antibody-based protein scaffolds into binding proteins, with the goal of both limiting the use of animals and developing binding reagents with qualities comparable with those of the antibodies.

1.4.2 Aptamers

Aptamers are oligonucleotide ligands that have received significant interest as a class of non-protein bio-recognition tools. The term ‘aptamer’ derived from the Latin word ‘aptus’ (to fit) and the Greek word ‘meros’ (part or piece) (Wang et al., 2018). The reported targets of aptamers range from small organic molecules, such as acetylcholine and ethanolamine (Mann et al., 2005;Bruno et al., 2008) to large complexes of proteins (Tang et al., 2007). Aptamers can exhibit nanomolar range binding affinities, which is comparable with that of mAbs (Jenison et al., 1994). To produce target-binding Aptamers, a large pool of either DNA or RNA synthetic oligonucleotide library is constructed and selected on different targets by a process called systematic evolution of ligands by exponential enrichment (SELEX) (figure 1.9) (Bayat et al., 2018).

1.4.2.1 Drawbacks of aptamers

Aptamer sequences against several target molecules have been reported and their successful applicability in a range of techniques have also been described (Keefe et al., 2010; Mairal et al., 2008). However, aptamers are susceptible to degradation in complex matrices, such as cell environment and blood serum. Furthermore, aptamers can be unstable over a range of temperatures and pHs as well as being more sensitive to cation concentration and digestion by nuclease (Ruigrok et al., 2011; Schutze et al., 2011). In addition, the backbone of oligonucleotides is self-repelling and that may result in conformational instability or unfolding during surface immobilisation. Extensive efforts to overcome these drawbacks by chemically modifying the aptamer is still ongoing (Mayer, 2009; Vaught et al., 2010).

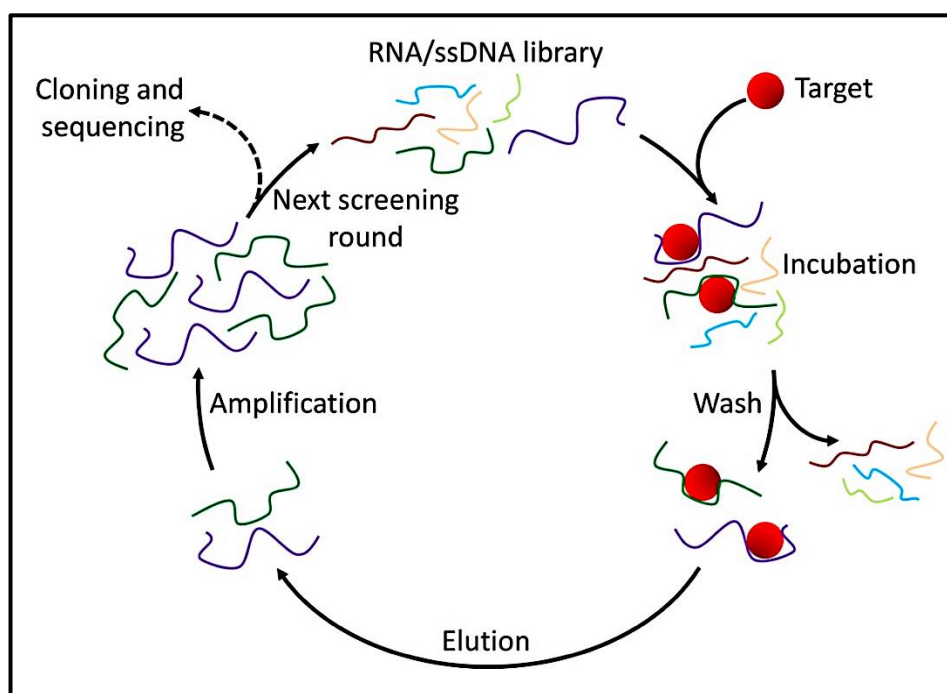


Figure 1.9 Selection of aptamers (SELEX). A library of random DNA or RNA fragments is selected on immobilised target followed by washing of the unbound sequences and eluted the bound ones are amplified in the PCR. The selection and amplification steps can be repeated and the finally obtained sequences are analysed and characterised. Adopted from (Schutze et al., 2011)

1.4.3 Engineered protein binding tools

In parallel to the development of new engineered antibody-based proteins and aptamers other studies have focused in generating non-antibody based protein modifying several natural occurring proteins into binding tools, with improved characteristics (Skerra, 2000; Skrllec et al., 2015). The principle of selecting the appropriate scaffold for

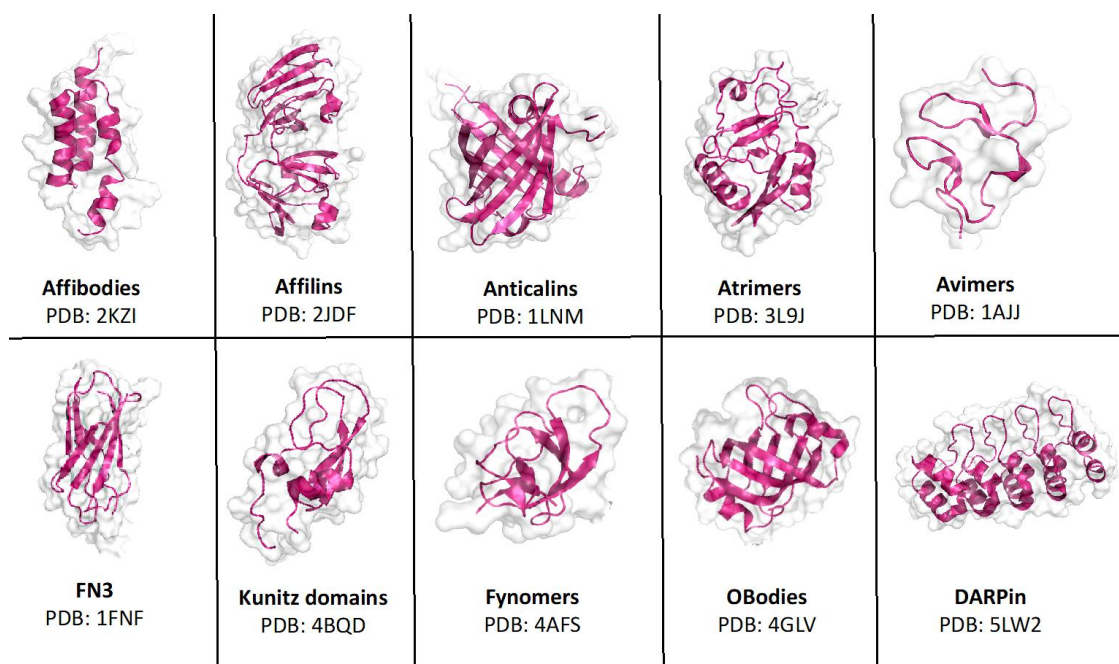
engineering into binding tool is based on the molecular structure of the antibody. The conventional structure of an antibody is a well-conserved rigid scaffold on which highly variable loops are situated. Likewise, binding proteins can be isolated from large libraries of protein variants with a constant scaffold and randomised variable regions that can interact with various target molecules. The recently developed binding proteins have potentials as affinity tools in many molecular recognition applications and as therapeutic agents for the treatment of diseases and cancers (Vazquez-Lombardi et al., 2015).

1.4.3.1 The diversity of the non-antibody-based protein scaffolds

Protein scaffolds represent an extremely diverse group of binding molecules that differ in their size, origin, engineering strategy, mode of interaction, structural topology and applicability (Skerra, 2000). An engineered binding protein against the cyclin-dependent protein kinase 2 (CDK-2) using a modified *E. coli* enzyme, known as thioredoxin (TrxA), was the first non-antibody based scaffold introduced by Roger Brent's group in 1996 (Colas et al., 1996). Since then, over 50 new alternative protein scaffolds have been reported as potential affinity reagents. The X-ray crystal structure as well as some main features of some successfully used protein scaffolds are illustrated in figure 1.10 (Vazquez-Lombardi et al., 2015). In addition to the different developed non-antibody scaffolds, Affimers has been recently developed and successfully applied as a potential theranostic tool (Tiede et al., 2014; Tiede et al., 2017).

Affimers are a class of non-antibody protein scaffold derived from cystatins. Cystatins are a large family of cysteine protease inhibitors that share sequence homology and common tertiary structure comprising of a single α -helix and anti-parallel β -sheet (Hall et al., 1995). There are two Affimer types derived from different proteins (figure 1.11) (Kyle, 2018). A plant-derived consensus cystatin sequence known as Affimer type II, initially known as Adhiron (Tiede et al., 2014), and one based on a human cystatin stefin A (SteA) (Woodman et al., 2005).

The plant derived-cystatin (phytocystatin) is a monomeric, single domain protein consisting of approximately ninety-nine amino acid units, lacking disulfide bond and glycosylation sites (Tiede et al., 2014). The inhibitory sequences within the two (Gln Val Val Ala Gly and Pro Trp Glu) variable loops of the consensus phytocystatin framework



Scaffold	Parental protein	Structure	Randomisation	MW (kDa)
Affibodies	Z domain (A protein)	Alpha-helical	Helix randomisation	6
Affilins	Gamma-beta-crystallin Ubiquitin	Beta-sheet Alpha/beta	Beta-strand randomisation Beta-strand randomisation	20 10
Anticalins	Lipocalin	Beta-sheet and Alpha-helical terminus	Loop randomisation Beta-strand randomisation	20
Atrimers	C-type lectin (tetralectin)	Alpha/beta	Loop randomisation	3x20
Avimers	A-domain	Ca ²⁺ binding disulphide constrained	Loop randomisation	4
FN3	Fibronectin (type III)	Beta-sheet	Loop randomisation Beta-strand randomisation	10
Kunitz domains	Serine protease inhibitor	Alpha/beta Disulphide constrained	Loop randomisation	7
Fynomers	SH3 domain (fyn kinase)	Beta-sheet	Loop randomisation	7
OBodies	OB-fold	Beta-sheet	Loop randomisation	12
DARPin	Ankyrin repeats	Alpha-helical and beta-turn	Helix randomisation Beta-turn randomisation	14-21

Figure 1.10 Structural features of some newly developed non-antibody-based scaffolds. The three dimensional structures are visualised by PyMol software, while all data provided in the table are mentioned elsewhere (Ruigrok et al., 2011).

has been replaced with nine randomised amino acids in each loop. After constructing the Affimer library as described previously (Tiede et al., 2014), specific binding Affimers are selected against different target molecules using phage display technology (Smith, 1985). Affimers are small, versatile, and stable in a broad range of both temperatures and pHs.

Affimers are produced in bacterial cells using standard conventional culturing equipment (Tiede et al., 2017). They are conformational proteins and thus their applicability is highly dependent on the conformation of their target molecule, which may limit their use in certain assays where a linear protein is need to be detected, such as the case in western blotting analysis.

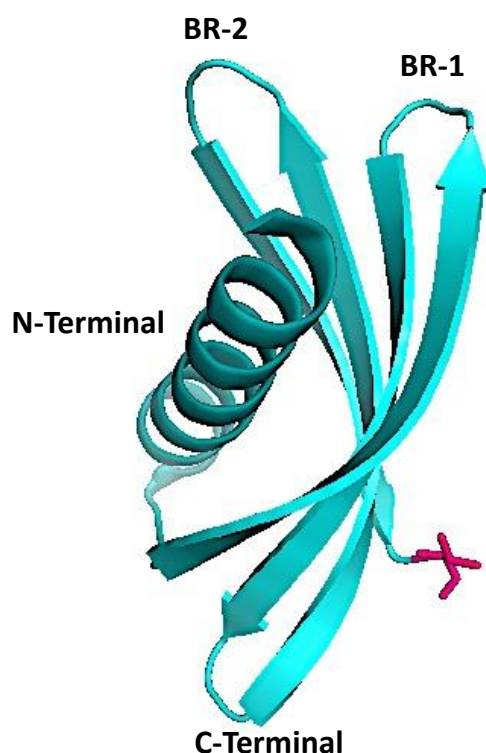


Figure 1.11 Three-dimensional structure of the Affimer scaffold. The Affimer structure was obtained from the Protein Data Bank (PDB) (ID: 4N6T) and constructed with PyMol software. The single alpha helix and the four anti-parallel β strands are shown in turquoise. The two binding loops (labelled as BR-1 and BR-2) where the randomisation occurs (peptide insertion of nine amino acids) produces the library, as described previously by Tiede (Tiede et al., 2014). The pink arm represents the site where a single cysteine residue can be inserted to enable site-specific labelling.

To generate this plant-derived consensus phytocystatin sequence, Tiede and co-workers (2014) established a construct from which the Affimer scaffold could be derived (Tiede et al., 2014). The structure of plant-based Affimer scaffold resembles that of a previously developed scaffold based on stefin A (Stadler et al., 2011;Woodman et al., 2005;Johnson et al., 2012), and both scaffolds are termed Affimers. Since the discovery of Affimers, their applicability in research has evolved at an incredible pace (Kyle et al., 2015;Kyle, 2018;Tiede et al., 2017;Robinson et al., 2018;Xie et al., 2017;Zhurauski et al., 2018). Several studies confirmed a successful utilisation of Affimers as equivalent detection alternatives for antibodies in IHC (anti-VEGFR2 and anti-TN-C Affimer reagents) and IF microscopy (anti-actin, anti-TRPV1, and anti-HER4 Affimer reagents) (Lopata et al., 2018;Tiede et al., 2017).

In cancer diagnostics, recent study has demonstrated the use of Affimers as captured reagents for the Glypican-3 (GPC3), which is a promising marker for hepatocellular carcinoma (Xie et al., 2017). Xie et al (2017) have developed a sandwich chemiluminescence immunoassay (CLIA) combining an anti-GPC3 Affimer with a monoclonal antibody to detect the presence of the protein in undiluted serum. Their study indicates that Affimers can be used to generate immunodetection kits for the use in in both research and clinics to enable the detection of biomarkers with high specificity and sensitivity, showing a detection range of detection rate of 0.03-600 ng/ml. In addition, Affimer reagents showed to be powerful detection reagents for recognising HER4 biomarker in undiluted serum samples using a novel Affimer-functionalised biosensor (Zhurauski et al., 2018). In recent future, Affimer-based biosensors against a range of potential serological biomarker can be developed and adapt in clinics.

In addition to the role of Affimer reagents in diagnostics, Affimer reagents also showed a promising potential as therapeutic agents by modulating the function of different protein, including a pain related biomarker (TRPV1) (Tiede et al., 2017) and IgG binding to the Fc gamma receptors (Robinson et al., 2018).

1.4.3.2 Generation of non-antibody binding proteins

A critical factor for successful design and engineering of a binding protein is the ability to produce large number of mutated derivatives. The well-known powerful high-throughput technology to fulfil the need for such production of variants is the molecular display, which combines the construction of large (poly) peptides libraries and a

following isolation for variant with desired biological and physiochemical features (Smith, 1985;Smith and Scott, 1993). Display technologies are based on a physical connection between a protein and its encoding gene, thus coupling phenotype and genotype. Although the most commonly applied display technology is the phage display (Paschke, 2006), other different display technologies including mRNA display (Josephson et al., 2014), ribosome display (Hanes et al., 1998;Zahnd et al., 2007), bacterial and yeast-cell surface display (Daugherty, 2007;Gai and Wittrup, 2007), have also been successfully used. This chapter, otherwise, will focus on describing phage display for the isolation of engineered non-antibody based binding proteins.

In phage display technology nucleotide sequences encoding variants of antibodies, peptides, or proteins are fused to a gene, which encodes phage coat protein. Following correct assembly, phage particles display the encoded (poly)peptide on their surface (Paschke, 2006). For library construction, the chosen vectors to use is based on the filamentous phage fd, M13, lytic phage γ and T7 phage (Sidhu, 2001;Pande et al., 2010). Most of non-IgG scaffolds are developed from M13 filamentous phage, such as the case for Affimer development. Filamentous phage particles are rod-shaped viruses (900 nm in length) enclosing a circular single-stranded DNA molecule (ssDNA) inside a cylindrical protein coat. The coat of proteins comprises of about 2700 copies of a major coat protein and other five copies of different minor coat proteins (figure 1.12). To construct a phage library, coat protein gene, commonly the pIII and pVIII gene, is modified and fused to the DNA sequence of the protein scaffold. This fusion is now known as a phagemid vector (Huse et al., 1992). *E. coli* cells are transformed with the phagemids and then infected with a helper phage to create the desired library of phage particles displaying the variant proteins (figure 1.13).

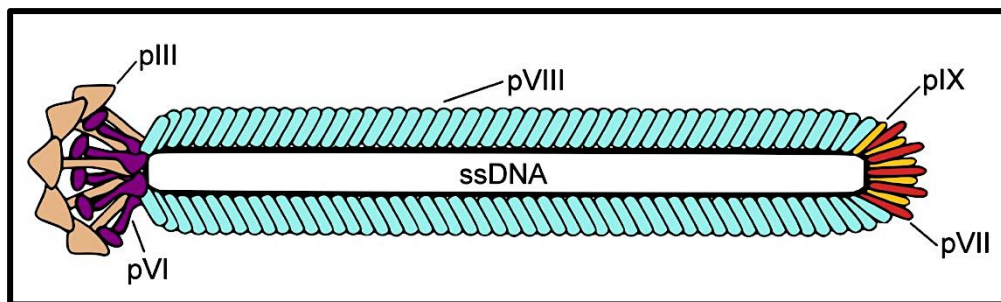


Figure 1.12 Schematic presentation of an M13 filamentous phage. The ssDNA is enclosed by a cylindrical coat of 2700 copies of the major coat protein pVIII. Other minor coat proteins include pIII, pVI and pIX found at low copy numbers of 5 copies per protein. Among all coat proteins, pIII and pVIII are the most commonly used for display purpose. In Affimer technology, pIII protein is the one used for Affimer-phage display. Adopted from (Loset et al., 2011).

The of phage displaying variant protein library is exposed to an immobilised non-target (negative selection) and target molecule (positive selection) (Finlay et al., 2017). As most protein binding scaffolds are conformational dependent, researchers have developed different selection strategies using tissue samples, and whole cells to generate reagents able to recognize the native structure of their target molecules. (Shukla and Krag, 2005;Sorensen et al., 2013;Sun et al., 2009) Following positive selection, both non-specific and non-binding phage are washed off, while the bound ones are eluted through different conditions, such as acidic buffers, which disrupt the interaction between the displayed protein and the target molecule. The eluted, binding phage are used to re-infect the *E.coli* cells to generate a highly-enriched library comprising an amplified population of binding phage. Selection, washing, elution and amplification steps are repeated for multiple rounds in process known as bio-panning (Bakhshinejad et al., 2016;Crepin et al., 2017;Lakzaei et al., 2018). Bio-panning results in enrichment of phage variants with increased specificity and affinity towards the target. After several rounds (normally between three to five), the output of isolated phage clones is screened by ELISA and identified by DNA sequencing analysis.

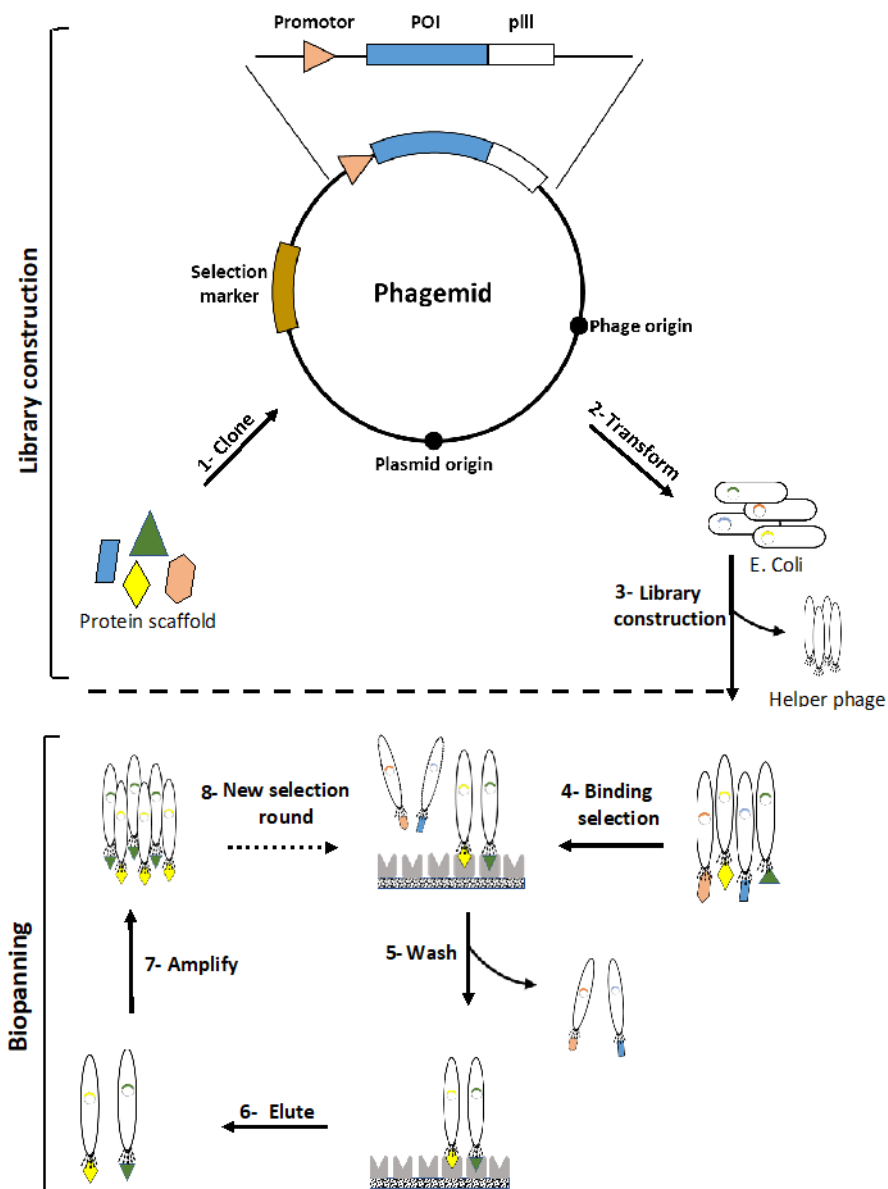


Figure 1.13 Phage display technology. Most non-antibody-based protein scaffolds, including Affimers are generated by bacterial phage display. Prior to the start of the phage screening process, a library of variants must be constructed. To create the library, bacterial cells are transformed with a phagemid vector, which carries the phage gene fused to the protein scaffold. After constructing the library, a bio-panning process is performed. The process starts with selecting the library on a target molecule that can be immobilised on solid surface or presented on cells or tissue sections. The unbound phage is then washed while the bound ones are eluted and amplified in bacterial cells with the aid of helper phage. The whole process of selection and amplification is repeated for several rounds to ensure for the enrichment of target specific binding phage.

1.4.3.3 Are some scaffolds better than others?

Selection of the appropriate scaffold to be engineered into a binding tool is based on the molecular structure of the antibody (Skerra, 2000;Skrllec et al., 2015). Antibodies conventionally take up a structure of a well-conserved rigid scaffold on which highly variable loops are situated. Likewise, binding proteins can be isolated from large libraries of protein variants which contain constant scaffolds and randomised variable regions that can interact with various target molecules. Recently developed binding proteins show potential as binding tools in many molecular-recognition applications and as therapeutic agents for the treatment of diseases and cancers (Vazquez-Lombardi et al., 2015).

High-affinity interactions require complementarity of shape and chemistry. This complementarity is accomplished by diverse secondary and tertiary structural elements in natural protein-protein interactions (Gilbreth et al., 2008). For example, DARPins recognise convex surfaces in their targets that are complementary to their concave binding sites; anticalins, which have a basket-like structure, cradle their target (Skerra, 2007). Furthermore, affibodies that contain flat binding sites recognise similarly flat surfaces in their targets. Scaffolds that contain loops, such as FN3 and nanobodies, exhibit more than one distinct binding mode, and this explains their ability to interact with cleft and convex epitopes (Skerra, 2007). Taken together, these data indicate that the topography of a scaffold binding site is closely related to the shape of epitopes that they recognise with high affinity.

The percentage of diversified positions that are in contact with the target molecule is another measure that indicates the suitability of the structure and therefore the success of the library design (Gilbreth et al., 2008;Koide et al., 2007). Among the structurally characterised scaffolds that interact with their targets in an antibody-like mode (using diversified loops as binding sites), Affimer/target complexes in which the target is human SUMO most closely match their library design. They exhibit an average of 70 per cent of diversified positions (nine randomised positions in the two binding loops) that are in contact with the target (Hughes et al., 2017). Similarly to Affimers, the fibronectin type III scaffold binds to its target via three diversified loops; however, only 51 per cent of its diversified positions have been shown to be involved in the binding interaction with the target molecule (Koide et al., 2012).

Therefore, it has been assumed that an increase in the diversification area would result in better interaction with target molecules and stronger binding affinity. This assumption

has been shown to be true. For instance, research found that if seven residues in each n-repeat of the DARPin scaffold (66 residues/n x 33) were randomised (Skrlec et al., 2015), an average of 75 per cent of the diversified sites were in direct contact with the target (Binz et al., 2004), while 90 per cent of the diversified region (13 residues in two helices) of the affibody scaffold were shown to be involved in target interaction (Hoyer et al., 2008; Wahlberg et al., 2003). However, one study showed that affibodies sometimes exert unexpected modes of interaction with a target, as in the case of the A β (1-40) peptide in which an altered structure to a β -sheet conformation was observed (Hoyer et al., 2008). Some affibodies are either partially or completely in-structured in the unbound state, which casts doubt on the integrity of the scaffold (Wahlberg et al., 2003). These data obtained from Affimer, FN3, DARPin and affibody systems highlight the value of structural analyses in the guidance of the development of new and improved library designs.

The success of all these developed platforms in the generation of binders that show high affinity to different targets therefore depends on several factors: the scaffold architecture, the sequence of the diverse amino acid sequences and the extent of the diversification that can be introduced without compromising the overall structure and stability.

1.4.3.4 Current status of antibody alternatives in disease diagnosis and treatment

Antibody alternatives were developed to overcome the inherent problems found with antibodies, including their large size, irreproducibility, high production cost and difficulties in modification and engineering. Today, various binding alternatives have been developed or are under development. Several literature reviews have highlighted the progress that has been made through the use of these novel agents in cancer diagnosis and therapy (Ruigrok et al., 2011; Skerra, 2007; Yu et al., 2017; Bedford et al., 2017). The reviews show that the intended benefits of such binding reagents compared with antibodies have been realised, and they offer tools with improved molecular recognition qualities for research and clinical use.

However, like antibodies, the developed binding alternatives demonstrate certain problems that need further improvement in order for their clinical implementation to become feasible. These problems are summarised and compared in Table 1.5, which

illustrates the advantages and disadvantages of utilising antibodies, aptamers, nanobodies and Affimers as binding tools in different molecular applications.

1.5 Research aims and objectives

Detection of cancer cells and analysing their surface markers provide crucial information for the diagnosis and treatment of cancers. Immunohistochemistry (IHC) is an example of a widely used assay in routine diagnostics that detects the expression level of different tumour related markers. However, using IHC for biomarker assessments can be challenging because of the lack of reproducibility. This project aims to isolate and characterise Affimers against EGFR, HER2 and HER3, in order to be used as detection reagents in IHC-like applications. In addition to biomarker detection, this project also explores the possibility of using Affimer-based phage display technology to identify new cancer specific biomarker.

Table 1.4 Examples of protein-display scaffolds, and their similarities and differences in relation to display strategy, pharmacokinetic properties and binding kinetics.

Scaffold	Display strategy	Expression	Half-life <i>in vivo</i>	Examples of binding affinity (K_d) to targets	Clinical trial phase	References
Affimers	Phage display	<i>E.coli</i> 10-100 mg/l	NA	17 nM to VEGFR2 2.8 nM to TN-C	NA	(Tiede et al., 2014;Tiede et al., 2017)
Affibodies	Phage display Ribosome display	<i>E.coli</i> 1-6 mg/l (Fc-fusion)	4-14 minutes (non-modified)	50 nM to ECD-HER2	Phase I (completed)	(Ronmark et al., 2002;Wikman et al., 2004;Baum et al., 2010)
Afflins	Phage display	<i>E.coli</i> 100 mg/l	20-56 hours (Fc-fused)	14 nm to extra-domain-B of fibronectin	Phase I (completed)	(Lorey et al., 2014;Hoffmann et al., 2012;Ebersbach et al., 2007)
Anticalins	Phage display	<i>E.coli</i> 2-20 mg/l	6 days (PEGylated)	1 nM to fluorescein*	Phase I (completed)	(Vopel et al., 2005;Eggenstein et al., 2014;Schlehuber and Skerra, 2002;Mross et al., 2013)
FN3/Adnectins	Phage display Yeast display mRNA display	<i>E.coli</i> 20-40 mg/l	53 hours (PEGylated)	2 nM to human EphA2 receptor	Phase II (completed)	(Park et al., 2015;Getmanova et al., 2006;Tolcher et al., 2011)
Kunitz domain	Phage display	<i>Pichia pastoris</i>	2 hours	11 pM to plasma kallikrein	Phase I	(Markland et al., 1996a;Markland et al., 1996b;Schneider et al., 2007;Simeon and Chen, 2018)
Avimers	Phage display	<i>E.coli</i> 1.4 g/l by fermentation	30 hours (Fc-fused)	5 nM to IL-6	Phase I	(Silverman et al., 2005;Braddock, 2007)
Fynomers	Phage display DNA display	<i>E.coli</i> 24-78 mg/l CHO 3.5-20.7 mg/l	68 hours in mice (Fc-fused)	0.9 nM to SH3 domain	Phase II (terminated)	(Silacci et al., 2014;Schlatter et al., 2012)

Table 1.4 Continued.

Scaffold	Display strategy	Expression	Half-life <i>in vivo</i>	Examples of binding affinity (K_d) to targets	Clinical trial phase	References
OBodies	Phage display	100-200 mg/l	NA	3 nM to hen egg-white lysozyme	NA	(Steemson et al., 2014)
DARPin	Ribosome display Phage display	<i>E.coli</i> 200 mg/l and 15 g/l (with fermentation)	More than 13 days (PEGylated) 3 minutes in mice (non-PEGylated)	4.4-22 nM to maltose binding protein	Phase III (completed)	(Binz et al., 2004; Binz et al., 2003; Campochiaro et al., 2013)
Atrimer	Phage display	<i>E.coli</i>	24 hours (parental protein)	90 pM to TNF	NA	(Byla et al., 2010; Weidle et al., 2013; Nielsen et al., 1997)
Nanobodies	Phage display mRNA display ribosome display	<i>E.coli</i> up to 10 mg/l	Few hours	1.5 nM to HER2	Phase I	(Bobkov et al., 2018; Van Audenhove and Gettemans, 2016; Siontorou, 2013)

Abbreviations: NA, not available; CHO, Chinese hamster ovary cells; TNF, tumour necrosis factor; *E.coli*, *Escherichia coli*; HER2, human epidermal growth receptor 2; IL-6, Interleuki

Table 1.5 Summary of the advantages and limitations of Affimers and other antibody alternatives in comparison with those of antibodies and aptamers.

		Detection of biomarkers	Molecular imaging	Study of intracellular protein function	Biomarker targeting and drug discovery
Advantages	Affimers/other alternative binding scaffolds	<ul style="list-style-type: none"> • High stability • Easy to conjugate with biotin and Fc-fragments • Suitable in applications such as: ELISA, pull-down, IHC, IF, super-resolution microscopy • Small size enables chip format Display technology can generate target to almost every molecule Synthesis is easy, fast and reliable 	<ul style="list-style-type: none"> • Rapid and homogeneous tumour accumulation • Easy conjugation • Rapid clearance rate 	<ul style="list-style-type: none"> • Small size • Intracellular stability/activity • Domain/function-specific modulation • Easy to fuse to chromogens 	<ul style="list-style-type: none"> • Suited for conjugation • Rapid tumour accumulation • Excellent binding affinity and inhibitory functions
	Antibodies	<ul style="list-style-type: none"> • Sub-nanomolar binding affinity • Suitable in applications such as: ELISA, western blot, FACS, IHC, IF • Easy immobilisation through adsorption 	<ul style="list-style-type: none"> • Sub-nanomolar binding affinity and target specificity 	<p>Their applicability in intracellular studies is limited: see disadvantages</p>	<ul style="list-style-type: none"> • Non-immunogenic (humanised) • Employ a contained Fc domain • Efficient binding affinity
	Aptamers	<ul style="list-style-type: none"> • SELEX can generate binders to almost every molecule • Synthesis is easy, fast and reliable • Bacterial and viral contamination is not problematic • Applied in IHC, ELISA, biosensors and IF 	<ul style="list-style-type: none"> • Suited to different modifications and labelling • Sub-nanomolar to picomolar binding affinities 	<ul style="list-style-type: none"> • Suitable for different labelling • High inhibitor function • Uniform activity regardless of batch • Target identification by shape, not by base-pairing • Binding target with the entire sequence 	<ul style="list-style-type: none"> • Non-immunogenic • Easily engineered to create multi-specific constructs • Efficient binding affinity

Table 1.5 Continued.

		Detection of biomarkers	Molecular imaging	Study of intracellular protein function	Biomarker targeting and drug discovery
Disadvantages	Affimers/other alternative binding scaffolds	<ul style="list-style-type: none"> • Increased performance, affinity and detection sensitivity are required • Aggregation due to cysteine incorporation • Conformational-binding dependent • Application dependent (no universal reagents for different applications) • Affected by frequent freeze and thaw cycles • Bacterial and viral contamination can be a problem • Cross-reactivity based on the display approach 	<ul style="list-style-type: none"> • Accumulation in liver • Enhanced signal detection required 	<ul style="list-style-type: none"> • Target specificity is affected by commercialised source of the protein used in the phage screen 	<ul style="list-style-type: none"> • Fast blood clearance • Lack of Fc • Immunogenicity • May need affinity maturation

Table 1.5 Continued.

		Detection of biomarkers	Molecular imaging	Study of intracellular protein function	Biomarker targeting and drug discovery
Disadvantages	Antibodies	<ul style="list-style-type: none"> • Irreproducibility • High-production cost • Instability for use in biosensors • Application dependent (no single Ab for different applications) • Difficult to modify • Affected by freeze and thaw cycles • Difficult to obtain against small, toxic and immunogenic molecules • Bacterial and viral contamination can be a problem • Tend to aggregate • Not stable at high temperatures and in a broad range of pH • Cross-reactive (pAb) 	<ul style="list-style-type: none"> • Low clearance rate • Cytotoxic • High-background level • Non-homogeneous distribution 	<ul style="list-style-type: none"> • Cannot tolerate the reducing environment of the cytoplasm • Require membrane penetration which is not possible due to their large size 	<ul style="list-style-type: none"> • High production cost • Toxic side effects
	Aptamers	<ul style="list-style-type: none"> • Tend to aggregate • Degraded by nuclease contamination • Not stable at broad pH • Complicated immobilisation • Cross-reactivity 	<ul style="list-style-type: none"> • Highly susceptible to serum degradation • Cross-reactivity • Binding affinity is susceptible to environment 	<ul style="list-style-type: none"> • Not stable at wide range of pH 	<ul style="list-style-type: none"> • Limited systematic delivery • High toxicity • Poorly understood pharmacokinetics • High-cost production in large scale • Short half-life

Abbreviations: pAb, polyclonal antibody; IHC, Immunohistochemistry; IF, Immunofluorescence; ELISA, Enzyme-linked immunosorbent assay; FACS, Fluorescence activated cell sorting assay. Data summarised in the table were obtained from various sources: (Tiede et al., 2017;Tiede et al., 2014;Bedford et al., 2017;Ruigrok et al., 2011;Skerra, 2007;Siontorou, 2013;Steeland et al., 2016;Van Audenhove and Gettemans, 2016;Hong et al., 2011;Chames et al., 2009;Lakhin et al., 2013)

CHAPTER 2

Materials and Methods

2.1 Materials

2.1.1 General reagents

Recombinant proteins used in the phage display screen (HER2-Fc tag, HER2, and HER3) were purchased from Sino Biological, UK, while all other reagents used in cell culturing, molecular cloning, Affimer production and characterisation, were purchased from Sigma (Gibco[®], UK), New England Biotechnologies (NEB, UK), and ThermoFisher Scientific, UK, respectively unless stated otherwise. Medias and in-house made buffers were prepared using sterile H₂O and were subjected to autoclaving before their use in the procedures. Primary and secondary affinity binding reagents were used as described in table 2.1, 2.2 and 2.3.

2.1.2 Mammalian cell lines and their characteristics

Different cell lines were a kind gift from Dr. Sandra Bell at the Leeds Institute of Biomedical and Clinical Sciences (LIBAC, Leeds, UK). A list of all the cell lines, their growth conditions, and properties are listed in table 2.4. The frozen cells recovered from a vial were passaged no more than twenty times (i.e., when the vial of frozen cells was given at say passage number twenty, it was used till it reached the passage number thirty-nine. Thereafter, a new vial was taken and the subsequent stocks were made. According to the Short tandem repeats (STR) profiling results provided by Dr. Sarah Perry at LIBAC, UK., all given cell lines had been tested for mycoplasma infection, and they were confirmed to be mycoplasma-free. According to the policy at LIBAC, cell lines were subjected to mycoplasma testing at intervals of three months.

2.1.3 Whole Tissue samples and Tissue microarrays (TMAs)

All the archival tissue blocks (normal breast tissues, cancerous breast tissues, and placenta tissue) and some breast TMAs were kindly provided, processed and sectioned by Professor Speirs and other groups in LIBAC in pursuance of their collaborative values.

Target	Origin	Clonality (ID)	Type	Conc. ($\mu\text{g/ml}$)	Time	App.	Source
VEGFR2	Rabbit	Monoclonal (55B11)	Un	1 $\mu\text{g/ml}$	1hr/ RT	IHC	Cell Signalling
fd- phage	Sheep	Monoclonal A-02-01	HRP	0.5 $\mu\text{g/ml}$	1hr/ RT	ELISA	Seramun Diagnostic
			Un	5 $\mu\text{g/ml}$		IF	
His-tag	Mouse	Monoclonal (ab18184)	Un	1 $\mu\text{g/ml}$	1hr/ RT	IF	Abcam
	Rabbit	Polyclonal (ab1187)	HRP	0.14 $\mu\text{g/ml}$		WB	
HER2	Rabbit	Polyclonal (A0485)	Un	0.1 $\mu\text{g/ml}$ 0.2 $\mu\text{g/ml}$ 1 $\mu\text{g/ml}$	1hr/ RT ON/4°C ON/4°C	IHC WB IF	DAKO
HER3	Rabbit	Monoclonal (ab32121)	Un	0.56 $\mu\text{g/ml}$ 3.4 $\mu\text{g/ml}$	ON/4°C ON/4°C	WB IF	Abcam
EGFR	Rabbit	Monoclonal (ab52894)	Un	0.02 $\mu\text{g/ml}$ 0.2 $\mu\text{g/ml}$	ON/4°C ON/4°C	WB IF	Abcam
Phospho-ERK1/2 (T202/Y204)	Mouse	Monoclonal (E10)	Un	0.5 $\mu\text{g/ml}$	ON/4°C	WB	Cell Signalling
Beta-Actin	Mouse	Monoclonal (8H10D10)	Un	1 $\mu\text{g/ml}$	ON/4°C	WB	Cell Signalling
Alpha-tubulin	Rat	Monoclonal (Sc-53029)	Un	0.06 $\mu\text{g/ml}$ 0.4 $\mu\text{g/ml}$	ON/4°C	WB IF	Santa Cruz Biotechnol-ogy
CK18	Mouse	Monoclonal (C8541)	Un	0.05 $\mu\text{g/ml}$	1hr/ RT	IHC	Sigma
				2 $\mu\text{g/ml}$	ON/4°C	IF	
				0.2 $\mu\text{g/ml}$	1hr/ RT	WB	
CK19	Mouse	Monoclonal (Clone-LP2K)	Un	10 $\mu\text{g/ml}$	ON/4°C	IHC IF	Central Resources (CRUK)
CK19	Rabbit	Monoclonal (ab52625)	Un	0.08 $\mu\text{g/ml}$	1hr/ RT	IHC	Abcam
				1.6 $\mu\text{g/ml}$	ON/4°C	IF	
				0.08 $\mu\text{g/ml}$	ON/4°C	WB	

Table 2.1 Primary antibodies. Details of origin, clonality, associated-conjugate, concentration, incubation, used application and source. App; Application, IHC; Immunohistochemistry, WB; western blot analysis, IF; immunofluorescence, RT; Room temperature, ON; Overnight, hr; hour, Un; unconjugated, HRP; Horseradish peroxidase.

Target	Origin	Clonality (ID)	Conjugate	Conc. ($\mu\text{g/ml}$)	Time	App.	Source
Rabbit IgG	Goat	Polyclonal (E0432)	Biotin	5 $\mu\text{g/ml}$	1hr/ RT	IHC	Dako
Sheep IgG	Rabbit	Polyclonal SA5-10054	DyLight488	1 $\mu\text{g/ml}$	1 hr/ RT	IF	Thermo-Scientific
Biotin	Strept-avidin	21130	HRP	0.5 $\mu\text{g/ml}$	1hr/ RT	ELISA	Thermo Scientific
Biotin	Strept-avidin	SA-5004	HRP	3.3 $\mu\text{g/ml}$	30min/RT	IHC	Vector Lab
Rabbit IgG	Goat	Polyclonal (ab97051)	HRP	1 $\mu\text{g/ml}$	1hr/ RT	WB	Abcam
Mouse IgG	Goat	Polyclonal (ab97025)	HRP	1 $\mu\text{g/ml}$	1hr/ RT	WB	Abcam
Rat IgG	Goat	Polyclonal (ab97057)	HRP	0.1 $\mu\text{g/ml}$	1hr/ RT	WB	Abcam
Mouse IgG	Goat	Polyclonal (A11032)	Alexa594	2 $\mu\text{g/ml}$	ON/4°C	IF	Invitrogen
		Polyclonal (A28175)	Alexa488				
Rabbit IgG	Goat	Polyclonal (A11008)	Alexa488	2 $\mu\text{g/ml}$	ON/4°C	IF	Invitrogen
		Polyclonal (R37117)	Alexa594				

Table 2.2 Secondary antibodies. Details of origin, clonality, associated-conjugate, concentration, incubation, used application and source. App; Application, IHC; Immunohistochemistry, WB; western blot analysis, IF; immunofluorescence, RT; Room temperature, ON; Overnight, hr; hour, min; minutes, HRP; Horseradish peroxidase.

Target	Conjugate	Dilution (Concentration)	Incubation	Application
VEGFR2	Biotin	1:25 (11 µg/ml)	1hr/ RT	IHC
	AP-fusion	1:2 (25 µg/ml)	2hrs/RT	IHC
	Unconjugated	1:10 (25 µg/ml)	ON/4°C	IF-Fixed cells
	Unconjugated	1:10 (25 µg/ml)	1hr/ 37°C	IF-live cells
	Mouse-Fc-fusion	1:200 (2.5 µg/ml)	1hr/ RT	IHC
	Rabbit-Fc-fusion	1:100 (5 µg/ml)	1hr/ RT	IHC
HER2	Unconjugated	1:10 (25 µg/ml)	ON/4°C	IF-Fixed cells
		1:10 (25 µg/ml)	1hr/ 37°C	IF-live cells
		1:2 (320 µg/ml)	ON/4°C	Pull-down
HER3	Unconjugated	1:10 (25 µg/ml)	ON/4°C	IF-Fixed cells
		1:10 (25 µg/ml)	1hr/ 37°C	IF-live cells
		1:2 (320 µg/ml)	ON/4°C	Pull-down
	Biotin	1:5 (50 µg/ml)	2hrs/RT	IHC
EGFR/HER1	Unconjugated	1:10 (25 µg/ml)	ON/4°C	IF-Fixed cells
		1:10 (25 µg/ml)	1hr/ 37°C	IF-live cells
		1:2 (320 µg/ml)	ON/4°C	Pull-down
CK19/18	Unconjugated	1:16 (15 µg/ml)	ON/4°C	IF-Fixed cells
		1:10 (25 µg/ml)	1hr/ 37°C	IF-live cells
		1:2 (320 µg/ml)	ON/4°C	Pull-down
	Biotin	1:25 (10 µg/ml)	2hrs/RT	IHC

Table 2.3 Affimer reagents. Details of associated-conjugate, concentration, dilution, incubation, and used application. IHC; Immunohistochemistry, IF; immunofluorescence, RT; Room temperature, ON; Overnight, hr; hour. All Affimers were identified by the Bioscreening Technology Group at the University of Leeds.

Regarding placenta tissue, three different placenta control-tissue blocks were used in this research. These control blocks were ethics-exempt anonymised, unidentifiable research gift tissue (lateral intercostal artery perforator, or LICAP) from the Department of Pathology and Tumour Biology, where the IHC work was performed. All normal breast tissue (from contralateral breast, reduction mammoplasty and risk-reducing surgery) and cancerous breast tissue was provided by Professor Valeri Speirs of the Leeds Breast Cancer Tissue Bank, BCNTB. These tissues were donated under the BCNTB authorisation code of 15/YH/0025. Other used breast tissue microarrays (TMAs) were purchased from USBiomax (BR243w, BR20819, BC081120). Characteristics of all the purchased TMAs are listed in table 2.5.

2.2 Methods

The university health and safety policy was adhered to while performing all the laboratory procedures. The Standard Operating Protocol (SOP) for each of the employed techniques was followed, and Personal Protective Equipment (PPE) was worn while handling

chemicals. Also, all the necessary COSHH (Control of Substances Hazardous to Health) forms were filed before beginning the procedures.

2.2.1 Mammalian Cell Culturing

2.2.1.1 Cell culture

Culturing of cells was carried out in a Class 2 laminar flow cabinet as was specified for secondary cell culturing. All contaminated fluid waste was decontaminated with 2% w/v Virkon (RELY+ON™ Virkon disinfectant, RMSupply™) prepared in ddH₂O.

Cell line	Tissue	Disease	Growth condition
MDA-MB-453	Mammary gland/breast; derived from metastatic site: pericardial effusion	Metastatic carcinoma	DMEM,10%FBS, 100U/ml P/S
MDA-MB-231	Mammary gland/breast; derived from metastatic site: pleural effusion	Adenocarcinoma	RPMI,10%FBS, 100U/ml P/S
MDA-MB-468	Mammary gland/breast; derived from metastatic site: pleural effusion	Adenocarcinoma	DMEM,10%FBS, 100U/ml P/S
MCF7	Mammary gland/breast; derived from metastatic site: pleural effusion	Adenocarcinoma	RPMI,10%FBS, 100U/ml P/S
BT474	Mammary gland; breast/duct	Ductal carcinoma	DMEM,10%FBS, 100U/ml P/S
HB2	Derivative from parental cell line (MTSV1-7); mammary luminal epithelial cell line	Non-tumorigenic, Immortalized	DMEM,10%FBS, 100U/ml P/S
HER2-HB2 transfected	Derivative from parental cell line (MTSV1-7); mammary luminal epithelial cell line; transfected with HER2	Tumorigenic	DMEM,10%FBS, 100U/ml P/S
U87	Brain	Glioblastoma	DMEM,10%FBS, 100U/ml P/S

Table 2.4 Mammalian cell lines characteristics and growth conditions. FBS; Foetal bovine serum, P/S; penicillin/streptomycin antibiotics, DMEM; Dulbecco's Modified Eagle Medium, RPMI 1640; Roswell Park Memorial Institute 1640 medium.

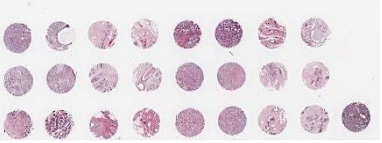
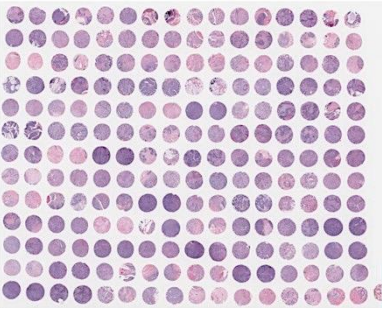
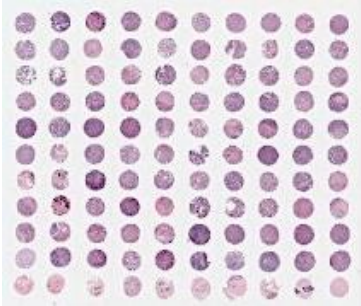
TMA	Cases	Cores	TNM Stage	IHC (ER, PR, HER2)	H&E image
BR243w	6	24 (quadruple core per case)	Available	Available	 <ul style="list-style-type: none"> • 6 breast invasive ductal carcinoma • 6 matched adjacent normal breast tissue
BR20819	104	208 (duplicated core per case)	Available	Available	 <ul style="list-style-type: none"> • 95 invasive ductal carcinoma • 1 mucinous carcinoma • 3 medullary carcinoma • 3 invasive lobular carcinoma • 1 lobular carcinoma in situ • 1 glycogen-rich clear cell carcinoma
BC081120	110	110 (single core per case)	Available	Not Available	 <ul style="list-style-type: none"> • 100 cases invasive ductal carcinoma • 10 adjacent normal tissue

Table 2.5 Purchased tissue microarrays (TMAs). Number of cases, cores per case, availability of clinic-pathological data (IHC marker and TNM staging) in addition to cancer subtypes. Images of the TMAs sections were obtained from the website of USBiomax from where these TMAs were purchased. H&E; Haematoxylin and eosin stain, TNM; (T; tumour site, N; lymph nodes involved, M: metastasis). IHC; immunohistochemistry, ER; Oestrogen receptor, PR; Progesterone receptor, HER2; Human epidermal growth factor 2 receptor.

All solid waste was autoclaved prior to discarding. Cells were routinely grown at 37°C in humidified air incubators containing 5% CO₂. Incubators were maintained, cleaned and checked for contamination in a regular basis.

2.2.1.2 Cell recovery, feeding, and passaging

Frozen vials of cells were taken out from LN2 storage facility and thawed in water bath at 37°C for one min. Cells were then diluted in 10 ml of media and pelleted by centrifugation at 200xg for five minutes. The supernatant was discarded, and the pelleted cells were resuspended in 5 ml of media supplemented with 10% foetal-bovine serum (FBS) and 100U/ml of penicillin/streptomycin antibiotics (Life Technologies) and placed in a T25 flask. The media on the cells was changed every three days (depending on the type of the cell line, table 2.4) and when cells reached the desired confluency for a specific assay (usually between 70% to 90%), they were harvested and passaged.

For cell passaging, media on cells was removed and cells were washed with 3/6 ml (T12/T75) Dulbecco's phosphate buffer saline (DPBS, Gibco®, Sigma). After washing, 0.5/1ml (T25/T75) of 0.25% Trypsin-EDTA (Gibco®, Sigma) were added on cells, and the cells were incubated at 37°C in incubators for five to twenty minutes (depending on the type of the cell line) to allow for complete detachment. Detached cells were collected in 5/10 ml (T25/T75) of media in 15 ml falcon tube and harvested by centrifugation at 200xg for five minutes at 4°C. The supernatant was discarded and the pelleted cells were split 1:5 or 1:10 based on the growth rate of cells and how confluent they should be before being passaged again.

2.2.1.3 Cell counting

To evaluate the viability of the cells and to count them, Countness™, the automated cell counter (Invitrogen, Life Technologies) was used. To obtain the count, 10µl of resuspended cells was mixed with 10 µl of trypan blue exclusion dye and placed in the cell counting chamber slide (Invitrogen) for analysis.

2.2.1.4 Cryopreservation

To freeze the cells, cultured cells grown in T75 flasks were washed, trypsinised and pelleted as mentioned in section 2.2.1.2. Pelleted cells were resuspended in 1 ml of freezing medium (80% of the respective growth medium, 10% of dimethyl sulphoxide (DMSO, Sigma), and 10% of FBS) and placed in cryovials. The vials were then labelled with the name of the cell line, passage number, and date. All the prepared vials were then placed in Mr. Frosty freezing container (Nalgene® Mr. Frosty, Sigma), which can freeze the cells at a controlled rate to -80°C for overnight in its enclosed-microenvironment containing isopropanol. For long-term storage, the cells were stored at a liquid nitrogen storage facility at Leeds University.

2.2.2 Affimers isolation by phage display

Phage display technology involves several steps, namely, target preparation, bio-panning, screening of positive hits, and hit analysis. Phage display technology was used to isolate Affimer binders by screening on known and unknown targets, which were either recombinant proteins or displayed on cells. For HER2, HER3 and EGFR targets, the Affimers were selected against the extracellular domain (ECD) of the receptors (Molecular weight of ~ 95kDa).

In a phage screen that involved whole cells, the selection of a suitable cell line to represent the negative and the positive source of the protein of interest was made on the basis of cells molecular Phenotypic data presented previously (Holliday and Speirs, 2011;Gostring et al., 2012). These data demonstrated the expression status of HERs proteins, particularly HER2 and HER3, on the cell surface of different cell lines. Cells overexpressing either HER2, HER3 or both were selected for positive screening of binders against HER2 and HER3 (target selection), while other cell lines that expressed neither of the receptors were chosen to be used in negative selection (depletion or non-target selection) where removal of non-specific binders, such as plastic binders and non-HER2, non-HER3 binders, was required.

2.2.2.1 Target preparation

2.2.2.1.1 Recombinant proteins

Before phage display, all HER2, HER2-Fc tag, and HER3 recombinant proteins were biotinylated using the amine-based biotin *N*-hydroxysuccinimide (EZ-Link® NHS-SS-Biotin) reagent. In a total volume of 100 µl of 1X PBS (137 mM NaCl; 10 mM Phosphate; 2.7 mM KCl; pH 7.4), 10 µl of protein (stock concentration of 1mg/ml prepared in 1X PBS, pH 7.4) and 7 µl of biotin NHS reagent (stock concentration of 5mg/ml prepared in DMSO) were mixed. The mixture was then incubated at room temperature before the removal of free biotin molecules by desalting using Zeba Spin Desalting Columns (7k MWCO). For prolonged storage of the biotinylated-recombinant protein at -20°C, 100 µl of 50% (v/v) glycerol was added to the mixture.

2.2.2.1.2 ELISA to assess the efficiency of biotinylation

After labelling the proteins with biotin, the efficiency of biotinylation was assessed by ELISA. On Nunc-Immuno™MaxiSorp™ strip, a range of different concentrations of the biotinylated proteins (1 µg to 0.03 µg) was prepared and added to a total volume of 50 µl of 1X PBS in seven of the eight wells, in the remaining well, the protein was not added. Biotinylated proteins were adsorbed to wells during overnight incubation at 4°C. The next day, 250 µl of PBST buffer (1X PBS, pH 7.4 and 0.1% (v/v) Tween-20) was used to wash all the wells once using the automated plate washer (TECAN HydroFlex). After washing, wells were blocked with 250 µl of 10x casein blocking buffer for 3 hours at 37°C.

Prior to the addition of 50 µl of diluted streptavidin-HRP (a dilution of 1:1000 dilution prepared in 2X blocking buffer), wells were washed thrice with PBST in the automated plate washer. 50 µl of 3,3',5,5'-tetramethylbenzidine substrate (SeramunBlue® fast TMB, Seramun Diagnostica, GmbH) was then added to all wells, and the oxidization reaction was allowed to take place for three to five minutes at room temperature. The absorbance of the developed oxidised substrate (blue colour) was then measured at 620 nm using a Multiskan Ascent 96/384 plate reader (MTX Lab Systems, Inc). The measured absorbance of the developed colour is directly proportional to the level of biotin molecules present in the solution. Therefore, an absorbance reading higher than 1.4 nm means better biotinylation efficiency (obtained by verbal communication from BSTG researchers).

2.2.2.1.3 Whole cells in 6-well plate: Fixed monolayer

Selected cell lines were grown to 100% confluent ($\sim 1.2 \times 10^6$ cell/ 2ml of media) in a 6 well-plate. After reaching the desired confluency, cells were washed once with 1X PBS (Invitrogen) for five minutes at room temperature to ensure the removal of unattached cell debris prior to fixation with 4% paraformaldehyde (PFA) for fifteen minutes at room temperature. The fixed cells were then washed thrice, for five minutes each time, in 1X PBS with 0.1% sodium azide to ensure complete removal of the fixative as well as to prevent bacterial growth before the addition of 2X casein blocking buffer (Sigma). Blocking of the non-specific binding sites was carried out overnight by incubating at 4°C.

2.2.2.1.4 Whole cells on a glass-slide: Formalin-fixed paraffin embedded (FFPE)

Different cells were grown to 100% confluency in T75 flasks. After the media was removed the cells were washed with 1X PBS, scraped and placed in a 15ml falcon tube for harvesting by centrifugation at 1000 rpm for fifteen minutes at 4°C. The high centrifugation speed resulted in a compact pellet of cells that were fixed in 5 ml of 4% formaldehyde prepared in 1X PBS overnight prior to adding 5 to 10 ml of 70% ethanol until the paraffin embedding. Dr. Filomena Esteves was kind enough to perform the process of cells embedding, block preparations and sectioning in LIBAC.

2.2.2.2 Bio-panning: selection rounds

2.2.2.2.1 Using recombinant proteins as the source of HER2 or HER3

The whole process of phage selection on the recombinant protein of both HER2 and HER3 is presented in figure 2.1. A total of three non-competitive panning rounds were performed. Non-competitive panning rounds are selection rounds that do not include a competitive elution with a non-biotinylated recombinant protein of the target (the competitor). The addition of the non-biotinylated target (the competitor) with an incubation period of 24 hours at 4°C as recommended by the BSTG phage screening protocol is enough to induce dissociation of the Affimer-displaying phage clone and to prevent it from re-binding. The binders that were not displaced in the presence of the competitor (binders with slow dissociation rates and thus high binding affinities) were eluted and subjected to further amplification rounds. However, in this research, the main aim was to recover as many binders as possible in order to obtain those able to perform

as detection reagents in IHC or those that exhibited potential therapeutic properties. Therefore, standard phage screens with no competitive elution steps were performed.

Biotinylated target proteins were immobilised onto a streptavidin coated wells for one hour at room temperature before the addition of 5 μ l of Affimer phage library (Tiede et al., 2014). The library was pre-panned/depleted on streptavidin coated wells containing no target protein. When the biotinylated HER2-Fc tagged protein was used as the target, the library was pre-panned on an additional well contained an Fc-tagged control protein in order to remove Fc-tagged binders. The pre-panning was performed at room temperature for a total of 120 minutes (forty minutes on each well). Following the depletion, the library was exposed to the immobilised target protein for two hours at room temperature and a shaking speed of 300 rpm.

Next, the plate was washed 27 times with 300 μ l PBST (pH 7.4) to remove the un-bound variants of the phage using the TECAN hydroflex automated cell washer, while the bound phage variants were eluted with 100 μ l 0.2 M glycine, pH 2.2, for ten minutes (neutralised with 15 μ l of 1 M Tris-HCL, pH 9.1) and with 100 μ l of 10mM Triethylamine for six minutes (neutralised with 1 M Tris-HCl, pH 7.0). A volume of 8 ml of *E. coli* strain ER2738 cells (Lucigen, UK) were then infected with the eluted phage for one hour at 37°C with a shaking speed of 90 rpm to enable for phage propagation and amplification. After that, 1 μ l of the 8 ml phage-infected bacterial cell culture was plated on a Luria-Bertani (LB) agar plates supplemented with 100 μ g/ml carbenicillin (50mg/ml carbenicillin stock prepared in ddH₂O, Invitrogen) and allowed to grow overnight at 37°C incubators. The remaining cells in the 8 ml phage-infected cell culture were harvested by centrifugation at 3,000xg for five minutes and resuspended in a 200 μ l volume of 2TY media and spread onto LB-carb plate, which is termed as “remaining cell plate”.

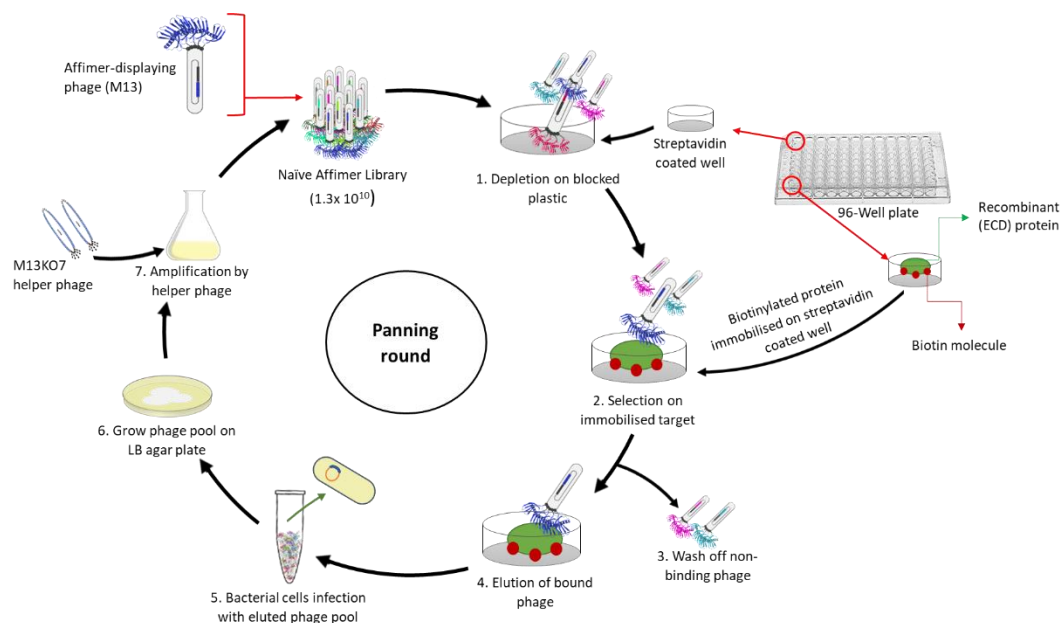


Figure 2.1 Isolation of Affimers by phage selection on immobilized-recombinant target protein. Naïve or enriched library of phage-displaying Affimers was depleted on blocked wells contained no target before the beginning of the selection process on an immobilized-recombinant target protein. Compared to naïve library, the enriched library refers to the library that has been selected previously on the target cells and contains target-binding specific phage clones. When the naïve library is selected on the target cells or protein in round one, the amplified phage pool obtained from this round is now termed as “Enriched library or enriched phage pool”. Here, the recombinant proteins of the ECD of all HER2, HER3 and EGFR were biotinylated. Next, irrelevant (non-binding) phage clones were washed off, while bound phages were eluted and used to infect bacterial cells for further phage-target specific amplification using M13KO7 helper phage. Bio-panning round were repeated thrice.

Following overnight incubation, all grown colonies in the remaining cell plate were scraped using 8 ml of 2TY media (per litre: 10 g yeast extract; 16 g tryptone; 5 g NaCl, pH 7.4) containing 100 µg/ml carbenicillin and then placed in a 50ml falcon tube in order to start the amplification process. Helper phage 0.32 µl M13K07 (titra ca. 10^{14} /ml) was used to infect bacterial cells for thirty minutes, at 37°C, with a shaking speed of 90 rpm. After the infection stage, 16 µl kanamycin (stock concentration of 25mg/ml, Invitrogen) was added and cells were grown overnight at 25°C, 170 rpm. Subsequently, the phage-infected culture was centrifuged at 3,500xg for 10 minutes and the phage-containing supernatant was transferred to a fresh 15ml falcon tube. From this supernatant, a 100µl phage aliquot was removed for use in the second panning round before proceeding to phage precipitation. The enriched pool of target-specific phage was precipitated in 2 ml polyethylene glycol-NaCl

solution (4% (w/v) PEG 8000, 0.3 M NaCl) and kept overnight at 4°C. After precipitation, the pool of phage variants was pelleted by centrifuging at 4816xg for thirty minutes followed by resuspension in 320 µl of TE buffer (10 mM Tris; 1 mM EDTA; pH 8.0).

Phage stocks were then prepared by adding equal volume of 80% glycerol (Sigma-Aldrich) and stored at -80°C for the next selection round and future use in different screens. In the next two rounds of selection, the same procedures were repeated using 5 µl of the phage stock obtained from the previous rounds. However, in both the second and third panning rounds, an equal volume of a depleted suspension of phage was added into target (recombinant protein) and non-target (no protein) containing wells to evaluate the efficiency of the screen. To achieve such evaluation, different concentrations of infected ER2738 cells (a volume range of 100, 10, 1, and 0.1 µl) were plated on LB-carbenicillin agar. The number of the recovered colony forming units (CFU) was counted and the difference in the number of recovered colonies from both target and non-target plates were assessed and compared. The overall enrichment rate of target-specific phage was also evaluated by examining the increase rate of the number of recovered colonies between all rounds.

2.2.2.2.2 Using FFPE cell sections on a glass-slide as the source of HER3

The enriched pool of HER3 binding phage variants was panned against FFPE sections of cells that overexpress HER3. About 5 µl of an HER3-enriched phage library, which was developed by previous phage screen on HER3-recombinant protein was diluted into 100 µl of blocking buffer before adding to cells. Two different screens were performed using different HER3 overexpressing cell lines. In screen-1, the positive cells were MDA-MB-231 cells, while MDA-MB-231 cells were employed in the screen-2. For negative selection, FFPE section of U87-MG cells that do not express HER3 were used. The overall on-slide-cell-based protocol is summarised in figure 2.2. Following deparaffinisation and rehydration of cell sections, the antigenicity was retrieved (see section 2.2.6.4), and the slides were placed in a rectangular plastic microscope glass holder (Fisher Scientific) that contained 2 ml of 10X casein blocking buffer.

Sections were blocked for 1 hour at room temperature before the start of library depletion on U87 cell sections. 100 µl of an enriched library of HER3 binding phage (1:20 dilution factor prepared in 10X casein blocking buffer) obtained from previous selection screen against the recombinant HER3 protein, was added on U87 cells and incubated for 1 hour

incubation at room temperature. After the negative selection step on U87 cells, the depleted pool of phage was then divided into equal volumes to be added on MDA-MB-453 and MDA-MB-231 cells for 1 hour at room temperature. Subsequently, cell sections were washed 10 times with 1 ml of 1X PBS, pH 7.4, and the bound phage were eluted and then plated out as described previously in section 2.2.2.2.1. The whole selection, reinfection and amplification process were repeated three times and the output of each round was evaluated.

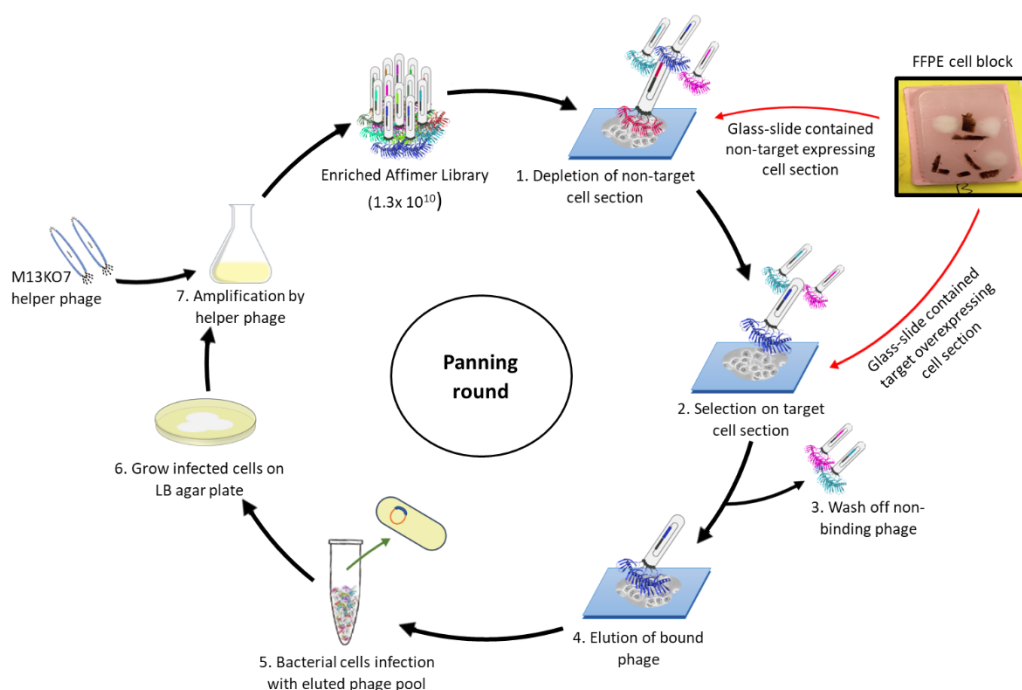


Figure 2.2 Cell-based phage screening strategy using FFPE cell sections on a glass-slide and enriched Affimer phage library. An enriched library was depleted on FFPE-non-target cells (U87-MG cell line) prior to selection on target cells (FFPE section of MDA-MB-231 cells in screen-1 or FFPE section of MDA-MB-453 cells in screen-2). Following selection, unbound phage clones were washed, while bound phages were eluted and used to infect bacterial cells for further amplification to start the next round.

2.2.2.2.3 Using fixed monolayer of cells in 6-well plate for isolation of HER2 or HER3 binding Affimers

To start the selection process of HER3 and HER2 binders on fixed-cells, 100 μ l of an enriched pool of phage obtained from 2/3 panning rounds against recombinant proteins (1:10 dilution factor prepared in 10X casein blocking buffer) was added to blocked well containing no cells for forty minutes followed by one hour depletion step on fixed U87-

MG cells (for HER3 phage screen) or MCF7 cells (for HER2 phage screen) . Summary of the overall phage screen on fixed monolayer of cells is illustrated in figure 2.3. After negative selection, an equal volume of the phage-containing suspension was transferred to target (MDA-MB-453) and non-target cells (either MCF7 or U87-MG), respectively. and incubated for two hours at 50 rpm shaking speed. Unbound phage variants were removed by 10 times of washing with 1 ml of 1X PBS, pH 7.4. According to the BSTG protocol, a stringent washing of the unbound phage is achieved when the plate is washed for 27 times with 1X PBS, pH 7.4, using the automated plate washer of for 10 to 12 times using manual washing in case of performing screens involving cells. Cell-bound phage were then eluted and replicated in bacterial cells to allow for the amplification of specific binders through three rounds of panning. All elution and replication steps were performed as described in section 2.2.2.2.1.

In each selection round, the efficiency of the screen was evaluated based on the number of the recovered colonies that was counted based on the number of colonies grown on the plates containing 1µl of cells. The number of counted colonies was then multiplied by 1000 to determine the number of colony forming units (CFU) per 1ml, or multiplied by 8000 (total volume of bacterial cell cultures used in the screens in order to grow and amplify phage-infected cells) to determine the total number of recovered, phage-infected cells. The overall enrichment rate of target-specific phage was also evaluated by examining the rate of increase of increase of the number of recovered colonies between all rounds. Furthermore, in each round of panning, the cells were visually examined under a light microscope to verify that they were still intact and had not been detached by the harsh washing and elution steps. Finally, the generated enriched phage library was precipitated, purified and stored at -80°C for future use.

We also performed a combined phage screen in which both biotinylated HER2-ECD recombinant protein and HER2 overexpressing cells (MDA-MB-453) were used in an alternative manner in order to isolate HER2 binders. In the first round of selection, 5 µl of naïve Affimer library was diluted in 50 µl of blocking buffer and depleted on 2 depletion wells (contained 2X blocking buffer) before selecting it on biotinylated HER2-ECD that was immobilised on streptavidin-coated plate as described in section 2.2.2.1.1 and 2.2.2.1.2. This round of selection was performed as mentioned in section 2.2.2.2.1 and the colonies of phage-infected cells were scraped with 8 ml of 2TY media to start the precipitation process. However, before precipitation, cells were centrifuged and 100 µl of the phage-infected cells were taken to be subjected to the second panning round on cells.

In the second panning round, the phage library obtained from the previous round was depleted on U87-MG cells and then selected on MDA-MB-453 cells as described previously in this section. The eluted phage clones were then propagated, amplified and plated out in LB-agar plate containing antibiotic in order to recover 100 μ l of the phage pool and use it in the third panning round on the HER2-ECD recombinant protein. The third panning round on protein was performed as illustrated in figure 2.1, section 2.2.2.2.1.

In another pure cell-based screen (no protein involved) to select HER2 binders on cells, 10 μ l of a naïve Affimer phage library (1:100 dilution factor prepared in 10X casein blocking buffer) was depleted against fixed monolayer of HB2 cells before selecting on the transfected counterpart (HER2-HB2 transfected cells) cells. Three rounds of screening were performed as described in figure 2.3, and as mentioned with the HER2 and HER3 combined phage screens containing cells and involving the use of an enriched phage library. The only difference in this new screen using HER2-HB2 transfected and non-transfected-HB2 cells is that the used library is the naïve Affimer library and the selection process was performed in a total of 4 rounds.

2.2.2.2.4 Phage display protocol for biomarker discovery

In accordance with the selection process illustrated in figure 2.3, 10 μ l of a naïve Affimer phage library (1:100 dilution factor prepared in 10X casein blocking buffer) was panned against fixed monolayer of cancerous (MDA-MB-453) and non-tumorigenic (HB2) cells to isolate Affimers for biomarker discovery. In the first panning round, the Affimer library was depleted on wells containing a fixed monolayer of HB2 cells for one hour of incubation at room temperature. Following negative selection, the depleted phage pool was transferred to wells containing a fixed monolayer of MDA-MB-453 and incubated for additional two hours, at room temperature, without shaking. Next, the wells were washed 12 times (five minutes each) using 1X PBS (pH 7.4), and the bound phage were eluted, replicated in bacterial cells and plated out on LB agar plates as previously described.

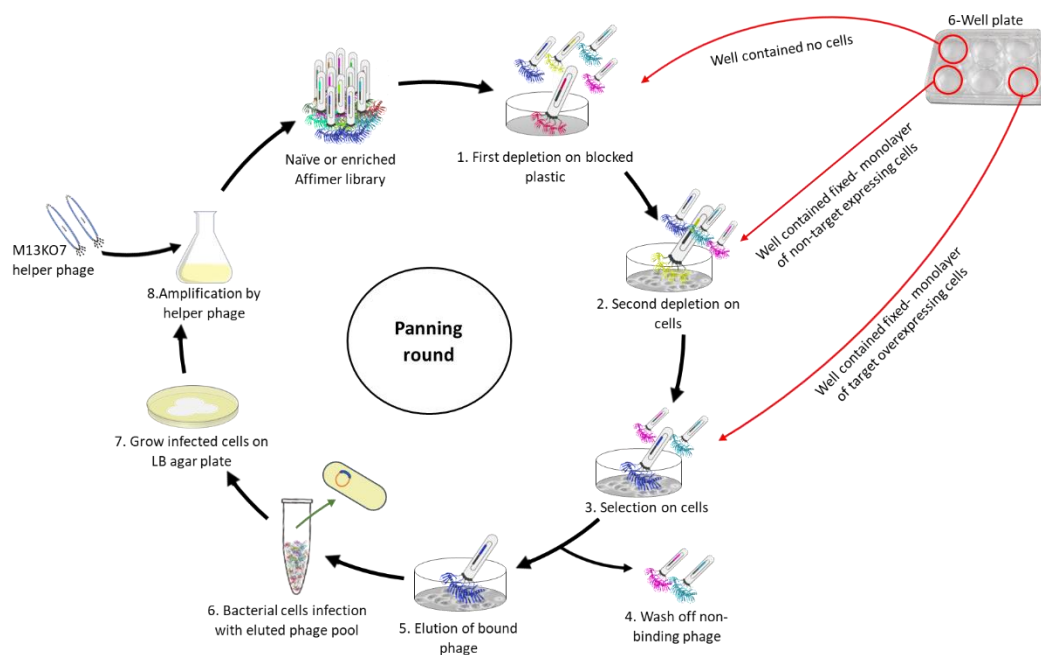


Figure 2.3 Isolation of Affimers on fixed monolayer of cells using phage display. Enriched library was depleted on wells contained either no cells or a fixed-monolayer of cells not displaying the target protein (MCF7 cells in HER2-screen or U87-MG cells in HER3-screen). Thereafter, depleted pool of phage was selected on fixed-monolayer of cells overexpressing the target protein (MDA-MB-453 cells was used for both HER2 and HER3-phage screens). Following selection, unbound phage clones were washed off, while bound phages were eluted and used to infect bacterial cells for further amplification to start the next round. Another screen to isolate HER2 binders from cells was performed using engineered and non-engineered cells (HER2-HB2 transfected and HB2 non-transfected cells) in addition to the naïve Affimer library in a total of 4 selection rounds.

In the second panning round, the stringency of the selection process was increased by prolonging the washing step (4 hours at room temperature using 1 ml of 1X PBS, pH 7.4 and interval change of the wash buffer in one hour interval) and increasing the number of depletion steps (using two depletion-wells containing HB2 cells instead of the one well only included in other rounds). Briefly, 100 μ l of phage supernatant from the first panning round was diluted in 10X casein blocking buffer (1:10 dilution) and added on HB2 cells to start the negative selection. The pool of phage was depleted twice on separate wells that contained HB2 cells for 1 hour at room temperature and shaken at 50 rpm. The depleted suspension of phage was then added to MDA-MB-453 cells for 1 hour at room temperature with a low shaking speed (between 30 to 50 rpm). To remove un-bound phage, the cells were washed with 1 ml of 1X PBS for 4 hours at room temperature with

a buffer renewal every hour. Next, the bound phage was eluted, replicated in *E. coli* cells and grown on LB agar as mentioned in section 2.2.2.2.1. The outcome of this second round was assessed (refer to section 2.2.2.2.1), and the grown colonies were scraped into 8 ml of 2TY media and amplified using helper phage to further enrich the pool with target-specific binders.

Two more rounds were performed using 100 µl of the enriched phage supernatant recovered from the previous rounds. After stringent selection in the second panning round, both the third and fourth rounds of panning were performed at the same conditions as were used in the first selection round. However, in these two rounds, the depleted supernatant of phage was divided into equal volumes and added on both HB2 and MDA-MB-453 cells to evaluate the final output of the whole screen by comparing the number of recovered colonies from both target (MDA-MB-453) and non-target (HB2) cells. After all the rounds, phage stocks were prepared and stored at -80°C. Cells were visually checked under the light microscope after each of the rounds.

2.2.2.3 Phage ELISA

2.2.2.3.1 Preparation of phage: colonies selection

In 96-well deep-V bottom plates (Greiner Bio-One) single picked colonies were grown for overnight at 37°C in a 2TY media with at a shaking speed of 1050 rpm. Next day, a fresh 96 well deep-V bottom plate was inoculated with 25 µl of the overnight culture. Glycerol stocks of the original 96-well overnight cultures were prepared by adding 50% (v/v) glycerol to the plate and stored at -80°C for long-term usage. The freshly inoculated plate was grown overnight at 37°C at the shaking speed of 1050 rpm for one hour. M13KO7 helper phage (diluted 1:1000 in 2TY media supplemented with 100µg/ml carbenicillin) was added to all wells. The plate was incubated at room temperature for thirty minutes with 450 rpm shaking speed. Later, growth selection of bacterial cells carrying the phagemid was made by adding 10 µl of 2TY media supplemented with 1.25 µg/ml of kanamycin (kanamycin stock of 25mg/ml prepared in ddH₂O). Following addition of the antibiotic, cells were grown overnight at room temperature with 750 rpm speed of shaking. Next day, the plate was spun at 3500xg for ten minutes at 4°C and 50 µl of the phage supernatant was transferred directly into the ELISA plate to perform the assay.

2.2.2.3.2 Positive hits conformation

After picking defined number of colonies randomly and grow them in 96-well deep-V bottom plates, their binding ability and specify towards the target protein was confirmed using different platforms of ELISA (i.e., protein-based and cell-based ELISA assays). Phage immunofluorescence (IF) staining was also used to visualise the binding pattern of some phage displaying Affimers as well as to determine the localisation of the proteins to which these tested phage clones bind to on cells. This section describes the ELISA assay, while detailed description of the phage IF protocol will be mention in section 2.2.6.1.

2.2.2.3.4 Protein-based ELISA assay

When protein-based ELISA was performed, streptavidin-coated 96 well plates was employed. The wells were blocked with 2X casein blocking buffer for overnight at 37°C. Biotinylated protein targets (HER2 and HER3) were diluted 1:1000 in 2X blocking buffer and 50µl of the diluted protein was aliquoted into the wells following the pattern illustrated in chapter 3 and 4. Added biotinylated-protein was incubated on wells for one hour, at room temperature and a shaking speed of 300 rpm. Next, wells were washed once with 1X PBST using automated plate washer and 50µl of phage supernatant containing 10µl of 10x blocking buffer were added into all wells, except of the ones used to test the phage clones against blocking buffer. Phage clones were allowed to bind to their target for 1 hour at room temperature, 300 rpm before washing and addition of 50µl anti-fd-Bacteriophage-HRP (1:1000 diluted in 10X casein blocking buffer) for one hour with 300 rpm. Afterwards, wells were washed for 12 times with 1XPBST using plate washer and 50µl of TMB substrate was added. The absorbance of the developed blue colour was measured at 620 nm, and the ability of a single phage clone to bind to its target was confirmed by comparing the absorbance readings of all wells contained target, non-target, and buffer control.

2.2.2.3.5. Cell-based ELISA assay

The cell-based ELISA required a seeding of ~8,000 cells in 100 µl into 96-well plates (Corning® Costar ® Sigma-Aldrich). Seeding and fixing of both target (cells overexpressing the target protein) and non-target (cells do not express the target protein)

cell lines was performed on a similar way to the 6-well plate mentioned in section 2.2.2.1. Before the assay, the plate was pre-blocked with 2X casein blocking buffer for overnight at 4°C. The next day, ELISA assay was conducted following the same way of performing a protein-based ELISA.

2.2.2.3.6 Characterizing the selected positive hits

ER2738 colonies containing the positive clones were grown in 3ml 2TY media (supplemented with 100 µl of carbenicillin) overnight at 37°C and 230 rpm shaking speed. Using QiAprep Spin Miniprep kit (QIAGEN), the plasmid DNA was extracted according to the manufacturer's protocol. Aliquoted samples of the pDHIS phagemid DNA were then sent for sequencing (Sanger sequencing, GENEWIZ) using an M13-26 Reverse primer: 5'–CAG GAA ACA GCT ATG AC-3'. Next, the amino acid arrangement of the variable loops of all sequenced hits were identified and further characterised using the MacVector 16.0.9 software (MacVector Inc, USA) and ProtParam tool (ExPASy, Bioinformatics Resource Portal) respectively.

2.2.3 *In vitro* production of soluble His₈-tagged Affimer proteins

To produce His₈-tagged Affimer proteins, the Affimer cDNA was subcloned from the phagemid vector into an expression vector containing a His₈-tag, such as pET11a (figure 2.4).

2.2.3.1 Molecular subcloning of Affimers

2.2.3.1.1 Amplification of Affimer sequence from the phagemid vector

Affimer DNA sequences were amplified by PCR following the conditions summarised in table 2.6. Prior to the amplification, 25 µl of PCR reaction mixture containing 1 µl of a phagemid DNA of a single clone was set up as described in table 2.7 and placed into PCR machine. It should be mentioned here that the sequence of the amplified Affimer can either contain a cysteine residue or not based on the reverse primer used (see primers list in table 2.8). To remove the phagemid from the amplified PCR product, 0.5µl of *DpnI* was added to all PCR reactions for one hour at 37°C. Next, all PCR products were purified

using QIAquick PCR purification kit (QIAGEN) according to the manufacturer's instructions, but with using sterile water to elute the product instead of the mentioned buffer.

Following purification, the PCR product was digested with 0.5 μ l of both *NheI* and *NotI* restriction enzymes. After digestion, Affimer sequences were purified using the same purification kit mentioned earlier. Finally, the concentration of DNA was measured using NanoDrop Lite Spectrophotometer at A260 nm (Thermo Scientific) and stored at -20°C.

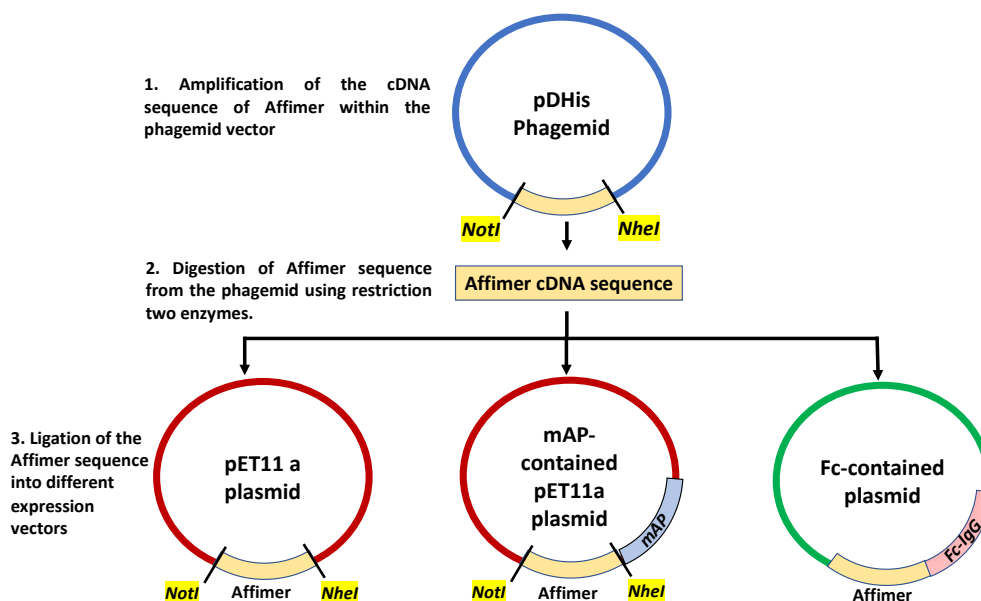


Figure 2.4 Schematic overview of the subcloning process of Affimer cDNA sequences from pDHis phagemid vectors into different expression vectors. The subcloning process starts with a standard PCR protocol to amplify the cDNA sequence of an Affimer in order to be digested. Double-site digestion of the sequence was performed using *NotI* and *NheI* restriction enzymes that facilitated the removal of the amplified-sequence of Affimer from the phagemid vector. The digested sequence (insert) was then ligated into different vectors that were already digested using the same restriction enzymes. Ligation occurred using T4 DNA ligase that fixed the ends of the Affimer and the vector together without the need for an additional PCR process. The vectors into which Affimers ligated included: pET11a vector, monomeric-alkaline phosphatase (mAP) contained-pET11a vector (subcloning process performed by BSTG), and Fc-IgG contained vector (subcloning performed by Avacta Life Sciences).

2.2.2.3.1.2 Ligation of the digested Affimer sequence into the pET11a vector

To ligate the digested Affimer sequence into the pET11a vector, 25 ng of the Affimer DNA sequence was added to the following 25 μ l volume of mixture; 2 μ l of 10X T4 DNA

ligase buffer, 1 µl of T4 DNA ligase and 75 ng of the DNA of a digested pET11a vector that was kindly provided by the BioScreening Group, and ddH₂O as required. Ligation in to the pET11a vector was carried out in a 1.5 ml Eppendorf microcentrifuge for overnight at room temperature. A reaction mixture where no insert (Affimer DNA) was added to the digested pET11a vector was included to serve as a negative control.

PCR Steps	Temperature	Time	Cycles
Initial Denaturation	98°C	30 seconds	1
Denaturation	98°C	20 seconds	30
Annealing	54°C	20 seconds	
Extension	72°C	20 seconds	
Final Extension	72°C	10 minutes	1
Hold	4°C	Hold	

Table 2.6 PCR condition for the amplification of Affimer sequence in the phagemid vector.

Component	25 µl Reaction
Sterile Water	13.8 µl
5X Phusion HF Buffer (NEB)	5 µl
dNTP Mix, 25 mM (MP Biomedicals)	0.2 µl (200 µM)
DMSO (NEB)	0.75 µl (3%)
Forward Primer (10 µM stock, Sigma)	2 µl (0.8 µM)
Reverse Primer (10 µM stock, Sigma)	2 µl (0.8 µM)
Phusion DNA Polymerase (NEB)	0.25 µl (0.02 units/µl)
Template DNA (Phagemid vector)	1 µl (5-10 ng)

Table 2.7 PCR Components of 25 µl reaction volume required to clone the Affimer sequence into a digested pET11a expressing vector.

Purpose	Primers sequence
Amplification of Affimer from phagemid vector	Forward: 5' TTCTGGCGTTTTCTGCGTCTGC Reverse: 5' TACCCTAGTGGTGATGATGGTGATGC
Cloning Affimer into pET11a vector	Forward 5' ATGGCTAGCGGTAACGAAAACCTCCCTG Reverse with C : 5'-TTACTAATGCGGCCGCACAAGCGTCACCAACCGGTTTG Reverse without C : 5' TACCCTAGTGGTGATGATGGTGATGC
Cloning Affimer into alkaline phosphatase (AP) contained pET11a vector	Forward: 5' ATGGCTAGCGGTAACGAAAACCTCCCTG Reverse without C : 5' TACCCTAGTGGTGATGATGGTGATGC

Table 2.8 Primers used in molecular subcloning of Affimers

The ligation mix was transformed into XL1-Blue supercompetent bacterial cells (Agilent Technologies). 1 µl of the ligation mix was added to 50 µl of competent cells and heat shocked at 42°C for forty-five seconds. Following heat shock the cells were recovered in 1 ml SOC media (Sigma, UK) (Froger and Hall, 2007). 100 µl of transformed bacterial cells were then plated on LB agar supplemented with 100 µl carbenicillin and incubated overnight at 37°C. The next day, single colonies were picked and grown in 5 ml of 2TY-carbenicillin media overnight at 37°C. Colonies were picked only when the negative control plate showed either no colonies or very few colonies compared to the other positive plates. The plasmid was extracted using the QIAprep Spin Miniprep Kit (QIAGEN) according to the manufacturer's instructions. Subsequently, an aliquot of the extracted plasmid DNA was sent for sequencing (GENEWIZ) using a T7 primer: 5'–TAA TAC GAC TCA CTA TAG GG. Before Affimer expression, DNA sequences were checked and the amino acid arrangements of the Affimers were analysed using the translate tool in the ExPASy Bioinformatics Resource Portal.

2.2.3.2 Production and purification of His₈-tagged Affimers

To produce the Affimers, 20 µl of the competent *E.coli* strain BL21 Star™ (DE3) (Life Technologies) cells were transformed. After transformation, a single colony was picked and placed into 2 ml of LB starter culture contained 100 µg/ml carbenicillin and 1% glucose (v/v) and incubated for overnight at 37°C. The following day, 50 ml of autoclaved LB media, in 250 ml flask, was inoculated with 625 µl of start culture and incubated at 37°C, 230 rpm until the cell density reached an OD_{600nm} of 0.7-0.8. After reaching the desired density, the temperature and shaking speed were changed to 25°C and 150 rpm, respectively and Affimers production was induced by 0.1mM Isopropyl-beta-D-thiogalactopyranosideI (IPTG, 1M stock prepared in ddH₂O). Cells were then harvested by centrifugation at 4816xg for twenty minutes at 4°C. Several strategies to maximize the expression of Affimers in bacterial cell system were examined (see chapter 3).

Cells were harvested by centrifugation and lysed with 1 ml of lysis buffer (table 2.9) for two hours at room temperature on a tube-rotator (Stuart™ SB2 fixed speed rotator, ThermoFisher Scientific). The lysate was incubated at 50°C in a water bath for twenty minutes followed by cell fractionation at 16,000xg centrifugation speed for twenty minutes. After centrifugation, the supernatant containing the soluble Affimer protein was transferred into a 1.5 ml Eppendorf tube contained 300 µl of previously washed nickel

beads (Amintra Ni-NTA slurry, Expedeon) and incubated for one hour on a rotator at room temperature to allow Affimers to bind. Next, saturated beads were washed with 1 ml of wash buffer (table 2.9) via centrifugation at 1,000 xg for one minute.

Washing was repeated several times until the absorbance measurements at 280 nm gave a consistent reading of < 0.04 nm. His₈-tagged Affimers were then eluted with 1 ml elution buffer containing a high concentration of imidazole (table 2.9). The elution was repeated until the spectrophotometer detected no more proteins. Proteins concentrations were determined using spectrophotometer (A_{280nm}) and bicinchoninic acid (BCA) assay according to the manufacturer's recommendations (Pierce™ BCA Protein Assay Kit). Prior use in further analysis, Affimers were dialysed in 1XPBS, pH 7.4, using Slide-A-Lyzer™ dialysis cassettes as instructed by the manufacturer.

Buffer	Components	pH
Bacterial cells Lysing buffer	<ul style="list-style-type: none"> • 1 ml lysis buffer (50 mM NaH₂PO₄; 300 mM NaCl; 20 mM Imidazole; 10% Glycerol(v/v)) • 1 X BugBuster® 10X Protein Extraction Reagent (Novagen) • 10U/ml Benzonase® Nuclease, Purity > 99% (25 U/μl, Novagen) • 1 X Halt Protease Inhibitor Cocktail (100X, Thermo Scientific) 	7.4
Wash buffer	<ul style="list-style-type: none"> • 50 mM NaH₂PO₄; 500 mM NaCl; 20 mM Imidazole; 0.01% Tween (v/v) 	7.4
Elution buffer	<ul style="list-style-type: none"> • 50mM NaH₂PO₄, 500 mM NaCl; 300 mM Imidazole; 10% (v/v) Glycerol 	7.4

Table 2.9 Lysis, wash and elution buffers used in Affimer production and purification protocol.

2.2.3.2.1 Sodium Dodecyl Sulfate Polyacrylamide gel electrophoresis SDS-PAGE gel

The efficiency of the expression and the purity of the obtained Affimers was confirmed by sodium dodecyl sulfate polyacrylamide gel electrophoresis SDS-PAGE. 10 μl of protein sample was mixed with 10 μl of SDS-PAGE sample loading buffer (prepared from mixing 50 μl of 2-mercaptoethanol, 14.2 M, and 2X Laemmli sample buffer, Bio-Rad). Before loading 10 μl of the sample protein into wells in a 4-20% Mini-PROTEAN® TGX™ gel (Bio-Rad), the mixture was heated at 95°C for ten minutes. As a negative

control, 5 μ l of the PageRuler™ Prestained Protein Ladder (10 to 180 kDa) was also loaded into a single well. The gel was run in 1X TGS running buffer (Tris/Glycine/SDS buffer, Bio-Rad, pH 8.4) for one hour at 150 mV.

Next, gels were stained for two hours with Coomassie brilliant blue stain (45% methanol, 7% acetic acid, 0.25% Coomassie blue, sterile water) followed by overnight de-staining step using destaining buffer (45% methanol, 7% acetic acid, sterile water) or dH₂O. Finally, gels were imaged using Amersham Imager 60 (GE Healthcare life sciences) and the purity of the Affimers were assessed. The mass of the expressed Affimers was calculated by ProtParam tool in the ExPASy Bioinformatic portal based on the amino acid sequence. When running the Affimer protein in SDS-PAGE gels, Affimer mass was further verified by comparing the observed molecular weight to the predicted one under the guidance of the used protein ladder.

2.2.4 *In vitro* production of VEGFR2 Affimer-Alkaline phosphatase (AP) fusion protein

2.2.4.1 Molecular construction of the fusion protein

To start constructing the fusion protein, digested-pET11a contained monomeric wild type bacterial alkaline phosphatase (AP) was a kind gift from Dr. Syzmonik from the Bioscreening group at University of Leeds. The Affimer sequence was then subcloned from the phagemid vector to the digested pET11a-AP contained expression vector following the same subcloning protocol mention in section 2.2.3.1.

2.2.4.2 Production and purification of the fusion protein

The fusion protein was expressed *in vitro* following the standard protocol of Affimer protein production in bacterial cells (section 2.2.3.2) with a few modifications. Several optimisation trials to maximise the yield of the fusion protein and, at the same time, maintaining the functionality of both enzyme and Affimer were performed (see chapter 5). The optimal expression protocol of AP-Affimer fusion protein in bacteria will be described. In brief, a start culture was setup for overnight at 37°C in 2 ml of super broth media (3% tryptone, 3% yeast extract, 1% MOPS, ddH₂O, pH 7.0) supplemented with 100 μ g/ml carbenicillin and 1% glucose. The next day, 50 ml of the same media was inoculated with 1ml of the start culture, and the expression of the fusion protein was

induced with 0.1mM at an optical density (OD_{600nm}) of 0.5 and incubated overnight at 25°C and 220 rpm.

The fusion protein was then extracted from cells, captured on nickel beads and eluted. To confirm the efficiency of the adapted expression protocol and to further check the purity of the obtained fusion, an SDS-PAGE gel electrophoresis was performed as mentioned in section 2.2.3.2. The concentration of the eluted protein was determined by BCA assay after six hours' dialysis in two changes of 3 L alkaline phosphatase storage buffer (0.15 M sodium chloride, 1 mM Magnesium chloride, 0.1mM zinc chloride, 0.05 M Tris, 50% glycerol in ddH₂O, pH 8.0).

2.2.4.2.1 Evaluating the catalytic activity of the AP enzyme using PNPP substrate

Next, the catalytic activity of the AP enzyme was examined using its related *p*-Nitrophenyl Phosphate (PNPP, NEB) substrate. In a 96-microplate (Falcon, VWR™), 25 µl of eluted protein was added to 25µl TBS buffer (pH 8.0) contained in the wells. To the 50 µl volume of the sample, 0.5µl of 500 mM PNPP was added and incubated at room temperature in the dark for ten minutes to allow the development of the yellow colour. Both negative and positive controls were used. One well that did not contain protein sample served as the negative control, while a control protein of known AP enzyme activity was kindly provided by BSTG was employed as the positive control.

2.2.5 *In vitro* chemical modification of Affimers

2.2.5.1 Bio-conjugation of horseradish peroxidase (HRP) enzyme to Affimers

In conducting HRP conjugation to Affimers, two approaches were followed. In the first approach, primary amines (-NH₂) suited on lysine were used, while in the second approach sulfhydryl groups (-SH) on cysteine residues were used (table 2.10, 2.11 and 2.12).

2.2.5.1.1. Approach 1: HRP labelling of Affimers via their lysine residues

Random conjugation of HRP molecule to Affimers by modifying the primary amines on lysine was performed. For this the lightning-link®HRP conjugation kit (Innova

biosciences) was used according to the manufacturer's recommendations of the used. Conjugation of HRP enzyme to Affimers occurred under a buffer pH of 8.0 (table 2.10).

2.2.5.1.2 Approach 2: Site-specific HRP labelling of Affimers via a single cysteine residue

In contrast with random conjugation, a site-specific labelling requires a cysteine residue and a thiol reduction to enable such conjugation (table 2.10). Therefore, Affimer proteins containing cysteine residues were employed, and the thiol bonds between two Affimer molecules holding a single cysteine residue was reduced using a tris-2-carboxyethylphosphine (TCEP) disulfide reducing gel (table 2.11). 150 µl of TCEP gel was washed by centrifugation at 1,000 *xg* for three times (1 minute each) using 1X PBS contained 1mM of EDTA. To the washed TCEP gel, 150 µl of 1 mg/ml Affimer protein and 5 µl of 1X PBS, pH, 7.2 (containing 50mM of EDTA) were added and incubated at room temperature, without shaking for one hour. The reduced Affimers molecules were recovered by one minute of centrifugation at 1,000 rpm and placed and mixed with maleimide-HRP activated reagent to achieve a mixture of maleimide-activated HRP and Affimers in 1:1 molar ratio. The conjugation took place overnight at room temperature before dialysis in 1X PBS, pH 7.0, using the Zeba™ Spin Desalting Columns, 40K MWCO.

HRP	Source	Characteristics	Molecular weight (Da)
Lightning link® HRP conjugation kit	Innova Bioscience	Random labeling via amine groups at pH 6.5-8.5	HRP: 44,000
Maleimide-Activated HRP	Innova Bioscience	Site-specific conjugation via sulfhydryls at pH 6.5-7.5	HRP: 44,000

Table 2.10 HRP- conjugation approaches.

2.2.5.2 Biotinylation of Affimer proteins

Site-specific biotinylation of Affimers via cysteine was conducted using different biotin linkers and thiol reducing agents (table 2.12 and 2.11, respectively) following the manufacturers protocol. Biotin conjugation was optimised by altering different conditions as described in chapter 5. In this section, the optimal biotinylation protocol will be summarised. Prior to biotinylation, proteins were reduced by 150 μ l TCEP-gel as mentioned in section 2.2.4.1. Reduced Affimers were then mixed with 0.1mM of Biotin-maleimide reagent (2mM stock reagent prepared in DMSO) and incubated for three hours at room temperature, without shaking. Following the labelling, excess unbound biotin linkers were removed by desalting with the Zeba™ Spin Desalting Columns, 7K MWCO.

Desalting of labelled Affimers was performed twice to ensure a complete removal of free biotin. In order to assess the efficiency of Affimer biotinylation, an ELISA assay was performed in the manner mentioned in section 2.2.1.1. Additional assessment of biotinylation efficiency by determining the ratio between biotinylated and non-biotinylated proteins was performed using mass spectrometry (MS) analysis. Before MS analysis, labelled-Affimer reagent was dialysed in 5L of 1X PBS, pH 7.4, overnight at 4°C using Pur-A-Lyzer™ Mini Dialysis Kit (Sigma). All mass-related analyses were performed by the members in mass spectrometry facility at the University of Leeds.

Thiol -reducing agent	Source	Characteristics	Application
Pierce™ immobilized-TCEP disulfide reducing gel	ThermoFisher-Scientific	<ul style="list-style-type: none">• 4% crosslinked agarose beads (supplied as 50% slurry)• TCEP concentration (8μmol/ml of gel)	Site-specific conjugation of maleimide-HRP and biotin molecules to Affimers
Pierce™ TCEP-HCL	ThermoFisher-Scientific	<ul style="list-style-type: none">• Molecular Formula: C₉H₁₆O₆PCl• MW: 286.65 Da• Soluble at 1.08 M	Site-specific conjugation of maleimide- biotin molecules to Affimers

Table 2.11 Thiol-reducing reagents. Details of type, characteristics, source. and applications used in.

Biotin linker	Source	Chemical Formula	Molecular weight (Da)	Spacer arm (Å)
Biotin-Maleimide	25mg, Sigma Aldrich	C ₂₀ H ₂₉ N ₅ O ₅ S	451.54	None
4-(n-maleimidomethyl)-cyclohexane carboxylic acid (BMCC)	50mg, ThermoFisher Scientific	C ₂₆ H ₃₉ N ₅ O ₅ S	533.68	32.6
Maleimide-PEG₁₁-Biotin	25mg, ThermoFisher Scientific	C ₄₁ H ₇₁ N ₅ O ₁₆ S	922.09	51.9
Reactive Groups	Maleimide, reacts with sulfhydryl at pH 6.5-7.5			

Table 2.12 Biotin-Maleimide linkers. Details of source, chemical formula, molecular weight and spacer arm length.

2.2.6 Functional characterisation of Affimers

2.2.6.1 Immunofluorescence (IF) microscopy on fixed cells

Prior to affinity/immunofluorescence experiments, cells were split, seeded, and grown on sterile glass-coverslips until they were 70% confluent. Next, cells were fixed in 4% paraformaldehyde (PFA) for 15 minutes at room temperature and washed thrice in 1X PBS (5 minutes each) before permeabilisation in 0.1% Triton X-100 (v/v) for 5 minutes at room temperature. In case of methanol-fixed cells, 1 ml of cold methanol (100%) was added to cells grown on glass-coverslips. After this, the plate of cells was immediately incubated at -20°C for two minutes to enable cell to be fixed without the risk of protein degradation due to the addition of an absolute methanol. Next, cells were washed three times with 1X PBS (5 minutes each wash) at room temperature with gentle agitation on a plate rocker before the start of the staining process.

Permeabilised-PFA fixed cells or methanol (non-permeabilised) fixed cells were then washed once in 1X PBS and blocked with 5% Marvel milk (prepared in 1X PBS) for 1 hour at room temperature. After blocking, the cells were incubated overnight at 4°C in 110 µl primary unconjugated affinity reagents (Affimers and antibodies, table 2.1 and

2.3) diluted with 1% Marvel milk. The next day, the cells were washed thrice in 1X PBS (each five-minute wash) prior to the addition of 110 μ l anti-his₈ tag antibody in 1% Marvel milk for one hour at room temperature to allow the detection of the his₈-tagged Affimer reagent. Subsequently, cells were washed thrice in 1X PBS to remove the unbound anti-his₈ tag antibody before adding 110 μ l of 1% blocking buffer containing Alexa Fluor-conjugated secondary antibodies (table 2.2) and 1 μ g/ml of DNA-binding dye (DAPI) and were incubated in cells for one hour at room temperature. Finally, the cells were washed and mounted on glass slide using 25 μ l of Fluoromount reagent. Images were acquired using EVOS fi digital inverted imaging system (Life Technologies) at 20X magnification or the Nikon Eclipse Ti-E widefield fluorescent inverted microscope (Nikon) at both 60X and 100X magnifications.

2.2.6.2 IF microscopy on live cells

To start IF staining of live cells grown on glass-coverslips, the cells were washed once with 1XPBS for one minute at room temperature before the addition of 5 μ g/ml Alexa Fluor-conjugated wheat germ agglutinin (WGA) membrane marker and incubated for fifteen minutes at 37°C in CO₂ supplemented incubator. Cells were washed once in 1X PBS and primary-unconjugated affinity reagents including Affimers and antibodies (table 2.1 and 2.3). The cells were incubated for one hour at 37°C. Thereafter, the cells were washed thrice in 1X PBS (each one-minute wash) at room temperature and then fixed with 4% PFA for fifteen minutes. After cell fixation, the cells were processed following the staining protocol mentioned in section 2.2.6.1.

2.2.6.3 Immunohistochemistry staining (IHC) staining

2.2.6.3.1 Paraffin blocks preparation and sample sectioning

Tissues and cell pellets samples were embedded in paraffin blocks after processing in graded ethanol and xylene using Leica ASP200 Vacuum tissue processor (Leica, UK). The paraffin-embedded blocks of cells and whole tissues were then cut into 4- μ M sections and mounted on poly-L-lysine extra-coated slides (Leica Biosystems). Sample sections (cells or tissues) were dried for overnight at 37°C before heating them on a hotplate at 60°C for twenty minutes.

2.2.6.3.2 Staining method

The sections were then deparaffinised and rehydrated starting with a series of three xylenes washes (three minutes in each solution) and followed by another series of three-minute washes in graded alcohols (100%, 95%, and 75%,) until finally being washed in water for five minutes. The pressure cooker was used for antigen retrieval by incubating the slides in a Tris-base retrieval buffer, pH 9.5 +/-0.5 (MenaPath Access Super RTU, A. Menarini Diagnostics) for two minutes at full pressure and maximum temperature of 121°C. Next, the slides were allowed to cool down by incubating them in water for five minutes. The activity of both endogenous peroxidases and alkaline phosphatases was blocked by treating the samples with 110 µl bloxall blocking buffer (Vector Laboratories) for twenty minutes.

When biotin-streptavidin detection system was used, an additional blocking step of all endogenous biotin, biotin receptors, and avidin binding sites is needed. To achieve the blocking, the biotin/avidin blocking kit (Vector Laboratories) was used following the manufacturer's recommendations. In between the blocking steps, sections were washed twice (five minutes each) in 1X TBST (20mM Tris-HCl pH 7.6, 137mM NaCl, 0.1% (v/v) Tween-20). Further, after blocking all endogenous molecules, non-specific binding sites were blocked by treating with 110 µl of 1X casein blocking buffer (Vector Laboratories) for one hour at room temperature. All primary Affimer reagents and antibodies (table 2.1 and 2.3) were diluted in 110 µl of antibody diluent reagent (Life Technologies) and sample sections were incubated at room temperature. Secondary reagents were then added based on the used detection system (table 2.2).

2.2.6.3.2.1 Biotin-Streptavidin detection system

Following incubation of biotinylated primary Affimers and biotin conjugated secondary antibodies, sections given two five-minute washes in 1X PBST at room temperature. After that, 110 µl of 1:300 diluted streptavidin-HRP conjugated reagent (Vector Laboratories) was added and incubated for thirty minutes at room temperature. Sections were washed twice with 1X PBS before the addition of one drop of Immimpact DAB peroxidase (HRP) substrate (Vector Laboratories) and left to stand for five minutes at room temperature.

2.2.6.3.2.2 Alkaline phosphatase detection system

After incubating the alkaline-phosphatase-containing primary/secondary reagents and other secondary-AP conjugated secondary antibodies in the dark for an hour, sections were washed and Impact vector red (AP) substrate was added and incubated on tissue for ten minutes in the dark, at room temperature.

2.2.6.3.2.3 Polymer-based detection system

To further improve the intensity of the detected signal, a polymer-based amplification kit (Novocastra Novolink™, Leica Biosystems) was used according to the manufacturer's instructions to detect the Fc-fragment of a rabbit and mouse IgG. As the used polymer conjugated to HRP enzyme, the Impact DAB peroxidase (HRP) substrate (Vector Laboratories) was used for visualisation.

2.2.6.3.3 Sections counterstaining, dehydration, mounting and image acquisition

Following the addition of the appropriate-substrate, sections were rinsed in water for one minute, counterstained in Mayer's Haematoxylin for thirty seconds, washed for one minute in water and then immediately treated with Scott's tap water for one minute before beginning the dehydration process. To dehydrate, slides were placed for one minute each in 75%, and 95% solutions of alcohol and 100% alcohol. This was followed by three xylene washes of one minute each. Finally, the sections were mounted in DPX (sigma) and images were captured at 16X and 20X magnifications using Axioplan Zeiss microscope fitted with AxioCam colour camera and AxioVision 4.8 software (Carl Zeiss, Germany). All microarray sections were scanned by the imaging facility in LIBAC and images were acquired by the WebScope software.

2.2.6.4 Pull-down assay and western blot (WB) analysis

2.2.6.4.1 Preparation of whole cell lysates

From T75 flasks, cells were quickly rinsed with ice-cold 1X PBS and scraped and pelleted as mentioned in section 2.2.1.2. Pelleted cells were lysed in 1 ml non-denaturing lysis buffer (25mM Tris-HCl, pH 7.0, 150mM NaCl, and 5% of glycerol) containing 1% of Nonidet-P40 (NP-40, Sigma) and 1X Halt protease inhibitor cocktail (100X stock reagent, ThermoFisher Scientific) for 35 minutes on ice and shaking at room temperature.

Cell debris was pelleted by centrifugation at 12,000 rpm for twenty minutes at 4°C, and the recovered supernatant was then subjected to different pull-down assays. Overall workflow of the pull-down assay involving cell lysates is summarised in figure 2.4.

2.2.6.4.2 Pull down assay

To 100 µl of cell lysate, 32.5 µg of the named Affimer reagent was added and incubated at 4°C for overnight. The next day, 15 µl of washed nickel beads (Amintra NiNTA slurry) were added to capture the Affimer-protein complex. After one hour of incubation at room temperature to capture most of the formed Affimer-protein complexes, the complexes were precipitated by centrifuging at 1000 xg for one minute and washed with 300 µl of wash buffer (table 2.9) for five minutes at 1000 xg centrifugation speed. Next, complexes were eluted in 30 µl of elution buffer (table 2.9). The eluates were mixed with 2X SDS loading buffer and subjected to SDS-PAGE electrophoresis as mentioned in section 2.2.3.2 and followed by western blotting analysis.

2.2.6.4.3 Western blot analysis

Proteins separated by SDS-PAGE gel electrophoresis were transferred onto nitrocellulose membrane (Amersham™ Protan™ supported 0.45 µm pore size, GE Healthcare Life Science) in transfer buffer (25mM Tris base, 192mM glycine and 20% (v/v) methanol, pH 8.3) at 25V for thirty minutes using the Trans-Blot Turbo transfer system (Bio-Rad). Next, membranes were blocked in either 5% BSA or 5% (w/v) Marvel milk prepared in TBST (20mM Tris-HCl pH 7.6, 137mM NaCl, 0.1% (v/v) Tween-20) on a rocker for two hours at room temperature. Membranes were washed once for ten minutes in TBST buffer before the addition of primary-unconjugated antibodies (table 2.1) followed by washing steps thrice. Secondary-HRP conjugated antibodies were then added for one hour at room temperature before washing in TBST (table 2.2). Chemiluminescent substrate (Luminta™ Forte western (HRP) substrate, Millipore) was added on to the membranes to enable the visualisation of the bound antibodies using Amersham Imager 60 (GE Healthcare life sciences).

2.2.6.4.3.1 Membrane Stripping for re-probing

In order to detect two different protein targets, membranes were washed in 5 ml of stripping buffer (0.2 M glycine, 0.1% SDS (w/v), and 1% Tween-20 (v/v), pH 2.2) twice for ten minutes, at room temperature. Next, the membranes were washed in 1XPBS followed by two washes in 1XTBST before blocking with either 5% Marvel milk or 5% BSA for one hour at room temperature. After blocking, all the primary and secondary reagents were added according to the standard WB protocol.

2.2.7 Cellular studies: treating cells with Affimers

Cells were serum-starved in their respective growth media for four hours and pre-treated with 100µg/ml Affimers for one hour at 37°C prior to stimulation with different concentrations of the NRG based on the type of the treated cells (25ng/ml for MDA-MB-453 cells or 100ng/ml for BT474 cells, NRG1-β1/HRG1-β1 ECD domain, R&D Systems, Chapter 4) or 25ng/ml EGF (Gibco™, ThermoFisher Scientific). Cells were washed, scraped and lysed as described in section 2.2.6.5 for western blotting using both primary and secondary antibodies listed in table 2.1 and 2.2.

2.2.8 Protein identification by pull-down assay and mass spectrometry (MS) analysis

Following pull-down assay and the separation of Affimer-protein complexes in SDS-PAGE gel, the gel was stained with Coomassie brilliant blue stain and then de-stained in H₂O for a week. Upon efficient de-staining, gels were sent to mass spectrometry (MS) facility at the University of Leeds to excise the desired protein bands from the gel and digesting them by trypsin before being subjected to the MS instrument (figure 2.5).

2.2.9 Data analysis and image construction

The histograms shown in the thesis were constructed by GraphPad PRISM version 7.0 software, while fluorescence-images were analysed by Image J software. Using PyMOL Molecular Graphics Software, and the 3D-structure of the proteins were viewed following the search in the protein data bank (PDB) ID for the desired protein.

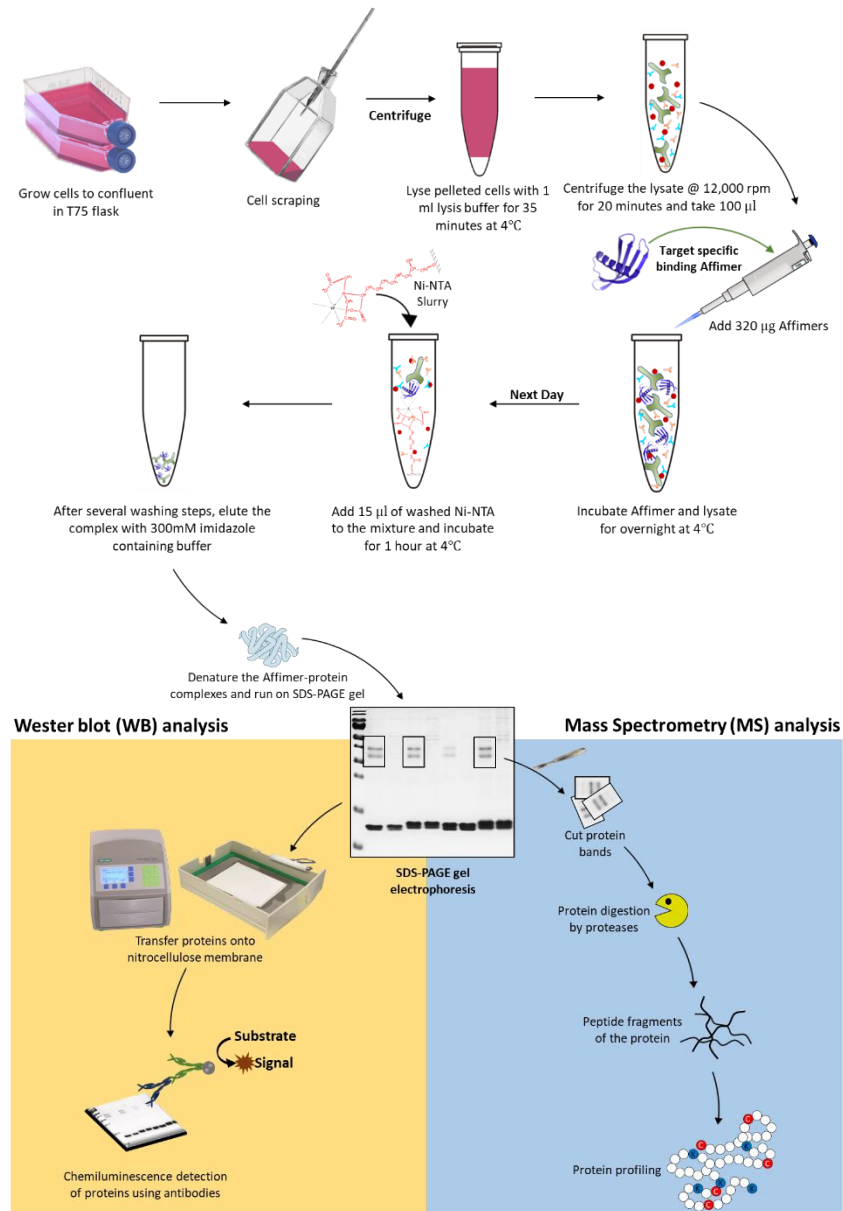


Figure 2.5 Workflow of pull-down assay coupled with either western blot (WB) or Mass-spectrometry (MS) analyses. Protein of interest was extracted from lysed mammalian cells and subjected to separation by SDS-PAGE electrophoresis prior to the start of either MS analysis or WB. In the case of MS analysis, the gel was stained with Coomassie blue stain and de-stained before sending to MS facility for further identification analysis. When WB analysis was performed, separated proteins were transferred into nitrocellulose membrane. Thereafter, protein detection was performed using a set of primary/secondary-HRP conjugated antibodies and HRP-substrate. Using chemiluminescence imaging system, proteins were visually examined.

CHAPTER 3

Phage display-based selection strategies to isolate Affimer reagents against HER2

3.1 Introduction

Among the HER family members, HER2, is the most established biomarker in breast (Hanna et al., 2007; Hicks and Kulkarni, 2008; Varga and Noske, 2015) and ovarian cancer (Tuefferd et al., 2007; Verri et al., 2005). Its overexpression is most commonly assessed by immunohistochemistry (IHC) in which antibodies are used to detect the expression of HER2 in tissue samples (Sarode et al., 2015). However, the historic lack of consistency in HER2 IHC testing initially cast doubt on the reliability of such tests (Tubbs et al., 2001; Press et al., 2005). In an effort to improve the accuracy of the IHC assay, the Food and Drug Administration (FDA) assessed and approved four commercial antibody-based kits to be used in diagnostic laboratories to test HER2 status (Perez et al., 2014a). However, the suboptimal performance of these kits, due to limitations of antibodies is still an issue (Gown, 2016). As such, the use of alternative affinity reagents could potentially address some of the reproducibility issues associated with antibody reagents and are therefore highly sought for diagnostic tests.

The most established method used to isolate alternative affinity reagents is phage display (Smith, 1985). Phage display involves sequential enrichment of a specific binding phage against the antigen of interest. Since the development of phage display in 1985, novel affinity reagents have been screened using this technology to isolate reagents against different targets using a soluble, purified antigen that is anchored to beads or plastic well (Chan et al., 2014; Finlay et al., 2017). Among such affinity reagents are Affimer proteins. To date, a range of Affimer reagents have been isolated and characterised successfully in different molecular applications (Tiede et al., 2017; Lopata et al., 2018; Robinson et al., 2018; Zhuravski et al., 2018).

A critical factor for attaining a successful screen is the quality and the stability of the antigen. Quality refers to not only the purity of the protein but also whether the protein is produced to include any post-translational modifications. Although expression of proteins, such as membrane receptors, in mammalian cells allows correct conformation,

maintenance of their native conformation still remains an issue (Rockberg et al., 2009). As such, many phage display techniques have been developed to screen against cells engineered to express membrane proteins (Lipes et al., 2008). Huang et al., reviewed different membrane protein presentation methods that allow the display of the membrane protein in its native conformation without the need of further expression and purification steps (Huang et al., 2016). Among these methods is the use of native and engineered (transfected cells) cells as the source of the membrane protein (Stark et al., 2017). Owing to the success of such screens in the development of a novel affinity reagents, this chapter assesses the use of cells in the phage display using an Affimer library to isolate reagents against HER2.

Affimer library (Ella2) is based on the 100-residue consensus sequence of plant-derived phytocystatins, which are protein inhibitors of cysteine protease. The library was constructed by controlled peptide insertion (nine amino acids) at the two variable loops for protein-binding activity as described earlier. The degenerate positions (NNN) were introduced into the loops as trimers that presented a single codon for each of the 19 amino acids, excluding the cysteine and other termination codons. This insertion of peptide was achieved by splice overlap extension (SOE) of two PCR products using a codon-selected-semi-trinucleotide primer synthesis system designed and purchased from Ella Biotech. In the first PCR, the synthesised product was extended from the DsbA coding sequence to the first variable loop, while in the second PCR, an introduction of two nine-amino-acid binding regions/loops (BRs) into the scaffold was attained (refer to Figure 1.12 in Chapter 1) (Tiede et al., 2014).

Using such synthesis, no biased amino-acid sequence insertions were detected and the obtained frequency of the different residues encoded at the phage level met the expected Poisson statistics at $5.26 \pm 2.3\%$ for trimer synthesised oligomers using a 19-amino-acid mixture (Tiede et al., 2014). Following ligation of library DNA, 126ng of the library DNA were electroporated into cells of *E.coli* (ER2738). This revealed a library size of 1.3×10^{10} clones, in which 86.5 per cent of clones showed the correct sequence of full Affimer (as verified by testing 96 clones). Only 3.1 per cent of the clones were comprised of the Affimer scaffold with no inserts, and 10.4 per cent of clones showed frame-shifts that occurred in the transition base between the standard nucleotide and trimer coupling (Tiede et al., 2014). Therefore Tiede et al., in 2014, proposed that use of fully-trimer-synthesised oligoes might improve the quality of the library through the reduction of the frequency of frame-shift mutants.

The main concern in designing the library was to keep a balance between the theoretical and the achievable library sizes to enable the majority of library sequences to undergo selection (Lendel et al., 2006; Wahlberg et al., 2003; Huang et al., 2018). In the Affimer library, a total of 18 positions were randomised (insertion of nine randomised residues per loop in which each residue reflected all 19 amino acids). This produced an unrealistic theoretical number of amino acid sequences (about 1.04×10^{23}) that could not be obtained following bacterial transformation (1.3×10^{10}), resulting in a limited library size and diversity (Table 3.1) (Tiede et al., 2014). However, this limitation in library design could be solved by limiting the theoretical library size to obtain a representative library, which could be attained by bacterial transformation (Huang et al., 2018). This could be achieved by only randomising the residues that seemed to be crucial for interaction with a target according to the available crystal structures of the Affimer complexes. Such exploration of the important residues has been published (Hughes et al., 2017) and currently remains the work in progress in different research (data obtained by verbal communication from the scientist creating the new Affimer-based phage libraries).

Library	Randomisation	Theoretical size	Number of individual clones	Percentage of correct Affimer sequences
Affimer (Ella2)-library	(NNN)- 19 amino acids Nine positions randomised per binding loop (total of 18 positions)	19^{18} 1.04×10^{23}	1.3×10^{10}	86.5 %

Table 3.1. Analysis of constructed Affimer (Ella2) library. The randomisation scheme is described by the degenerated nucleotides (NNN), in which all 19 amino acids were used except the cysteine and stop codons. The actual (theoretical) size of the library was calculated based on the randomisation position and the number of amino acids used in the scheme. The number of individual colonies was calculated to indicate the experimental size of the library by performing a serial dilution after bacterial electroporation. The percentage of correct sequences of Affimer within the phagemid vector (pDHis) was verified by DNA sequencing of 96 randomly picked clones from the library (Tiede et al., 2014).

Following the approach to reduce the theoretical size of the library, the quality and diversity of the affibody library was improved through construction of a new library of a theoretical size of 2.4×10^9 (Cyranka-Czaja and Otlewski, 2012). In this new library, only eight binding essential amino acids were randomised using the degenerative synthesis approach (NNC; hard randomisation) instead of the procedure used with the original affibody library, in which 13 amino acids located at two of the three helices were randomised. Even with this smaller theoretical size, the researchers obtained a representative phage library after bacterial transformation with a size of 2.1×10^9 with an 86 per cent level of correct sequences as verified by the sequencing of 36 random clones (Cyranka-Czaja and Otlewski, 2012).

Furthermore, the researchers also proposed that the application of soft randomisation schemes (such as, KMT or HWC) in which only four to six amino acids were used to randomise more than eight positions could generate binders of low-nanomolar affinity, which would mimic the affinity achieved with the full-length antibodies (Cyranka-Czaja and Otlewski, 2012). It was also shown that such minimal diversity enabled the selection of high-performance single domain binders. Another factor that can affect the library performance is the efficiency of displaying phage on cells. The display level of phage was found to be improved through use of a polyvalent display approach (fusion to M13-pVIII coat protein) instead of the monovalent system (fusion to M13-pIII coat protein) adapted by most libraries, including the Affimer library (Ledsgaard et al., 2018).

In this chapter, we characterise and assess different strategies for phage selection of Affimer reagents targeting HER2. We performed a recombinant-protein based screen, whole-fixed cells based screen (HER2 transfected *vs* non-transfected cells), and we also did a combined-phage screen alternating fixed-cells overexpressing HER2 and the recombinant purified ECD of the receptor. In addition, any generated HER2 binding Affimers may represent a useful molecular recognition tool in different diagnostic applications, involving cell staining.

3.2 Results

3.2.1 Isolating Affimers against the recombinant protein of the ECD of HER2

The extracellular domain (ECD) of HERs have a high number of intramolecular disulfide bond and are also highly glycosylated making them difficult to express in a bacterial system. In addition these receptors are glycosylated, masking potential epitopes that affinity reagents may bind to (Rockberg et al., 2009). However, these proteins can be expressed in other systems and numerous alternative affinity reagents, including affibodies (Lee et al., 2008), Affimers (Tiede et al., 2017) and DARPins (Goldstein et al., 2015) have been successfully isolated against a range of membrane targets using recombinant proteins. In addition to these published targets, the Bioscreening Group at Leeds has also isolated Affimer reagents against HER2. The amino acid sequence of the variable regions, also known as binding loops, of all HER2 binding Affimers is shown in table 3.2.

Binder name	Binding loop-1	Binding loop-2
D11	H F V G K F Y H N	E F Q M G G I W K
H7	R Y E G R G Y H N	H Y I M K Q H W H
D7	W H K S W S P T T	S L I N A Y Y D I
E8	Y Q S Q G K P L E	A D G S A A F M F
F9	M E P D A S W W D	Y E E L S G Q H Y
E12	S W H Y Q S - - -	V E M L E Y Q T W
H9	N W F Y N S - - -	T E V Y N N K K M
H8	R F W D S H Y Q H	C G G G F Y Y H Y

Table 3.2 Amino acid sequence of the binding loops of eight different HER2 binding Affimer. These binders were recovered from panning against the recombinant protein of the ECD of the HER2 receptor. The bio-panning was kindly performed by the Bioscreening Group (University of Leeds, UK). See appendix A for amino acid details.

3.2.2 Selection of Affimers on whole-fixed cells engineered to overexpress HER2

Given the possible structural changes of HER2 upon cell fixation (Li et al., 2017) and due to the high specificity of Affimers for protein conformation (Tiede et al., 2014), it was questionable whether the isolated eight binders would bind to HER2 in fixed cells. Therefore, we decided to test the potential of isolating binders from fixed-HER2 transfected cells. The reasons for using transfected fixed cells include: (1) fixing cells with 4% paraformaldehyde is widely used procedure in IF (Webster et al., 2010); (2) using fixed monolayer of cells enables vigorous washing steps without the risk of losing cells during the screen, thereby removing non-specific phage more efficiently; (3) many studies have demonstrated the advantageous use of transfected cells in phage display screens (Lipes et al., 2008; Yoon et al., 2012; Yuan et al., 2008).

Prior to the start of the screen, the transfection efficiency and stability were confirmed by immunofluorescence staining, in which the HER2-HB2 transfected cells showed high level of HER2 expression compared to the non-transfected (HB2) cells (Figure 3.1 A). After confirming the transfection efficiency, we started the screen by depleting the naïve Affimer library on non-transfected HB2-cells followed by a selection process on the HER2-HB2 transfected cells. After four cycles of panning, 32 colonies out of 1.9×10^6 of total recovered colonies from the last panning round were randomly picked and screened by cell-based phage ELISA (figure 3.1 A and B). As a common practice in BSTG, a range of 24 to 48 colonies considered as a manageable number of colonies to be assayed using low throughput ELISA assay. So, initially this range of colonies was selected randomly and assayed in order to evaluate the binding specificity. If ELISA assay showed 50% of colonies were target-specific no more colonies were selected, but when no binding colonies were obtained, then more colonies were picked and assayed to determine whether to stop the screen or to start a new screen.

Based on the poor enrichment level of the number of recovered colonies between target and non-target in all selection rounds, we decided to perform an initial phage ELISA assaying 32 colonies only in order to evaluate the binding specificity of phage clones towards target cells (HER2-HB2 transfected cells).

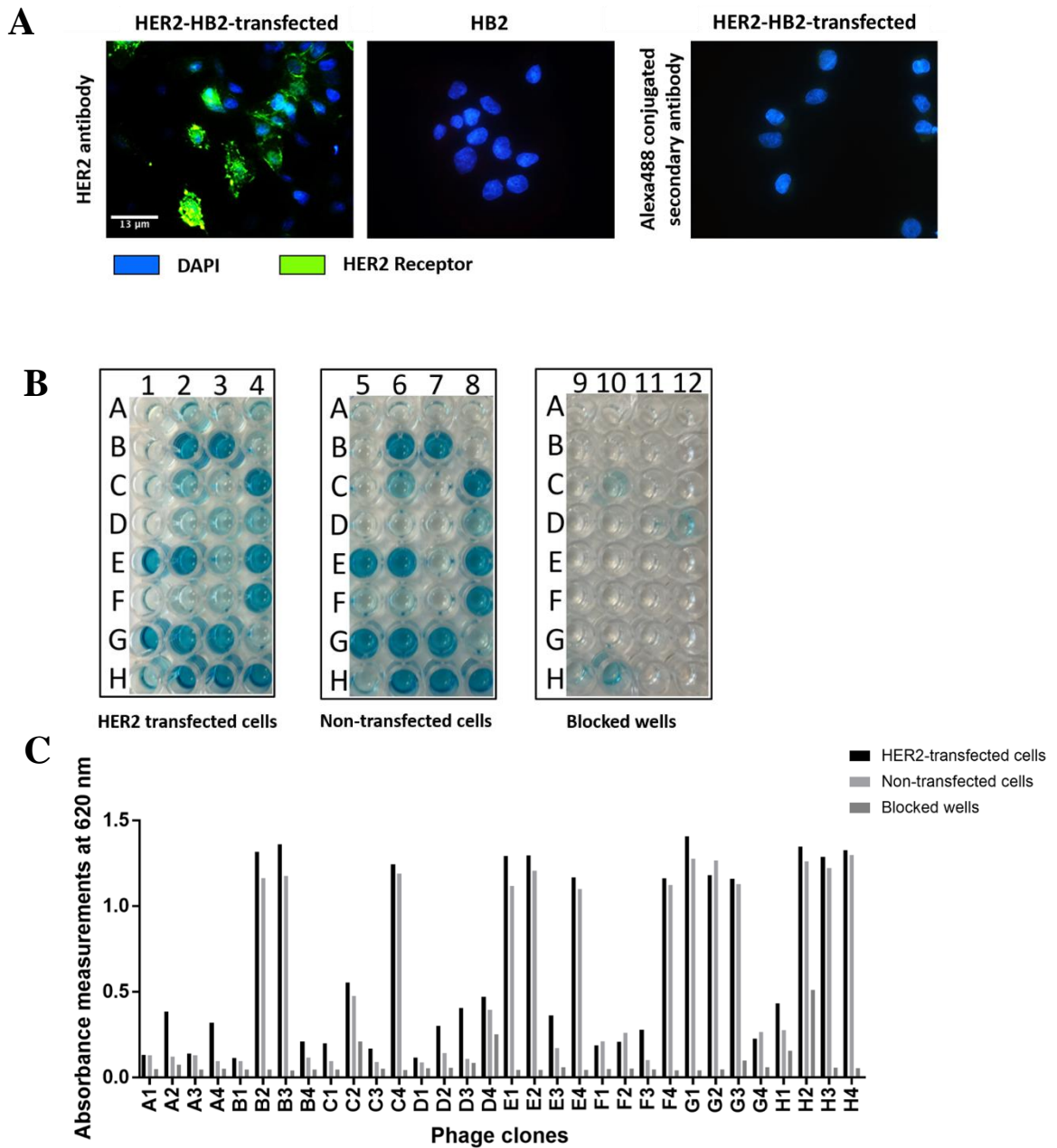


Figure 3.1 Demonstrating the unsuccessful isolation of Affimers using cell-based screen against HER2-HB2 transfected cells. (A) Immunofluorescence staining showing an efficient transfection of HER2-HB2 transfected cells with high expression of HER2 (green colour) compared to the other HB2 (non-transfected) counterpart. The HER2 was identified using rabbit anti-HER2 polyclonal antibody followed by anti-rabbit (IgG) Alexa488 conjugated antibody (scale bar = 13 μ m). (B) Following four rounds of panning, 32 colonies were randomly picked and screened in ELISA assay. Each clone was tested against transfected cells, non-transfected cells, and wells containing 2X blocking buffer. (C) The absorbance measurements at 620 nm for each well showed equal binding preference to all wells containing transfected, non-transfected cells or no cells. The absorbance measurements plotted in the histogram represent the mean value of duplicated measurements of one experiment. ($n = 2$ for both IF immunofluorescence staining of cells and phage ELISA).

Wells with no cells, containing 2X blocking buffer, were also included to serve as negative controls (figure 3.1 B). Binding of the phage clone with HER2 was detected using an anti-fd phage antibody conjugated with HRP and the 3,3',5,5'-tetramethylbenzidine (TMB) substrate. Absorbance readings for each well was measured at 620 nm, as shown by the histogram in figure 3.1 C. Interestingly, none of the isolated Affimers showed specific staining for HER2 expressing cell strain (figure 3.1 C). This highlighted the need to further optimise our panning strategy. The whole screening process and the outcome of the screen is illustrated in figure 3.2 A and B, respectively. The phage screen was performed only once; however, a repeat of the screen using non-engineered HER2 overexpressing cell line is planned as part of the future work.

3.2.3 A combined phage selection strategy

It was speculated that we could alternate panning rounds using recombinant HER2 protein and a cell line overexpressing HER2 to isolate Affimer reagents that show specific binding to native HER2 protein. Recombinant proteins have been shown previously as a way of limiting the background of non-specific binders when using only cells for phage display (Andersen et al., 1996). Following this strategy, the first and the third panning rounds were performed using HER2 protein while the second used a breast cancer cell line (MDA-MB-453).

Two recombinant proteins of the ECD of HER2 (Fc-tagged and non-tagged protein) were purchased and biotinylated. Biotinylation is used to present proteins on streptavidin coated plates, helping to maintain conformation. Biotinylation of the Fc-tagged HER2 protein and HER2 was determined by ELISA (figure 3.3). The HER2 protein failed biotinylation showing low levels by ELISA after two repeats while the Fc-tagged version showed successful biotinylation. It was hypothesised that the purchased non-tagged HER2 protein may be degraded. This could be confirmed with SDS-PAGE gel coupled with western blotting or via the use of ELISA in which the protein would be detected by HER2 antibody.

The percentage of biotinylated protein present in the mixture was not determined by highly sensitive and quantitative techniques such as MS. However, the adapted protocol for random biotinylation of the protein (section 2.2.2.1.1 and 2.2.2.1.2) had been optimised previously by the BSTG, indicating that an A_{620nm} of ≥ 1.4 represented 100% biotinylation (data obtained through verbal communication).

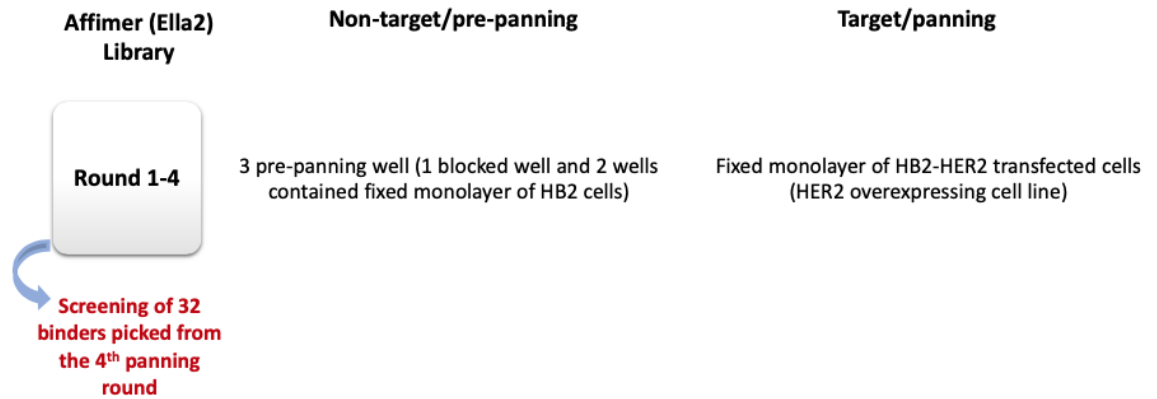
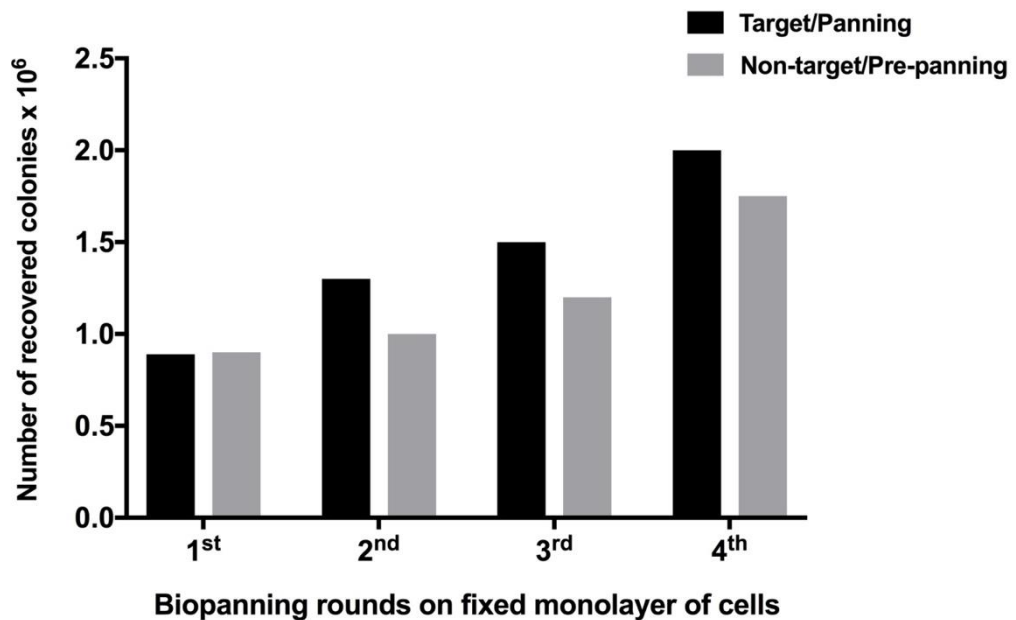
A**B**

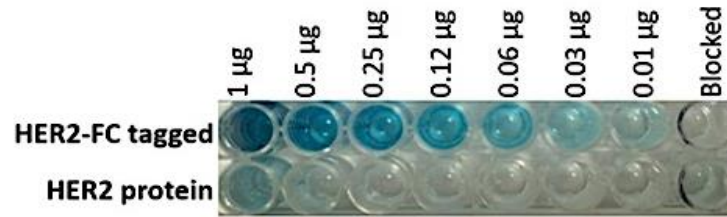
Figure 3.2 Phage screen on fixed monolayer of engineered (HER2-transfected) HB2 cells to isolate binders against HER2 using the naïve Affimer phage library. (A) Schematic overview of the cell-based phage screen on engineered HB2 cells to isolate binders against HER2 by phage display using naïve Affimer library. Four rounds of selection were conducted, including pre-panning steps on two HB2 cells (non-HER2-transfected) and blocked wells to ensure complete removal of the non-HER2 binding phage clones. From the final panning round (4th round), 32 colonies of a total of 1.9×10^6 of recovered colonies, were randomly picked to be assayed in phage ELISA for the characterisation of their binding specificity towards HER2 expressing cells (HB2-HER2-transfected cells). (B) The outcome of the screen was estimated by the number of total colonies recovered from target plate of HER2-HB2-transfected cells compared with control non-target samples (HB2 cells). The numbers of colonies plotted in the histogram represent the mean number of duplicate counts that was performed manually using a marker pen. All colonies were counted from 1 μ l plates and then multiplied by the total volume of phage-infected bacterial cell cultures (8 ml). ($n = 1$)

As such, there indicated absorbance measurement was used as a cut-off point to estimate the degree of the biotinylation in relation to the determined absorbance shown in figure 3.3.

Owing to the successful biotinylation of the Fc-tagged HER2 protein, we decided to only use this protein in the bio-panning process. In pan rounds 1 and 3, a negative selection step was performed using a different Fc-tagged protein to remove any Fc binders. During the panning round against MDA-MB-453, a fixed monolayer of U87-MG cells (glioblastoma cell line with no detectable HER2 levels) was used to pre-pan. The outcome of this strategy was evaluated by phage ELISA, in which the binding ability of the 40 picked clones of total 2×10^6 colonies recovered from the target plate of the final panning round (3rd round) was assessed. A control Fc-tagged protein and blocked wells were also, used as negative controls. Based on the absorbance measurements, four clones showed specific binding to HER2 protein (Figure 3.4 A and B). Most of the 40 screened colonies were not functional, as they showed no binding events. After DNA sequencing, all the HER2 specific binders were appeared to be one binder, which was the **D11** (Figure 3.4 C and table 3.2). Figure 3.5 illustrated the schematic overview of the combined-phage screen (A) in addition to the overall outcome (B) indicating the efficiency of the screen based on the total number of recovered colonies after each panning round. Although we managed to isolate one HER2-binding reagent (**D11**), the outcome of the screen (figure 3.5 B) was poor compared to previous screens against other protein targets. As such, we continued to further optimise the screening strategy.

The combined phage screen to isolate HER2 binders was performed only once and due to its outcome, we speculated that further optimisation adopting another strategy, in which cells were introduced after 3 rounds of selection on recombinant protein would be the optimal approach to sort out the outcome of the protein-based screens using cells. As such, we decided not to repeat the combined phage screen but instead go forward and try another approach of cell-containing phage screen.

A



B

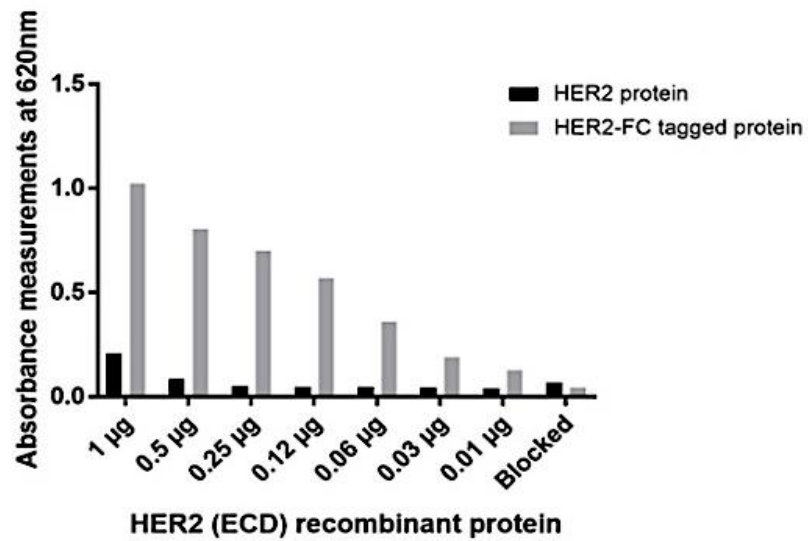
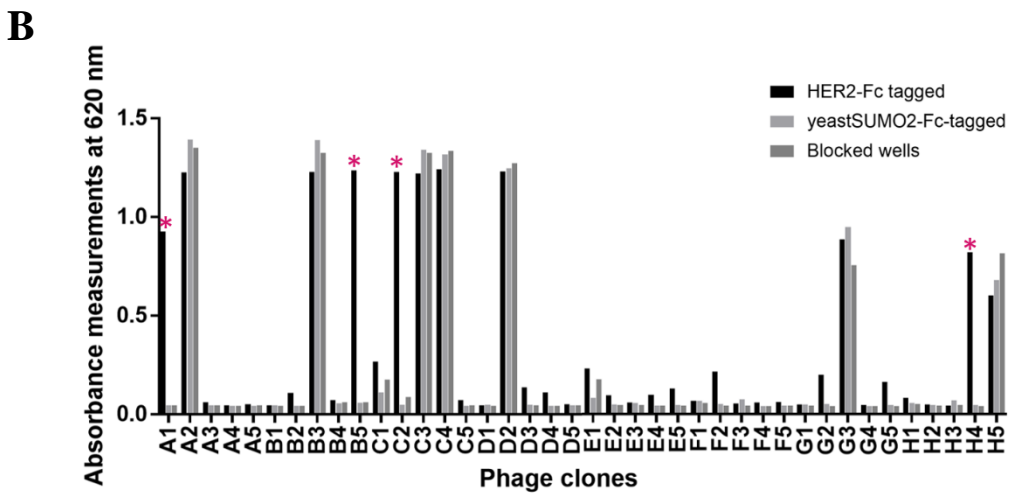
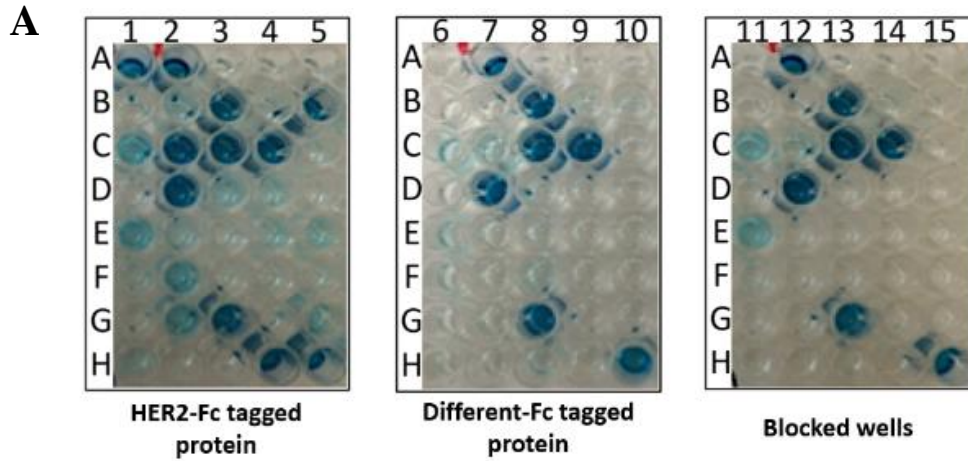


Figure 3.3 ELISA assay examining the efficiency of the amine-based biotinylation of the HER2-ECD protein used for the phage display screening. (A) Showing the strip for different dilutions of the biotinylated recombinant protein. Negative control (PBS) was included. (B) Presenting the absorbance measurements of the wells taken at 620 nm. The plotted absorbance measurements represent the mean value of duplicated measurements of one experiment. ($n = 2$).



C

Binder name	Binding loop-1	Binding loop-2	Frequency
* Anti-HER2 (D11) Affimer	H F V G K F Y H N	E F Q M G G I W K	4

Figure 3.4 Showing the phage ELISA results from isolating Affimers using alternate proteins and cell-based screening. (A) After three panning rounds, 40 colonies were randomly picked and tested against the HER2 (ECD) protein, yeast SUMO-Fc tagged (negative control protein), and wells containing 2X blocking buffer. (B) Graph showing the results from the phage ELISA. Hits are highlighted with an *. The plotted absorbance measurements in the histogram represent the mean value of duplicated measurements of one experiment. (C). Sequences results of the specific binder showed the isolation of a single reagent, which is the **D11** binder. See Appendix A for amino acid details. ($n = 2$ for phage ELISA assay and DNA sequencing).

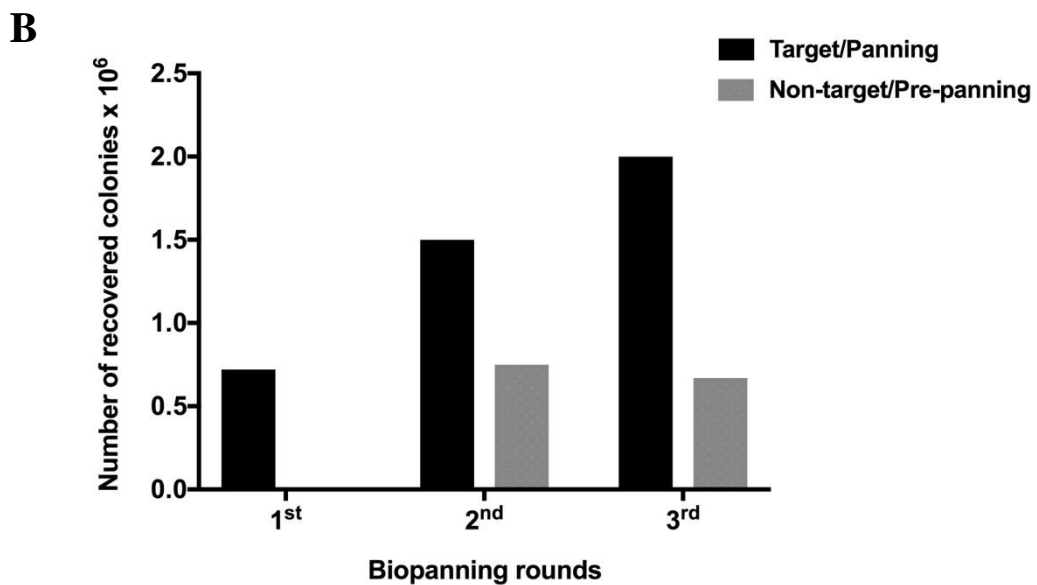
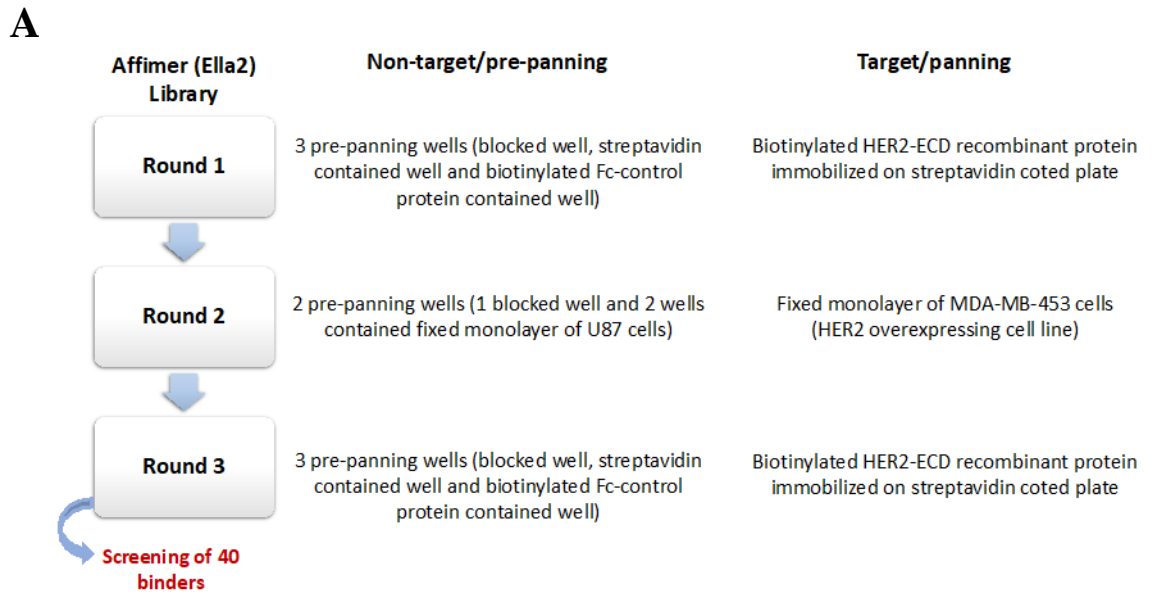


Figure 3.5 Selection outcome of the combined-phage screen to isolate HER2 binder.

(A) Schematic overview showing that for the first and third selection rounds, the naïve Affimer library was pre-panned on three pre-panning wells (blocked well, streptavidin-contained well and a third that contained immobilised biotinylated Fc-control protein) before panning on biotinylated HER2-ECD target protein immobilised on streptavidin-coated wells. For the second panning round, the library was pre-panned on three wells (one blocked well and two wells that contained U87 cells, which do not express HER2) and then selected on the target-expressing cell (fixed monolayer of MDA-MB-453 cell line). From the library pool after the last round of selection, 40 randomly picked binders were screened for binding to HER2-ECD recombinant protein using phage ELISA assay.

(B) Histogram showing the total number of colonies recovered from each panning round as counted from the 1µl agar-plate containing the phage-infected bacterial cells (ER2738 cells). The counted number was multiplied by the total volume (8ml) of bacterial cell culture. The colonies were counted twice, manually, using a marker pen and the plotted numbers represent mean value of duplicated counts. ($n = 1$).

3.2.4 Selecting enriched pool of HER2-binding Affimers on cells enhanced the diversity of isolated binders

It was speculated that increasing the panning against cells using an enriched HER2 phage pool may increase the number of clones isolated that can bind to native HER2 (Gijs et al., 2016). Therefore, we proposed an approach to increase the rounds of panning against HER2 protein followed by two selection rounds on cells. We chose to use the enriched library pool of the third panning round from the screen against HER2 recombinant protein in order to start the selection process against fixed MDA-MB-453 cells. The enriched library was derived from the screen performed by the Bioscreening group as it contained diverse variants of HER2-specific phage clones compared to the screen performed against the HER2-Fc protein. During the panning rounds on cells, a depletion step on the HER2 negative fixed cancer cells (MCF7 breast cancer cell line) was performed in the first round only (figure 3.6 A). The use of a depletion step at this stage was made to remove binders, which were not able to recognise epitopes at the fixed conformation of the receptor, thus allowing the amplification of specific binders (section 2.2.2.2.3).

After the final round of selecting the enriched pool on fixed cells, 48 colonies out of a total recovered 3×10^6 colonies (figure 3.6 B), were randomly picked and screened by cell-based phage ELISA (figure 3.7 A). The absorbance measurements at 620 nm of each wells confirmed the binding ability of 20 clones as they showed increased binding of cells overexpressing HER2 (figure 3.7 B). From experience, cell-based phage ELISA, generally show weak signals in negative controls. Following ELISA, all the 20 positive hits were sequenced, and sequencing revealed isolation of two binders (**D11** and **H7**). The **D11** binder appeared 19 times in the screen compared to the **H7** that appeared only once (figure 3.7 C, table 3.1). The outcome of this screen strongly suggests that **D11** is the best binder that can bind to HER2 on cells and recombinant protein. In addition, preselecting Affimer library on pure recombinant protein for multiple panning rounds prior to selecting it on cells can lead to higher enrichment of Affimer reagents. The phage screen was performed only once as proof-of-principle examining a new approach of selection combining cells and proteins in a single screen. However, using such approach for selecting binders against other targets could be performed in the future to further assess the efficiency of the selection approach.

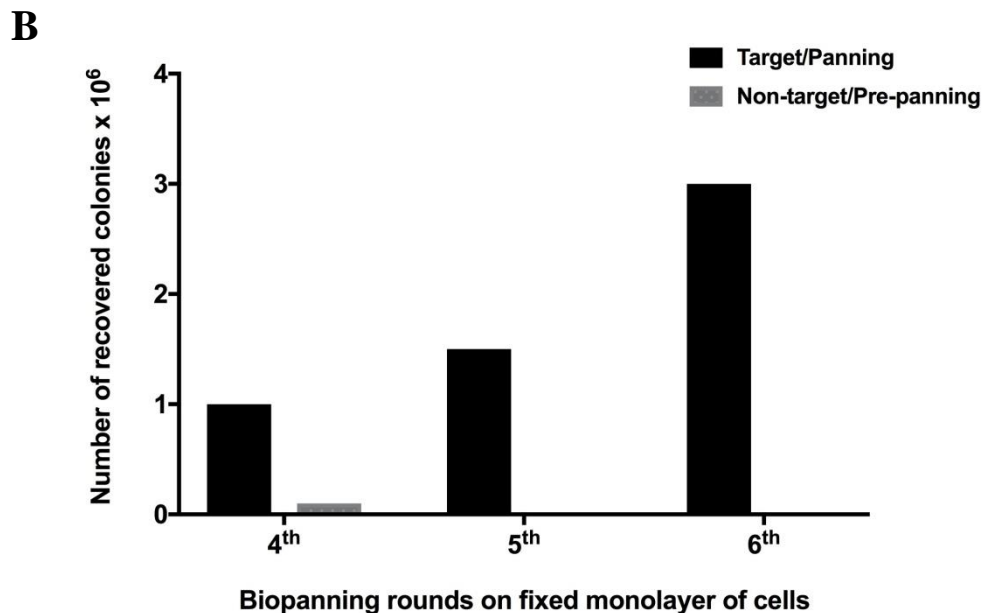
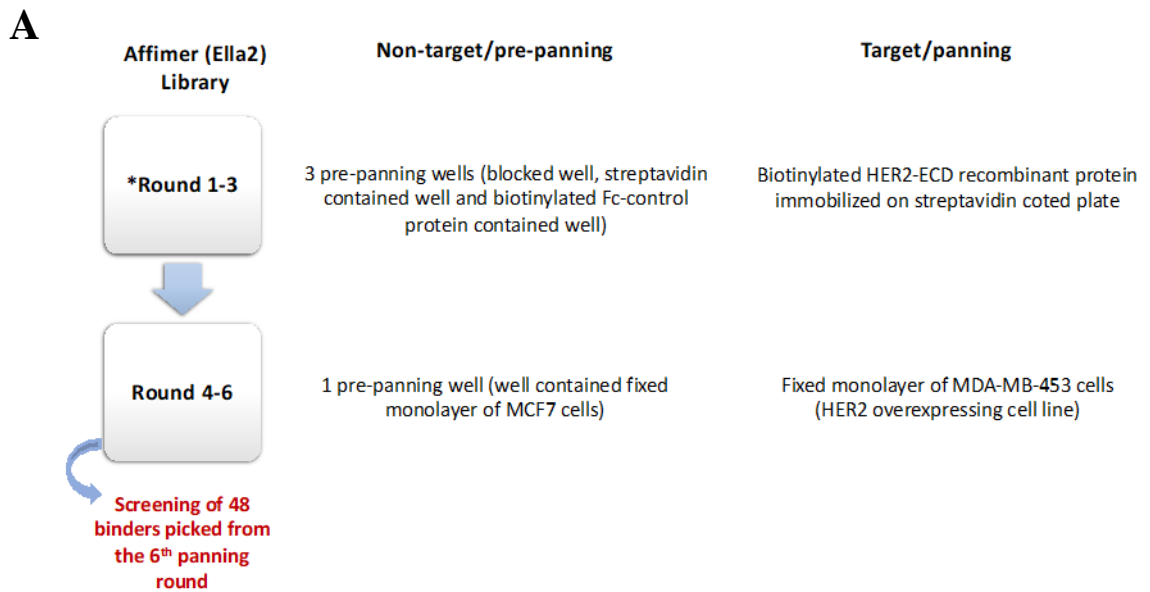


Figure 3.6 Affimer phage screen on HER2-overexpressing cells (MDA-MB-453) after multiple enrichment rounds on biotinylated HER2-ECD recombinant protein.

(A) Affimer phage library was selected on biotinylated HER2-ECD recombinant protein immobilised on streptavidin-coated wells to isolate binders against HER2. After three panning rounds on recombinant protein, the phage pool from the third panning round was used to start the selection on cells. The enriched phage pool (from panning round three) was used to start phage sorting on fixed monolayer of MDA-MB-453 after being pre-panned on MCF7 cells (HER2-deficient cells). The (*) indicates that protein-based screen (round 1-3) was performed by the BSTG. After 3 rounds on protein and three other rounds on cells, 48 colonies from the last round on cells (6th round) were randomly picked and assayed in phage ELISA. (B) Histogram showing the output of the screening after three selection rounds on cells. The plotted numbers of colonies in 1 μ l plates multiplied by the total volume of phage-infected ER cells (8 ml) represent the mean of duplicated counts, which was calculated manually using a marker pen. ($n = 1$)

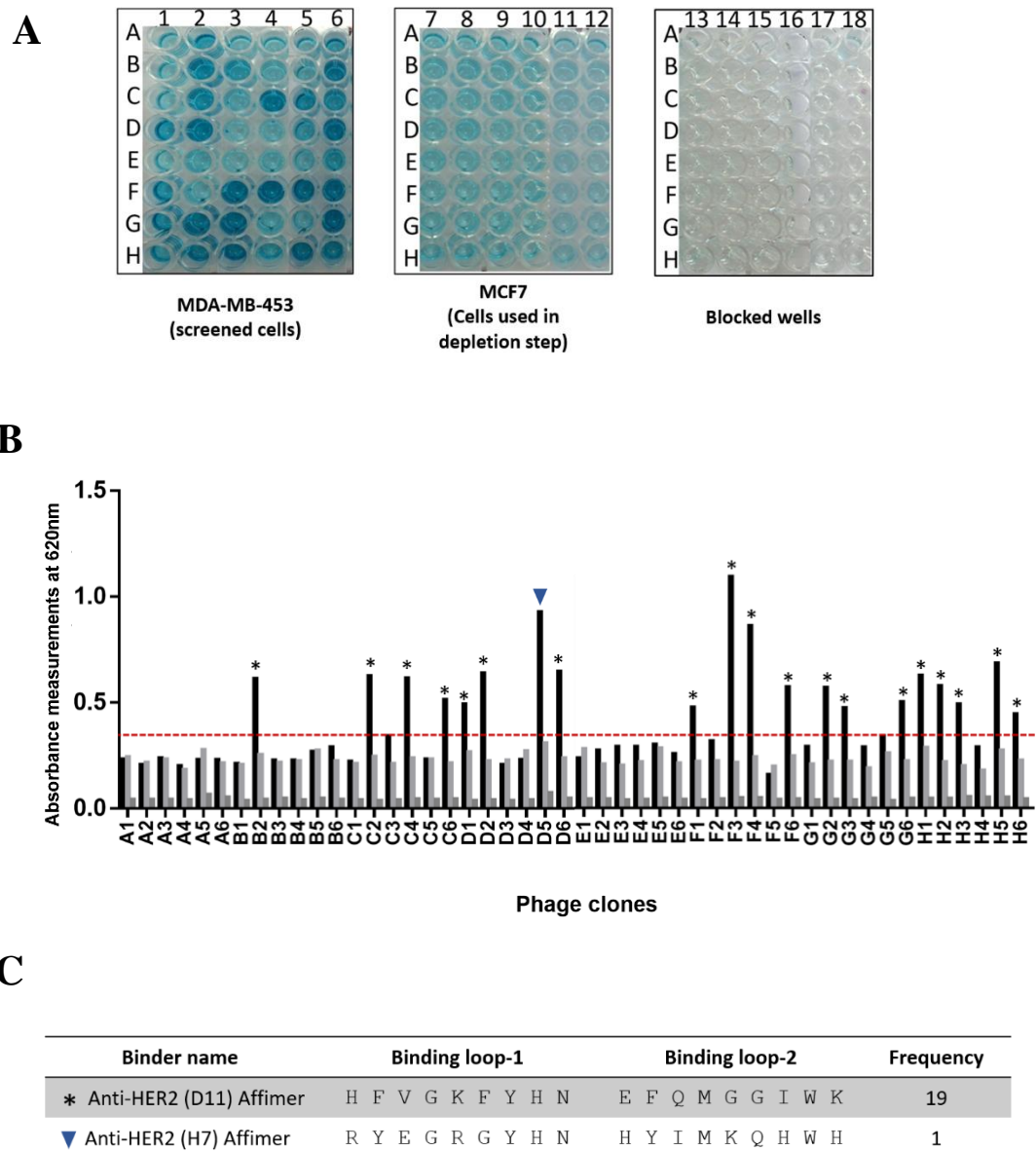


Figure 3.7 Showing the phage ELISA from clones isolated after three panning rounds against recombinant protein and three against cells. (A) 48 colonies were randomly picked, and a phage ELISA was performed. In column 1 to 6, the selected clones were tested against fixed monolayer of MDA-MD-453 cells. Whereas, MCF7 fixed cells along with the 2X blocking buffer were used as corresponding negative controls in column 7 to 18. Phage binding was detected using anti-fd bacteriophage HRP conjugated antibody and visualised with TMB. **(B)** The absorbance measurements at 620 nm of each well were taken and blotted in a histogram. An arbitrary cut-off (red line) was used to determine which clones would undergo sequence analysis based on the differences in the signal intensity (clones showed a ≤ 2 -fold increase in the intensity of the signal detected in target cells were eliminated). Indicated columns are the ones taken forward. **(C)** Showing the amino acid sequence of the binding loops of the recovered clones (**D11** and **H7**). See Appendix A for more details about amino acids.

3.2.5 Molecular cloning, bacterial production, and purification of eight isolated HER2-binding Affimers

All HER2-binding Affimers listed in table 3.2 were amplified by PCR using primers containing *NheI* and *NotI* restriction site (section 2.2.3.1) and cloned into the pET11a expression vector (data not shown). The cDNA of each binder was extracted from colonies and sequenced to confirm successful cloning (GATC, biotech AG, data not shown). Affimer cDNA were transformed into BL21 (DE3) cells for protein expression.

E.coli is the most commonly used system for the production of recombinant proteins. However, the achievement of high level of protein expression can be a challenge. To overcome possible challenges and maximize the yield of produced Affimer proteins, some parameters that affect cell growth and protein expression must be optimised (Kaur et al., 2018). The ideal scenario would be obtaining an optimal condition in which both protein yield per cell and cell densities per volume are high, but this cannot always be reached. Therefore, we focused on optimizing the cell growth conditions to obtain high cell densities compensating for possible low protein production per cell. Our optimisation experiments involved altering some growth conditions such as aeration (shaking speed), temperature, induction, and the cell density at which induction was started.

3.2.5.1 Optimisation of temperature, shaking speed and time for production of Affimers

Generally, 200-250 rpm is the standard speed for most shake flask culture, therefore, we decided to examine two shaking speeds, 230 rpm and 150 rpm in 30 ml cultures. Post-induction, cultures were incubated for 6 hours and overnight (16-18 hours) at 25°C. Affimer protein from the two shaking speeds at different intervals was purified and the yield was measured. There was little difference in total yield of proteins (figure 3.8 B), however, a large amount of Affimer proteins was left unbound (figure 3.8 A) in overnight cultures at both 230 and 150 rpm suggesting overnight culture produces more protein overall. Unbound protein is most likely due to the too little NiNTA resin being used during purification.

It is worth mentioning that a control lysate of non-transformed bacterial cells was not included and this could be a drawback affecting the authenticity of the experiment; however, it was suggested by BSTG that a lysate of the non-transformed cells would not

represent the appropriate negative control as it would not show the level of the leaky expression of non- isopropyl β -D-1-thiogalactopyranoside (IPTG) induced cells (Studier and Moffatt, 1986). Vectors encompass the T7 promoter system, such as the pET11 vectors, in which the target gene (in the case of this research, it is the Affimer sequence) is cloned behind a promoter that is recognised by the T7 RNA polymerase (T7 RNAP), which is usually provided by the bacterial genome (DE3 strain of BL21 cells) (Studier and Moffatt, 1986).

T7 RNAP is under the transcriptional control of the lac UV5 promoter and thus when the system is induced by lactose or its non-hydrolysable analogue, IPTG, the conformational structure of the active repressor that blocks the T7 RNAP from binding to the T7 promoter region will change, rendering it inactive to bind and thus initiate the transcription of Affimers (Moffatt and Studier, 1987;Stano and Patel, 2004;Fernandez-Castane et al., 2012). As such using the non-induced lysate will evaluate the tightness of the control provided from the used BL21 (DE3) bacterial strain in comparasion to the IPTG-induce lysate. In our research, using the indicated bacterial strain provided sufficient control of Affimer expression as the level of the leaky expression of Affimer in the uninduced cultures was very small compared with the expressed amount of Affimers in the induced counterparts as confirmed by western blot analysis (data not included and confirmed by different researchers). After purification, the uninduced cultures yielded about 0.02 mg/ml of Affimer protein compared with a yield of 1.5-2 mg/ml in the induced cultures (data provided from other Affimer-based research).

Next, the incubation temperature post induction was optimised. Using the optimized shaking speed (150 rpm), a sample of 2ml from 50 ml cell culture was harvested at 2, 4, 6 and 16 hours. The amount of Affimer protein produced was assessed on an SDS-PAGE gel (figure 3.6). 0.5mM of IPTG was added to all cultures after inoculation with the overnight culture and the incubation was started when an OD_{600nm} reached 0.7-0.8. After 6-hour, the amount of protein produced was greatest at highest temperature, however, in the overnight cell cultures started to die at 30 and 37°C based on the measured optical density measured after overnight culturing. Therefore, for shorter incubation times 37°C is the best at shaking speed of 150 rpm and for longer incubation time 25°C at 150 rpm is the best. Our results here further confirm the advantageous effect of both low temperature and low shaking speed on the production level of Affimers.

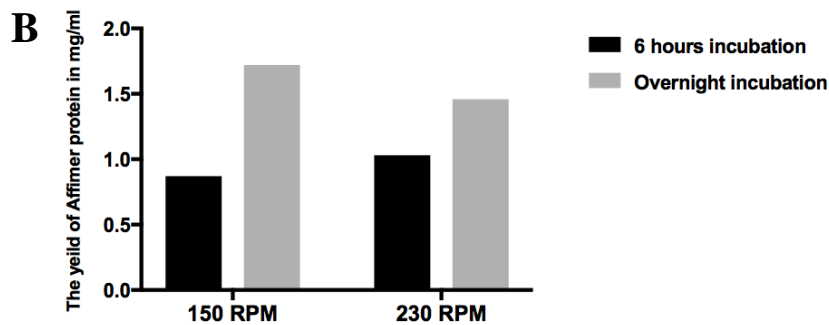
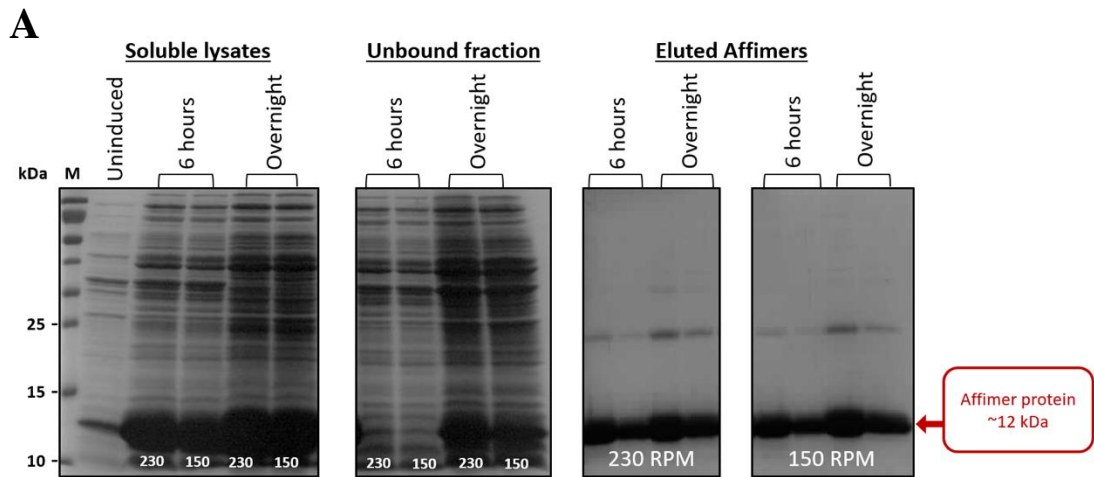


Figure 3.8 The effect of different shaking speeds on the production of Affimer proteins. The expression was induced by 0.5mM IPTG at 25°C for overnight and different shaking speeds (rpm). (A) 5 μ l of sample volume of soluble lysates, unbound fractions and purified Affimers obtained after overnight or 6 hours at 230 and 150 rpm shaking speed were loaded and the gel was stained with Coomassie blue. A culture where the expression of Affimers was not induced by IPTG used as negative control. (B) Column chart showing that the highest increase seen at 150 rpm speed of which most of the Affimers were captured on the agarose beads compared to the 230 rpm. Due to the incorporation of cysteine residue, formation of Affimer dimers were detected at an approximate mass of 24 kDa. ($n = 1$)

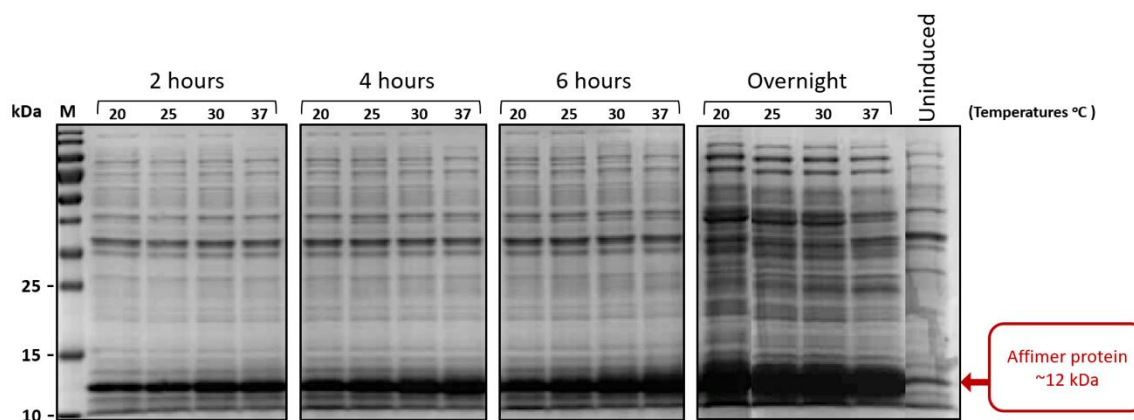


Figure 3.9 SDS-PAGE analysis of Affimer protein produced at different temperatures. The expression was induced with 0.5 mM of IPTG started at optical density (OD_{600nm}) of 0.7-0.8 and incubated at 20, 25, 30 and 37°C for overnight with 150 rpm shaking speed. 3 μ l of soluble lysates was loaded in to an SDS-PAGE gel and the gel was then stained with Coomassie blue. Un-induced cell culture was used as negative control. ($n = 1$)

3.2.5.2 Optimisation of induction of Affimer production

After optimising the temperature and the shaking speed, the next step was to determine the optimal OD of the culture for induction and the optimal concentration of IPTG. Initially, two 50 ml cultures were inoculated with 2 ml of start culture and incubated at 37°C at 230 rpm until the optical densities (OD_{600nm}) of 0.5 and 0.7 were reached. The reason behind choosing these two optical densities is that they represent the lowest and the highest densities usually used in our laboratory to produce different Affimer proteins. The cell cultures were then divided into four subcultures containing 50 ml each in order to add a range of different IPTG concentration starting with 0.05, 0.1, 0.5 and 1mM. Un-induced transformed cells were also used as a negative control. The cells were then allowed to grow overnight at 25°C at 150 rpm after the addition of IPTG. At the end of the incubation time, the optical density of all cultures was measured, and cells were harvested for purification. 5 μ l of both soluble and unbound protein fraction of each subculture were analysed by SDS-PAGE gel (figure 3.10 A).

Cell cultures that were induced at 0.7 OD_{600nm} showed slightly higher cell densities. However, there was little difference in cell density between cultures induced with different IPTG concentration at an OD_{600nm} of 0.5 and 0.7 (figure 3.10 B). Both 0.05 and 0.1mM of IPTG showed the highest level of soluble Affimer protein (figure 3.10 A). The lower level in yield at higher concentrations of IPTG could be due to overwhelming the

folding machinery in the cell leading to protein accumulation in the insoluble fraction (Sorensen and Mortensen, 2005). A basal level of Affimer production was observed in the un-induced transformed cell culture, and that may indicate the need of optimising the amount of glucose in the media to suppress the T7 promoter. Although starting the induction at an optical density of 0.7 with low IPTG concentrations did show better protein synthesis, no difference was noticed in the yield of Affimer proteins obtained after the purification (data not shown). This can be reasoned to the limited capacity of the agarose beads used in the purification process which affected the capturing of the protein as proved by the observed bands in the unbound fraction of different cultures (figure 3.10 A).

To further confirm the best OD_{600nm} for induction we set another experiment where a range of cell densities from 0.4 up to 1 were tested. In this experiment, bacterial cell cultures were grown till reaching the desired optical density prior to induction with 0.1 mM of IPTG. After overnight culture at 25°C at 150 rpm, cells were harvested, and cell densities were measured. In addition, the Affimer proteins were purified and the yield was measured. 5 µl of all soluble and the unbound fractions alongside the first batch of eluted Affimer proteins were run on an SDS-PAGE gel (figure 3.11). Little difference was observed in all tested time points as cells were able to produce high level of Affimer protein albeit at slightly lower level at 0.4 OD_{600nm} (figure 3.11 A). However, by calculating the yield (figure 3.11 B), we concluded that inducing at OD_{600nm} of 0.8 yield slightly more protein. Our conclusion was based on increase in the OD of cells and the amount of purified Affimer (figure 3.11 B).

Cultures induced at low density of 0.4 showed low protein outcome (figure 3.11). Thus, starting at low optical density was too early for cells to produce enough protein. On the other hand, inducing cells at late-exponential phase (OD_{600nm} of 0.9 and 1) resulted in a slight reduction of cell density and the concentration of protein (figure 3.11 B).

This reduction in both cell density and production level of Affimers may suggest that cells died because of their declined metabolic rate caused by the consumption of the nutrients in growth media as reported earlier (Balbas, 2001).

The optimised protocol was used to produce the HER2 binding Affimer reagents. A representative SDS-PAGE, Coomassie-stained gel shown in figure 3.12 confirming the purification of relatively pure, soluble anti-HER2 Affimers with a concentration range

between 1mg/ml to 3 mg/ml. Protein concentration was determined spectrophotometrically and by BCA assay prior to dialysing in PBS, pH 7.4 buffer.

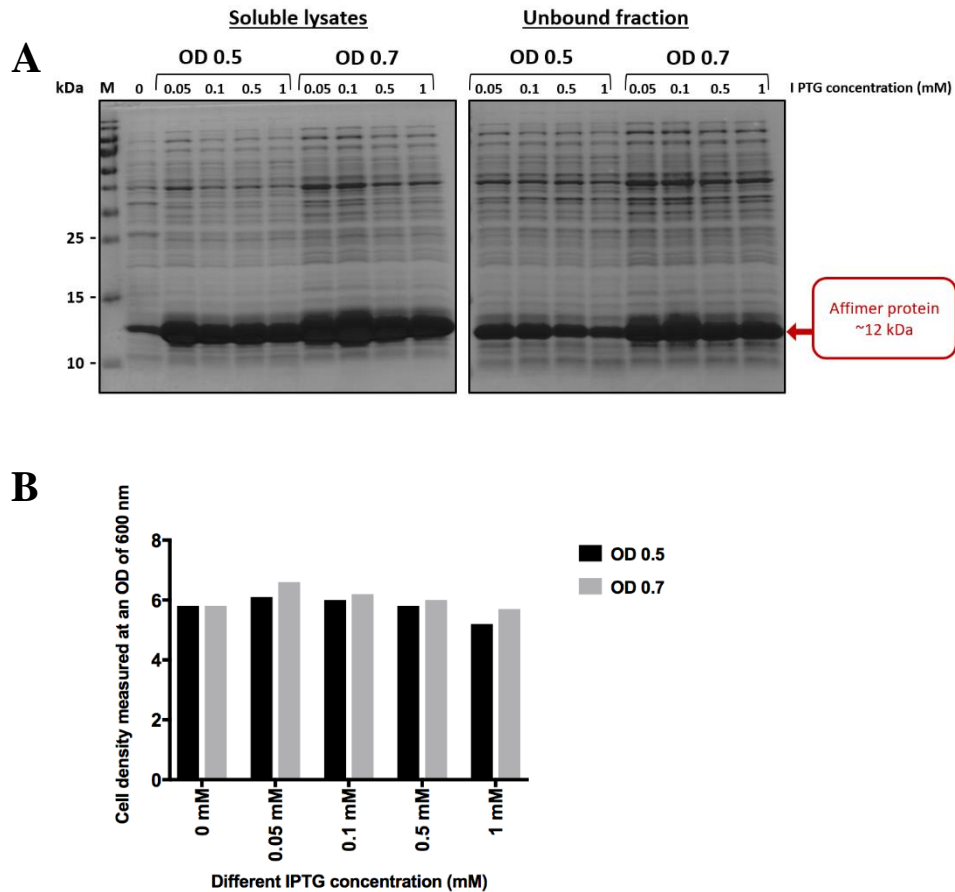


Figure 3.10 The effect of using different IPTG concentrations on both cell density and Affimer production. A range of different IPTG concentration (0.05, 0.1, 0.5 and 1mM) were added at two different optical densities (an OD_{600nm} of 0.5 and 0.7) and cells were allowed to grow for overnight at 25°C with 150rpm. **(A)** 3 µl of soluble lysates and unbound fractions obtained from cultures with different ODs and concentration of IPTG were ran on SDS-PAGE gel and stained with Coomassie blue. **(B)** A graph showing the measured post-induction optical density of cultures induced at different OD start point and different concentration of IPTG. (*n* = 1)

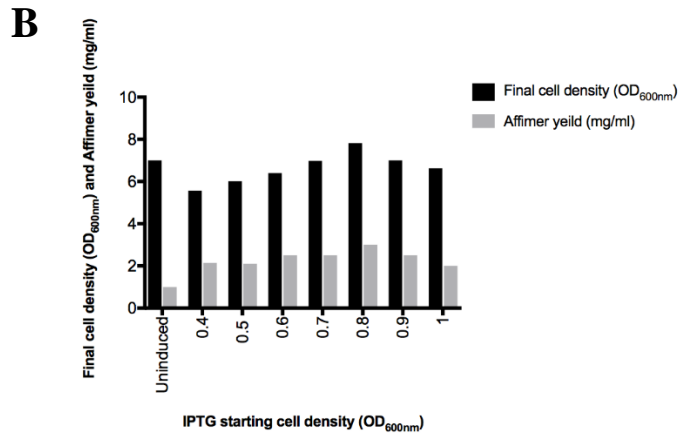
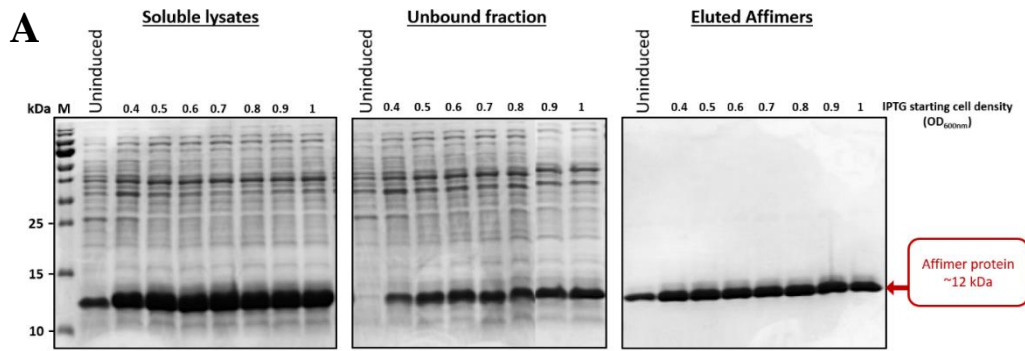


Figure 3.11 Optimising the induction of Affimer production at different OD of cultures. Bacterial cultures were induced with 0.1mM of IPTG at optical densities (OD_{600nm}) of 0.4, 0.5, 0.6, 0.7, 0.8, 0.9 and 1 and incubate at 25°C for overnight to grow while being shaken at 150 rpm. (A) SDS-PAGE gel of 3 μ l soluble lysates, unbound fractions and purified Affimers were ran on gel and stained with Coomassie blue. (B) Graph showing the measured post-induction optical density of cultures as well as the yield of produced Affimer at different pre-induction culture densities. ($n = 1$)

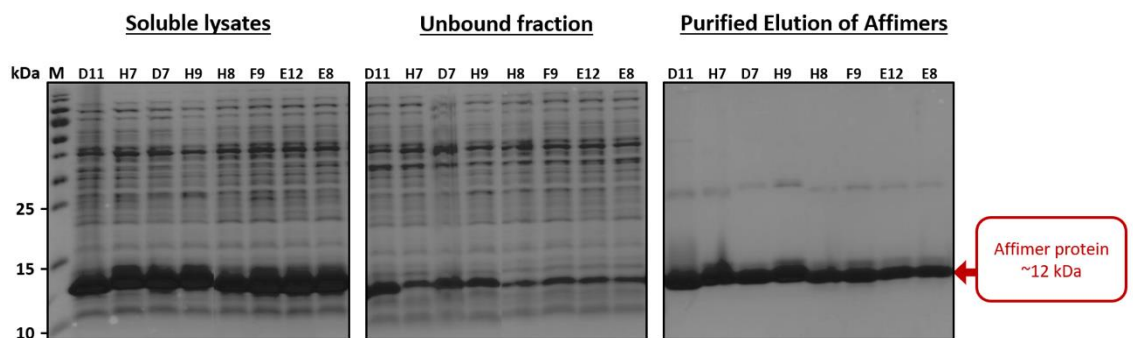


Figure 3.12 SDS-PAGE showing the purification of anti-HER2 Affimers. Eight isolated anti-HER2 Affimers were produced in *E.coli* by growing the transformed cells for overnight at 25°C with 150 rpm under induction at 0.1mM of IPTG that started at 0.8 OD. 5 μ l of soluble lysate, unbound fraction and eluted protein was added in the indicated lanes. Proteins were visualised with Coomassie blue stain. ($n = 1$)

All optimisation experiments were performed only once and the optimised expression protocol was then evaluated and tested to express about 28 Affimers. Approximately 89 % of the expressed Affimers were produced in a high yield of 100-250 mg/l as described in the article that was published in 2017 (Tiede et al., 2017). Another optimisation experiment performed by researchers in the BSTG group confirmed the efficiency of the conditions presented by our optimal Affimer-expression protocol mentioned here and summarized in chapter 2, section 2.2.3.2 (data obtained by verbal communication).

3.2.6 Characterising the binding ability of anti-HER2 Affimers on a panel of breast cancer cells

All eight isolated Affimers were then subjected to binding analysis to determine their ability to recognise HER2 on cells by IF and affinity precipitation.

3.2.6.1 Immunofluorescence staining of HER2 using Affimers

Affinity/immunofluorescence staining (AF/IF) was performed on HER2 overexpressing cells (MDA-MB-453, BT474 and HER2-HB2 transfected cell lines) and immortalized breast cells (HB2 cell line) that do not express HER2 (Holliday and Speirs, 2011). After being fixed with 4% PFA, mouse conjugated Alexa 594 and anti-his₈ tag antibody was used to detect the Affimer (section 2.2.6.1). All Affimer proteins (table 3.2) were added to fixed cells and their staining pattern was compared to a commercial polyclonal HER2 antibody. The background level caused by anti-his₈ tag antibody binding to cells was tested and used as a negative control. In addition, yeast SUMO2 (YS15) Affimer reagent (Hughes et al., 2017;Tiede et al., 2017) was also included in the analysis to serve as a non-HER2 targeting control Affimer. Interestingly, the cellular localisation of Affimer staining was inconsistent when compared to the antibody (membrane and/or cytoplasmic staining patterns on both BT474, MDA-MB 453, but cytoplasmic mainly on transfected cell lines, respectively, figure 3.13) with little staining observed in the negative control cell line. The observed inconsistency in the staining pattern could potentially indicate the need to optimise the fixative as recent laboratory experience has indicated Affimer reagents showed better staining results with fixatives other than paraformaldehyde. In addition, both Antibody and Affimers were raised against different regions of the receptor

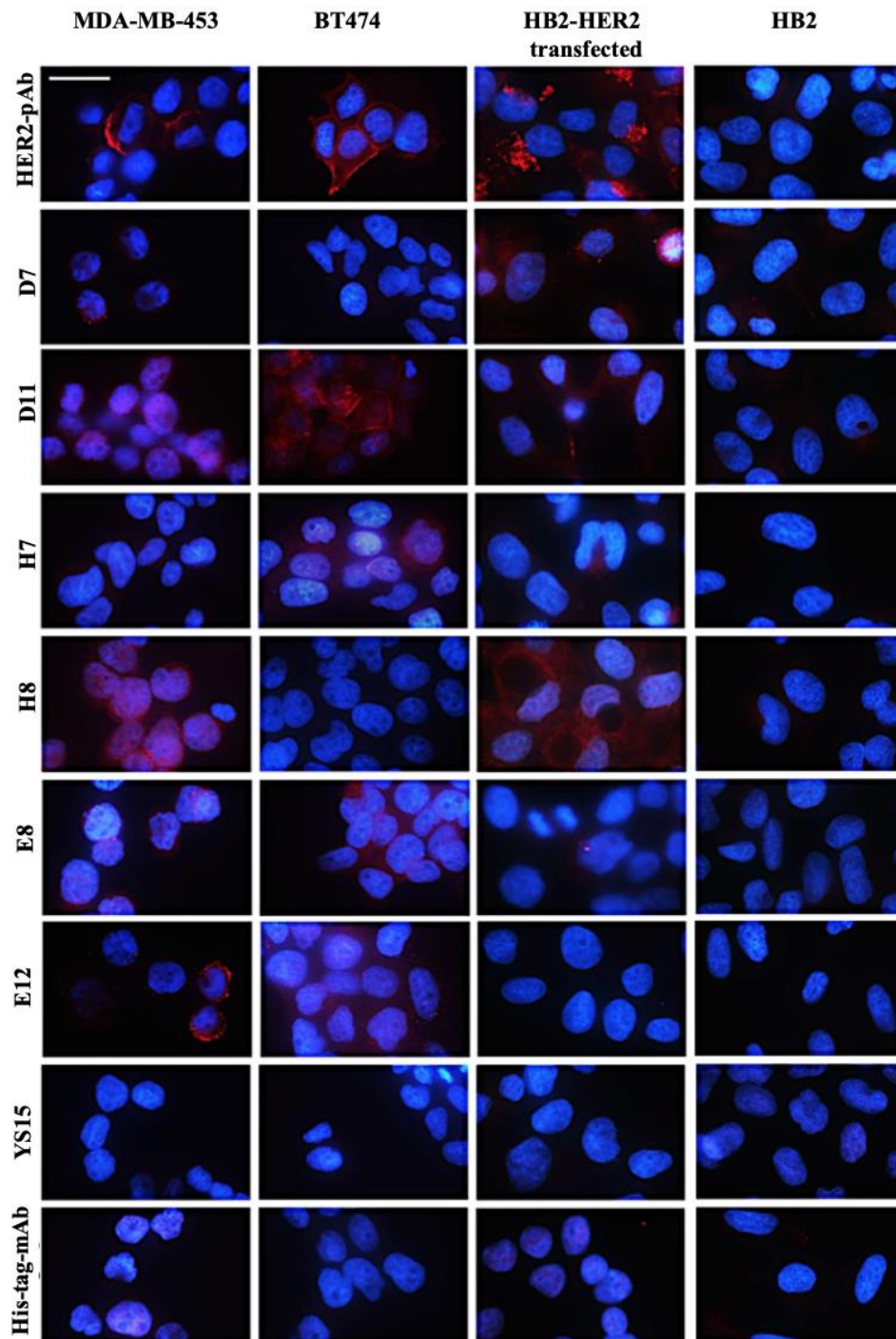


Figure 3.13 Immunofluorescence staining of HER2 receptor on fixed cells. The staining was performed on a panel of HER2 overexpressing cell lines, HER2-HB2 transfected and non-HB2 transfected cells. The molecular binding of Affimer proteins to the receptor was identified by the mouse anti-his₈tag antibody and visualised with Alexa 594 conjugated antibody. The binding interaction between the HER2 antibody and its cognitive receptor was visualised by anti-rabbit conjugated Alexa 594 antibody. In the anti-his₈tag control, no Affimer protein was added, while anti-YS15 Affimer reagent was included as a negative control and scale bar = 20 μ m. ($n = 2$)

and that can further indicate the need of treating them differently in relation to fixing and permeabilisation. Therefore, we decided to test if adding Affimers to cells prior fixing them will enable us to evaluate their binding ability to HER2 without the need of further optimisation of cell fixing.

3.2.6.2 Testing anti-HER2 Affimer reagents on live cells

We started our AF/IF staining by adding the Affimer molecules on BT474 cell line, a HER2 overexpressing cell line, for one hour at 37°C followed by a fixation step with 4% PFA. Bound Affimer variants were then localised using an anti-his₃tag antibody and an anti-mouse Alexa 488 conjugated antibody (section 2.2.6.2). The Affimer yeast SUMO2 (YS15) was used as a negative control. Out of eight tested Affimer variants, only **D11**, **H7** and **E12** showed binding of HER2 on live cells (figure 3.14). Interestingly, **H7** and **E12** Affimer proteins also displayed internalisation into cells. As shown in figure 3.14, both **H7** and **E12** localised as green dots in the cytoplasm indicating internalisation into lysosomes. Compared to **H7** and **E12**, the **D11** variant demonstrated a little cellular uptake with the majority of cells demonstrating specific staining. Very little staining was observed in the negative controls. The commercial polyclonal anti-HER2 antibody could not serve as a positive control because of its inability to detect HER2 on live cells (as recommended by its manufacturer).

3.2.6.3 Anti-HER2 Affimers pull down endogenous HER2 from cell lysates

To examine the ability of the anti-HER2 Affimers to pull down the endogenous HER2 from cell lysate, a pull-down assay was used. Our optimal assay involved incubating Affimer binders with cell lysate overnight prior to precipitating the Affimer-HER2 conjugated complex using NiNTA agarose beads. The cells were lysed under a non-denaturing condition. The pulled down complexes were eluted and ran on SDS-PAGE gel for western blot analysis. The selectivity of the Affimer binders as examined by blotting for the presence of HER2, HER3 and actin. Negative controls included were an anti-yeast SUMO2 (YS15) Affimer and MDA-MB-231 (HER2 negative) cell lysate. In addition, anti-actin Affimer was used as a positive control for the pull-down assay due to its ability to pull down actin.

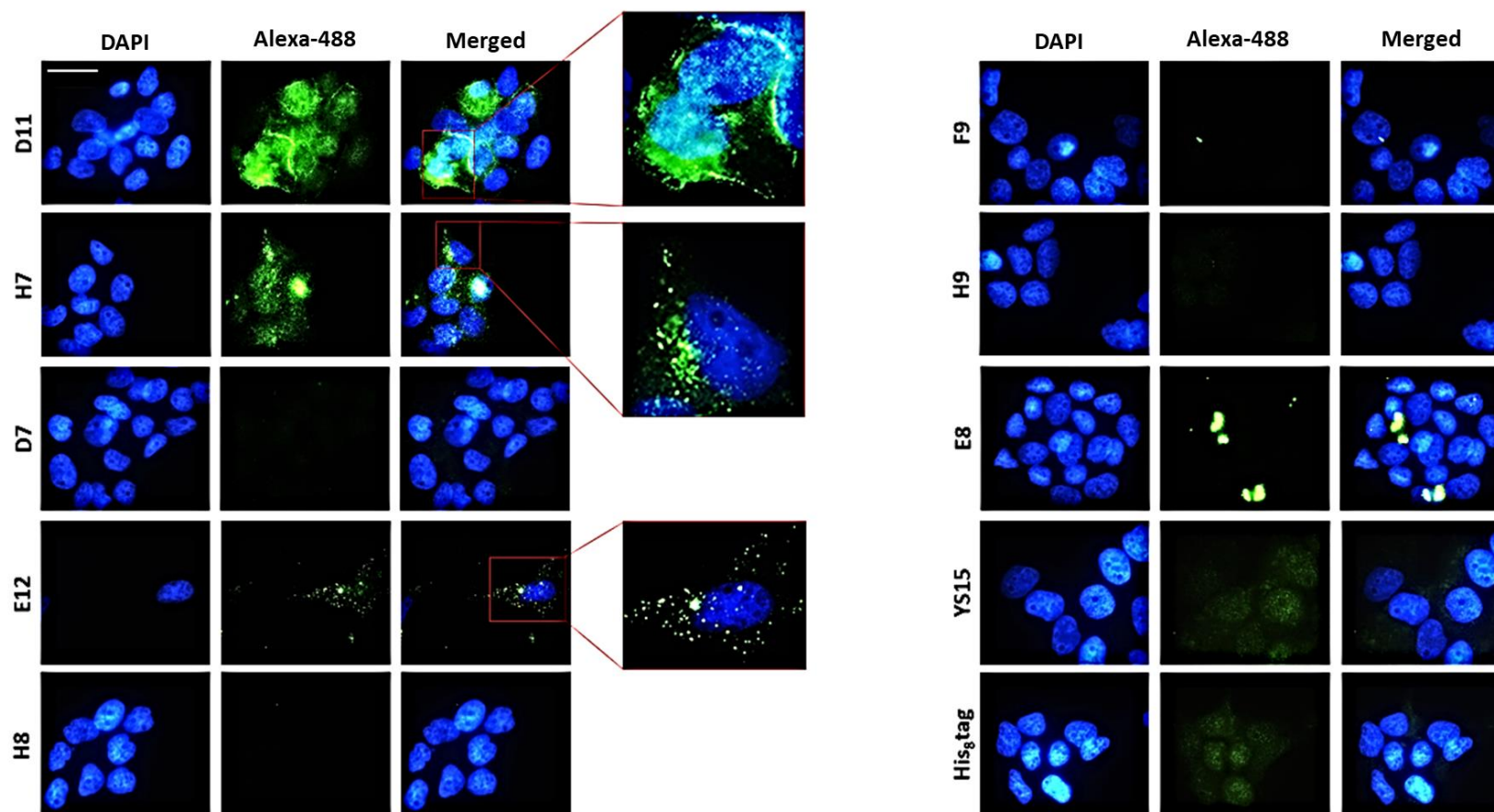


Figure 3.14 Immunofluorescence staining of HER2 binding Affimers on live BT474 breast cancer cells. Affimer proteins (25 $\mu\text{g/ml}$) were added to adherent BT474 cells for one-hour incubation at a 37°C incubator, supplemented with CO₂, before fixing them with 4% PFA. The positive binding (green colour) was visualized by mouse anti-his₈tag antibody followed by anti-mouse (IgG) Alexa 488 conjugated antibody. YS15 Affimer reagents and cells stained with anti-his₈tag antibody only were included as negative controls ($n= 2$, scale bar = 20 μm).

Affimer **D7**, **D11**, **H8** and **E8** pulled down endogenous HER2 from the cell lysate (figure 3.15). However, D11 and D7 pulled down the most HER2, compared to **H8** and **E8** which showed a faint band upon blotting against the HER2. Interestingly, **E8** was the only Affimer protein that showed only pulldown of HER2. In contrast, both **H8** and **D11** showed interaction with HER3.

In addition, the D7 Affimer protein, actin protein was observed alongside other proteins. No bands were detected with the negative YS15 control and other tested Affimer variants. Our positive control, the anti-actin Affimer reagent managed to pull down actin with a weak interaction towards HER2. The observed interaction of the anti-HER2 reagents with either HER3, actin or both may indicate their cross-reactivity or could be due to the fact that these represent protein complexes (Jain et al., 2012). In this context, the pull-down assay can be an indication of how Affimer binders interact with HER2. For example, both HER2 and HER3 interact together by their dimerization arm located at domain II of the extracellular region of the receptor, therefore any HER2 binding reagent such as D7 and D11 may not affect this interaction and therefore precipitate the complex (Rubin and Yarden, 2001). On the other hand, E8 may be binding to at point on HER2 that is occluded when it is in complex with HER3 and therefore only precipitate HER2 protein.

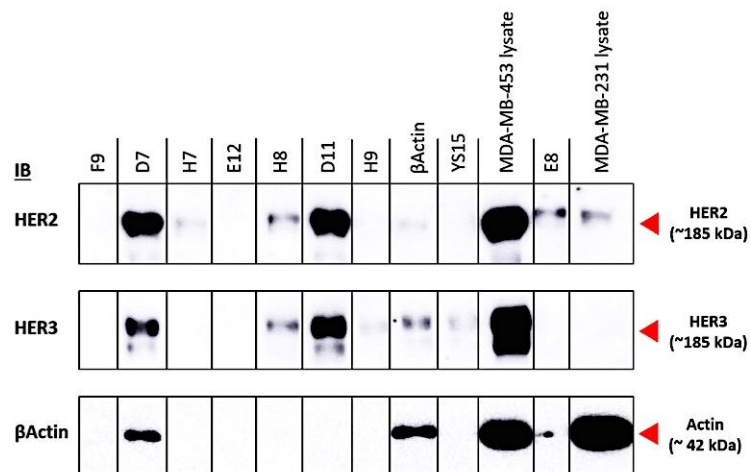


Figure 3.15 Anti-HER2 Affimers showed ability to pull-down HER2 complexes. Affimer proteins were incubated with MDA-MB-453 cell lysate overnight at 4°C. The Affimer-HER2 complex was precipitated using NiNTA agarose beads, washed and eluted. The eluates were separated on an SDS-PAGE gel and blotted against HER2, HER3 and actin antibody. Anti-actin Affimer was used as a positive control in addition to the yeast SUMO2 (YS15) Affimer protein, which served as a negative control. MDA-MB-231 whole cell lysate was used as control to further validate the specificity of the anti-HER2 antibody.

3.3 Discussion

This chapter has described the isolation of Affimers against the extracellular domain of HER2 from the Affimer phage library (Ella2) *in vitro* using different phage-selection strategies that involved biotinylated-HER2-ECD recombinant proteins, and fixed-monolayers of established and engineered cell lines that overexpressed HER-2. The selected Affimers were partially characterised and demonstrated an ability to bind to the receptors on cells, and to pull cells down from a cell lysate. However, this characterisation can only be considered as a preliminary result and further confirmation is currently in process in order to characterise fully the binding specificity and selectivity of the HER2-binding Affimers towards HER2 exclusively in the HER family.

The selection experiments were performed on biotinylated HER2-recombinant proteins and on cells. Regarding the protein-based phage screen that involved the use of biotinylated HER2-ECD only, the BSTG group isolated eight different HER2 binders out of 48 tested clones that were selected from the third panning round. Comparing this screen output with other screens, screening the DARPIn library on adsorbed HER2-ECD protein using ribosome display resulted in the isolation of five different DARPins after the assay of 120 clones that were recovered from the 6th and final panning round (Zahnd et al., 2007; Zahnd et al., 2006). Seven different affibody proteins were isolated after testing 49 individual phage clones picked from the 4th and final panning round following the use of the affibody library and phage-display technology (Wikman et al., 2004). Based on these data, we can suggest that the selection of an Affimer library on immobilised (biotinylated) protein in a minimum of three panning rounds can result in a good level of HER2-binder enrichment. However, the affinity of the isolated binders requires analysis in order to compare it further with the affinity of other generated binders, such as DARPins and affibodies that binds to HER2 in a nanomolar range.

In addition to the need to explore the affinity of the isolated Affimers, the use of random biotinylation to biotinylate the recombinant protein in order to immobilise it on a streptavidin-coated plate to preserve its conformation may block some active sites or binding sites involved in the interaction of the commercial antibody with the different HER2-ECD domains. Therefore, it would be interesting in the future to perform a protein-based screen in which the recombinant protein was adsorbed to the plastic well, as such adsorption seems not to affect the conformation of most of the epitopes as reported in the DARPIn screen (Zahnd et al., 2006). In Zahnd and co-workers' research using adsorption

instead of protein biotinylation to present the protein in the screen, they isolated HER2 binders that recognised the receptors on cells. That group used molecular-recognition applications such as IF and IHC. In addition, the generated DARPins showed specificity towards HER2 as they did not bind to other non-HER2 tested proteins, including EGFR (Zahnd et al., 2007;Zahnd et al., 2006).

Beside using recombinant protein as the source of the ECD of HER2, we tried different cell-based selection strategies to check if we can isolate different reagents. We also wanted to develop a strategy that can help in sorting out the outcome of a recombinant protein-based screens without the need of a time-consuming and laborious characterisation steps especially with many binders to do so. In contrary to the reported success of isolating reagents from a cell-based screen on whole-cells (Jones et al., 2016), our cell based screen using HER2-transfected *vs* non-transfected cells was failed and what we isolated were non-specific binders. We reasoned our screen failure to multiple factors, including library quality and experimental parameters. In relation to the library quality as mentioned in section 3.1, the diversity of the Affimer library may have limited the isolation of binders that were able to recognise the receptor under fixed conditions, under which cross-linking of proteins could be a drawback causing fewer epitopes to be exposed in the screen. Another factor was that Affimers were displayed on a truncated M13-pIII bacteriophage coat protein and this might have resulted in steric hindrance that may have prevented the displayed Affimers from binding to epitopes (As suggested by Dr. Darren Tomlinson). More scaffold flexibility is needed to improve identification and binding to differently structured epitopes.

Various experimental parameters, such as the washing of the unbound phage clones, the use of negative (depletion) selection steps to remove the non-target binding phage and the number of selection rounds required to achieve good enrichment rates have been shown to have a critical impact on the outcome of the phage screen (Alfaleh et al., 2017). In our work, we pre-panned the library in multiple pre-panning wells prior to the start of the selection process on wells that contained the target for the purpose of depleting the library from the non-target binding clones. However, we did not manage to enrich the library with target-specific phage clones compared with the control colonies recovered from the control samples. So, we speculated that since the detected amplification of phage was seen with the phage-infected bacterial cultures of both target and non-target, the problem was likely to be with the applied stringency of washing (as described in section 2.2.2.2.3). Therefore, and in order to remove the non-target binders, more stringent

washing may be required (>10 times per round) of unbound phage in addition to more prolonged pre-panning steps (one hour per step) against the non-transfected cell line to remove efficiently the non-specific binders (Alfaleh et al., 2017). Furthermore, an increase in the number of panning rounds to six or more instead of four could result in improvement in the enrichment of HER2-binding clones compared with the control samples.

On the other hand, cells represent an adverse mixture of antigens, which leads to a complex process to isolate binders against a single specific antigen. To overcome such complexity, several studies have adapted the competitive elution strategy to isolate specific binding clones through use of known physiological ligands or specific blockers to displace the bound phage (Alfaleh et al., 2017; Duan and Siegmund, 2010). For example, the T24 human bladder carcinoma cell line is known to overexpress cytokeratin (CK)-7, CK18 and CK8 (Meulemans et al., 1995; Meulemans et al., 1994). A competitive elution using anti-CK8 monoclonal antibody was useful to isolate binders against CK8 only, as confirmed by the binders' specificity and selectivity towards CK8. The researchers used various molecular applications, such as ELISA, IF and IHC (Meulemans et al., 1995; Meulemans et al., 1994). This strategy could be adapted in future to isolate binders against HER2 using HER2 antibody or HER2-recombinant protein from a cell-based phage screen.

Another solution to overcome the admixture environment of cells is to use a transfected cell line and its non-transfected counterpart as a way to enrich the screen with unlimited supply of a specific target, as well as to ensure the elimination of the common binding phage when using the equivalent non-engineered cells (Alfaleh et al., 2017). As such we performed a cell-based screen on a HER2-HB2 transfected cell line and at the same time we used the HB2 (non-transfected) counterpart for the negative (pre-panning) selection to isolate HER2-binding reagents. However, it was clear that transfected cells may not have been the appropriate source of HER2. In our case, transfected cells (HB2-HER2 transfected cells) did not present the right localisation of the HER2, as most of the receptor protein was expressed in the cytoplasm instead of in the plasma membrane.

In addition, it is known that the protein expressed upon transfection may exhibit inappropriate folding and not proper localisation and thus offer contradictory staining results (Kim and Eberwine, 2010). Therefore, using a non-engineered, HER2-overexpressing cell line in future cell-based screens may result in a successful cell-based

screen after optimisation, according to earlier reports (Gijs et al., 2016). An additional advantage of using a non-engineered cell line is that most HER2-overexpressing cell lines also overexpress the transforming factor (TGF- β) that is required to recruit actin (Figure 3.16) and therefore provide the necessary stabilisation for HER2 on the cell membrane, thus enhancing cell motility, invasiveness and survival (Wang et al., 2006a).

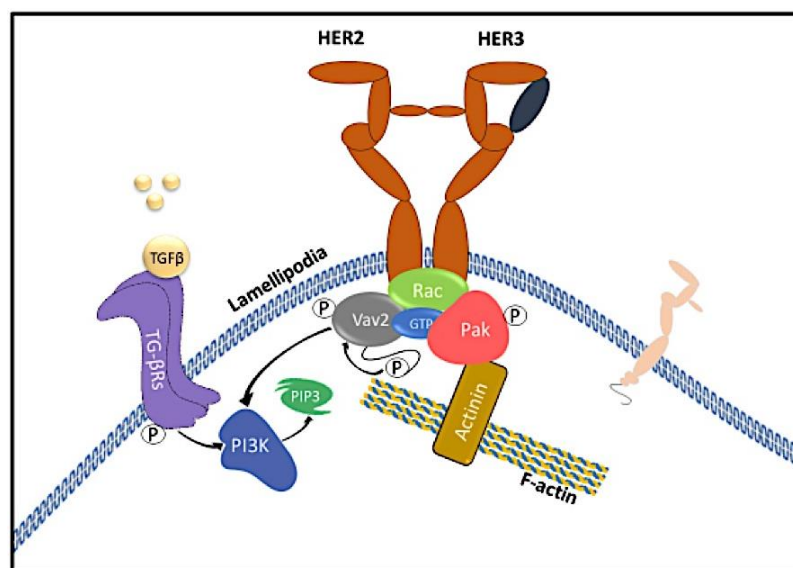


Figure 3.16 Mechanism of stabilising the HER2 receptor on the cancer cell surface.

Upon HER2 activation, TGF- β receptor induces PI3K above a necessary threshold required for the recruitment and stabilisation of F-actin and HER2 complex at cell protrusions, thus leading to prolonged activation of RacI, cell movement, and increased survival on cell detachment (Wang et al., 2006a). Rac: Ras-related C3-botulinum toxin substrate; PIP3:phosphatidylinositol(3-4,5)-triphosphate; PI3K:phosphoinositide-3-kinase; TGF- β : tumour growth factor beta; TG- β Rs: tumour growth-beta receptors; p: phosphate; Pak: p21-activated protein kinase; Vav2: vav guanine nucleotide exchange factor 2; GTP: Guanosine-5'-triphosphate.

Although our cell-based screen did not work, we managed to develop a novel strategy to generate Affimer reagents able to recognise their target on cells. We first adopted the developed alternate display strategy in which the library is selected on both cells and recombinant protein (Andersen et al., 1996). We believe that introducing cells early in the screen is not efficient as the pool of phage in that point was still enriched with non-specific binders, and changes in the screen platforms from blocked wells to wells contained non-HER2 expressing cells was not helpful for efficient elimination of such

binders. In addition, using protein-based ELISA to screen for hits may not be the optimal option as it would not reflect the ability of binders to bind to cells. Therefore, using a cell-based ELISA for screening hits is a factor to consider when such strategy is to be repeated in future. To further enhance the outcome of the screens, another crossover selection strategy was adopted (Gijs et al., 2016).

In conclusion, selecting anti-HER2 Affimer reagents against the recombinant ECD protein of the receptor is less challenging than using whole cells. However, the latter approach can be more efficient and less complex when combined with recombinant protein of the same target. Beside the vast production of Affimers in bacterial cells, the anti-HER2 reagents generated are promising tools for *in vitro* detection of HER2 on cells and its quantification or imaging *in vivo*. Finally, due to the internalisation ability that some Affimer reagents exhibit they could also be utilised in cancer therapeutic for delivery of drug conjugate

CHAPTER 4

Isolation and characterisation of anti-EGFR and anti-HER3 Affimers

4.1 Introduction

For the last two decades, antibodies have been used to detect and target specific antigens on tumour cells (Pento, 2017). Numerous antibodies to different cellular receptors have been approved to be used as diagnostic tools for detecting the presence of tumours in patients (Sampath et al., 2007; Warram et al., 2014). However, owing their large size antibodies have a slow clearance rate and therefore give relatively high background signal in different imaging applications (Divgi, 1995). To overcome this problem, there is an increasing interest in smaller antibody-like derivatives, such as Fab, single-chain Fv (scFvs), diabody, nanobody, minibody and their fusions (Holliger and Hudson, 2005). There are numerous reports on their use as *in vivo* imaging tools (Freise and Wu, 2015; Tavaré et al., 2014). Other alternative-affinity binding molecules have been used for *in vivo* imaging including, monobodies (Koide et al., 1998), protein-A-derived affibody molecules (Hogbom et al., 2003), PDZ domains (Schneider et al., 1999), Src homology domains 2 and 3 (Brasher et al., 2001), designed Ankyrin repeat proteins (DARPs) (Binz et al., 2004), lipocalins (Beste et al., 1999) and Affimers (Tiede et al., 2014) which have recently entered this field have been developed.

Tyrosine kinase receptors, such the HER family of receptors, are part of a complex signalling network involving intracellular stimulation of diverse pathways leading to cell growth, differentiation and survival (Yarden, 2001). As such, they have been considered as attractive targets for the development of new diagnostic and therapeutic agents (Krause and Van Etten, 2005). So far, monoclonal antibodies (mAbs) and small molecule tyrosine kinase inhibitors targeting both EGFR (Arteaga, 2003) and HER2 (Sakamoto and Mitsuyama, 2000) have been developed and approved to be used in clinics. Recently, focus has turned towards HER3 as it plays a significant role in drug resistance against the existing HER2 and EGFR targeting agents (Aceto et al., 2012). Over the last 10 years, HER3 targeting reagents have been undergoing clinical trials and thirteen mAbs are currently in phase 1 and 2 (Lyu et al., 2018). Targeting single biomarker has been proven to be limited (de Melo Gagliato et al., 2016; Lockwood et al., 2017), highlighting that

combination treatments targeting multiple HER family members may improve clinical outcome when treating various solid tumours.

Such advantage of using combined HER targeting therapy provoked us to isolate binders against other members of the HERs family as well as HER2. In this chapter, we described the selection of Affimer reagents against both EGFR and HER3 using phage display. Furthermore, the ability of the isolated binders to identify their specific targets on cells or in cell lysates was evaluated using Affinity/immune-fluorescence (AF/IF) staining and affinity pull-down assay, respectively. Finally, the potential of anti-EGFR and anti-HER3 binding Affimers to modulate the function of the receptor by inhibition the stimulation of downstream signalling is further explored.

4.2 Results

4.2.1 Selection of HER3-binding Affimers

Phage display was used to isolate Affimer reagents binding to the extracellular domain of HER3. The isolation of binders was achieved using Affimer phagemid library in bio-panning selection process against a biotinylated recombinant protein. The biotinylation and phage selection process was performed according to the protocols mentioned in section 2.2.2.1.1 and 2.2.2.1.2, respectively. Based on ELISA results (figure 4.1), HER3 recombinant protein showed efficient biotinylation and thus suitable as a target to start the phage screen against. A total of three bio-panning was performed as shown in the schematic overview in figure 4.2 A. In all panning rounds, depletion steps were performed to remove phage binders that bind to the solid matrix of wells.

A total of 48 colonies out of 6.3×10^6 of recovered colonies, were randomly selected from the third panning round (figure 4.2 B). This number of colonies were picked as only 48 of the total colonies grown in the 1 μ l agar plate was found to be as individual colonies. For future screens, titering phage to less than 1 μ l would be of advantage enabling to select more colonies. Phage ELISA examining all the selected clones against biotinylated HER3, HER2 and blocked wells was performed. HER2 was used as a control owing to the high degree of homology between all members of the HER family (Sierke et al., 1997; Yarden, 2001), After discarding the non-specific and weak binding clones to both proteins, 18 colonies that showed binding to HER3 with low binding to the control wells

(figure 4.3 A and B) were sequenced, identifying 11 unique reagents against HER3 (figure 4.3 C) with low cross-reactivity to HER2 (figure 4.3 A and B).

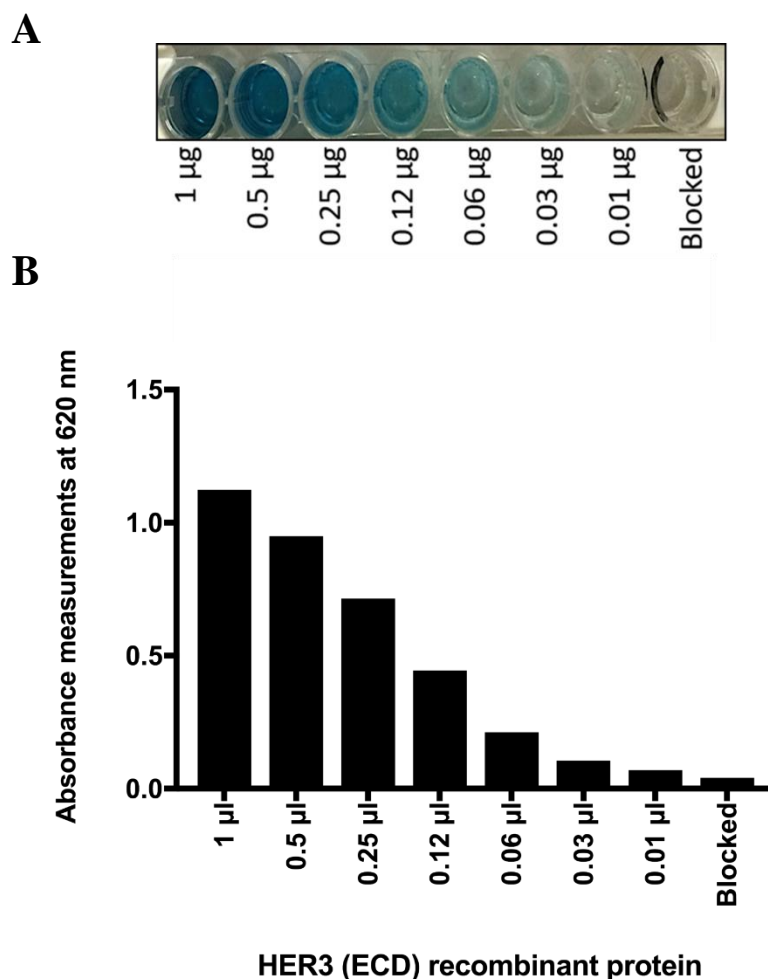


Figure 4.1 Evaluating the efficiency of HER3 (ECD) recombinant protein biotinylation for use in phage display screen. The recombinant protein was biotinylated using the NHS-amine based biotinylation reagent. (A) Showing the strip of different dilutions of the biotinylated recombinant protein detected with streptavidin conjugated with HRP and TMB. PBS was used as a negative control. (B) Graph showing the absorbance measurements of all wells at 620 nm. The plotted measurements represent the mean value of duplicate measurements of one experiment ($n = 2$).

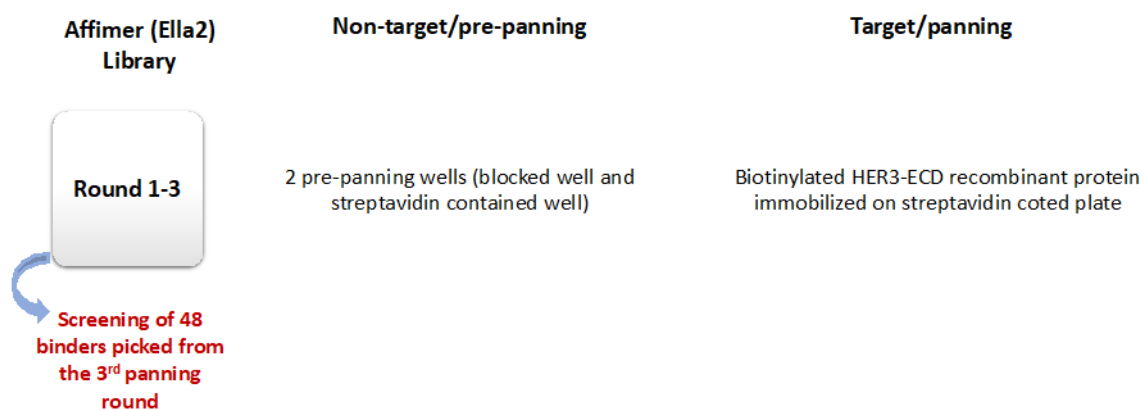
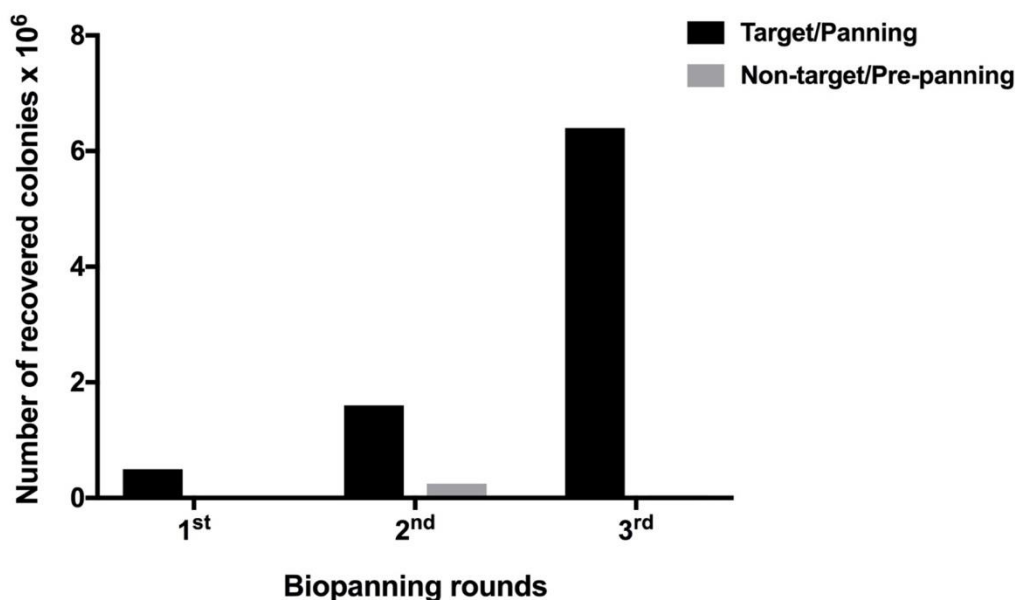
A**B**

Figure 4.2 Phage-display screen against biotinylated recombinant HER3-ECD protein to isolate binders against the ECD of the receptor. (A) Schematic overview of the total three panning rounds. In all rounds, the naïve Affimer library was pre-panned on two wells containing blocking buffer and streptavidin in order to remove non-target-specific binders before the start of selection of the library on the biotinylated HER3-ECD protein immobilised on streptavidin-coated plate. From round three, 48 colonies were randomly picked and assayed for their binding specificity using phage ELISA. **(B)** Histogram showing the total number of recovered colonies in all rounds. After each round, the numbers of recovered colonies were counted twice by manual marking using a marker pen. The count was then multiplied by the total volume of phage-infected *E.coli* culture (8ml) to determine the total number of phage-infected cells. ($n = 1$).

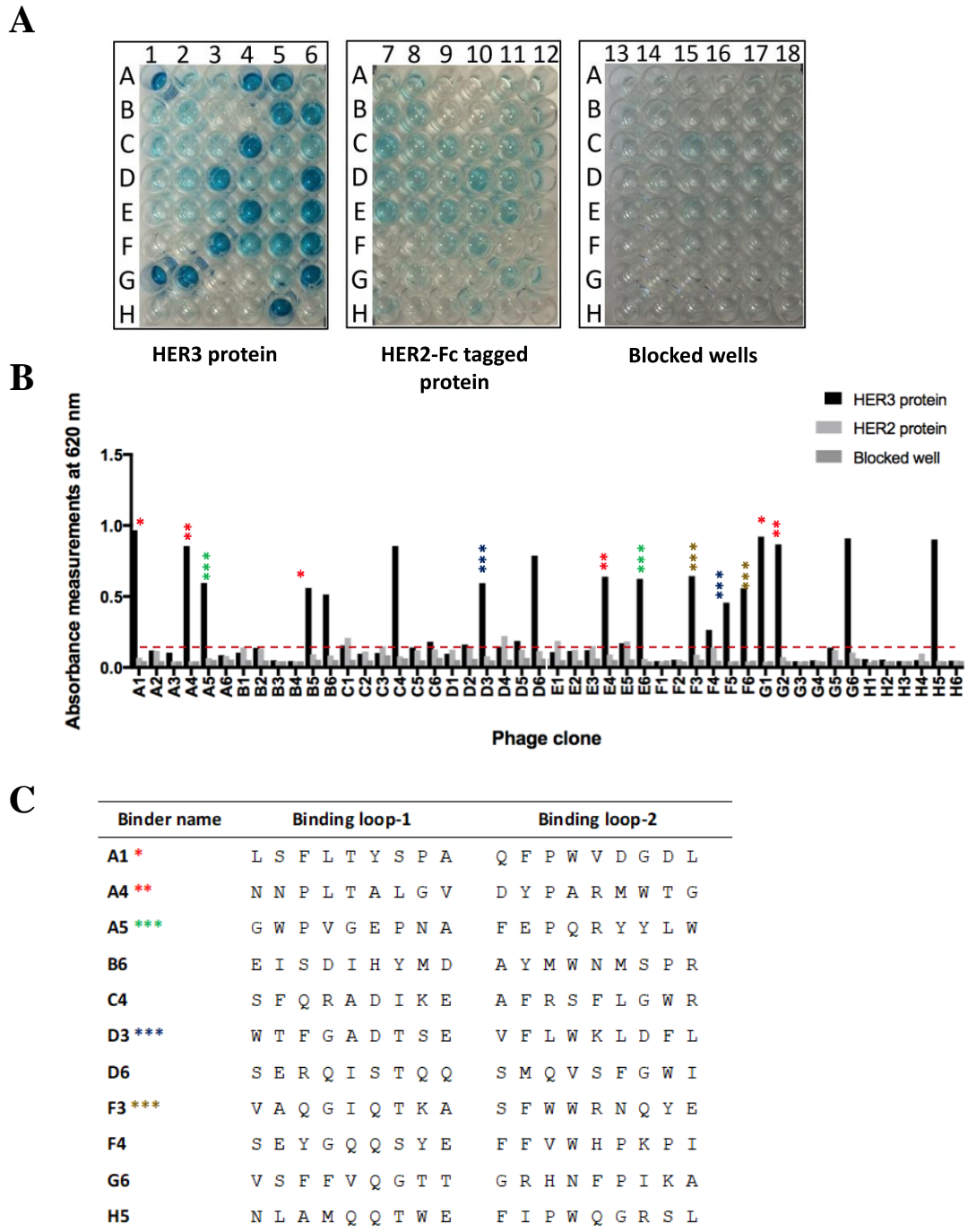


Figure 4.3 Phage ELISA of 48 picked clones after 3 panning rounds against the HER3 recombinant protein. (A) The 48 selected clones were tested against the HER3 recombinant protein in column 1 to 6. Whereas, HER2-Fc tagged recombinant protein and blocked wells containing 2x blocking buffer were used as negative controls in column 7 to 18. Phage binding was detected using anti-fd bacteriophage HRP conjugated antibody and visualised with TMB. (B) The absorbance measurements at 620 nm of each well were taken and blotted in a histogram. An arbitrary cut-off (red dotted line) was used to determine which clones would undergo sequence analysis. Indicated columns are the ones taken forward. The plotted absorbance measurements represent the mean value of duplicated measurements of one experiment. (C) Showing the amino acid sequence of the binding loops of the recovered 11 clones. Amino acid details found in appendix A. ($n = 2$ for phage ELISA and DNA sequencing but as phage screen it was performed only once).

In addition, we wanted to identify the clones that can bind to HER3 on cells. Therefore, we selected the enriched pool of HER3 binding phage on either fixed monolayer of cells or on FFPE cell sections. In relation to the use of FFPE cell sections as the source for HER3, two different screens were performed using two different HER3 overexpressing cell in each screen (Takagi et al., 2014). In the first screen (figure 4.4 A), we selected the enriched pool on fixed monolayer of MDA-MB-231 cells (HER3 overexpressing cell line) after depleting it on HER3 negative cell line (U87-MG, glioblastoma cell line) as described in section 2.2.2.2.1, while in the second screen (figure 4.4 B), the enriched pool was selected on MDA-MB-453 cells after depletions on U87-MG (HER3 negative) cells.

With regard to the cell-contained phage screen against fixed monolayer of cells, one screen was performed using MDA-MB-43 cells as target cells and U87-MG cells as non-target cells figure 4.4 C). In all three screens against HER3 overexpressing cells, a total of three selection rounds were performed (figure 4.4). The number of recovered colonies, after the final panning rounds of the three selection screens were counted and plotted in a column chart (figure 4.5). Comparing the counted number of recovered phage colonies in both target and non-target agar plates, no enrichment of HER3 binding Affimers was seen from the screen on fixed monolayer of cells (figure 4.5 C). In contrast, a slight increase in the number of phage colonies was seen in the selection screens against FFPE cells (figure 4.5 A and B). However, the minor enrichment of phage clones in the FFPE cell-based screens was not enough to be assessed as a successful screen based on our experience with other performed cell-based screens.

Non-successful cell-based screening against HER3 can be an indication of how complex it is using cells in the screen as a source of target. In addition, using one cell-based screening approach as a standard selection strategy to isolate binders against different membrane-associated target may not be optimal. Therefore, modifications to the developed strategy alongside several optimisation trials is necessary for future screens. However, we screened the 11 phage clones that showed binding to HER3 recombinant protein in a cell-based ELISA using a fixed-monolayer of two HER3 overexpressing cells (MDA-MB-453 and MCF7 breast cancer cell lines). The histogram in figure 4.6 demonstrates the ability of the isolated binders to recognise HER3 receptor on fixed cells, albeit at relatively low levels. Hence, the binders were taken forward and tested using different assays to confirm binding to HER3.

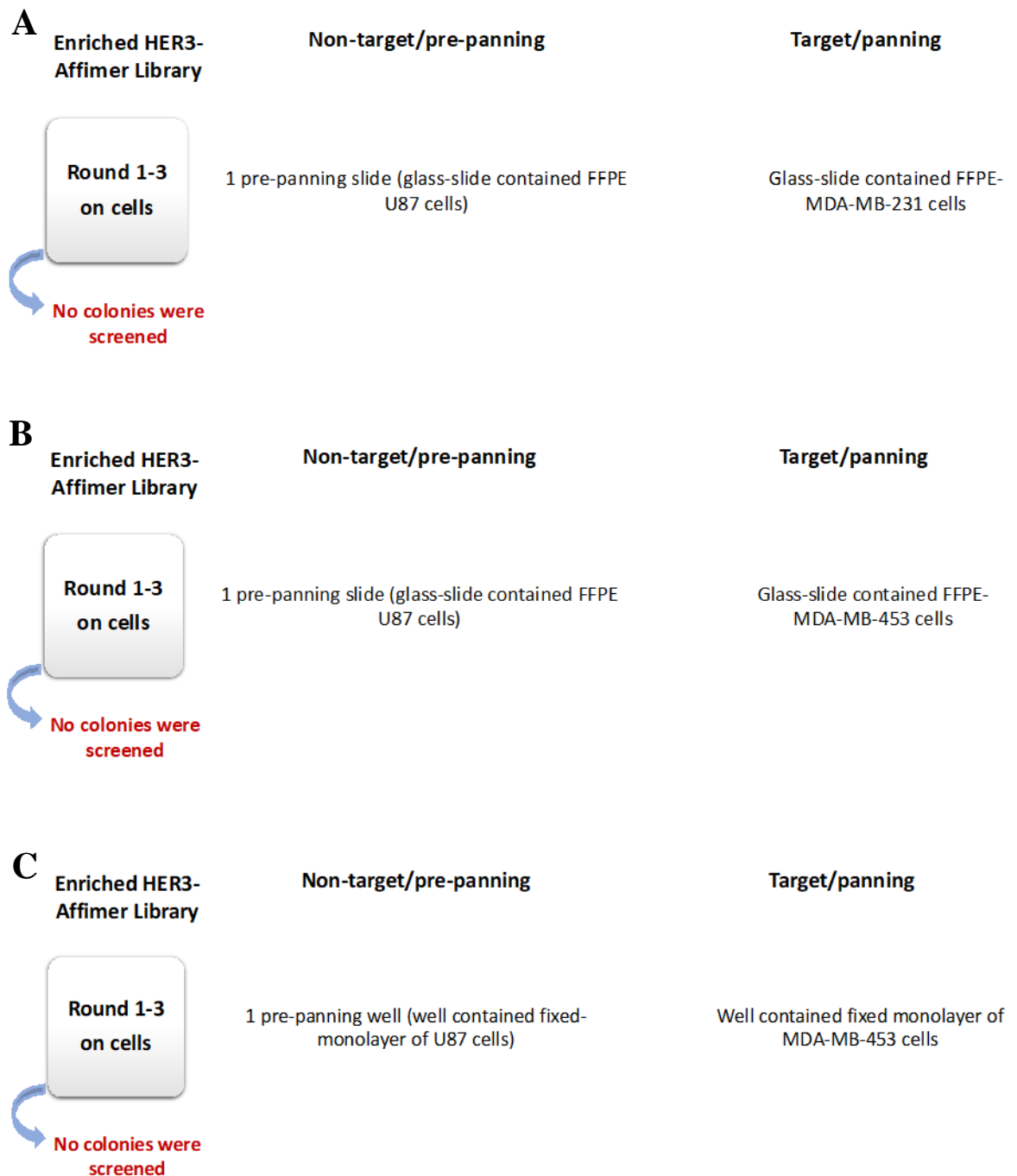


Figure 4.4 Schematic presentation of the three phage screens performed against HER3-overexpressing cells after three rounds of library enrichment on HER3-ECD recombinant protein. From all screens, no colonies were assayed. (A) and (B) represent the phage screens against FFPE cells. This screen aimed to sort the enriched HER3 phage library by the isolation of binders that could identify the receptor on cells. (C) shows the selection of the enriched library on a fixed monolayer of HER3-overexpressing cells (MDA-MB-453). ($n = 1$)

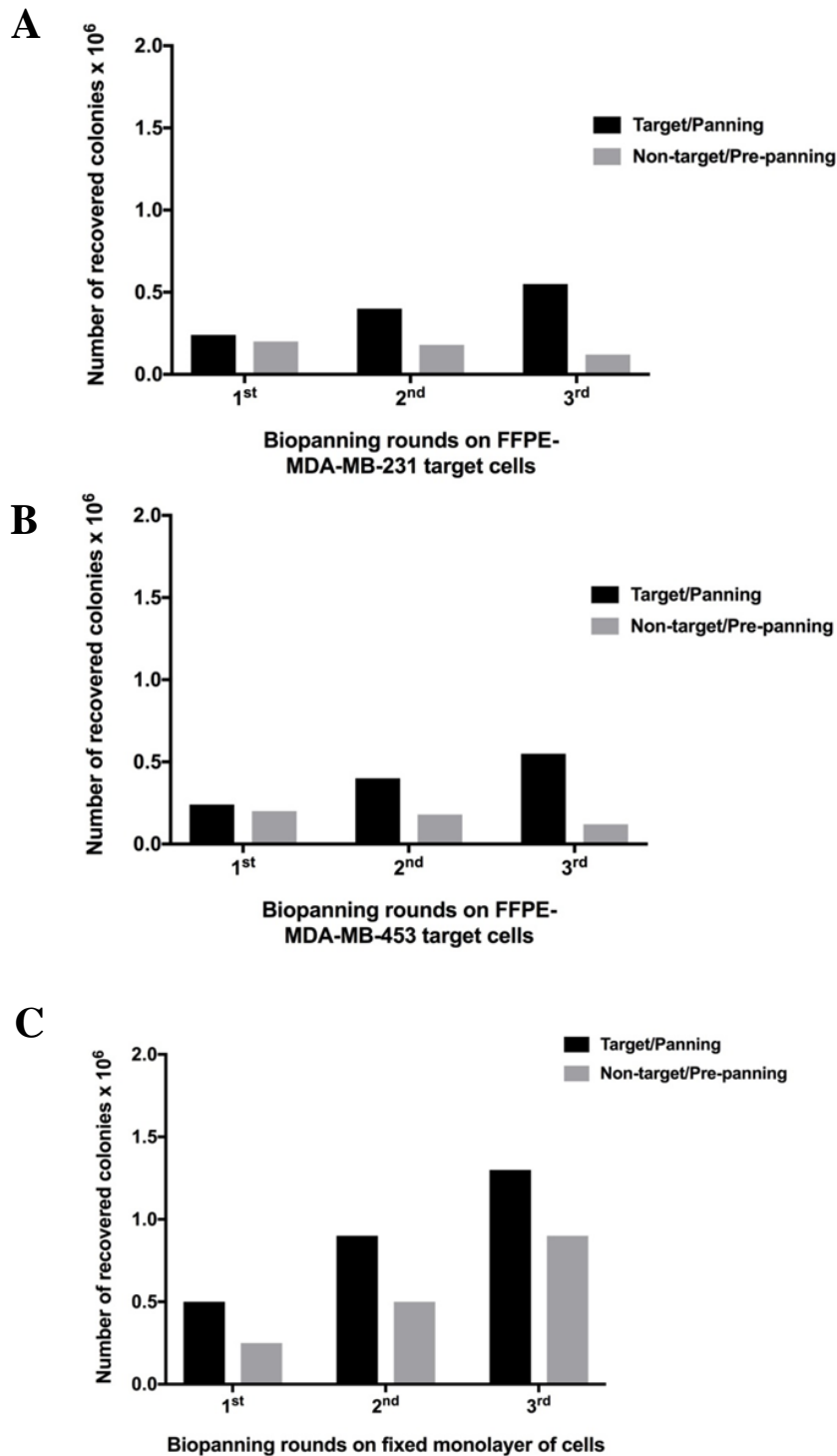


Figure 4.5 The phage output of the three different phage screens on cells that overexpressed HER3 using an enriched-HER3 phage library. In each screen, three panning rounds were performed on either FFPE-MDA-MB-231 cells (A) or FFPE-MDA-MB-453 cells (B) or a monolayer of fixed MDA-MB-453 cells (C). The numbers of the recovered colonies were counted twice (manually) using a marker pen. The obtained number of colonies was then multiplied by the volume of the phage-infected bacterial cell culture in order to determine the total number of phage infected cells, as shown in the plotted values. ($n = 1$).

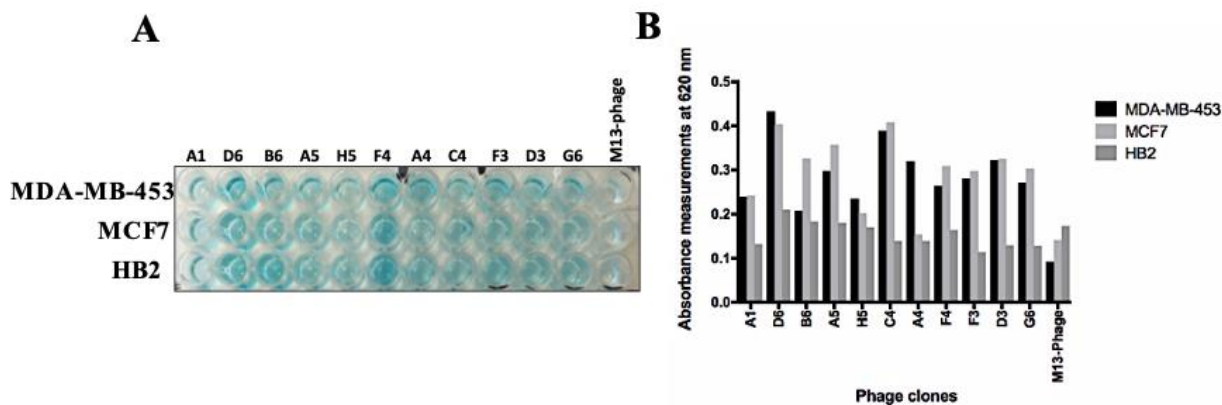


Figure 4.6 Cell-based phage ELISA to examine the ability of 11 isolated HER3 Affimers to bind the native receptor on fixed cells. (A) 11 isolated anti-HER3 phage clones were tested for their binding ability to identify the native receptor on fixed cells with different expression level of HER3. The used cells include the MDA-MB-453 (HER3 intermediate expression level), MCF7 (HER3 overexpression), and HB2 (low expression). Helper (M13K) phage was used as negative control. (B) Absorbance measurements at 620 nm for all wells were measured and blotted in a histogram. The absorbance measurements plotted in the histogram represent a mean value of duplicated measurements taken from one experiment. ($n = 2$).

4.2.2 Isolating Affimers against the extracellular domain of EGFR using a recombinant protein

Following the successful selection of HER2 and HER3 Affimer binding reagents from protein-based screens, the Bioscreening group at Leeds university also succeeded to isolate 6 unique binders against the extracellular domain of the EGFR using a recombinant protein. The amino acid sequences of the binding loops of the 6 isolated binders are illustrated in table 4.1. Due to mixed results from cell-based screens and therefore the further need to optimise the whole selection process, we decided to assess and characterise the binding ability of all 6 selected binders by Immunofluorescence staining and pull-down assay.

Binder name	Binding loop-1	Binding loop-2
A3	V E H P R L L M G	P L I V F I H S K
G10	E I V W L K A H S	G N Y I D N L L Y
H3	I I W A K H V K N	L N G F L T E Y I
H4	H A E W A T F G Q	V L F S Y R E L E
H9	M S Q W L D A V D	K M P I M N Y N T
H91	T W Q W L N A Q D	N W R M Y Q E I R

Table 4.1 Amino acid sequences of the binding loops of 6 different EGFR binding Affimers. These binders were recovered from biopanning against the biotinylated recombinant protein of the ECD of EGFR. The phage screen was kindly performed by the Bioscreening group (University of Leeds, UK). See Appendix A for more amino acid details.

4.2.3 Molecular cloning, production and purification of anti-HER3 and anti-EGFR Affimer proteins

The isolated Affimer reagents (table 4.1, and figure 4.2 C) were amplified by PCR and cloned into the pET11a expression vector after being digested with two digestion enzymes (data not shown, see method section 2.2.3). The PCR amplification also introduced a cysteine residue before the histidine₈-tag. The cysteine residue allows for site-directed chemical modification of the Affimers, such as biotin-conjugation (section 2.2.5.2). Chemical biotinylation of Affimers enables them to be detected by streptavidin conjugated reagents used in multiple detection applications (Ternynck and Avrameas, 1990). All the Affimers were sequences prior to being produced in BL21(DE3) bacterial cells.

Affimer proteins were produced *in vitro* under the induction of the T7 promotor by adding 0.1mM of IPTG at an OD_{600nm} of 0.8. After the induction of IPTG, cells were grown overnight at 25°C with a shaking speed of 150 rpm. SDS-PAGE analysis showed a vast production of soluble anti-HER3 (figure 4.7 A) and anti-EGFR (figure 4.7 B) binding Affimers. With regards to HER3 binding Affimers, SDS-PAGE gel showed that all binders did highly expressed in bacterial cells as confirmed by the soluble lysate fraction, except of the **D3** Affimer. Therefore, the anti-HER3 (**D3**) protein was excluded from further characterisation analysis. We speculate that the low level of D3 production is due

to the need for different expression conditions that needs further optimisation to improve its production in BL21(DE3) bacterial cell.

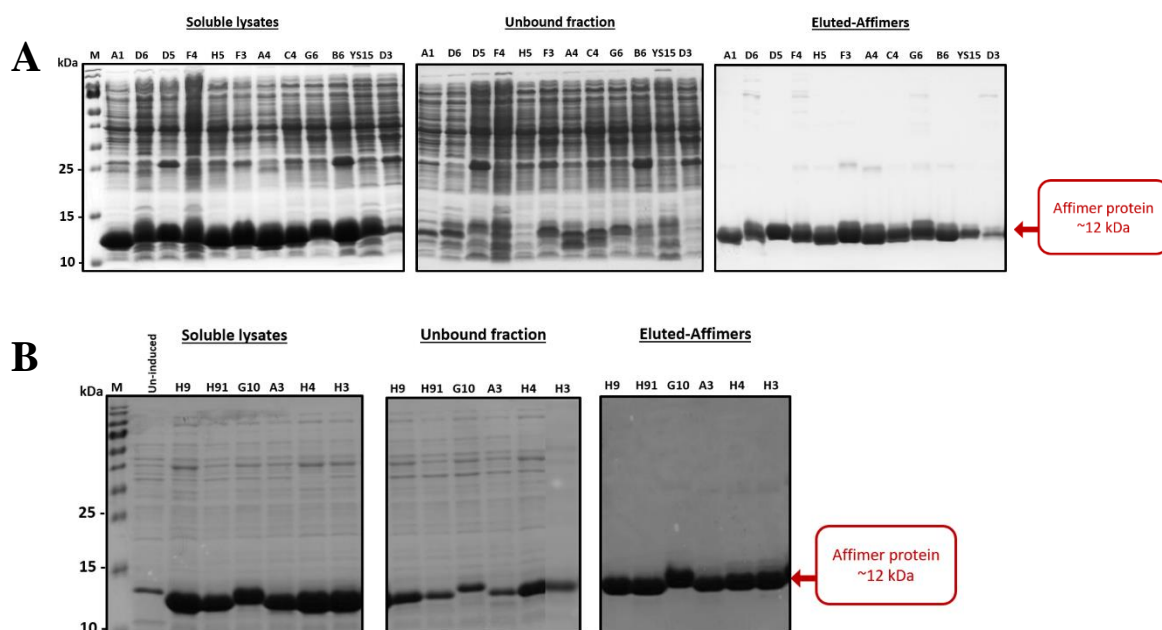


Figure 4.7 SDS-PAGE gel showing production and purification of Affimer proteins. Affimers were induced by IPTG and grown overnight at 25°C with a shaking speed of 150 rpm. After production the cells were harvested, lysed and Affimer proteins were purified on nickel agarose beads. 5 µl of Purified Affimers, soluble lysates and unbound fractions were denatured, ran on SDS-PAGE gel and Stained with Coomassie blue to examine the production efficiency and purity. **(A)** All 11 isolated anti-HER3 Affimers were produced in bacteria, except of the **D3** Affimer that showed very low production level. **(B)** All 6 anti-EGFR Affimers were efficiently produced in bacteria ($n = 4$).

All EGFR binding Affimers showed high expression level and thus a high yield of protein was obtained for each binder. SDS-PAGE gels also confirmed the efficiency of the performed single-step purification on nickel beads as all eluted Affimer reagents were relatively pure. After purification, Affimers were dialysed in PBS, pH 7.4 and subjected to binding analyses to assess their ability to recognise their receptor on cells or pull down of endogenous proteins from cell lysates.

4.2.4 Anti-HER3 Affimers can recognise the receptor on cells and in cell lysate

Binding capability of the isolated anti-HER3 Affimers to their target on both fixed and live cells was assessed by immunofluorescence microscopy study (figure 4.8 and 4.9). Their ability to pull down endogenous receptor from a cell lysate were also examined (figure 4.10). Finally, we evaluated the applicability of our anti-HER3 Affimer as reagents in IHC using formalin-fixed-paraffin embedded (FFPE) cells (figure 4.11).

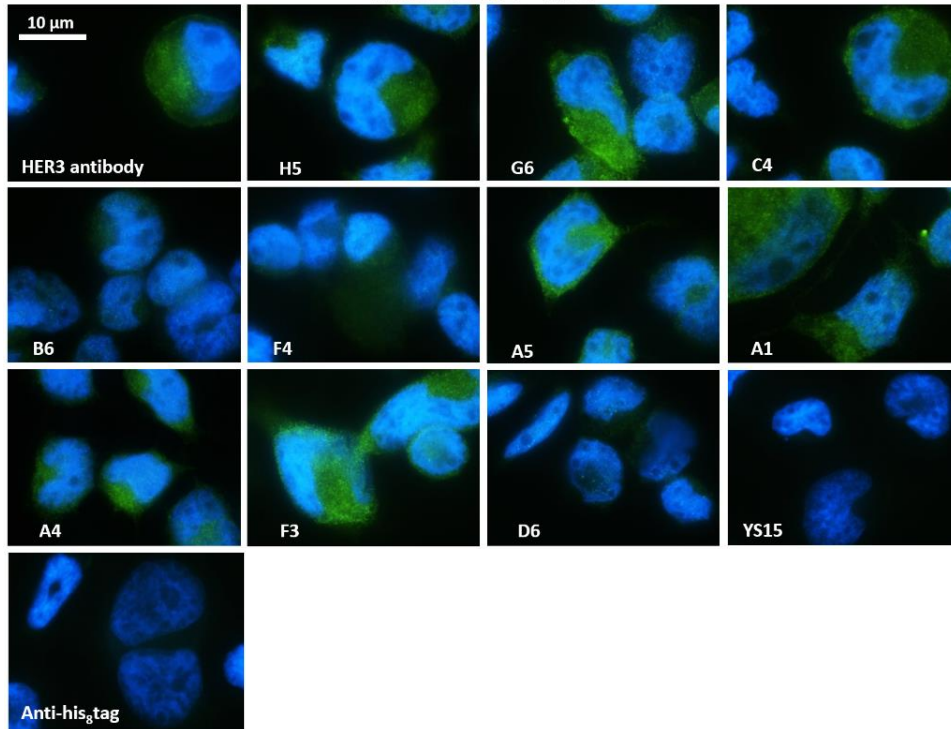
4.2.4.1 Binding characterisation by immunofluorescence microscopy

The binding of anti-HER3 Affimer reagents to native HER3 was assessed on fixed and live cells by fluorescent microscopy (figure 4.8 and 4.9). Affimers were incubated overnight on fixed monolayer of two cell lines (MDA-MB-453 and MCF7), which are known to overexpress HER3 (Gostring et al., 2012). Affimer reagents were detected using an anti-his₈tag antibody and fluorescently tagged secondary reagent. All Affimers, except of **B6** and **D6**, showed staining similar to the anti-HER3 antibody (Figure 4.8).

Five of anti-HER3 Affimers showed consistent binding to both cell lines (**G6**, **A5**, **A1**, **A4**, and **F3**) similar to the antibody. The background level, which can result from binding of anti-his₈tag antibody to other proteins in the cellular entity, was also assessed by incubating the fixed cells with anti-his₈tag antibody without Affimers. In addition, anti-yeast SUMO2 (YS15) Affimer reagent was used as a negative control. No positive staining of cells was seen with both anti-his₈tag and YS15 reagents.

Further studies of anti-HER3 Affimers on live cells, showed the ability of 4 Affimers (**G6**, **A5**, **A4**, and **F3**) to bind HER3 expressing cells prior to fixing them (figure 4.9), but their binding specificity towards HER3 needs to be confirmed with co-staining studies using a validated HER3 antibody. All Affimer molecules were incubated with MCF7 cells (overexpressing HER3) for one hour at 37°C, with CO₂ supplementation, prior to fixing and permeabilising them to add the antibodies. All four Affimers showed internalisation ability, while others revealed aggregation-like pattern of staining which may indicate that Affimer reagents were aggregated prior to use in the assay due to the presence of the cysteine residue and that may limit their ability to work. Therefore, a repeat of the staining using fluorescently conjugated Affimer reagents or a cysteine-free Affimers is needed.

MDA-MB-453



MCF7

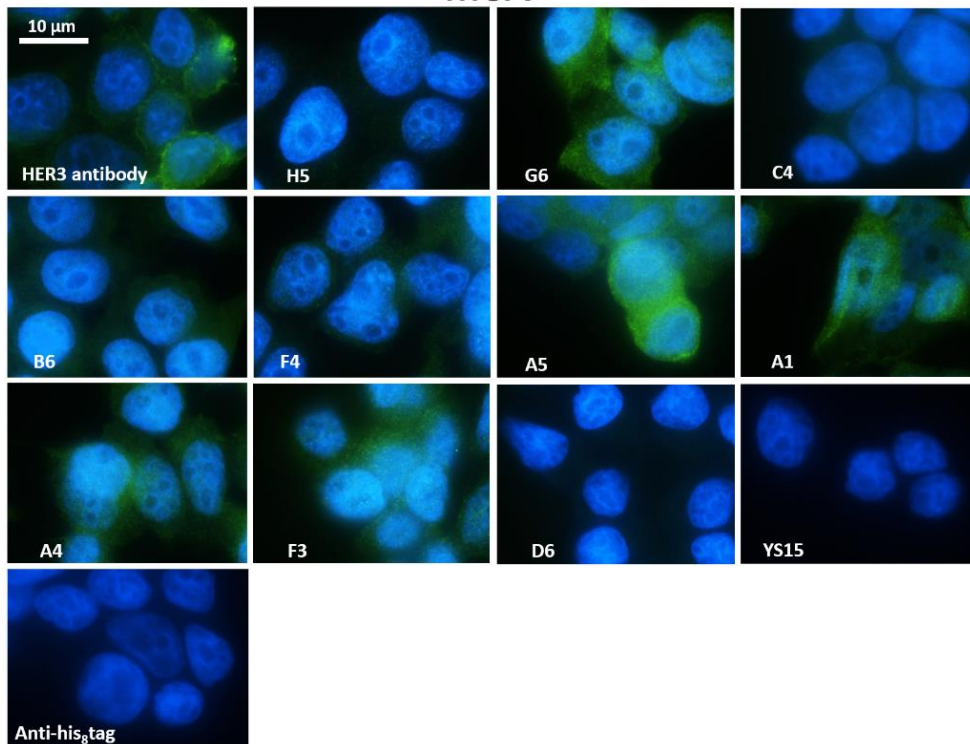


Figure 4.8 Immunofluorescence microscopy confirming the ability of anti-HER3 Affimers to bind the HER3 on fixed cells. Cells were fixed with 4% paraformaldehyde and all Affimers were incubated with cells for overnight at 4°C. Bound Affimers were detected by mouse anti-his₈tag and visualised with the anti-mouse Alexa488 conjugated antibody. All images were merged in which cell nucleus was stained with DAPI (blue), while green colour indicates the binding of both anti-HER3 Affimers and antibody. Yeast SUMO2 (YS15) binding Affimer and anti-his₈tag alone were used as negative controls. Scale bar: 10μm (*n* = 2).

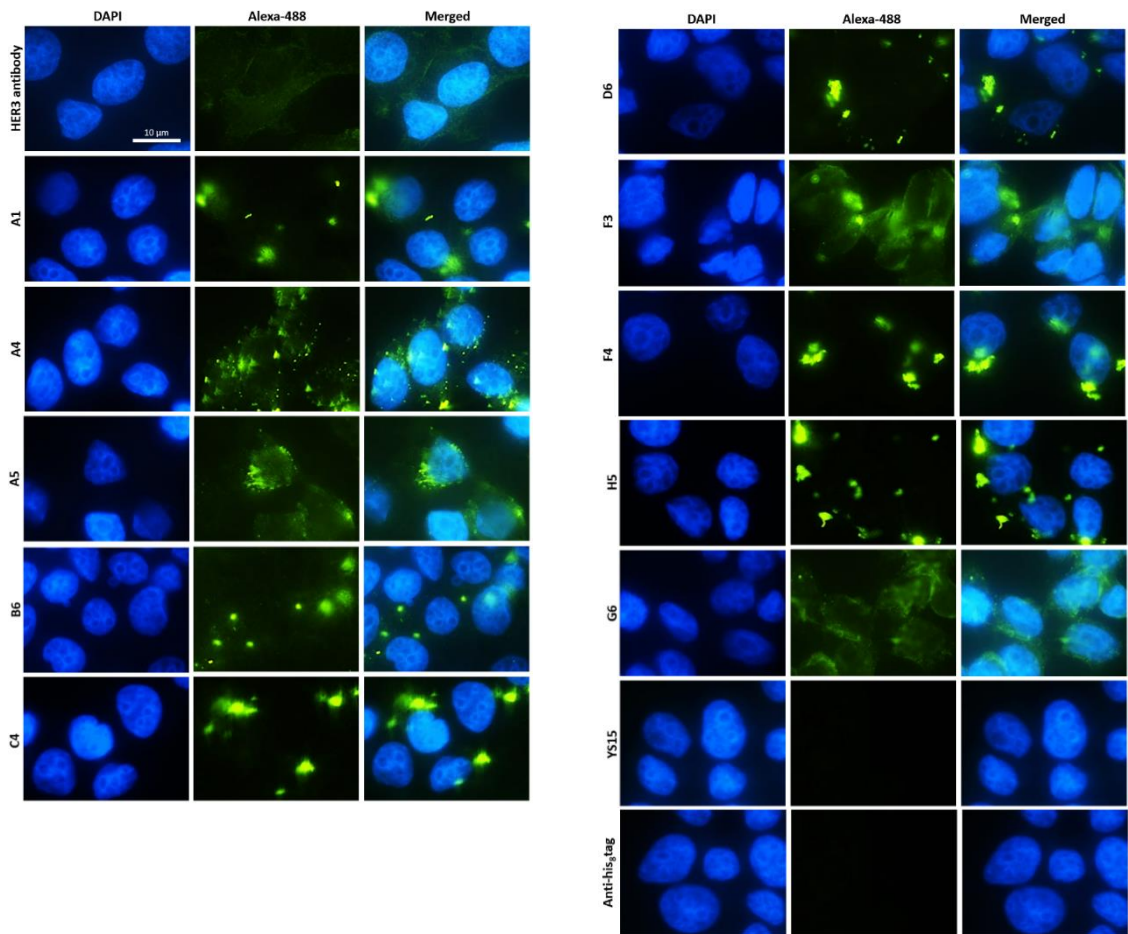


Figure 4.9 Immunofluorescence microscopy showing the capability of anti-HER3 Affimer reagents to bind native receptor on live cells and causing it to internalise. All Affimers were incubated with live cells for 1 hour under physiological conditions prior to fixing them. Bound and internalised Affimers were detected by mouse anti-his₈tag and visualised with the anti-mouse Alexa488 conjugated antibody. All images were merged in which cell nucleus was stained with DAPI (blue), while green colour indicates the binding of both anti-HER3 Affimers and antibody. Yeast SUMO2 (YS15) binding Affimer and anti-his₈tag alone were used as negative controls. Scale bar: 10µm (*n* = 2).

In contrast to our Affimer reagents, HER3 antibody showed weak fluorescence (green) binding signal because of its inability to bind the ECD of HER3. No staining was detected with both negative controls used in this experiment, including the anti-YS15 Affimer and the anti-his₈tag antibody.

4.2.4.2 Anti-HER3 Affimers pulled-down the endogenous HER3 protein from different cell lysates

MDA-MB-453 (overexpressing HER3 and HER2) and MCF7 (overexpressing HER3 only) cells were lysed using non-denaturing cell lysing reagents. Non-denaturing reagents were used to maintain the native conformation of HER3 (Duquesne et al., 2016; Duquesne and Sturgis, 2010). Anti-HER3 Affimers were incubated with cell lysates for overnight at 4°C. Following incubation, the complexes were precipitated with nickel agarose beads. The captured complexes were then eluted with 300mM imidazole containing buffer after being washed multiple times. Finally, the eluates were denatured and ran in an SDS-PAGE gel to start western blot analysis using anti-HER3 and HER2 antibodies. Negative controls including anti-YS15 Affimers, cell lysate prepared from HER3 deficient (MDA-MB-468) cell line, and PBS were included in each run.

The first remark we noticed from the blots is that MCF7 cell lysate do contain high level of HER2 protein. Our result contradicts other reports that stat MCF7 cells have low levels of HER2 (Khan et al., 2017; Holliday and Speirs, 2011; Subik et al., 2010). However, it was recently revealed that MCF7 cells can develop heterogeneous cell variants overexpressing HER2 upon culturing, and thus resulting in discrepancy reported in regards to the HER2 expression level in MCF7 cells (Khan et al., 2017). Therefore, we could not rely on the pull-down assay results for determining the selectivity binding of our anti-HER3 Affimers towards HER3 only. The optimal option to evaluate the cross-reactivity of our reagents in such assay is by using HER2 knockdown cell line to serve as the negative control.

All of the anti-HER3 Affimers (**A1, D6, B6, H5, F4, G6**) affinity precipitated (pull down) endogenous HER3 but also interacted with HER2 protein (figure 4.10). However, **F3, A5** and **A4** Affimers pulled-down HER3 but potentially showed weaker interaction with HER2 protein. The ability of Affimers to precipitate both HER2 and HER3 is most likely due to the level of HER2-HER3 complex in cell lysates, as none of the reagents show

cross-reactivity to recombinant protein (figure 4.3). Also previous research has shown that HER2-HER3 dimerization is highly likely to occur in cancer cells that overexpress HER2, such as the MDA-MB-453 cells (Takagi et al., 2014). As such HER2 protein would be expected to be pulled down by the anti-HER3 reagents.

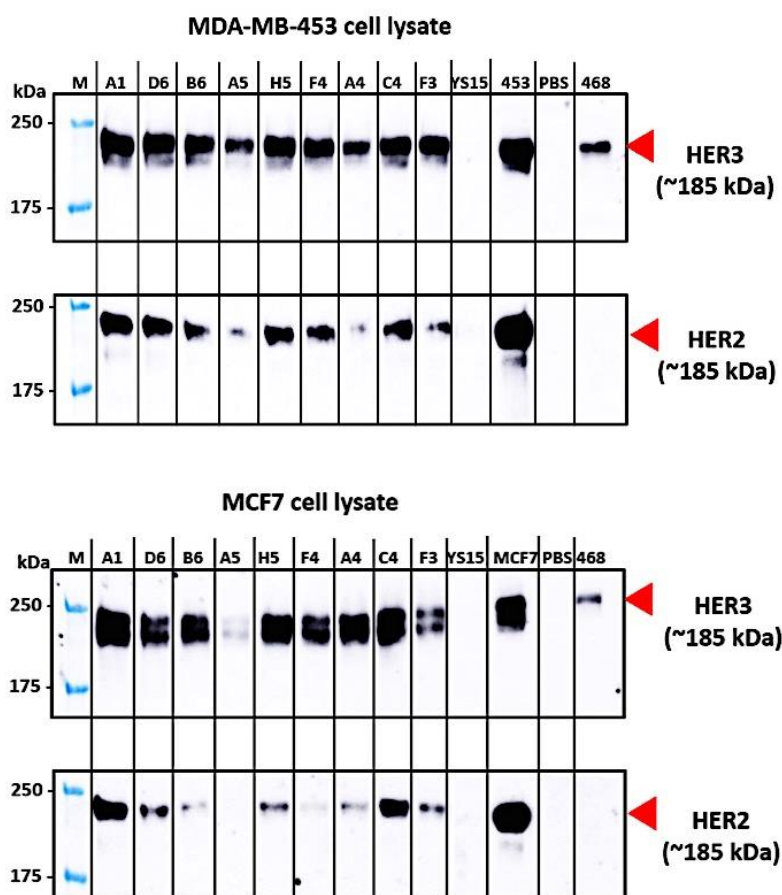


Figure 4.10 Anti-HER3 Affimers showed ability to pull-down endogenous HER3 overexpressed in MDA-MB-453 and MCF7 cancer cells. Affimers were incubated with the cell lysates prepared from both cell lines for overnight at 4°C. The Affimer-HER3 complex was then precipitated using NiNTA agarose beads, washed and eluted. The eluates were separated on an SDS-PAGE gel and blotted against HER3 and HER2 antibody. The yeast SUMO2 (YS15) Affimer reagent, PBS, and MDA-MB-468 (low HER3 expression) were used as negative controls ($n = 2$).

4.2.4.3 Anti-HER3 Affimers as biotin-conjugated reagents for use in IHC

Immunohistochemistry (IHC) is the primary technique used to determine the expression status of the HERs receptors in a formalin-fixed paraffin embedded (FFPE) tissue or cell

samples (Duraiyan et al., 2012). Therefore, affinity reagents, including Affimers, that work in such applications would represent promising alternatives to antibodies in this technique. To test the ability of our isolated anti-HER3 Affimers, we initially labelled them with biotin. Optimisation of biotinylation is further discussed in chapter 5. According to the optimised biotin conjugation protocol mentioned in section 2.2.5.2, Affimers were labelled with single biotin molecule via the cysteine residue at their C-terminal. The efficiency of biotin-labelling was evaluated by ELISA using TMB substrate against the streptavidin-conjugated HRP (section 2.2.2.1.2). The measured absorbance at 620 nm showed the extent of biotinylation of all Affimers. Based on the absorbance reading, all HER3 binding Affimers were efficiently biotinylated (figure 4.11).

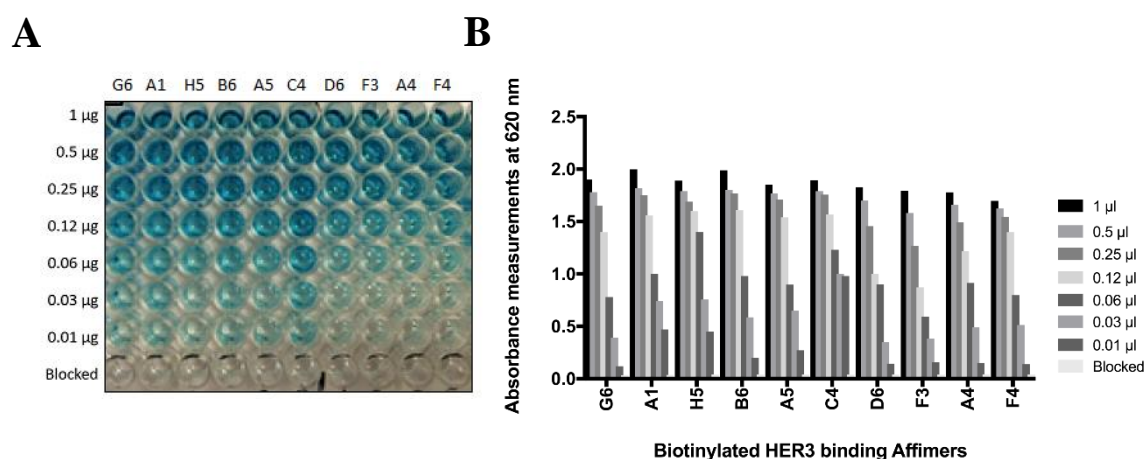


Figure 4.11 ELISA confirming the efficiency of biotinylated anti-HER3 Affimers. Affimers were biotinylated via cysteine residue introduced in their C-terminal domain of the scaffold using maleimide- site specific-thiol based reagent. (A) Showing the colour change for samples in a strip for different dilutions of biotinylated anti-HER3 Affimers. PBS was used as negative control added to blocked wells. (B) presenting the absorbance measurements at 620 nm for all wells from A were measured and plotted in a histogram ($n = 3$).

After successful biotinylation, the labelled Affimer reagents were tested in IHC using a panel of two HER3 overexpressing cancer cell lines (MDA-MB-453 and MCF7) and an immortalised breast cell line (HB2). A polyclonal mouse HER3 antibody was used as a positive control (see table 2.1). To evaluate the efficiency of blocking endogenous biotin, streptavidin conjugated HRP was added to cells to serve as negative control. Anti-HER3 Affimers, **G6, A5, B6, C4** and **A4** showed positive by weak staining of the cancer cell

lines (figure 4.12). No staining was observed in samples where streptavidin-HRP was added. As well as the weak staining, the localisation pattern was different compared to the polyclonal anti-HER3 antibody. This may indicate that HER3 binding Affimers may not be suitable for the use in IHC or that the biotinylation efficiency of Affimers should be confirmed prior to the use of Affimers in any application as the presence of non-

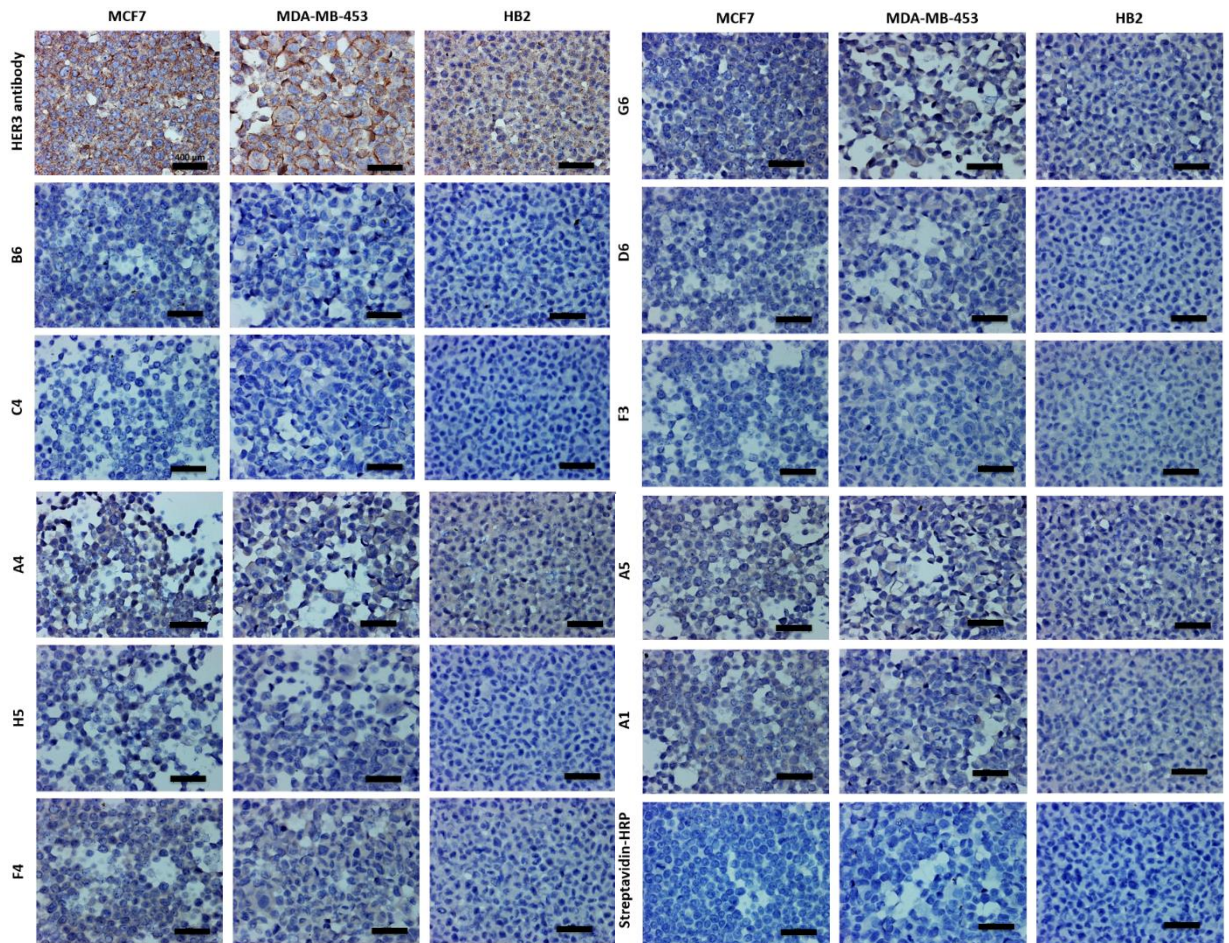


Figure 4.12 Staining of anti-HER3 Affimers on a panel of FFPE cancerous and non-cancerous breast cells. All biotinylated-Affimers were incubated with cells on slides for one hour at room temperature after deparaffinising the wax coating layer and retrieving the antigenicity with heat. Biotinylated-Affimers were detected with streptavidin-HRP and visualised with DAB that gives (brown). Endogenous biotin was blocked with avidin-biotin blocking kit to block further non-specific binding of streptavidin reagent. Negative control where no Affimers were added was used as negative control, while anti-HER3 antibody served as a positive control. Scale bar: 20 μ m and images were taken at 16X magnification ($n = 1$ per sample section and 2 in total as 2 different FFPE blocks of each cell line were used).

biotinylated Affimers may compete with the non-biotinylated ones causing false-negative results. In our case, we could not conclude the reason that caused Affimers to not work in IHC as we did not evaluate the biotinylation efficiency using a sensitive, quantitative technique, such as mass spectrometry. Also, the anti-HER3 antibody is polyclonal and therefore has the advantage of signal amplification compared to biotinylated reagents (Ivell et al., 2014), and thus an ideal comparison would be by using monoclonal HER3 antibody. In chapter 5, different signal amplification strategies will be further discussed and explored.

4.2.5 Inhibition of downstream cell signalling by anti-HER3 Affimers

HER3 is activated by neuregulin (NRG1 β) growth factor binding to its extracellular domain inducing conformational changes, transautophosphorylation and downstream signal transduction stimulation (Yarden, 2001). To test the ability of the anti-HER3 Affimers to inhibit receptor activation, three different breast cancer cells (MDA-MB-453, BT474 and MCF7) were cultured with 100 μ g/ml of anti-HER3 Affimers for 60 minutes prior to stimulation with either 25 or 100 ng/ml of NRG1 β .

Initially, the optimal concentration and time of NRG1 β treatment was assessed by measuring the level of MAPK activation via measuring phosphorylation of ERK by western blotting (data obtained by personal communications). In both MDA-MB-453 and MCF7 cells, ERK1/2 activation was detected after 5 minutes of culturing with 25 ng/ml of NRG1 β . In BT474 cells, activation of the ERK1/2 required highly concentrations of NRG1 β (100 ng/ml). Using these conditions, all cells were treated with anti-HER3 Affimers and their inhibitory effect on the downstream signalling was assessed by their ability to inhibit phosphorylation of ERK1/2 by western blot analysis (figure 4.13). Tubulin was used as loading control.

In HER2 overexpressing cells (MDA-MB-453 and BT474), the activation of ERK1/2 was completely inhibited by **D6** and **C4**, while **A1**, **F4** and **A5** anti-HER3 Affimers partially inhibited the activity of ERK1/2 signalling pathway binding Affimers (figure 4.13 A and B). In MCF7 stimulated-cells, no inhibition of the ERK1/2 protein activity was detected upon treating the NRG1 β -induced cells with all anti-HER3 Affimers (figure 4.13 D). In all cell types the control anti-YS15 Affimer did not affect phosphorylated ERK1/2.

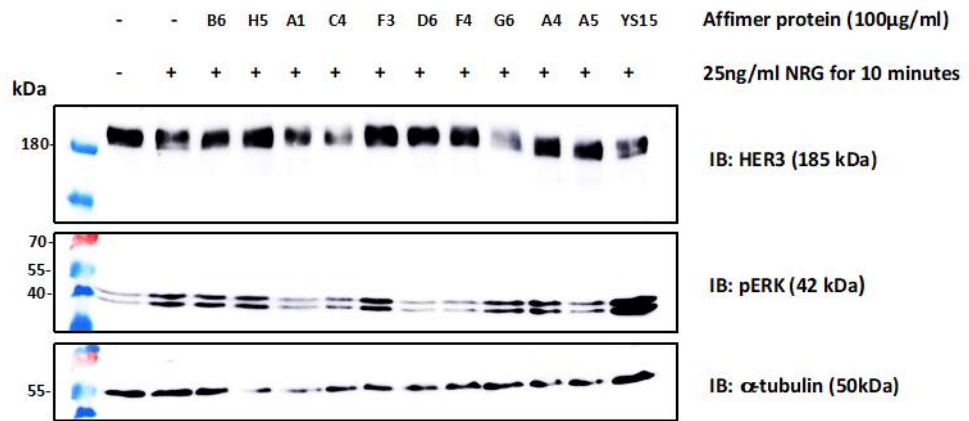
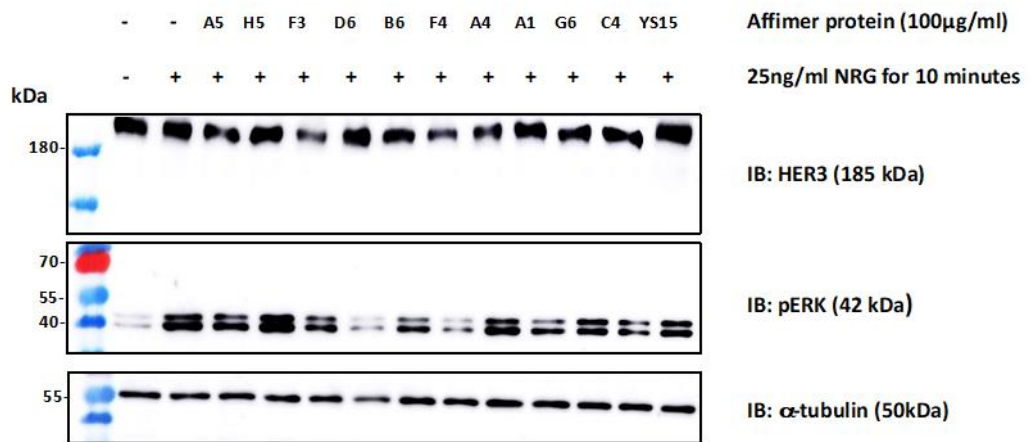
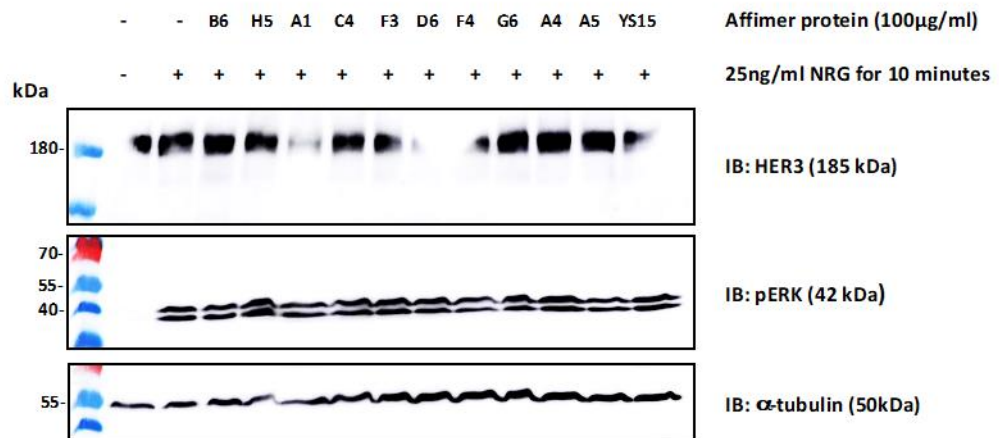
A**B****C**

Figure 4.13 Western blots indicating the inhibitory effect of HER3-binding Affimers on downstream signalling pathway (MAPK/ERK1/2) after NRG stimulation in various HER3-overexpressing cells. HER2 overexpressing breast cancer cells MDA-MB-453 (A), and BT474 (B), in addition to the HER2 deficient cells, which are the MCF7 (C) ones were cultured with 100 µg/ml of Affimers for 60 minutes prior to 25 or 100 ng/ml NRG stimulation. Cells were then lysed, and the lysates were ran on SDS-PAGE gel for western blot analysis using HER3, phosphorylated-ERK1/2 (T202/Y204), and tubulin antibodies (n = 1).

Tubulin antibody confirmed that all lysates contained similar amount of protein. Our preliminary results showed the potential of using Affimers to target and inhibit these receptors. However, confirmation of the results is currently in progress as the experiment illustrated here was performed only once due to time constraints. Targeting HER3 in such tumours would be of advantage when combined with other HER2 targeting agents. Furthermore, our preliminary findings also revealed that HER3 overexpressing cells, such as MCF7, may compensated the activity of the MAPK signalling pathway independently to HER3.

4.2.6 Ability of EGFR binding Affimers to recognise the receptor in different applications

The anti-EGFR Affimers were evaluated by immunofluorescence microscopy and affinity precipitation on cell lines.

4.2.6.1 Anti-EGFR Affimers bind to cells

Anti-EGFR Affimers were assessed for their binding ability to bind to MDA-MB-468 (a cell line that expresses high levels of EGFR) and three cell lines that express low levels of EGFR (MDA-MB-453, BT474 and HB2). The protein expression level of EGFR on these cells was confirmed by western blot analysis (data not shown) which confirmed by previously reported results (Buick et al., 1990; Hyatt and Ceresa, 2008).

The anti-EGFR Affimers were initially assessed using fixed cells. Binding was detected with anti-his₃tag and mouse anti-IgG Alexa488 conjugated antibody. All Affimers showed positive binding to EGFR on all cells, showing a localisation pattern similar to that seen with the EGFR antibody (figure 4.14). No staining was observed in both negative controls (anti-YS15 Affimer and cells stained with anti-his₃tag antibody only).

Next, we further assessed the binding ability of all anti-EGFR Affimer on live cells, in which Affimers were added to cells prior to fixation (section 2.2.6.2). Bound Affimers were detected with anti-his₃tag and anti-mouse Alexa488 conjugated antibody (green colour). In this experiment a membrane marker, include wheat germ agglutinin (WGA) Alexa-594 conjugated (red colour signal) was used to visualise the plasma membrane of cells. All Affimers showed binding to cells with **H9**, **G10**, and **H91** showing potential

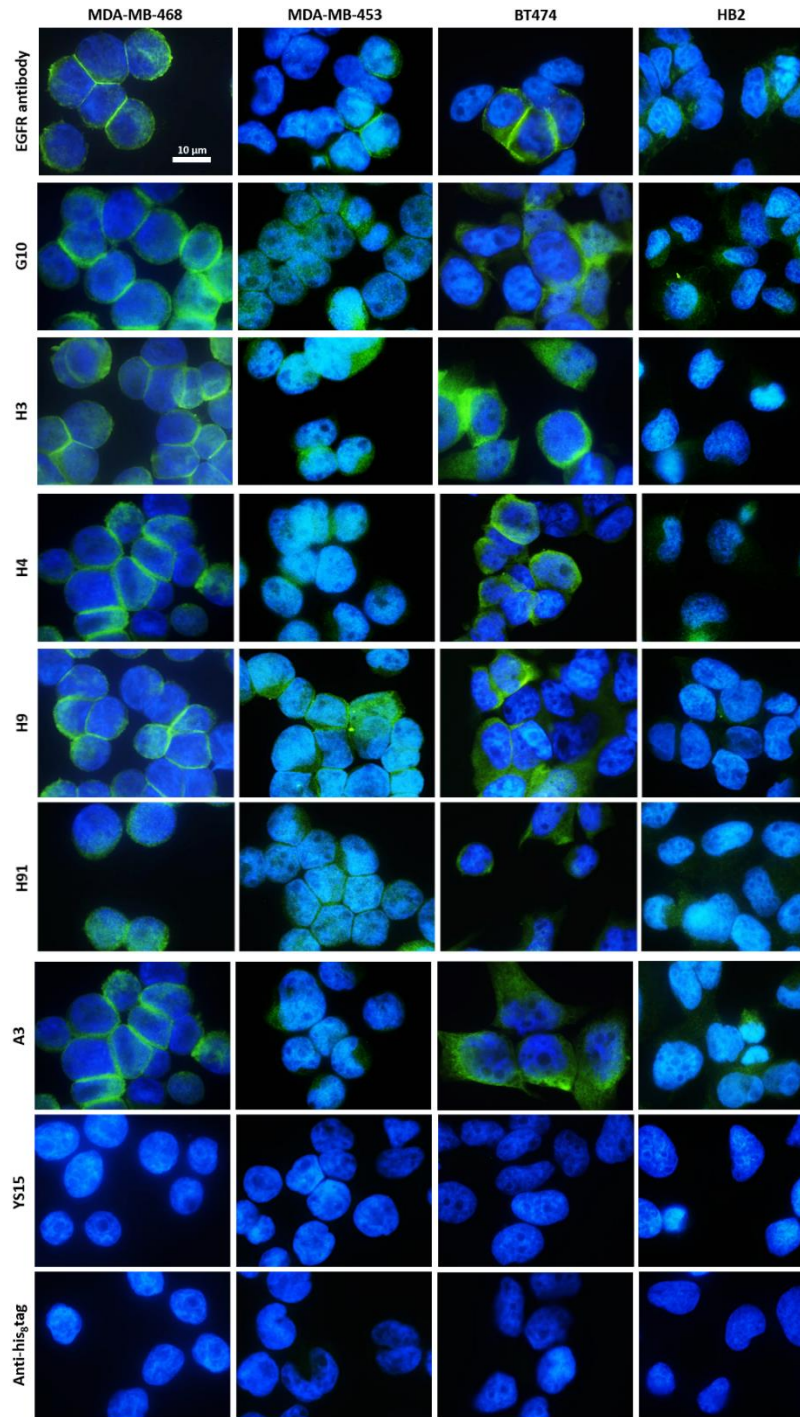


Figure 4.14 Immunofluorescence microscopy showing the ability of anti-EGFR Affimers to bind the native EGFR. Cells were fixed with 4% PFA and Affimers were incubated with cells for overnight at 4°C. Affimers were detected by mouse anti-his tag and visualised with the anti-mouse Alexa488 conjugated antibody (green). All images were merged in which cell nucleus was stained with DAPI (blue). Yeast SUMO2 (YS15) binding Affimer and anti-his tag alone were used as negative controls. Scale bar: 10μm ($n = 3$ for MDA-MB-468 and $n = 2$ for all other cell lines).

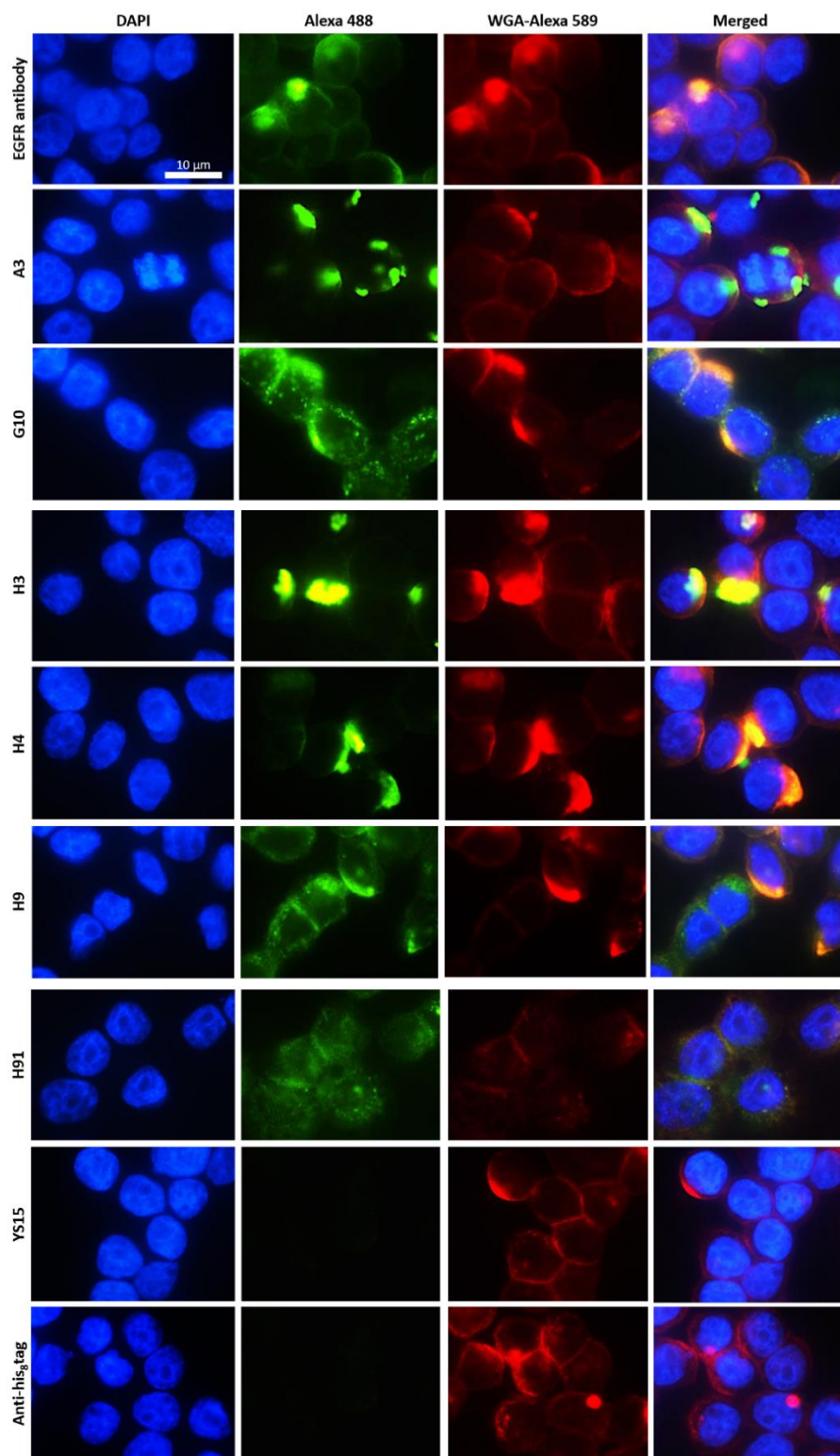


Figure 4.15 Anti-EGFR Affimers bind to MDA-MB-468 cells in live cell culture. All Affimers were incubated with MDA-MB-468 for one hour prior to fixing in PFA. Wheat germ agglutinin (WGA) Alexa 594 conjugated marker was used to stain membranes (red). Affimers were detected by mouse anti-his₈tag and visualised with the anti-mouse Alexa488 conjugated antibody (green). Cell nuclei were stained with DAPI (blue), and the yellow colour represents the co-localisation of Affimers with the membrane marker. Yeast SUMO2 (YS15) binding Affimer and anti-his₈tag alone were used as negative controls. Scale bar: 10μm (*n* =2 with and without the use of WGA).

ability to internalise into cells (figure 4.15). No positive binding signals were seen with both anti-YS15 Affimer and anti-his₈tag antibody negative controls. In figure 4.15, not all cells displayed positive membrane staining. The mechanism of membrane lectin staining involves the binding of the WGA to the exposed *n*-acetylglucosamine residues at the peptidoglycan outer membrane layer (Emde et al., 2014; Higashi et al., 1988). Therefore, when the plasma membrane is damaged due to cell death or cellular permeabilisation, no staining can be detected, which was thought to have occurred in the two repeats of immunofluorescence staining of live cells using anti-EGFR Affimers.

As shown in figure 4.15, no negative control cell line (non-EGFR expressing cell line) was included. This represents a major drawback of the performed experiment, but our main intention was to examine the possibility of the anti-EGFR Affimers to bind to HER2 expressing cells and causing receptor internalisation in order for the work to be pursued by other researchers.

The microscopy results on both live and fixed cells confirmed the binding ability of three anti-EGFR Affimers to EGFR expressing cells and thus making them promising tools to be used for future *in vitro* diagnostics and *in vivo* imaging. The internalisation capability of four EGFR binding Affimers may suggest the critical role that our reagents may play in the development of novel cancer-targeting therapy. Despite all the observed staining on both fixed and live cells using anti-EGFR Affimers, we cannot confirm the specificity of these Affimers towards EGFR, as no MS analysis or co-localisation study to confirm their specificity were performed. Therefore, assessment of the specificity of the Affimers and their binding affinity is of need and it is currently a work in progress.

4.2.6.2 All anti-EGFR Affimers pulled down the endogenous receptor from cell lysate

The ability of anti-EGFR Affimers to affinity precipitate EGFR from cell lysate was assessed using MDA-MB-468 (EGFR overexpressing) cell line. Following the pull-down protocol mentioned in section 2.2.6.5, the eluted Affimer-protein complexes were denatured and ran on SDS-PAGE gels for western blot analysis. Nitrocellulose membranes were blotted against EGFR antibody. Figure 4.16 confirmed the binding of Affimers to EGFR by pulling it down from the EGFR overexpressing cell lysate. No protein was pulled down with the negative control anti-YS15 Affimer reagent.

Using pull-down assay and Immunofluorescence test, we were unable to detect the Affimers selectivity towards EGFR only. As such, future studies using EGFR knockdown cell lines to perform binding assays will provide further characterisation to assess the binding selectivity of our isolated anti-EGFR reagents.

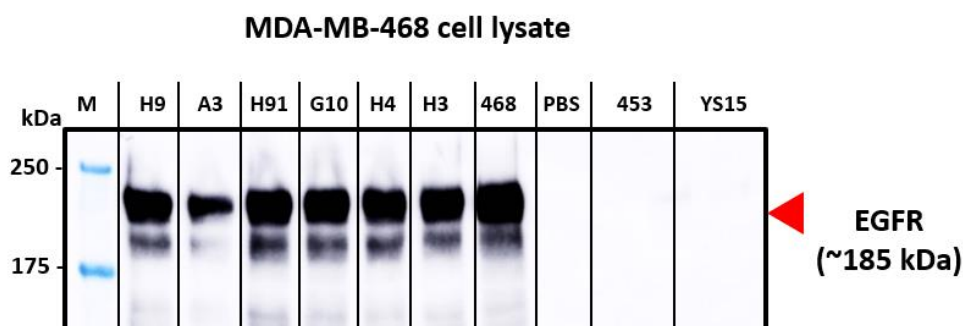


Figure 4.16 Anti-EGFR Affimers pulled-down EGFR from cell lysate prepared from MDA-MB-468 cancer cells. Affimers were incubated with the cell lysates prepared overnight at 4°C. EGFR-Affimers complexes were precipitated using NiNTA agarose beads, washed and eluted. The eluates were separated on an SDS-PAGE gel and blotted against EGFR antibody. The yeast SUMO2 (YS15) Affimer reagent, and PBS were used as negative controls. (n = 2)

4.2.7 Anti-EGFR Affimers downregulated the MAPK-ERK1/2 signalling activation in HER2 overexpressing cells

In immunofluorescent microscopy, **G10**, **H9**, **H91** and **A3** anti-EGFR Affimers showed internalisation into the MDA-MB-468 cells. To investigate potential effect of the EGFR binding Affimers on MAPK pathway, ERK1/2 phosphorylation was assessed using western blot analysis. Degradation of receptor was evaluated by blotting against the total EGFR using the rabbit monoclonal EGFR antibody. In many EGFR overexpressing cells, including MDA-MB-231 and MDA-MB-468, the MAPK pathway is constitutively active due to activated mutated Ras or Raf effector proteins (Nagarja et al., 2017). Therefore, we tested other EGFR expressing cell lines include MDA-MB-453 and BT474. EGFR trigger cell survival signalling through its activation with EGF-ligand (Yarden, 2001). When we stimulated both MDA-MB-453 and BT474 cells, with different concentrations of EGF-ligand, BT474 was the only cell line that showed efficient ERK1/2 activation after 5 minutes.

After culturing BT474 cells with 100 $\mu\text{g}/\text{ml}$ of anti-EGFR Affimers prior to EGF-induced activation, **G10**, **H9** and **H91** showed inhibition of the EGF-induced ERK1/2 phosphorylation (figure 4.16). In addition, the level of the total EGFR in cells treated with the three Affimers (**G10**, **H9** and **H91**) was reduced (figure 4.17). No inhibition of ERK1/2 phosphorylation was observed when cells were treated with Anti-YS15 control Affimer. Blotting of tubulin indicated equal loading of proteins in each lane. The preliminary findings suggest anti-EGFR Affimers **G10**, **H9** and **H91** may cause increased receptor degradation by lysosomes. As such, anti-EGFR Affimers may represent novel therapeutic agents for treating EGFR expressing cancers that are resistance for other targeted therapies and can also be used in combination with the other selected HER3 Affimers to create dual cancer-targeting agents to further enhance the inhibitory effect against tumour growth. However, our results are preliminary, as it performed only once due to our time limitation, and a repeated experiment to confirm the obtained results is required.

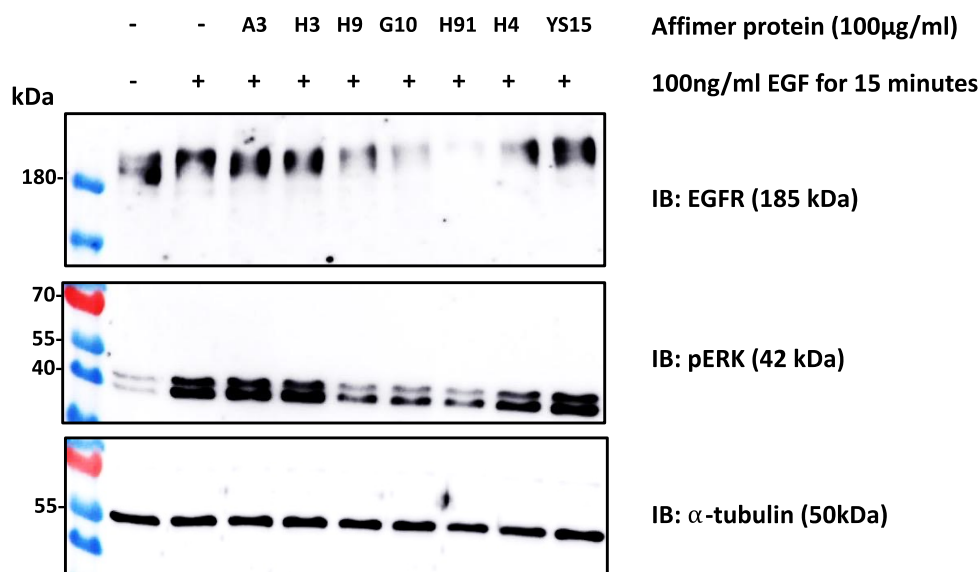


Figure 4.17 EGFR binding Affimers inhibit EGF-stimulated signal transduction in BT474 cells. BT474 cells were cultured with 100 $\mu\text{g}/\text{ml}$ of Affimers for 60 minutes prior to 100 ng/ml EGF stimulation. Cells were then lysed, and the lysates were run on an SDS-PAGE gel for western blot analysis using EGFR, phosphorylated-ERK1/2 (T202/Y204), and tubulin antibodies ($n = 1$).

4.3 Discussion

In this chapter, we demonstrated isolation of Affimer reagents against the extracellular domain (ECD) of HER3 and EGFR using phage display. However, their selectivity towards their target proteins remains questionable as no negative control cell lines were employed and thus full characterisation of their binding selectivity and specificity is still under investigation through use of a confirmatory application such as MS coupled with pull-down assay, a co-localisation study with receptor specific antibody, or competitive assays using monoclonal antibodies against the receptor of interest.

For instance, all anti-HER3 reagents pulled-down endogenous HER3 and HER2 protein. As the reagents showed little cross-reactivity to HER2 by ELISA, this suggests that the Affimers are affinity precipitating HER2/HER3 complex rather than showing cross reactivity with HER2. However, this will need to be confirmed by knocking down the individual proteins using siRNA and repeating the experiment. In addition to pull downs, we demonstrated the lack of sensitivity of the reagents in IHC. Successful utilisation of reagents in IHC requires the reagent to be at high binding affinity (nanomolar to picomolar) to work in IHC-like assays (Orlova et al., 2006), perhaps suggesting the reagents have lower affinity than expected binding affinity of 50 nM observed with the only anti-HER2 affibody binding reagent, which can work in IHC and as molecular imaging reagent (Baum et al., 2010;Gostring et al., 2012;Wikman et al., 2004). However, using the most common formaldehyde fixatives creates methyl cross-linking bridges between amino acid residues of the protein altering by that the structure of the protein and lowering the accessibility of antigen sites (Li et al., 2017).

Therefore, different antigen retrieval (AR) methods break the cross-linking and thus expose the epitopes but, at the same time, they may result in protein denaturing (Singh and Sood, 2017). Given the fact that affinity reagents are dependent on conformation of target, reagents suitable for IHC are potentially more difficult to identify. This reason might explain why anti-HER3 affibodies were used to stain HER3 in Cryo-sections where no AR retrieval process is involved (Orlova et al., 2006) while other binding DARPins (Zahnd et al., 2006) used proteolytic enzyme method to ensure complete unmasking of the protein. Another factor that may cause weak staining of the Affimers is the need for a sensitive signal detection system (Kohler et al., 2000). Hence, to improve the performance of the our HER3 binding reagents in IHC, it may be necessary to investigate

their binding affinity, perform affinity maturation, attempt different AR methods and develop signal amplification system.

Despite the vast growth of the development of various HER3 targeting agents, none have been approved for cancer treatment to date (Jacob et al., 2018). Here we demonstrated the ability to inhibit HER3 signalling similar to previously published results using affibodies (Gostring et al., 2012). Anti-HER3 affibodies were able to inhibit NRG-induced cancer cell growth by blocking the MAPK activation. However, the reported inhibitory effect of the affibodies was detected only in MCF7 cells but not in the other tested HER2 overexpressing cells (SKBR3) (Gostring et al., 2012). In their study, anti-HER3 affibodies showed competitive binding with the NRG1 β ligand. As they did not confirm if the Affibody reagents do not cross react with other receptors, there is a high chance that affibodies were binding to both HER3 and HER4, which found to be overexpressed in MCF7 (Gerarduzzi et al., 2016), preventing the NRG1 β ligand from binding to both receptors (figure 4.18).

In HER2 overexpressing cells, the dimerization between HER2 and HER3 could create a binding pocket for more NRGs to bind (Claus et al., 2018). Therefore, targeting agents against such conformational dynamics would be of help for inducing complete inhibition of cell growth by preventing such conformational change (figure 4.18). The developed anti-HER3 affibodies could not inhibit receptor structural change and that confirmed by their inability to inhibit the downstream signal activity in the SKBR3 (HER2 overexpressing) cells where high level of HER2-HER3 complexed were detected (Gostring et al., 2012). In contrast to affibodies, we suggest that our anti-HER3 Affimers can prevent the occurrence of HER3 conformational change by inhibiting its dimerization to HER2. Our suggestion is in line with the inability of HER3 binding Affimers to inhibit the phosphorylation of ERK1/2 in MCF7 cells (HER3 and HER4 overexpressing cells). In NRG1 β -induced MCF7 cells, both active HER3 and HER4 will simulate further downstream signalling. In future studies, it would be interesting to further investigate the effect of HER3 binding Affimers in NRG1 β -induced HER4 and HER3 overexpressing tumours by blocking the activity of HER4 using the previously developed anti-HER4 Affimer reagents (Tiede et al., 2017; Zhuravski et al., 2018). These studies will also explore further the differences of the involved downstream signalling pathways between different tumours which can eventually result in better treatment.

EGFR is another valuable target for cancer therapy (Seshacharyulu et al., 2012). Three of the anti-EGFR Affimers showed binding to the native EGFR protein on live cells comparable to that seen with the antibody and comparable to previously developed protein scaffolds, including DARPins (Boersma et al., 2011), Aptamers (Li et al., 2011) and affibodies (Friedman et al., 2007). **G10**, **H9**, and **H91** anti-HER3 Affimer reagents also showed an internalisation ability similar to what has been observed with anti-EGFR affibody (Friedman et al., 2007).

The potential internalisation observed with the Affimer may cause receptor degradation and then reduce further activation of the downstream signalling (Henriksen et al., 2013). To test this possibility, EGF-induced cells were pre-treated with anti-EGFR Affimers. In EGF-induced BT474 cells, all **G10**, **H9** and **H91** Affimers reduced the phosphorylation activity of ERK1/2 protein but also caused a reduction in total EGFR. This reduction of total EGFR was not observed with other monomeric scaffolds (Friedman et al., 2007). However, when a bivalent DARPIn was added to EGF-induced cells a similar complete loss of the total EGFR was seen (Boersma et al., 2011). Introducing cysteine residue at the C-terminal region of the Affimer scaffold can cause Affimers to dimerise and that may create a bivalent effect as the one observed with the engineered construct of DARPIn (Boersma et al., 2011).

The synergistic effect of targeting both HER2 and EGFR on tumour cell survival (Yu et al., 2018), highlights the need to develop bivalent Affimers to inhibit both receptors. Recent study on different HER2 overexpressing cell lines (BT474 and SKBR3), revealed that blocking EGFR with monoclonal antibody or tyrosine kinase inhibitors in such cells is not effective (Dietel et al., 2018). Inducing growth of HER2 overexpressing cells with EGF ligands will over-activate other non-membrane associated proteins, particularly the protein tyrosine kinase interacting protein 51 (PTKIP51), that found to maintain a basal level of MAPK pathway activity under conditions where EGFR is blocked (Dietel et al., 2018). This role of other downstream MAPK regulating proteins further explains the limited effect we saw upon blocking EGFR in the EGF-induced, HER2 overexpressing cells (figure 4.16). By investigating the mechanism that caused total loss of EGFR, researchers showed that the used bivalent DARPIn constructs bound to the receptor, induced its internalisation and, at the same time, inhibited its recycling back to the cell surface (Boersma et al., 2011). Our Affimers may follow similar mechanism but further investigations on EGFR overexpressing cell lines could be done in future.

In conclusion, we have successfully developed Affimer reagents against the extracellular domain of both HER3 and EGFR. These reagents represent a novel antibody alternatives in cancer diagnostics, *in vitro* imaging and potentially in therapeutics.

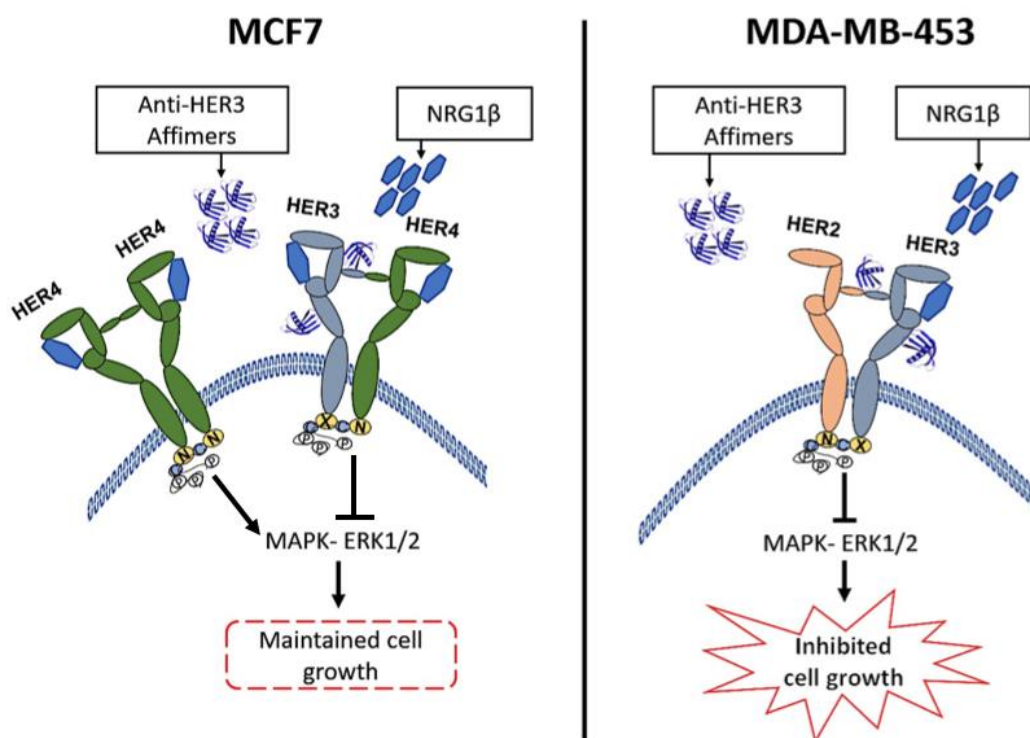


Figure 4.18 The suggested mechanism of anti-HER3 Affimers modulating the stimulatory effect on NRG-stimulated signal transduction in cells with different HER2 expression level. In HER2 overexpressing cells (MDA-MB-453), Affimers showed inhibition of the downstream signalling activity and that can be addressed to Affimers blocking the conformational change of HER3 resulted from its dimerization to NRG. However, in HER2 deficient cells including MCF7, blocked HER3 activity can be compensated by the active HER4. As such the downstream signalling activity via the MAPK-ERK1/2 pathway was maintained.

CHAPTER 5

Modified Affimer reagents for improved biomarker detection in IHC

5.1 Introduction

Numerous pathophysiological biomarkers are routinely used in diagnostic (Perlis, 2011; Selleck et al., 2017). In patients' samples, biomarkers can be detected using various types of assays, including immunohistochemistry (IHC). This assay helps in the detection, visualisation and semi-quantification of a defined protein in tissue sections without the destruction of the histologic architecture (Farr and Nakane, 1981). Recent advances in techniques for unmasking antigens in formalin-fixed, paraffin-embedded archival tissues in addition to the development of different endogenous blocking kits have further expanded the use of IHC as a tool for biomarker exploration and validation of affinity reagents in research (Bussolati and Radulescu, 2011; Radulescu and Boenisch, 2007; Shi et al., 2011).

Due to the considerable progress in automation and standardisation of IHC, more sensitive and efficient detection systems are required. This aims at achieving similar or better sensitivity of the immunoreactivity with less concentrated primary reagent, shorter incubation time, fewer steps in the procedure, and faster turnaround time. Several IHC multistep detection systems (figure 5.1) have been developed and used routinely (Ramos-Vara, 2011). These include using the avidin-biotin complex method, phosphatase-anti-phosphatase, and peroxidase-anti-peroxidase (figure 5.1 A and B). Despite the ability to achieve signal amplification with various labelled monoclonal and polyclonal antibodies, these systems suffered from major drawbacks, such as the difficulty in staining standardisation, time-consuming multi-step process and the suboptimal detection of low abundant antigens (Kim et al., 2016).

In 1993, the enhanced polymer one-step staining (EPOS) system (Dako) was introduced which covalently binds the primary antibody and horseradish peroxidase (HRP) to an inert dextran polymer (Pastore et al., 1995). Dako, in 1995, has developed a new detection system, using up to 100 peroxidase enzyme molecules with 20 secondary antibodies,

which are linked directly to the backbone of an activated dextran polymer (Wiedorn et al., 2001).

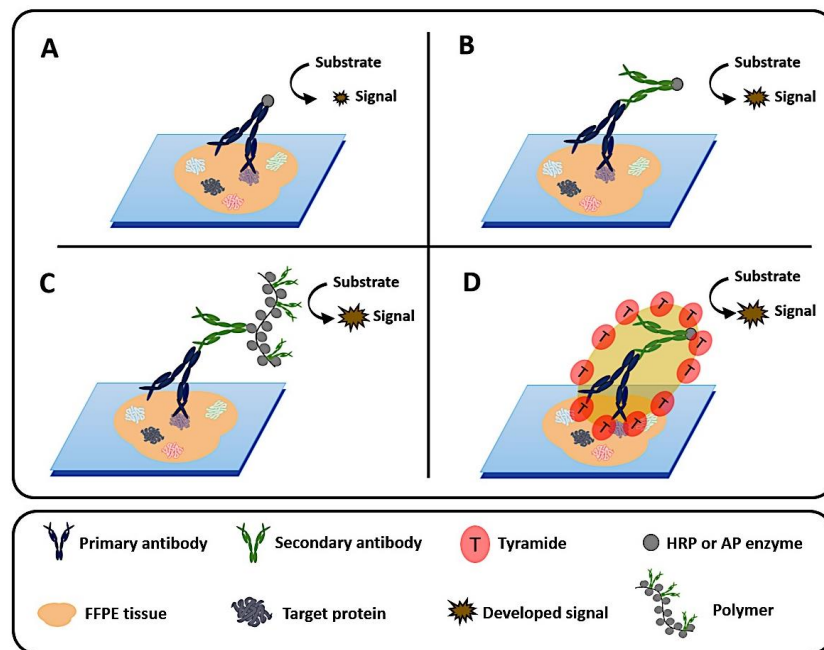


Figure 5.1 Schematic overview of the different methods used in IHC to detect the biomarker of interest. Protein biomarkers in tissues can be detected either directly using a single, primary labelled antibody (A), or indirectly (B) involving a second, labelled antibody. For improved signal intensity, two amplification systems have been developed, the polymer reagent (C) and the tyramide technology (D).

The use of dextran polymer (figure 5.1 C) led to the development of a rapid, single and two-step assays that enhance the sensitivity and the reliability of IHC. However, the high molecular weight of the dextran-based polymeric conjugate limits its ability to bind to different intracellular and nuclear proteins (Russo et al., 2003). To overcome the limitation of the size of the dextran polymer, a second-generation of polymer was developed by Shi and colleagues (Shi et al., 2016). These are polymer conjugates of small, linear and less-branched multi-functional reagents that polymerize under controlled conditions with secondary antibodies and enzymes.

In addition to polymeric conjugates, catalysed reporter deposition technique (CARD), which is also known as tyramine signal amplification (TSATM), has been developed to improve signal amplification (Faget and Hnasko, 2015; Zaidi et al., 2000). It is based on the activation of multiple copies of the derivative of tyramide by HRP at the site of

antigen-antibody formed complexes (figure 5.1 D). Although this technique has increased the detection sensitivity of the IHC by at least 50 folds it has not been widely applied in diagnostics. Its limited applicability in diagnostics is mainly due to its multi-step process and high background staining (Dhawan, 2006). As the TSA method showed equal sensitivity to the polymer-based amplification system, the two-steps polymer conjugate remains the most commonly used detection system in routine diagnostics and research (Yuan et al., 2012).

Modification of antibodies is commonly used in detection systems and can be achieved chemically by various reagents that conjugate functional molecules, such as biotin, enzymes, or fluorescent groups, to specific side chains on the amino acids of the protein (Spicer and Davis, 2014). The amino group in lysine and the thiol group in cysteine are among the most predominantly used side-chains for labelling strategies (Boutureira and Bernardes, 2015). In addition to chemical modification methods, genetic fusion of enzymes, such as alkaline phosphatase to single-chain variable fragment (scFv) (Wang et al., 2006b; Harper et al., 1997) and the variable domain of a heavy chain antibody (also known as nanobody) (Liu et al., 2015) have been assessed. These fusions represented a new format of detection reagent for the use in immunoassays allowing for simple and rapid antigen testing.

Here, we provide an assessment of different approaches to generate chemically modified Affimer reagents. We also present the development of Affimer-alkaline phosphatase and Affimer-Fc fusions as protein detection tools in IHC. The functionality of the modified reagents was examined and their obtained sensitivity compared with different commercial reagents and polymer-based amplification kits.

5.2 Results

5.2.1 Affimer-Alkaline phosphatase fusion protein as a rapid, single-step detection tool for IHC

Simple and fast detection of alkaline phosphatase (AP) and horseradish peroxidase (HRP) activity is of an advantage for diagnostic and analytical applications, including the IHC assay (Matos et al., 2010). Most histochemical methods for alkaline phosphatase produce highly stable final reaction product (Chida, 1993), and there are few reports showed the ability of using the enzyme in different fluorescent approaches (Nobori et al.,

2018;Murray and Ewen, 1992). As such, we constructed an Affimer-alkaline phosphatase fusion protein to use as detection protein.

5.2.1.1 Construction of a monomeric alkaline phosphatase (mAP)-fused Affimer

To use mAP as a signal generator in the IHC assay, we constructed a fusion protein consisting of a VEGFR2 binding Affimer and a monomeric alkaline phosphatase (mAP). All anti-VEGFR2 Affimer were kindly provided by the BSTG in the University of Leeds, UK. The anti-VEGFR2 Affimer was inserted into an pET11a expression vector containing the AP enzyme with the aid of *NotI* and *NheI* restriction enzymes (figure 5.2 A). No linker was added in between the Affimer scaffold and the C-terminus fused AP enzyme. Cloning the Affimer into the alkaline phosphatase enzyme-pET11a expression vector resulted in a lack of a histidine tag and protein purification with nickel affinity chromatography was dependent on the number of histidine residues present in the enzyme.

5.2.1.2 Monomeric alkaline phosphatase-fused Affimer production, its catalytic activity and stability

Initially the optimisation of the production of the Affimer-mAP fusion was performed by altering growth conditions and IPTG concentration. Bacterial cells were transformed with the Affimer-mAP plasmid. Three different growth media were used; super broth (SB), Luria Bertani (LB) and terrific broth (TB) media (see method section 2.2.4.2). Using super broth media, the fusion protein was expressed in cells after IPTG (0.1mM) induction at an OD_{600nm} of 0.7. In addition to SB media, LB media was used and the fused Affimer-mAP protein was produced in cells after the addition of 0.1, 0.5, and 1mM of IPTG at a bacterial cell culture density of 0.7. Auto-induction media where no IPTG is needed was also used. In all different media, the fusion protein was produced overnight at 25°C, with a shaking speed of 220 rpm.

As shown in figure 5.2 B, the mAP-Affimer fusion protein was confirmed to be highly expressed using 0.1mM of IPTG induction at 25°C using the super-broth media. Coomassie stained SDS-PAGE gel displayed a single band with an expected molecular

size between 58 to 60 kDa, meeting its suggested theoretical size. Parallel with our result, super-broth media has been previously shown to be superior to other medias for reaching higher cell densities (Rosano and Ceccarelli, 2014;Shafiee et al., 2017). As the number of cells per liter increases, oxygen availability becomes a critical factor that impacts the growth. The simplest way to increase oxygen levels is by increasing the shaking speed (Somerville and Proctor, 2013).

After fusion protein production, we checked the catalytic activity of the AP enzyme in all eluates obtained from different expression conditions, using a colorimetric assay, with *p*-nitrophenyl phosphate (pNPP) as the substrate. As shown in figure 5.2 C, the AP was active and its catalytic activity was maintained even after the overnight dialysis and buffer exchange with tris buffered phosphate (TBS), pH 8.0. Our colorimetric result further indicated that the genetic fusion of the anti-VEGFR2 Affimer protein to mAP did not affect the catalytic activity of the alkaline phosphatase. It was previously reported that the free monomeric alkaline phosphatase enzyme suffers from thermal instability and results in its activity loss (Boulangier and Kantrowitz, 2003). Therefore, we repeated the colorimetric assay of the same eluates after 14 days of production and storage at 4°C. The assay showed a major loss in the catalytic activity (data not shown). We reasoned that the observed precipitation, which may result from improper storage buffer could cause the loss of fusion protein functionality. The use of additives, such as zinc and magnesium, has been proved to be successful in maintaining the activity of the AP enzyme (Bosron et al., 1977); however, we could not see an improvement in the fusion stability after long-term storage (data not showed) in the presence of such additives.

5.2.1.3 Direct affinity staining of the VEGFR2 protein on tissue using the mAp-Affimer fusion

To assess the ability of using the Affimer-mAP fusion protein for a direct single-step IHC (figure 5.3), we used the fusion as an affinity reagent to detect the VEGFR2 protein reveal its expression pattern on formalin-fixed, paraffin embedded (FFPE) placenta tissue. The binding specificity of the fusion protein was also examined based on the localisation specificity in addition to the presence or absence of a background non-specific staining. The anti-VEGFR antibody that was detected by a polymer-based kit was also employed in the run to serve as positive control. A tissue section, where no fusion protein or

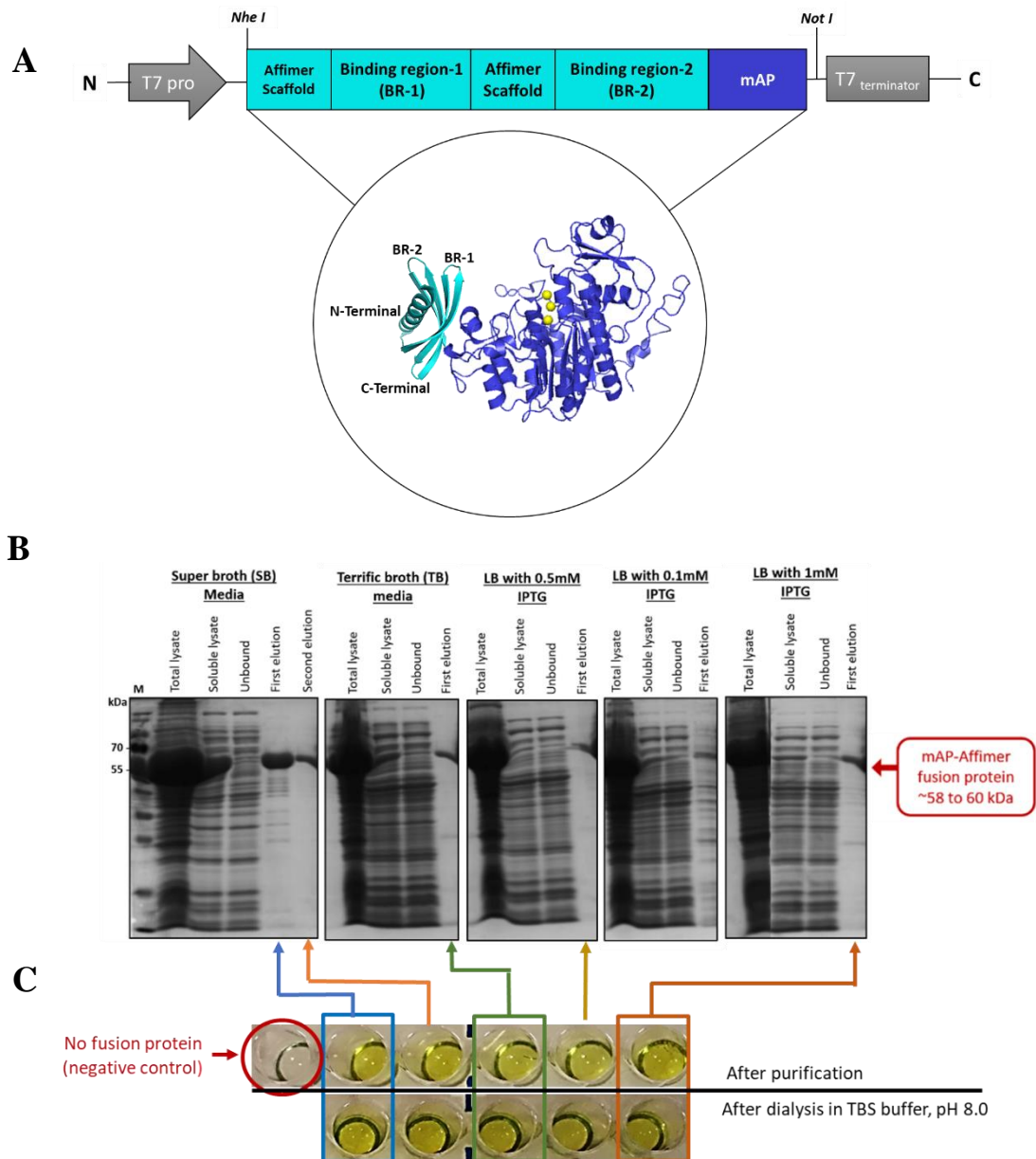


Figure 5.2 Production and characterisation of a monomeric alkaline phosphatase (mAP)-fused VEGFR2 binding Affimer. (A) Schematic illustration of a fusion protein containing both Affimer protein (cyan) and the mAP (blue). (B) Coomassie stained SDS-PAGE gel showing the production of the fusion protein using the super broth, terrific broth and LB growth media with different concentrations of the IPTG in LB growth media. In SDS-PAGE stained gel the molecular size of the fusion protein was detected as 58 to 60 kDa. (C) The catalytic activity of the monomeric alkaline phosphatase enzyme in the fusion was evaluated with the pNPP (yellow) substrate after purification and dialysis steps (performed in duplicates). Crystal structures were obtained from PDB; Affimer (**4N6U**) and *E.coli* alkaline phosphates (**1ED8**). ($n = 2$).

antibody was added, was considered to be our negative control. Such a negative control was included to evaluate the efficiency of the endogenous peroxidase blocking, which may result in a non-specific binding of the primary reagent.

Following the optimised staining protocol mentioned in section 2.2.6.3.2.2, the Affimer-mAP fusion showed binding specificity to the VEGFR2 protein expressed on the endothelial cells surface demonstrated by pink staining of the cell membrane around the blood vessels (figure 5.3). No staining was observed on the negative control section, while an intense signal was obtained after the addition of the AP substrate (red colour) was visualised with the antibody reagent. The high intensity accompanied with the antibody was most likely due to the use of a polymer-amplification approach. Despite the weak signal detected with our fusion protein, its specificity indicates that the binding ability and specificity of the VEGFR2 binding Affimer was not affected by its fusion to another protein. However, it is not yet possible to use the fused mAP-Affimer proteins as an affinity-detection reagent in IHC, as further optimisation studies are required to allow for long-term storage without the loss of the fusion functionality. To overcome the stability issue with fusing AP enzyme to the VEGFR2 binding Affimer, different chemical modification approaches involved labelling of Affimers with HRP enzyme and biotin molecule were developed and assessed.

5.2.2 Development of the optimal bio-conjugate via chemical modification of Affimers

Bio-conjugation is the attachment of one molecule to another through a covalent bond to create a complex comprising of both molecules linked together (Alt et al., 2015). One of the oldest methods for detecting biomarkers in IHC is by using antibody-enzyme conjugates. As such, we initially tried to directly link Affimer proteins to HRP enzyme using a lightning link system (see section 2.2.5.1). After successful conjugation of the HRP to Affimer proteins, as demonstrated by ELISA, a high, non-specific background staining of cells was observed with the Affimer-HRP conjugate compared to the commercial-HRP conjugated antibody (data not showed). We reasoned that the obtained non-specific staining was due to the conjugation technology offered by the kit. The lightning system targets the amine functional group of lysines. Due to the abundance of the lysine residues in the Affimer scaffold and its variable two loops, their binding ability to the target could be blocked because of the linked HRP.

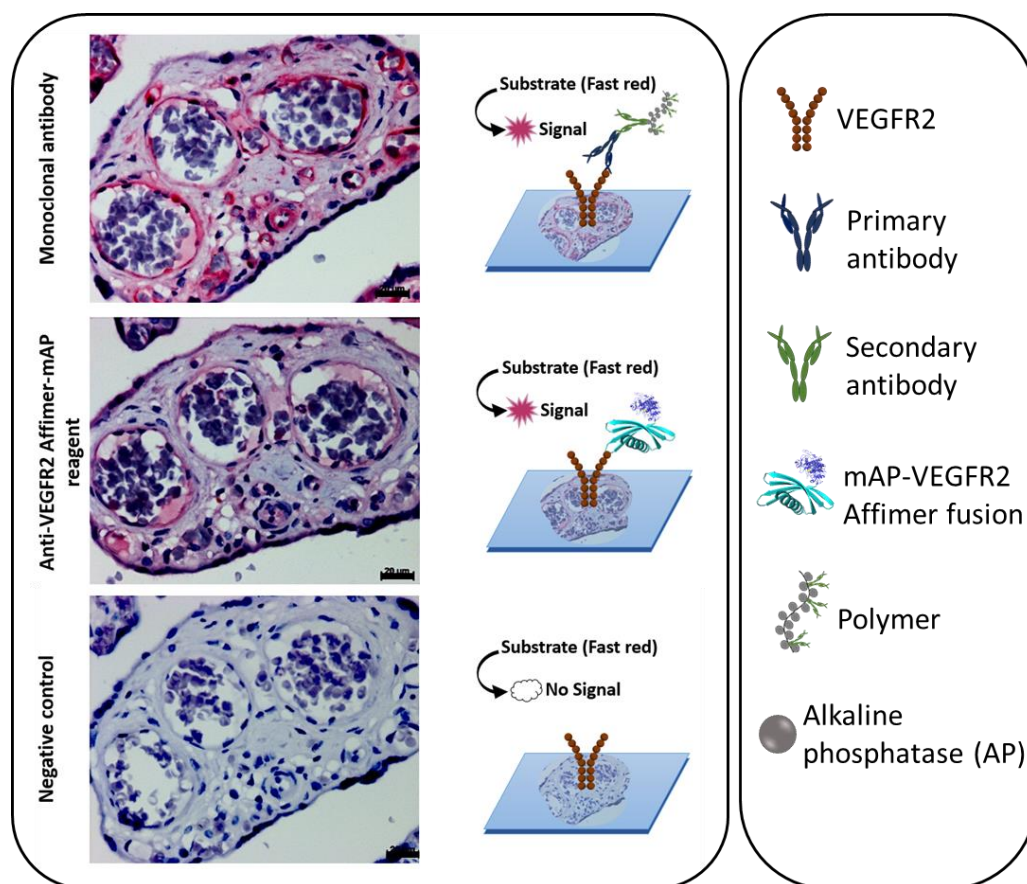


Figure 5.3 Fused mAP-Affimer protein for staining VEGFR2 in human placenta tissue. The expression of the VEGFR2 in placenta tissue was detected by both monoclonal antibody and the mAP-Affimer fusion protein. Bound affinity molecules were visualised with fast red substrate (red). Difference in the multi-step detection process was illustrated with the schematic diagrams. Negative control contained no primary affinity reagents was included. Images were taken at 20X magnification ($n = 2$ on different human placenta tissue sections).

We introduced a cysteine residue in the C-terminal end of the Affimer scaffold to enable us to perform a site-specific conjugation without affecting the binding loops (figure 5.4 A). Based on their capability to work in IHC as we demonstrated in published work (Tiede et al., 2017), both cysteine-contained anti-Tenascin C (TN-C) and anti-vascular endothelial growth factor receptor 2 (VEGFR2) Affimers were used. They were produced in bacterial cells and their purity was confirmed in Coomassie-stained SDS-PAGE gel (Figure 5.4 B). We optimised Affimers site-specific labelling using anti-TNC Affimer, but the effectiveness of the labelling protocol and its applicability in IHC was examined with another Affimer protein, which is the VEGFR2 binding Affimers. The reason of using anti-VEGFR was mainly due to the scant availability of mouse xenograft section overexpressing TN-C biomarker and the fact that the optimised labelling protocols can

be applied to all Affimer proteins. Conjugation efficiency of the HRP enzyme to the anti-VEGFR2 Affimer was evaluated by ELISA and assessed in IHC like application using placental tissue (figure 5.5).

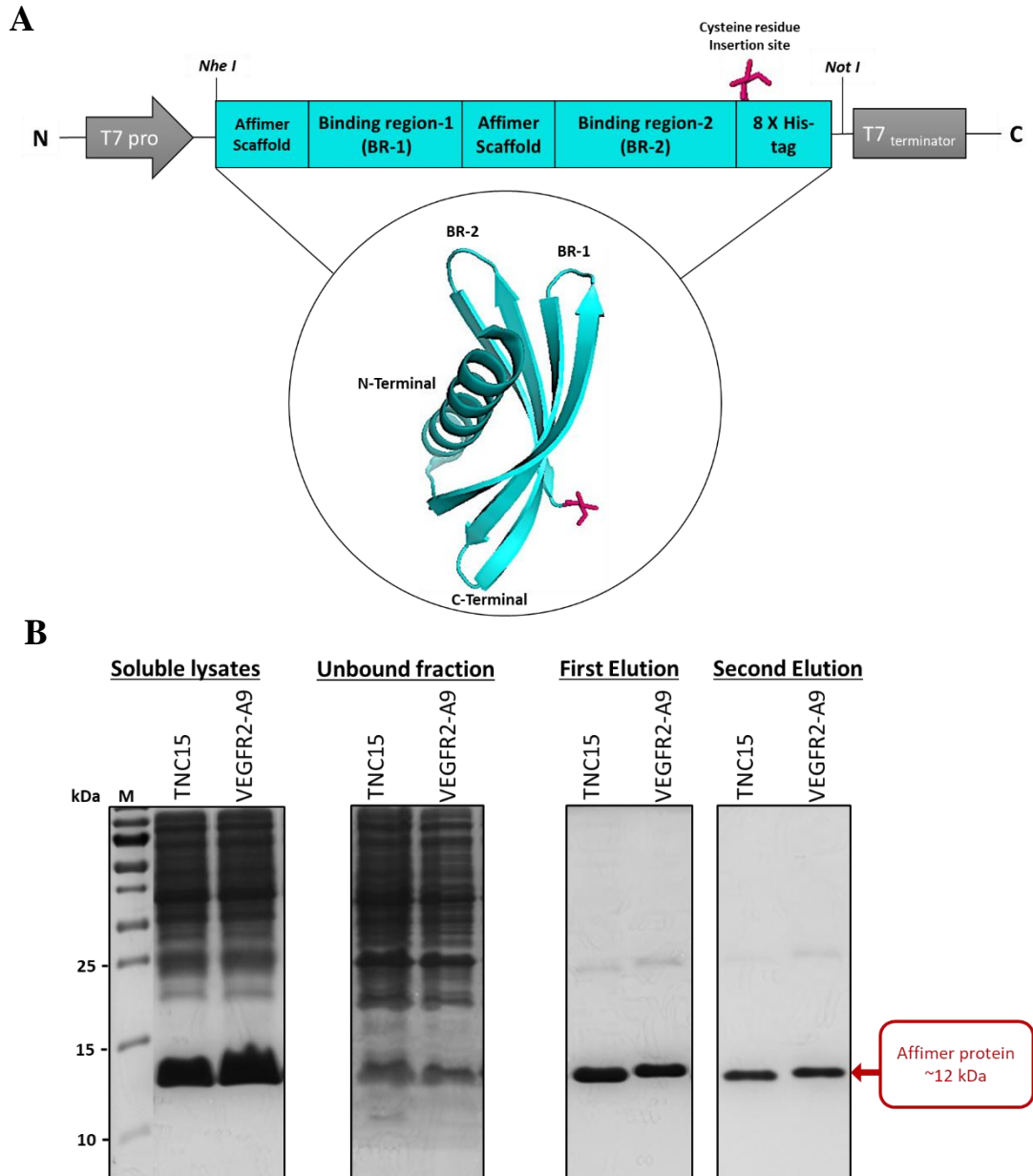


Figure 5.4 Cloning and producing of an Affimer containing a single cysteine residue. (A) Schematic of the Affimer construct showing the cysteine residue (pink arm) at the C-terminal region of the Affimer protein. (B) Coomassie stained, SDS-PAGE gel showing a high level of Affimer protein production in the soluble lysates. After single-step nickel affinity chromatography, pure soluble Affimer proteins were obtained as seen in the elution fractions ($n = 5$ for Affimers productions). The crystal structure of the Affimer was obtained from PDB (4N6U) and developed by PyMOL software.

Placental tissue is divided into three parts, maternal, middle and foetal (Isaza Mejia et al., 1971; Stegeman and Treffers, 1980). Since the middle region contains rich homogenous villous tissue, placenta represents a model tissue for evaluating affinity reagents (Meng et al., 2016). Although the ELISA confirmed the HRP conjugation based on the obtained absorbance measurements at 620nm (figure 5.5 A), the staining of the HRP-anti-VEGFR2 Affimer did not localise at the sites where VEGFR2 protein expressed (figure 5.5 B). As such it was not possible to confirm the specificity of the HRP-labelled Affimers and thus we considered the staining pattern as non-specific. We speculated that the lack of the specificity may be caused by unbound HRP due to inefficient conjugation and subsequent purification which requires further optimisation.

A recent report demonstrated that affinity reagent that use biotin-streptavidin interactions can result in high sensitivities (Lakshmipriya et al., 2016). In order to develop the procedure for biotinylating Affimer reagents, optimisation of the biotinylation approach was performed. This included reaction conditions (time, temperature, and protein-to-biotin molecule ratio), type of disulfide reducing agents, and the length of the spacer arm that links biotin to the maleimide group. It should be mentioned here, in all optimisation experiments, a concentration of 1 mg/ml of anti-Tenascin (TN-C) Affimer reagent was used.

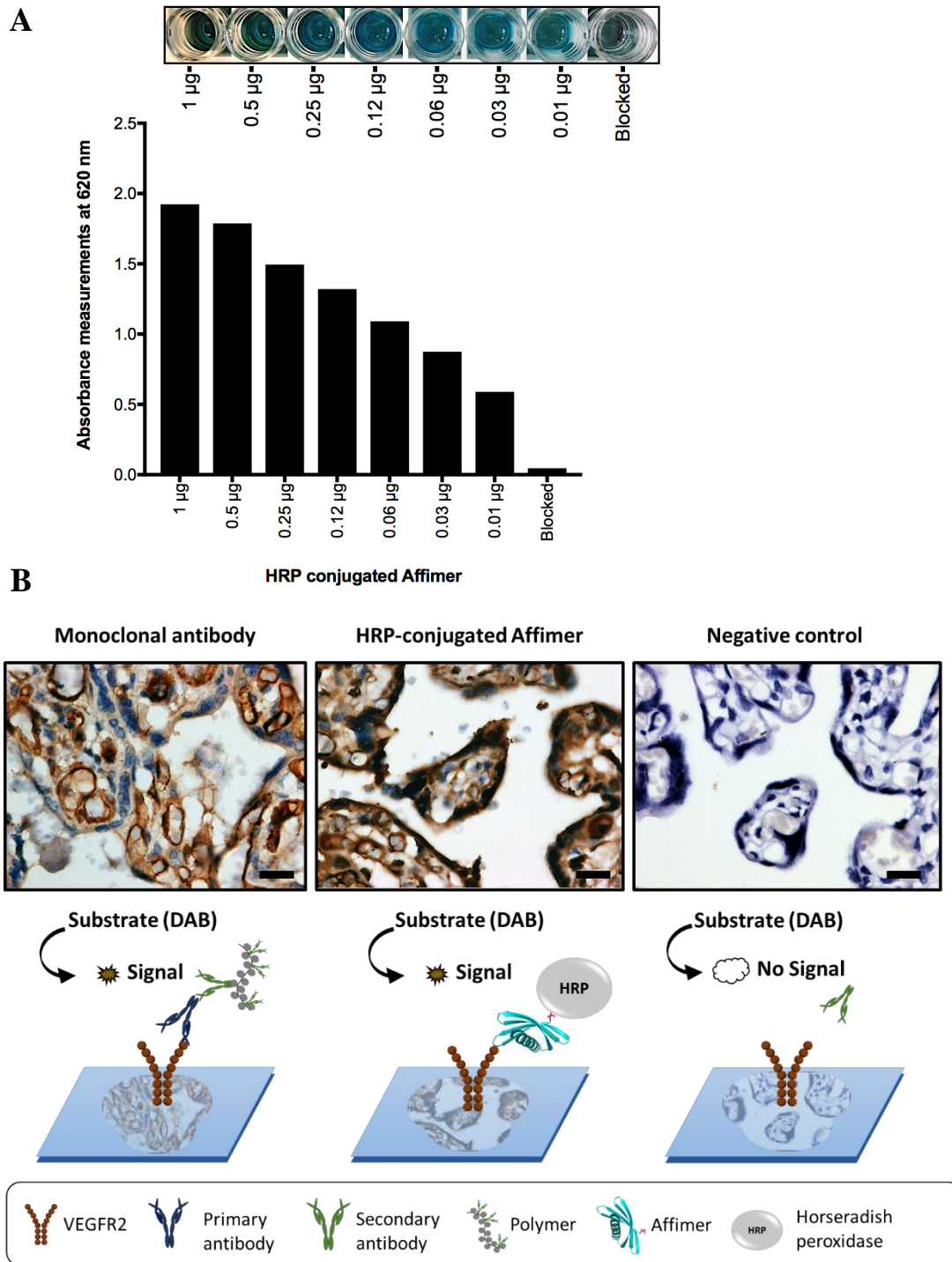


Figure 5.5 HRP-conjugated Affimer showed low specificity in IHC. The anti-VEGFR2 Affimer reagent was conjugated to HRP enzyme via cysteine residue using maleimide chemistry. (A) The efficiency of Affimer labelling was evaluated by ELISA prior to the start of IHC staining. (B) HRP-conjugated Affimer was added to FFPE placenta tissue to enable the detection of the VEGFR2 protein expressed on the surface of the endothelial cells surrounding the vessels. Protein visualisation was enabled by DAB substrate (brown) and tissues were then counterstained with Mayer's haematoxylin (blue), dehydrated and mounted. Monoclonal antibody against the VEGFR2 was used as positive control, while tissue section where no primary reagents were added served as negative control. Images taken at 20X magnification ($n = 2$).

5.2.2.1 Optimisation of biotinylation incubation time, biotin concentration and temperature

Initially, we looked at the optimal labelling reaction temperature to be used to enable a labeling reaction to occur. The biotinylation reagent was incubated with Affimer proteins at 4°C, 37°C, and room temperature (22-25°C) for a recommended 2-hours reaction time. The excess unbound biotin molecules were removed from the solution by desalting. The biotinylation obtained at different temperatures were checked and assessed by ELISA using streptavidin-HRP conjugated reagent (see section 2.2.2.1). After adding TMB enzymatic substrate, the signal intensity of the developed colour was measured at 620 nm. As negative controls, both non-biotinylated Affimer protein and wells containing diluted blocking buffer were used. In figure 5.6, different reaction temperatures showed similar efficiency of biotin-labeling. Therefore, we decided to use the room temperature as the standard conjugation temperature to make the approach more practical.

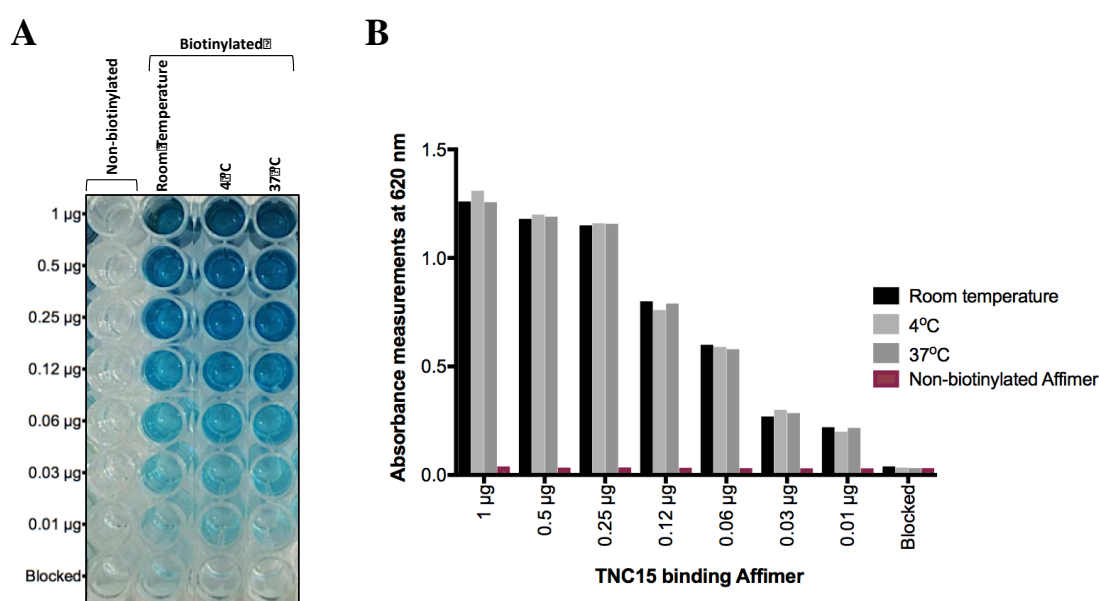


Figure 5.6 ELISA showing the efficiency of biotin labeling of Affimers at different temperatures. TN-C binding protein was biotinylated at room temperature, 4°C, and 37°C. The efficiency of the biotin conjugation was evaluated by ELISA. (A) Each protein was passively adsorbed onto plates at different concentrations as shown by the ELISA strips. Biotinylated Affimers were detected with streptavidin-HRP reagent and visualised using the TMB substrate. Negative control wells containing no protein was included. (B) The absorbance measurements of the all developed signals were taken at 620 nm and blotted in a histogram as a mean value of duplicated measurements obtained from one experiment. ($n = 1$).

The next step was to alter the biotinylation conditions testing different coupling reaction times. A biotin-labeling reaction was carried out at room temperature and 100 μl of sample was taken after 3, 4, 5, 6 and 18 hours (overnight) of incubation. The mixtures were then dialysed in PBS buffer of pH 7.4, for further analysis. After checking the biotinylation efficiency by ELISA (data not shown), the extent of biotinylation was determined by mass spectrometry (MS) analysis in a semi-quantitative way showing the percentage ratios between biotin-labelled (molecular weight of **12855** Da) and non-labelled (molecular weight of **12403** Da) Affimers. MS analysis showed that the most efficient (90 to 95%) Affimer protein biotinylation occurred after 6 hours incubation (Figure 5.7).

Different concentrations of linkers 1, 2, 4, 6, 8, and 10 μM were added in a conjugation mixture containing 1 μM of Affimer reagent. As reported earlier, 10 fold excess of biotin reagent in the reaction can cause 4 to 6 biotin molecules to bind to the protein if the reaction is not cysteine specific (Kay et al., 2009). However, in this case, only one biotin molecule will be attached to the cysteine residue though potentially the increase in biotin molecules may lead to more Affimers being biotinylated. Samples containing either non-biotinylated Affimer protein served as a negative control. Using ELISA, it was shown that biotinylation efficiency increased with the increase in ratio of biotin reagent (figure 5.8). A molar ratio of 8:1 or 10:1 μM of biotin linker to Affimer was the most efficient for biotinylation.

In summary, the highest biotinylation efficiency was achieved after a 6-hour incubation at room temperature with a 10-molar excess of biotin linker to Affimer.

5.2.2.2 Testing different biotin linker lengths

The length of the spacer arm, which is the chemical chain between two reactive groups, defines how flexible a conjugate will be (Harlow and Lane, 2006). Previous studies have suggested that the great flexibility that long spacer arms exhibit can minimize the steric hindrance related to streptavidin binding and thus improve the efficient capturing of biotinylated proteins (Chen et al., 2013). To test this idea, three conjugates were created using three different biotin-linkers with different spacer arm lengths (see section 2.2.5.2). Despite the difference in the lengths of the arm, all linkers have a maleimide moiety in

addition to a high aqueous solubility (figure 5.9 A).

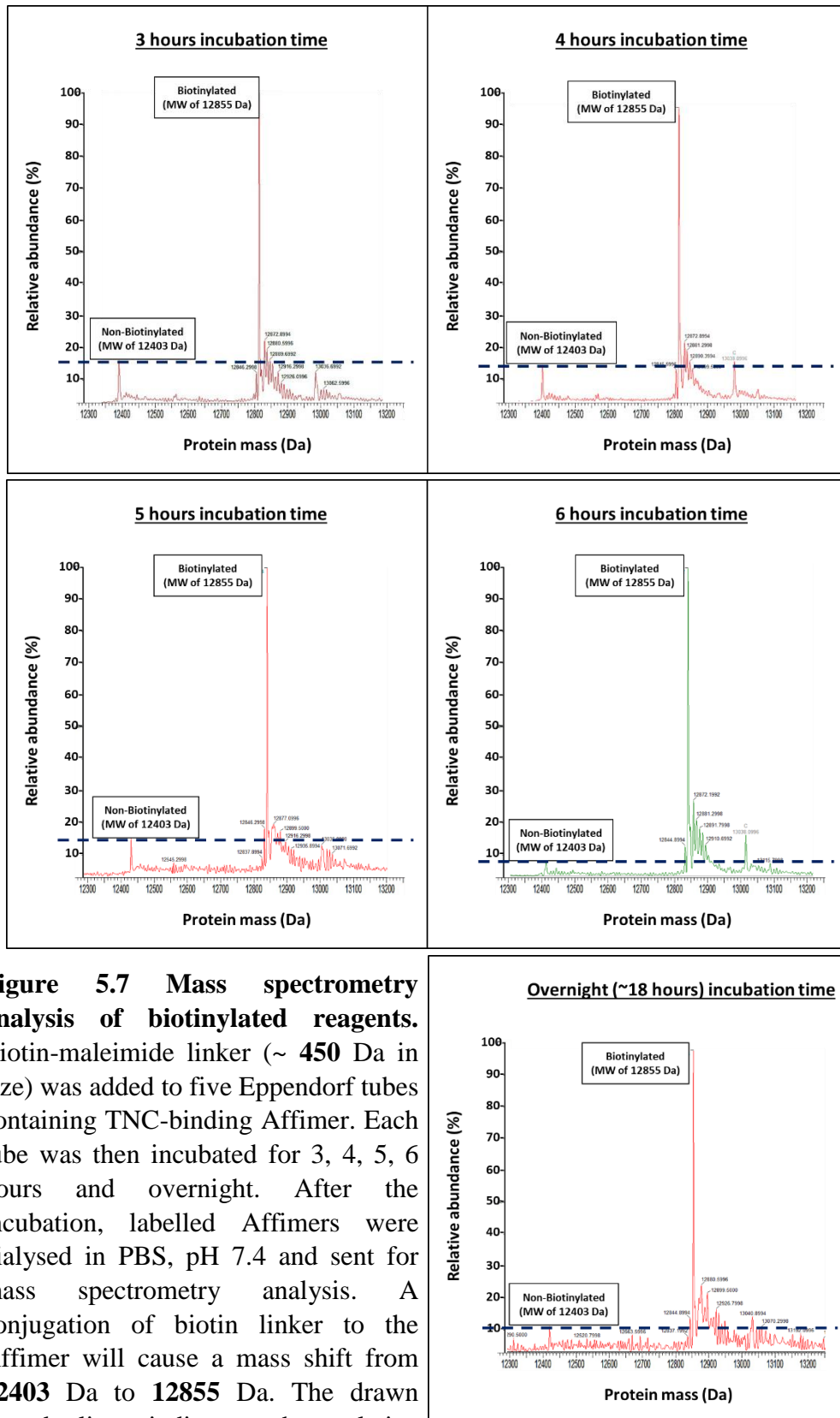


Figure 5.7 Mass spectrometry analysis of biotinylated reagents. Biotin-maleimide linker (~ 450 Da in size) was added to five Eppendorf tubes containing TNC-binding Affimer. Each tube was then incubated for 3, 4, 5, 6 hours and overnight. After the incubation, labelled Affimers were dialysed in PBS, pH 7.4 and sent for mass spectrometry analysis. A conjugation of biotin linker to the Affimer will cause a mass shift from **12403 Da** to **12855 Da**. The drawn dotted line indicates the relative abundance (%) of the non-labelled Affimer in the mixture. ($n = 1$)

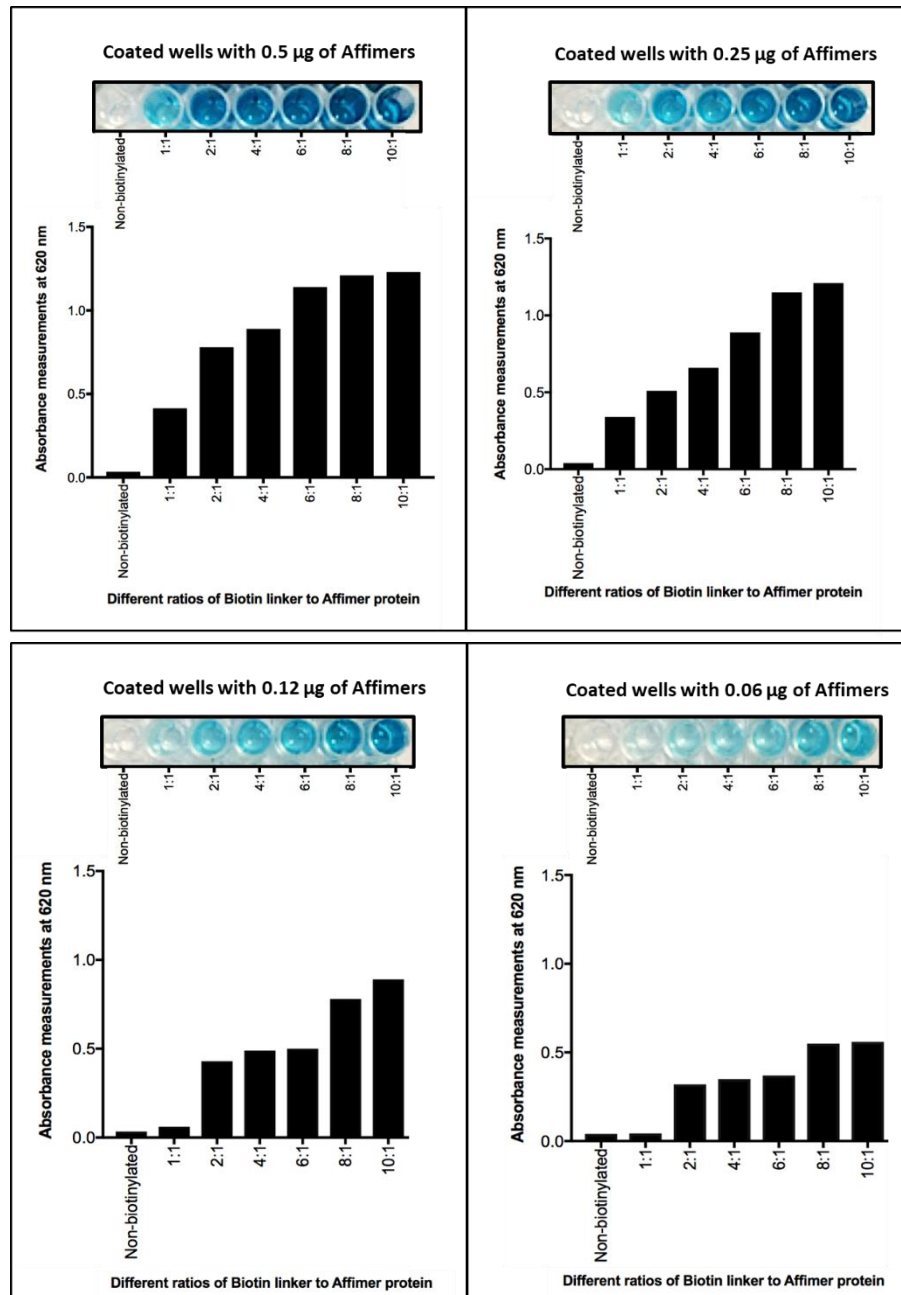


Figure 5.8 Graphs showing optimisation of Affimer:biotin ratio. 1mg/ml of anti-TN-C Affimer was incubated with different excess folds of biotin molecule that were calculated based on the molar ratio between both biotin linker and the Affimer. All Biotinylated proteins were coated to well at different concentrations (0.5 to 0.06 µg). ELISA assay was used to determine the biotinylation efficiency of the different ratios by measuring and plotting the absorbance readings that were taken at 620 nm. ($n = 1$)

The biotinylation reagent that has been used so far had a very short-sized linker. Two further linkers were tested: BMCC and PEG₁₁-Biotin maleimide, containing either a cyclohexane ring or a poly (ethylene glycol, PEG) increasing by the distance between the biotin molecule and maleimide to 36.2 and 59.1 angstroms, respectively. The biotinylation efficiency using the reagents was checked by ELISA. The assay showed that the longest linker was the best for obtaining an efficient detection (figure 5.9 B). It would be helpful to verify if the enhanced ELISA signals obtained by the long arm linker is due to improved detection with streptavidin reagent or because of better biotinylation.

Therefore, a mass spectrometry analysis to examine the extent of biotinylation between the different linkers was performed. Based on the change in the molecular mass between labelled and non-labelled proteins, the extent of biotinylation was interpreted by the relative difference in the abundance between the two masses in the mixture (figure 5.9 C). For Affimer linked with the biotin maleimide linker (~ 450 Da) a mass shift from 12403 Da (non-biotinylated) to 12855 Da (biotinylated) was seen. With BMCC linker (~ 533 Da), the mass of the non-biotinylated Affimer will change was 12937 Da. A third mass shift of the non-biotinylated protein to 13227 Da was observed in the conjugation reaction with the PEG₁₁-biotin linker was used (~ 922 Da).

This analysis suggests the observed improved signal by ELISA is due to the increased detection of biotin molecules by the streptavidin reagent as the mass spectrometry result suggests lower biotinylation efficiency using these reagents. With an increase in the spacer arm length, less Affimers gets biotinylated (figure 5.9 C). It has been reported that conjugates with long- arm linkers have the tendency to fold over themselves, masking the ligand they are coupled to and thus affecting biomarker detection or capture (Lalli et al., 2018).

In addition, to mass spectrometry analysis and ELISA results, the three differently biotinylated reagents have been tested by other researchers to stain the TN-C biomarker on FFPE xenograft tissue samples, and it was found that the reagent with longer spacer arms produced higher background and non-specific staining than the other two reagents which contained shorter or no spacer arms (data obtained from verbal communication with Dr. Filomena Esteves in LIBAC). As such, we decided to use the shortest of the three linkers tested, which contained no spacer arm (biotin-maleimide linker) for further optimisation of the biotinylation protocol as it appeared to be the best option to develop conjugated-Affimer reagent able to work efficiently in IHC.

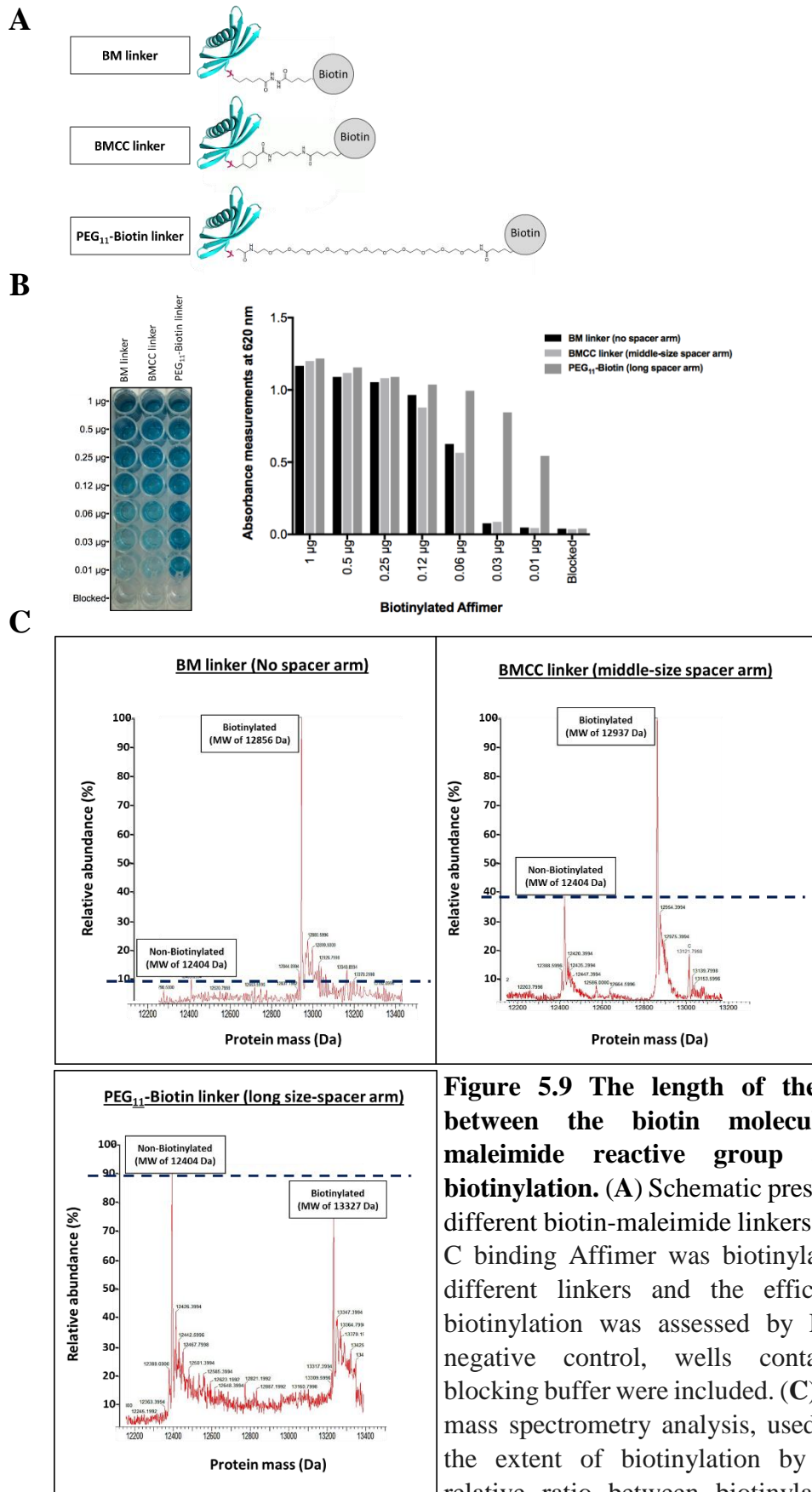


Figure 5.9 The length of the spacer-arm between the biotin molecule and the maleimide reactive group affected the biotinylation. (A) Schematic presentation of the different biotin-maleimide linkers used. (B) TN-C binding Affimer was biotinylated using the different linkers and the efficiency of the biotinylation was assessed by ELISA. As a negative control, wells contained diluted blocking buffer were included. (C) Illustrates the mass spectrometry analysis, used to determine the extent of biotinylation by showing the relative ratio between biotinylated and non-biotinylated Affimers in the mixture. A dotted line was drawn to indicate the abundance of the non-labelled Affimer in percent. ($n = 1$)

5.2.2.3 Testing different reduction techniques for biotin labelling

As we mentioned earlier, a cysteine residue has been introduced into the Affimer scaffold to allow us to perform site-specific modifications. This introduction of cysteine residue forms disulfide bonds between Affimers, which then hindered the residues from being biotinylated. Therefore, the disulfide bond must be cleaved using a thiol reductant agent, such as dithiothreitol (DTT), 2-mercaptoethanol (2-ME), or tris (2-carboxyethyl) phosphine (TCEP) (Lu and Chang, 2010). However, an efficient reduction of the disulfide bond can only be achieved after optimising several reduction conditions including reductant concentration and time as well as the reduction approach (reductants in solution vs bound to agarose beads).

In our optimisation experiments, TCEP was used as it is significantly more stable in a broad pH range, faster acting, and is non-reactive with other functional groups compared to other reducing agents (Getz et al., 1999;Liu et al., 2010). Numerous conditions have been optimised by the Bioscreening Technology Group (BSTG) and the School of Chemistry, demonstrating treatment with a 10-fold excess of the TCEP-HCl for one hour was optimal reduction condition (data obtained by personal communication). Therefore, we compared the biotinylation efficiency of an Affimer reagent after thiol-reduction with TCEP in solution and agarose-immobilized. After checking the biotinylation efficiency of the Affimer by ELISA (figure 5.10 A), samples were sent to mass spectrometry analysis to determine the extent of biotinylation. Mass spectrometry analysis further confirmed the ELISA results in which a reduction with immobilised TCEP resulted in improved overall biotinylation (Figure 5.10 B).

5.2.3 Applicability of the biotinylated, single cysteine Affimer as a detection reagent in IHC

To assess the performance of Affimer proteins compared with a conventional monoclonal antibody, we used an Affimer reagent, which was developed against VEGFR2 biomarker. FFPE placental tissue section was used to directly compare the staining specificity and sensitivity of the anti-VEGFR2 Affimer reagent and its corresponding monoclonal antibody. To ensure an even comparison, we chose a commercial antibody that has been

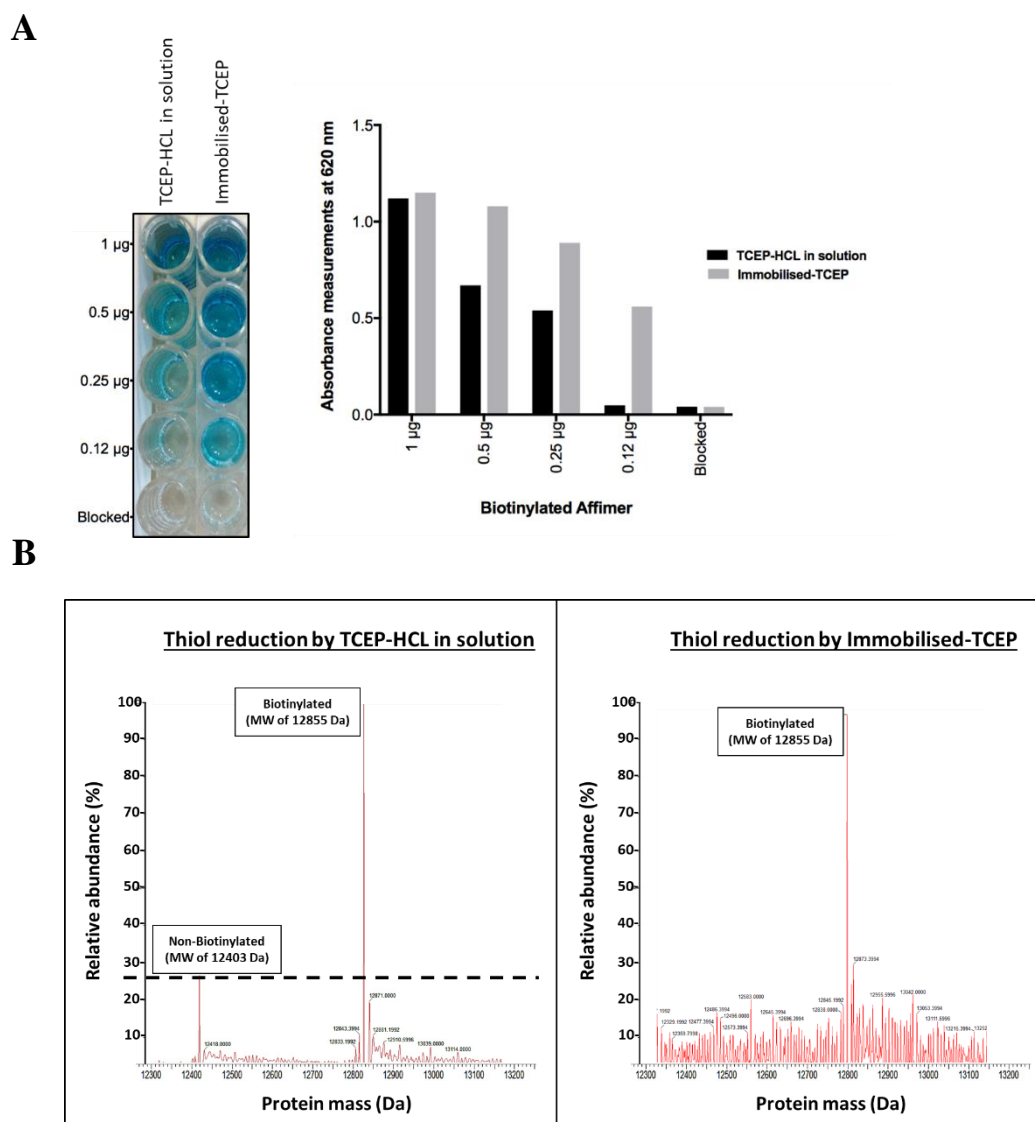


Figure 5.10 Comparing the efficacy of different reducing approaches. Thiol reduction was achieved with TCEP; either in solution or immobilised to agarose-beads were compared. Upon disulfide bond reduction, TN-C binding Affimers was biotinylated, dialysed in PBS, pH 7.4, and checked for presence of biotin by ELISA (**A**). As negative control in ELISA wells containing blocking buffer was included. The extent of biotinylation was further evaluated by mass spectrometry analysis (**B**). In this experiment, the biotin-maleimide linker (~ 450 Da), which has no spacer arm was used and the Affimers were reduced for 1 hour at room temperature followed by a reaction time of 6 hours. As a negative control in ELISA, wells contained diluted blocking buffer were included. ($n = 1$)

previously referenced (Oladipupo et al., 2018), validated, and optimised in the Leeds Institute of Medical and Molecular Research (LIMR, UK). In addition to the selection of primary affinity reagents, an important consideration in IHC application is whether to use directly labelled primary antibodies (direct method) or use another secondary-labelled reagent (indirect method). Due to the flexibility, low cost, and signal intensity obtained with the indirect methods, a number of IHC staining approaches use the indirect detection method (Hammond et al., 1982). However, when several steps are involved in a single indirect antigen detection method, the risk of non-specific binding increases, in addition to the requirement of a longer process time and extra reagent costs.

An alternative method is to use direct detection that involves using labelled primary affinity reagents without the requirement for secondary and tertiary reagents. To create a streamlined, cost effective Affimer-based IHC detection system, we chemically biotinylated VEGFR2 binding Affimer by attaching a biotin molecule to the C-terminus-cysteine residue using maleimide chemistry. Efficient biotinylation of the Affimer reagent was confirmed by ELISA, as illustrated in figure 5.11 A, in which measurements were taken at 620 nm and the obtained signals were compared to negative control wells that contained a diluted blocking buffer. To represent a typical amplification system, we used an anti-rabbit secondary biotinylated reagent for detecting signals in tissue stained with VEGFR2 targeting monoclonal antibody.

The staining of the primary reagents was compared with placenta tissue stained with no primaries as a negative control. Our results confirm the binding ability and specificity of all Affimers and antibody reagents (figure 5.11 B). Consistent with published data (Miettinen et al., 2012), VEGFR2 staining is intense in the membrane of the endothelial cells surrounding the vessels. Although chemically biotinylated anti-VEGFR2 Affimers eliminates the need for secondary antibody reagents, an amplification method of the detected signal may still be required to further enhance the sensitivity of the detection system (Tiede et al., 2017).

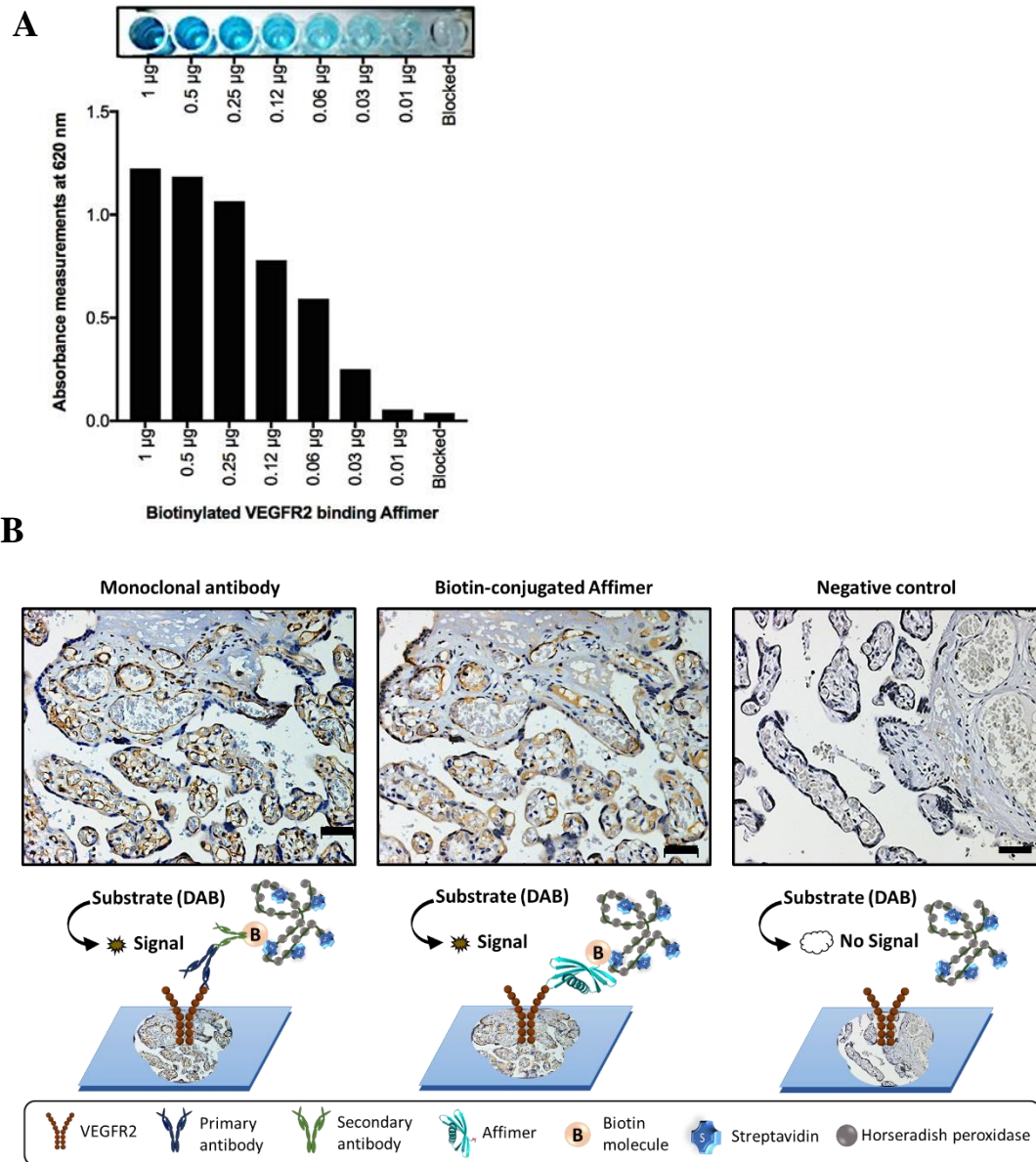


Figure 5.11 Applicability of the biotin-labelled-VEGFR2 binding Affimer as a detection reagent in IHC. After confirming biotinylation efficiency by ELISA (A), 25 µg/m of Affimer was added to placenta tissue for one hour at room temperature (B). A tissue section where no primaries were added was used as negative control, while other section which contained anti-VEGFR2 monoclonal antibody served as a positive control. Both VEGFR2 binding reagents were detected using the streptavidin-HRP conjugated reagents and visualised by DAB (brown). Next, Mayer's haematoxylin counterstaining, dehydration and mounting were performed. A schematic overview represents the multi-steps involved in the staining process. Scale bar: 50 µm and images were taken at 16X magnification ($n = 3$).

5.2.4 Signal amplification achieved by the introduction of two cysteine residues into the Affimer scaffold

Next, we tried to increase the signal by increasing the number of biotinylation sites on the Affimer. It was speculated that if the number of biotin molecules could be increased, we could potentially increase the number of streptavidin-HRP and therefore increase the signal intensity without the use of other amplification systems such as polymers or TSA. After several trials in choosing the right site for the incorporation of a second cysteine residue into the Affimer scaffold, the Bioscreening Technology Group (BSTG, Leeds, UK) have found that the approximate end of the N-terminal region of the scaffold is the most flexible site that allows for better biotin-linker accessibility, and thus more efficient biotinylation. The resulting modified, double cysteine Affimer reagents were termed as “Affimer Plus_{2C}” (figure 5.12 A). To determine if the Affimer Plus_{2C} reagents can result in signal amplification, we compared the signal intensity obtained from monoclonal antibody to the VEGFR2 binding Affimer Plus_{2C} reagents. While monoclonal antibody was detected by a secondary-polymer reagent, Affimer Plus_{2C} was detected by streptavidin-HRP conjugate only. Prior to the employment of the newly developed Affimer proteins in the IHC application, its binding specificity and biotinylation efficiency was assessed by ELISA and mass spectrometry analysis, respectively (data obtained from personal communication).

In IHC staining, we used all primary reagents to detect the VEGFR2 protein in placental formalin-fixed paraffin embedded (FFPE) placenta tissue. We also included the biotinylated-single cysteine VEGFR2 binding Affimer to further examine the effect of adding another cysteine residue on the intensity of the detected signals, in comparison to the observed signal with the single, cysteine Affimer. As a next step, we compared the signal amplification achieved by the Affimer Plus_{2C} reagent to the signal intensity of the developed signals obtained with the polymer-antibody-based detection system (figure 5.12 B). Placenta tissue section where no primaries were added served as negative control. 25µg/ml of biotinylated-single-cysteine Affimer and the Affimer Plus_{2C} proteins were incubated on tissue sections for 1 hour at room temperature, and the bound Affimers were detected by streptavidin-HRP conjugated reagent and visualized with DAB substrate (brown colour precipitate). In contrast, 11µg/ml of the monoclonal VEGFR2 binding antibody has been used. Bound antibody molecules were then detected with secondary polymer based reagents followed by visualization using DAB substrate.

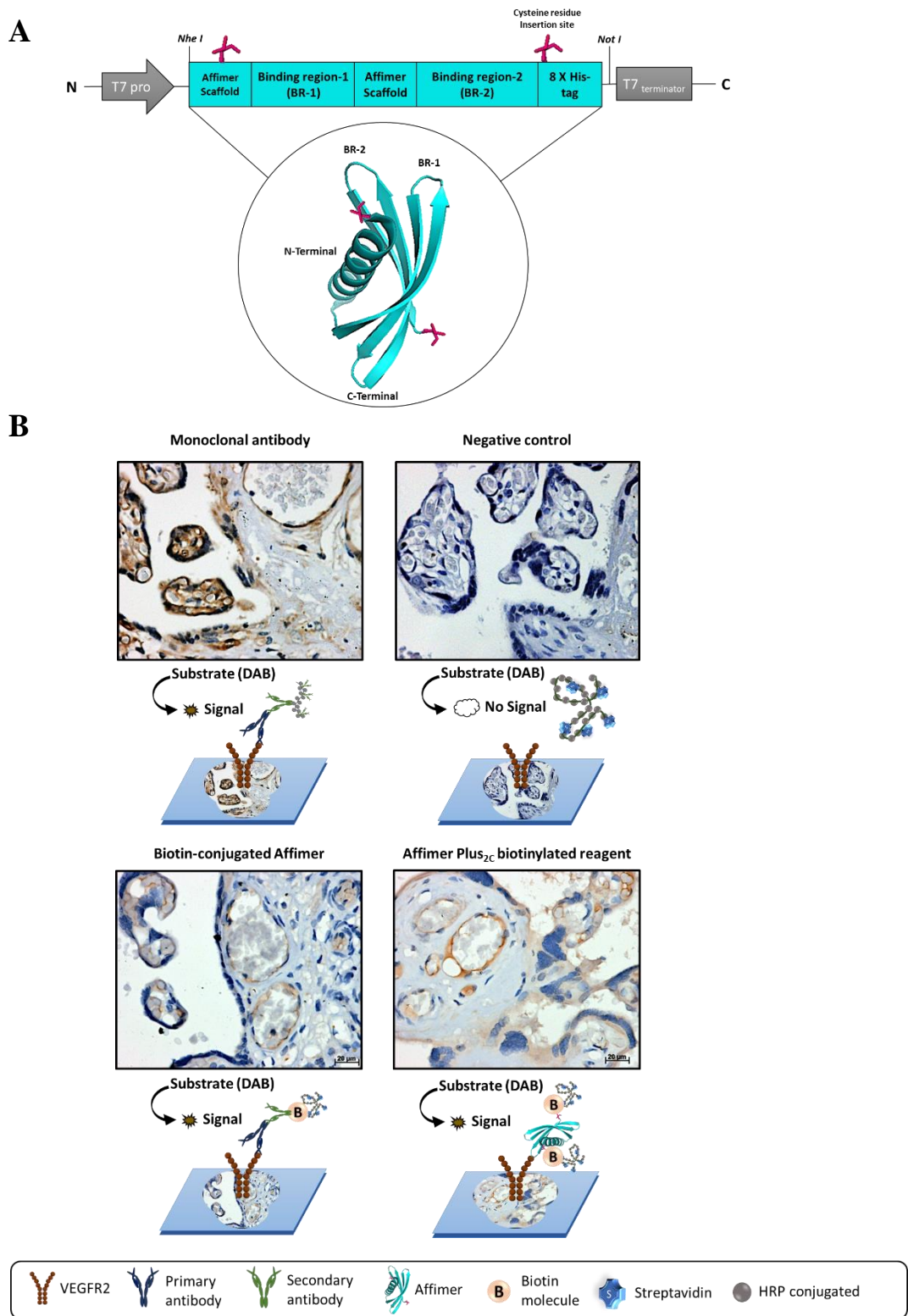


Figure 5.12 B showed an enhanced detection signal with the double-cysteine, Affimer Plus_{2C} variant as compared to the single cysteine one but, at the same time, the level of signal intensification was not equivalent to the level of amplification seen with the polymer-based amplification system. No staining was observed in the negative control tissue section. Although our results offer an approach for improving the detection of proteins with different abundance in cells, the amplification obtained by the polymer system remains the best. As such, we further studied an alternative approach for Affimer detection by creating Affimer-fusions that can detect the protein of interest in an amplified manner with or without the involvement of a polymer-detection system.

5.2.5 Characterisation of Affimer-Fc chimeras in IHC diagnostic application

Fc-based fusion proteins are comprised of an immunoglobulin Fc domain that is directly linked to another protein. Affimer-Fc chimeras were constructed by the genetic fusion between VEGFR2 binding Affimer and an Fc fragment (figure 5.13), derived from both mouse and rabbit IgG. Both construction and production of the Affimer-Fc protein was performed by the Avacta life sciences company (Avacta®, UK). Herein, we focused on characterising the binding ability of the constructed Affimer-Fc chimeras and their specificity towards the target protein, which is the VEGFR2. Both Affimer-rabbit Fc and Affimer-mouse Fc protein reagents were utilised in an IHC assay following an optimised protocol that was illustrated in section 2.2.6.4. Briefly, both reagents were added to FFPE placenta tissue sections at a concentration of 5 and 2.5 µg/ml (a dilution of 1:100 and 1:200, respectively) and incubated for 1 hour at room temperature. In addition, the rabbit monoclonal VEGFR2 antibody was also used at similar staining conditions but with a lower concentration (1 µg/ml). All bound affinity reagents were detected by polymer-amplification kit (Novolink kit, Leica Biosystems, UK) and the formed antigen-affinity reagent complexes were visualised by an HRP substrate, known as DAB (brown colour precipitate) followed by Mayer's Hematoxylin counterstaining (blue colour) (figure 5.13). A negative control section, where no primary reagents were added, was included in the run.

Figure 5.13 confirms the binding ability of both Affimer-Fc chimeric reagents. The signal intensity and the staining localisation pattern was consistent with the pattern observed with the commercially used monoclonal antibody. No staining was seen in the negative

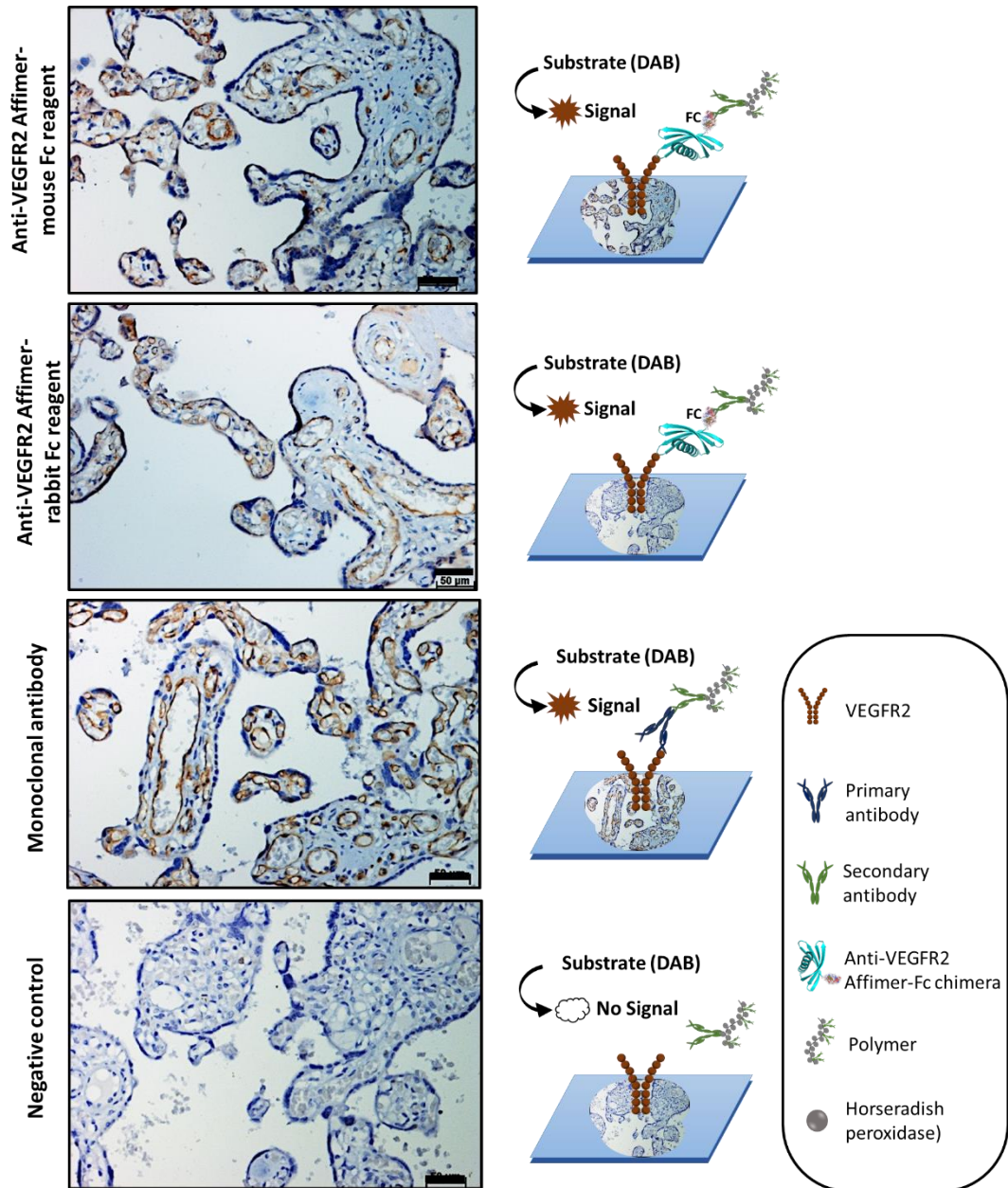


Figure 5.13 Characterisation of the developed Affimer-Fc chimeras in IHC. Using placental tissue sections, 2.5 $\mu\text{g/ml}$ of VEGFR2 Affimer-mouse Fc fusion protein (dilution of 1:200), 5 $\mu\text{g/ml}$ VEGFR2 Affimer-rabbit Fc fusion protein (dilution of 1:100), and 1 $\mu\text{g/ml}$ of monoclonal anti-VEGFR2 antibody (dilution 1:100) were used. After one-hour incubation of affinity reagents, detection and visualisation steps were started with both polymer-HRP based system and DAB (brown) substrate, respectively. Tissue section contained no primary reagents served as negative control. After the addition of DAB, tissues were counterstained with Mayer's haematoxylin, dehydrated and mounted. The whole staining process was summarised in the schematic diagrams. Images were taken at 16X magnification (Scale bar: 50 μm). ($n = 2$)

control tissue section. Although both constructed chimeras showed successful staining, the one containing a mouse Fc fragment gave more specific localisation as well as a higher sensitivity as compared to the rabbit Fc-Affimer reagent. This noticed difference in the specificity and the sensitivity between the chimeric proteins has been reported previously with several rabbit and mouse monoclonal antibodies that were raised against the same antigen (Lipman et al., 2005).

5.3 Discussion

Revealing the expression and spatial arrangement of different molecules within a tissue through immunohistochemistry (IHC) is an invaluable tool in research and diagnostics. Choosing both the appropriate primary affinity binding reagent and the signal detection system is paramount to the pathological interpretation of the tissue sample at hand. The use of single domain Affimer proteins promise robust and consistent results in different molecular recognition applications (Kyle, 2018;Lopata et al., 2018;Robinson et al., 2018;Xie et al., 2017;Zhurauski et al., 2018), but they are rarely used as an alternative to the conventional antibodies in IHC-like method. As such, this chapter provides an insight in the applicability of Affimer reagents as a detection tools for different tissue-based biomarkers.

In 2016, a published study has suggested an alternative way of creating a detection protein tools for the use in ELISAs (Seo et al., 2017). They successfully fused a monomeric alkaline phosphatase enzyme to a repebody scaffold, also known as leucine-rich repeat (LRR) scaffold. Their fusion protein introduced a new format of highly sensitive affinity reagents that can be utilised in immunoassays as a direct, simple, cost-effective, and single-step detection process. To test the applicability of their idea in an IHC assay, an anti-VEGFR2 Affimer-monomeric alkaline phosphatase (mAP) fusion reagent was successfully constructed, produced, and characterised. The fusion was expressed at high level in *E.coli* and retained a catalytic activity of alkaline phosphatase enzyme in addition to the binding specificity of the VEGFR2 binding Affimer, as shown in figures 5.2. and 5.3. Based on the IHC results, the construct confirmed the binding specificity of the Affimer in the fusion but detected a low signal compared to the signal obtained with the commercial VEGFR2 monoclonal antibody.

The main reasons for the observed difference in the signal intensity is the employment of a polymer-detection system with the antibody and the use of monomeric bacterial alkaline

phosphatase instead of the highly active dimeric human alkaline phosphatase as the enzyme source for constructing our fusion protein. Several studies have suggested the introduction of a single-point mutation in the bacterial alkaline phosphatase enzyme as a way to improve its efficacy (Muller et al., 2001; Halford et al., 1972). Their strategy can be adopted in future studies for further amplification of the detected signal, in addition to the maintenance of the thermal and functional stability of such Affimer-mAP protein reagents.

To overcome the stability issue encountered with the Affimer-mAP fusion protein and further achieve the desired stability, a single cysteine residue was introduced to the Affimer scaffold to enable the performance of site-specific chemical labelling of HRP and biotin. After unsuccessful conjugation of HRP to the Affimer proteins due to inefficient labelling technique and subsequent purification steps (figure 5.5), we developed bio-conjugates in which biotin molecule was linked to an Affimer by an optimal biotinylation protocol. The optimised protocol can be efficiently applied to other cysteine contained Affimer proteins displaying different target specificity. By biotinylating the anti-VEGFR2 Affimer reagent and testing it in placental tissue, our results show that biotin labelled Affimers are a valuable tool with an equal detection specificity to the conventional monoclonal antibodies (figure 5.11). Other alternative protein-based scaffolds, such as affibody, also showed a similar ability to the Affimers in detecting protein targets using IHC application (Orlova et al., 2006). Although we bypassed the need for a secondary-labelled antibody by using directly biotinylated Affimers, the obtained signal was less intense than the one observed by the monoclonal antibody involving the use of a secondary biotin conjugated antibody.

The next step was to amplify the signal in a free-antibody detection system. To achieve such amplification, we genetically modified the Affimers to duplicate the number of the incorporated cysteine residues as a method for increasing Affimers sensitivity and improving the intensity of the detected signal. With the newly modified reagent (Affimer Plus_{2C}), the desired amplification can be achieved by the increase in the number of biotin-molecule to be linked to the Affimer and thus leading to a signal amplification at the site of the protein of interest caused by the high chance of more streptavidin-HRP agent to bind. The Affimer Plus_{2C} protein showed promising enhancement of the signal intensity when compared to the single cysteine one. Although incorporation of the Affimer Plus_{2C} reagent to the IHC staining protocols represents a simple and cost-effective way of signal

amplification, no sensitivity improvement of the IHC was detected when compared to the sensitivity obtained by other polymer-based amplification kits (figure 5.12).

In contrast to our results, a recently published data showed that the approach of increasing the number of biotin molecules is efficient when applied it to nanobody (Wong et al., 2018). The genetically modified nanobody reagents showed to surpass the traditional amplification methods in relation to sensitivity and detection efficiency. The only difference between our study and their study is the protein target we evaluated our modified reagents against. As such, it is speculated that the binding affinity of both Affimers and nanobodies may contributed in the inconsistency between results. Therefore, it would be beneficial in future studies to re-examine the efficiency of the double-cysteine signal amplification approach by generating various two cysteine constructs containing different multiplicities of Affimer binding proteins. Furthermore, it would be of benefit to use different labels, including quantum dots (Medintz et al., 2008), fluorescent dyes (Figueroa et al., 2014;Lopata et al., 2018) and nanoparticles (Zahavy et al., 2012). These labels will not only expand the applicability of Affimers but it may also contribute in the development of more sensitive diagnostic reagents involved in different applications.

To improve the sensitivity of Affimer reagents and ease their use in diagnostics, in which routine IHC is dependent on the use of polymer-amplification kits, Affimer-Fc chimeras were developed and assessed using the IHC technique. Using such Fc-fusion proteins enabled the use of a polymer reagent, which further increased both the sensitivity and the intensity of the detected signal to levels comparable with those detected with the used antibody (Figure 5.13). To our knowledge, Affimer-Fc reagents against VEGFR2 are the only one-step protein-based Fc chimeras that have proved successful in IHC applications. The commercialised affibody reagent (Abcam, anti-ErbB2 Affibody molecule, ab31889, UK) requires detection by another anti-affibody labelled reagent that may not offer as strong signal amplification and as high sensitivity as the Fc-containing constructs.

The promising results obtained with the Fc-based Affimer reagents can expand their applicability into disease diagnostics, as well as in the development of therapeutic agents and vaccines. As therapeutic reagents, the presence of the Fc domain can prolong the therapeutic activity of the reagents by increasing their plasma half-life through their interaction with the different neonatal Fc-receptors (FcRn) found on immune cells (Czajkowsky et al., 2012;Yang et al., 2017), representing an effective activation of the

defence mechanism important for use in oncological therapies and vaccines. From a technical point of view, use of the Fc region enables cost-effective purification by protein-G/A affinity chromatography during production or evaluation using applications that involve precipitation of protein-complexes (Shukla et al., 2001). Furthermore, although the Fc-fusion proteins are expressed as homodimers, it is easy to modify the avidity of the reagents by polymerisation into well-defined complexes that comprise 12 fused partners (Ha et al., 2016; Czajkowsky et al., 2012). Such improvements in the avidity may enhance the analytical detection sensitivity by enabling the use of small sample volumes as desired in micro-applications, such as microarrays (Gonzalez, 2012; Husain et al., 2019).

From a biophysical perspective, the Fc domain folds independently, and this characteristic may improve the stability and solubility of the fused partner protein (such as Affimers) during *in vivo* production (Czajkowsky et al., 2012; Yang et al., 2017). However, these Fc-fusion proteins tend to unfold and aggregate upon exposure to various factors (Lowe et al., 2011) including agitation (Torisu et al., 2017), high temperature (He et al., 2011), low pH (Perico et al., 2009), freeze-thaw cycles (Zhang et al., 2012), transportation (Fleischman et al., 2017) and long-term storage (Cleland et al., 2001), which may restrict the development of such Fc-based reagents and limit their use as therapeutic reagents. In our research, the Fc-based Affimers were stored at 4°C to prevent freeze and thaw cycles, and their stability was examined by IHC staining. Placental tissue was stained using two-month-old Fc-VEGFR2 Affimer fusion reagent that had been stored at 4°C, at the same working concentration that was used with freshly obtained reagents prior to their storage, and the results obtained showed consistent staining intensity (data not shown).

Despite the promising results observed with these fusion reagents, tests must be performed with numerous Fc-based Affimer proteins that target different biomarkers, and their biophysical properties must be examined in order to confirm fully the effectiveness and applicability of these reagents as both detection and therapeutic agents.

In conclusion, this chapter further emphasize the feasibility of the Affimer proteins to be genetically modified and fused to different functional proteins without loss in their binding ability and specificity. Furthermore, the developed class of Affimer-Fc chimeric protein could represent a promising alternative to monoclonal antibodies in IHC. The

successful fusion of the Fc fragment to the VEGFR2 binding Affimer could also lead to the development of new other chimeras for the use in diagnostics and therapeutics.

CHAPTER 6

Identification of cancer specific Affimers using phage display

6.1 Introduction

A large degree of heterogeneity between and within breast cancer patients has always been a challenge for effective detection, diagnosis and treatment (Polyak, 2011). The heterogeneous nature of breast cancer has led to the identification and use of predictive and diagnostic protein biomarkers including oestrogen receptor (ER), progesterone (PR) receptor and human epidermal growth factor receptor 2 (HER2). These biomarkers aid the classification of breast cancer into five molecular subtypes, which differ in their prognosis and treatment response. These subtypes include luminal A (ER+, PR+/-, HER2-), luminal B (ER+, PR+/-, HER2+), basal/triple negative (ER-, PR-, HER2-) and HER2 (ER-, PR-, HER2+) subtypes (Correa et al., 2009; Holliday and Speirs, 2011). However, each subtype only represents the difference in the molecular signature between different breast tumours (inter-heterogeneity) but not within the same tumour (intra-heterogeneity).

Intra-heterogeneity affects cellular morphology, growth, metastasis, escape from therapeutic interventions and disease recurrence (Marusyk et al., 2012). Several factors including genetic and epigenetic alterations, changes in protein expression and modulation of signalling pathways all contribute to the diversity within a single tumour (Almendro et al., 2013; Marusyk and Polyak, 2010). In addition, it was recently demonstrated that many extrinsic factors can also result in the intra-tumour heterogeneity observed in breast cancers (Park et al., 2000). It has been reported that development of carcinoma is influenced by surrounding stroma cells, extracellular matrix, paracrine factors and local hypoxia (Knowles and Harris, 2001; Tlsty and Coussens, 2006). The complex interaction between the tumour and the surrounding environment plays a critical role in controlling protein expression, which influences therapeutic responses (Junttila and de Sauvage, 2013; Pietras and Ostman, 2010). When considering all factors that contribute to tumour intra-heterogeneity, expanding the number of clinical-relevant biomarkers may further improve the characterisation of breast cancer enhancing the

capability to accurately stratify cancer patients, predict their response, and identify disease recurrence.

Genomic, metabolic, transcriptomic and proteomic studies have all been used to identify new biomarkers (Adam et al., 2003; Benetkiewicz et al., 2006; Bullinger et al., 2007; Mohammed et al., 2017). However, the lack of reagents has limited the development of new diagnostic assays (Drucker and Krapfenbauer, 2013). Thus, the ability to isolate reagents with high affinity and specificity is crucial factor developing diagnostics in cancer research (Sanchez-Martin et al., 2015). Techniques, such as phage display have demonstrated a great capability to identify such reagents for a wide variety of targets including proteins (Brown, 2000), nucleic acid (Wolcke and Weinhold, 2001), inorganic materials (Whaley et al., 2000), whole cells and tissues (Alfaleh et al., 2017; Jones et al., 2016). In biomarker discovery, phage display is more advantageous compared to *in vivo* immunization as it does not rely on the immunogenicity of antigen, but rather depends on the binding interaction between the antibody and its target epitope (Chan et al., 2014).

After the successful isolation of different Affimer reagents described in previous chapters and recently published (Tiede et al., 2017) we further assessed the use of Affimer-based phage library for the discovery of new cancer biomarkers. In this biomarker discovery approach, Affimers were selected based on ability to bind to a fixed-monolayer of MDA-MB-453 breast cancer but not the control cells. The binding ability of the isolated Affimers against their target was assessed and characterised using a panel of cancerous and non-cancerous breast cells and tissue microarrays (TMAs). Such discovery of novel Affimer reagents that specifically recognise biomarkers defining breast cancer subpopulation may have a great clinical potential in cancer diagnosis and treatment.

6.2 Results

6.2.1 Selection and screening for cancer specific Affimers

Cell-based phage display is a proven technique for isolating cancer specific affinity reagents against surface expressed biomarkers on cancer cells (Jones et al., 2016). Here, a total of four selection rounds against a breast cancer cell line (MDA-MB-453) were performed including negative selection against an immortalised-breast cell line (HB2) and cancerous breast cell line (MDA-MB-453), respectively (see section 2.2.2.2.4). In all panning rounds, the selection was performed for one hour at room temperature with the

aim to target proteins expressed on the cell surface. To further increase the stringency, prolonged washing step of up to four hours were performed in the second panning round only. This application of prolong washing step of unbound phage clones caused a drop in the number of recovered colonies from the target MDA-MB-453 cells as seen in figure 6.1 A. However, the overall output of the screen after the fourth round of bio-panning was successful. This success was indicated by the increased in colony number of target-specific phage clones. Figure 6.2 summarises the whole process of the phage screen performed.

A total of 48 colonies out of 5.7×10^6 recovered colonies in the last panning round (4th round) were randomly picked and screened by phage ELISA against MDA-MB-453 and HB2 cells (see section 2.2.2.3). Phage clones that bound equally well or better to immortalised (HB2) cells but not to blocked wells, were considered to bind to proteins common between cell lines and were not further characterised. On the other hand, 13 colonies showed increased binding to cancer cells compared to HB2 cells indicating their selectivity towards cancer-specific proteins (figure 6.1 B and C). All 13 clones were selected and sent for DNA sequencing, which revealed 8 unique cancer-specific binders (figure 6.1 D)

To further assess the binding selectivity of the isolated 8 phage clones against cancer cells, we performed phage ELISA against MCF7 cells and compared binding to other cell lines used in the phage screen (MDA-MB-453 and HB2 cells). This demonstrated the Affimers also bound to MCF7 cells (figure 6.3 A and B). Helper M13KO7 phage showed only a low level of binding to the cells. Next, we aimed to visualise the phage binding to the cells to ensure that the isolated colonies were not binding to anomalies, such as dead cells or cell debris. To achieve this, phage binding was detected and visualised with an anti-fd phage antibody and a secondary Alexa488 conjugated antibody as mentioned in section 2.2.6.1. M13KO7 helper phage were used as negative control. The four tested phage clones showed positive binding to cells controls (figure 6.3 C). However, the binding visualisation of the tested clones by fluorescence microscopy did not produce conclusive results in relation to their binding specificity towards cancer cells only, because of the absence of stained control cells (HB2 cells). Thus the results obtained cannot be used as confirmation of the phage ELISA results. Therefore, it was decided to proceed to further characterisation tests of the eight isolated Affimers and to identification of the protein entity to which they were bound.

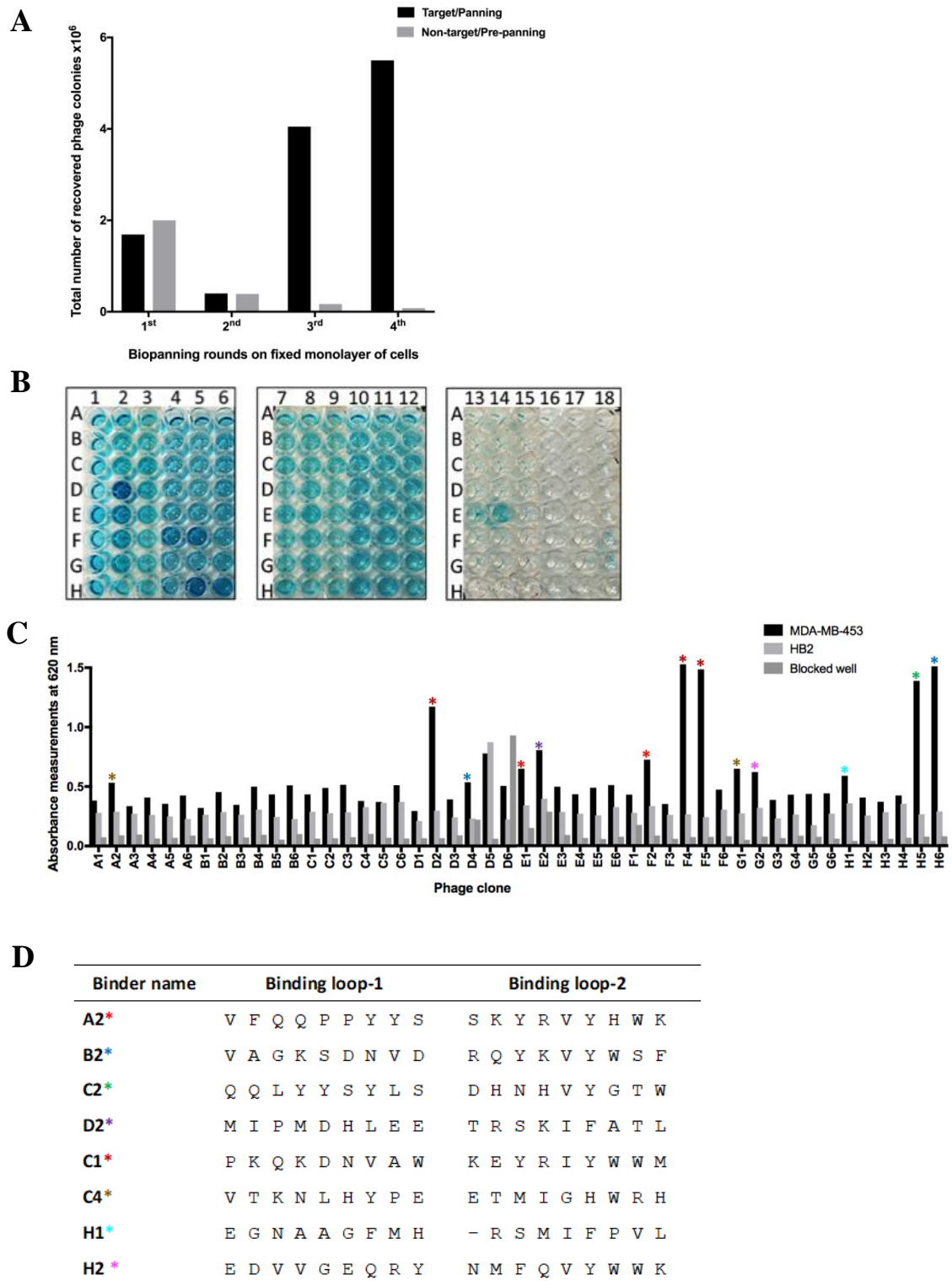


Figure 6.1 Isolation of eight cancer-specific binders after 4 rounds of panning on MDA-MB-453 breast cancer cells. (A) Graph represents the total number of recovered phages after each panning round. (B) A total of 48 randomly picked phage colonies were screened for binding on MDA-MB-453 and HB2 cells using ELISA. The phage binding on cells was detected by anti-fd bacteriophage antibody and visualised by HRP enzyme substrate. The absorbance of each well was then measured at 620 nm and blotted in histogram as illustrated ($n = 2$) (C). Thirteen indicated phage clones were sent for DNA sequencing and the amino acid arrangement of the variable loops (binding regions) revealed the identification of eight unique binders (D). See appendix A for more details about amino acids. ($n = 1$ for the phage screen)

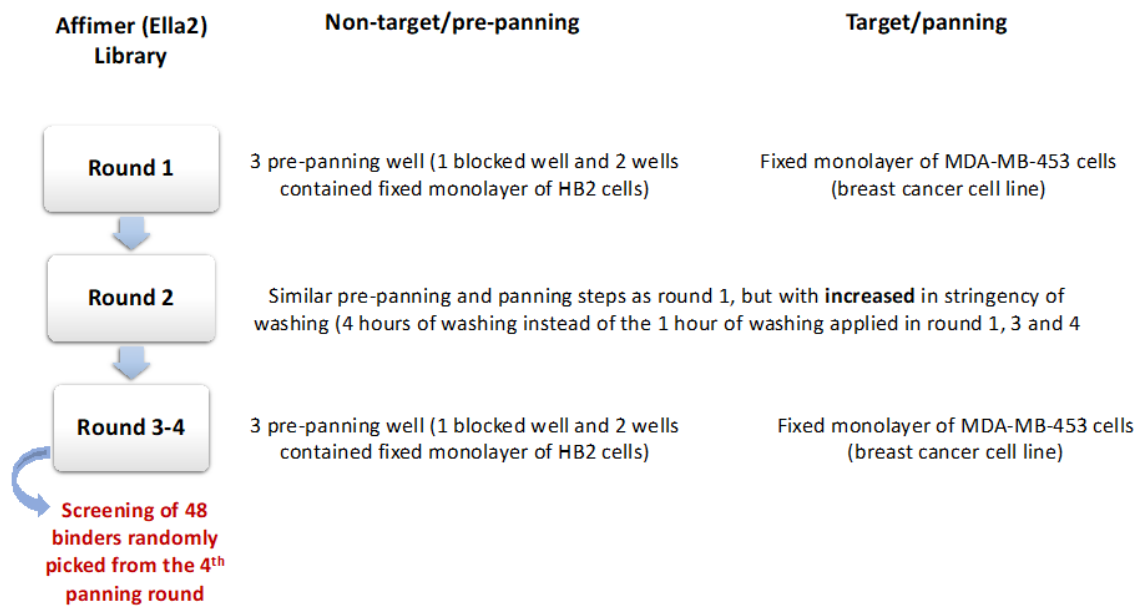


Figure 6.2 Schematic overview of the panning rounds to isolate Affimers against unidentified protein biomarkers. A total of four phage selection rounds was performed on fixed monolayers of cells in which the naïve Affimer phage library (Ella2) was pre-panned and then selected on fixed HB2 (non-tumorigenic cells) and MDA-MB-453 (cancerous cell line), respectively. In round 2, the selection pressure was increased by using prolonged washing to remove the non-binding phage in addition to other weak binders. After library selection on the target cells (MDA-MB-453), cells were washed for four hours instead of the one hour of washing that was used in rounds 1, 3, and 4. During the four hours of washing, the buffer that contained the non-bound phage was replaced with new buffer every hour. Then 100 μ l of the phage pool from round 2 was recovered and subjected to a third round of selection using the standard stringency of washing (one hour). A fourth panning round was performed similarly to round 3. From the final, 4th cycle of selection, 48 colonies were randomly selected and assayed in phage ELISA to assess their binding specificity towards cancerous cells but not to the normal counterpart.

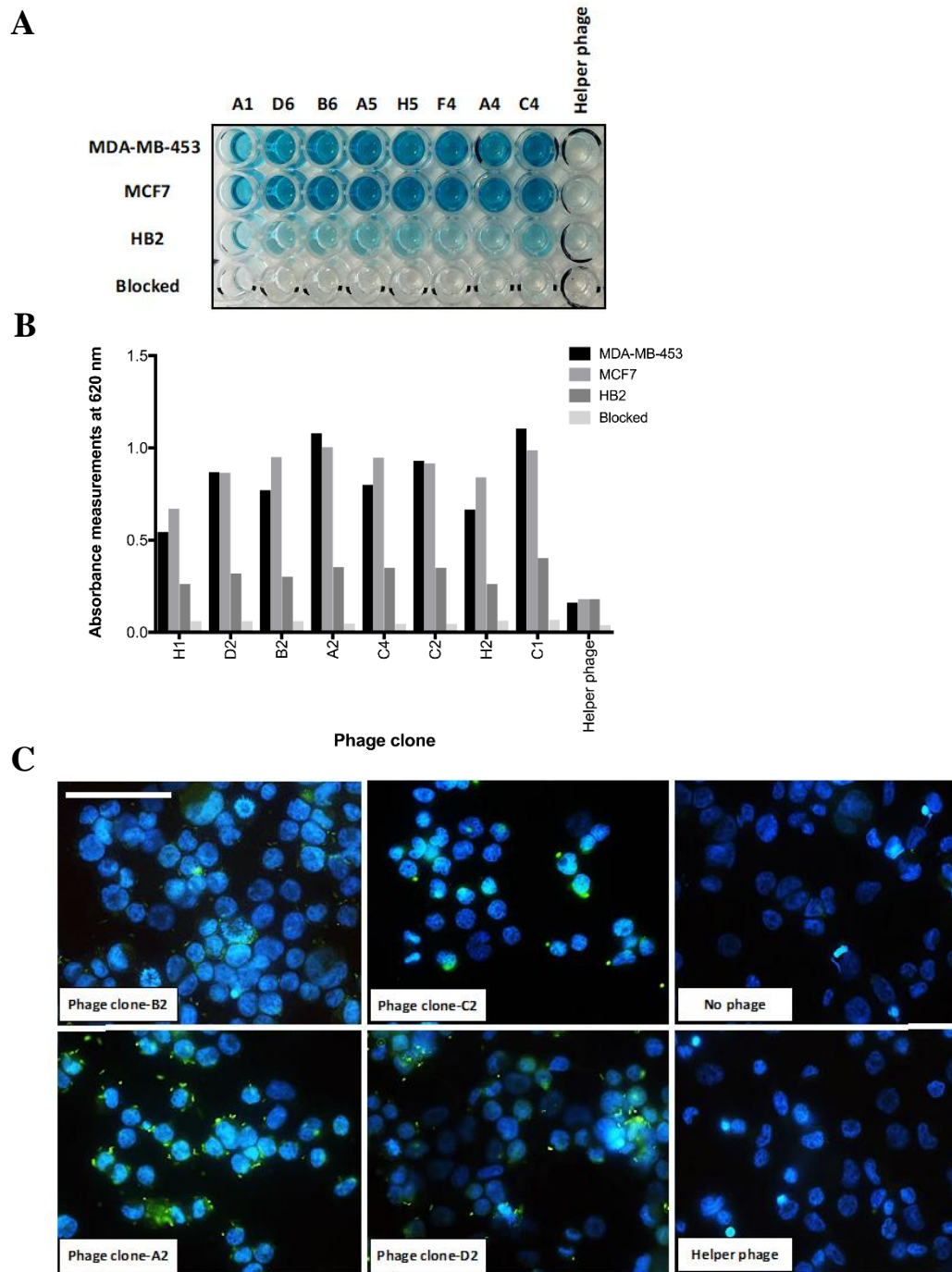


Figure 6.3 Binding of selected phage clones by ELISA and immunofluorescence. (A) The binding specificity of the phage clones to cancer cells were tested by cell-based ELISA on MDA-MB-453 and MCF7 cancer cells, and the non-tumorigenic HB2 cells. Wells containing 2x blocking buffer and the addition of helper phage were also used as controls. Phage binding event was detected by anti-fd bacteriophage antibody and visualised by HRP enzyme substrate. Figure represent a picture of the ELISA plate prior to reading using a spectrophotometer. (B) Graph representing the absorbance values at 620 nm of the plate. The plotted absorbance readings represent the mean value of duplicated measurements obtained from one experiment ($n = 2$) (C) Immunofluorescence microscopy showing the binding of the phage clones on MDA-MB-453 breast cancer cells. Fixed cells were incubated with phage hits, helper phage or no phage for 1 hour prior to addition of anti-fd antibody and secondary conjugated Alexa488 (green) and DAPI (blue). Scale bar: 20 μm ($n=1$ with duplicated staining of each phage clone).

6.2.2 *In vitro* production of cancer-specific binding Affimers

For further analysis, all 8 isolated Affimers were sub-cloned into pET11a vector using primers to include a cysteine in the C-terminal region of the scaffold as previously described (see section 2.2.3.1). The cysteine site-directed modification of the Affimers by chemically conjugating biotin molecule using maleimide. Biotinylation enabled the ability to characterise the binding ability of the Affimer proteins in IHC. The successful insertion of the cysteine residue and cloning of the Affimer scaffold into pET11a vector was confirmed by DNA sequencing. Plasmids were transduced into BL21 (DE3) and proteins produced as previously described (section 2.2.3.2). SDS-PAGE and Coomassie was used to visualise the production of Affimers (figure 6.4). Interestingly, only low levels of **H1** were produced in these cells and therefore, was not used in subsequent experiments. All Affimers were dialysed in a PBS, pH 7.4 and concentrations were determined by spectrophotometric analysis and BCA assay (data not shown).

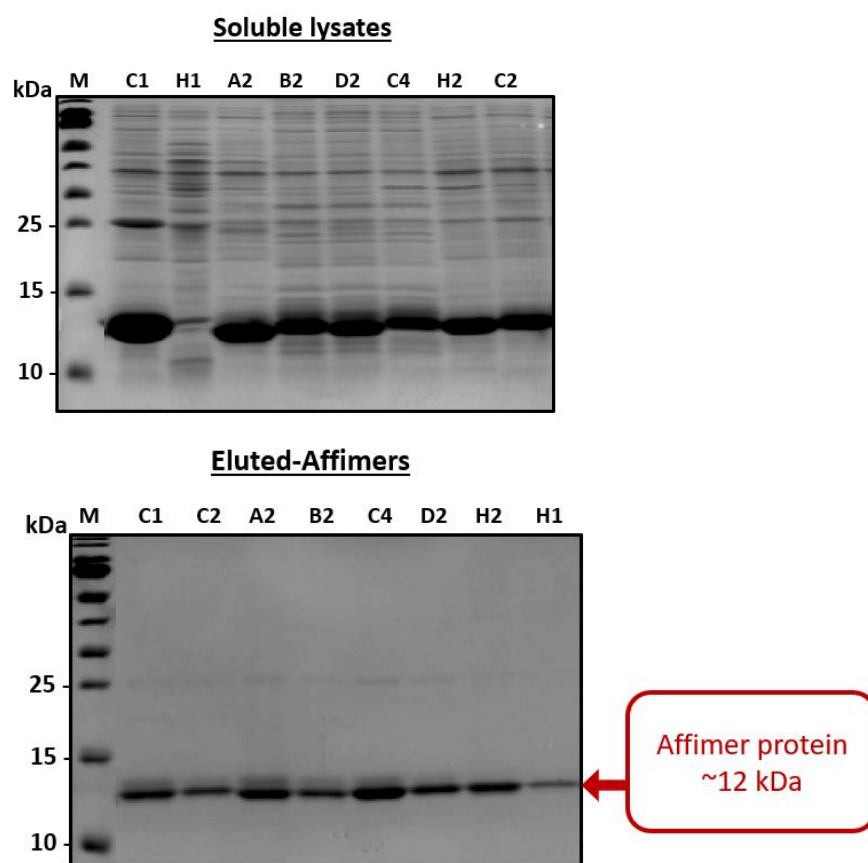


Figure 6.4 Coomassie stained SDS-PAGE gel showing production of Affimers. 3 μ l of soluble lysates and purified Affimers were run on SDS-PAGE. The major species observed on the gel is a band at ~12 kDa which is the approximate size of an Affimer protein ($n = 5$).

6.2.3 Validation of Affimer binding specificity towards cancer cells

6.2.3.1 Immunofluorescence microscopy

To evaluate the binding selectivity of 7 isolated Affimers towards cancer cells, IF and IHC assays were carried out on both cancerous and non-tumorigenic, immortalised cells. In IF study, all Affimers were detected using monoclonal mouse his₈-tag antibody and visualised with secondary Alexa488 conjugated antibody. As negative control, the his₈ tag antibody was added to cells without the presence of Affimers to check the background level of non-specific staining caused by the antibody. Commercial antibodies, in this case HER2, were used to stain cells (MDA-MB-453) as positive control (data not shown). All the tested Affimers showed staining of MCF7 and MDA-MB-453 breast cancer cells with no or little staining observed on HB2 breast cells (figure 6.5). No staining was seen in the negative control sample (figure 6.5).

6.2.3.2 Staining on formalin-fixed paraffin embedded cell pellets

For IHC, Biotinylated Affimers were used to enable their detection by a biotin-streptavidin based system. The interaction between the bound biotinylated Affimer reagent and the streptavidin-HRP conjugated agent was visualised with HRP substrate, known as 3,3'- diaminobenzidine (DAB), which forms brown colour precipitate upon oxidation. After successful site-specific biotinylation of Affimers (figure 6.6 A and B, detailed biotinylation protocol in section 2.2.2.1), the reagents tested to determine ability to detect antigen on formalin-fixed paraffin embedded pelleted breast cell lines, including MDA-MB-453, BT474, MDA-MB-468 and HB2 in addition to HEK293 kidney cell line that a kind gift from Dr. Filomena Esteves (see section 2.2.6.4 for details IHC method).

A2 and **C1** showed a high level of staining on MDA-MB-453, MCF7 and BT474 cell lines with weak expression level detected in a triple negative (MDA-MB-468) cell line. No staining was observed using the **A2** and **C1** Affimers on the control cells (HB2 and HEK293). Affimer **C4**, **D2** and **C2** also showed positive staining on the cancer cells but their staining pattern varied between different cells. The three Affimers showed strong positive localisation in BT474 cancer cells, while displaying weak to no staining in other

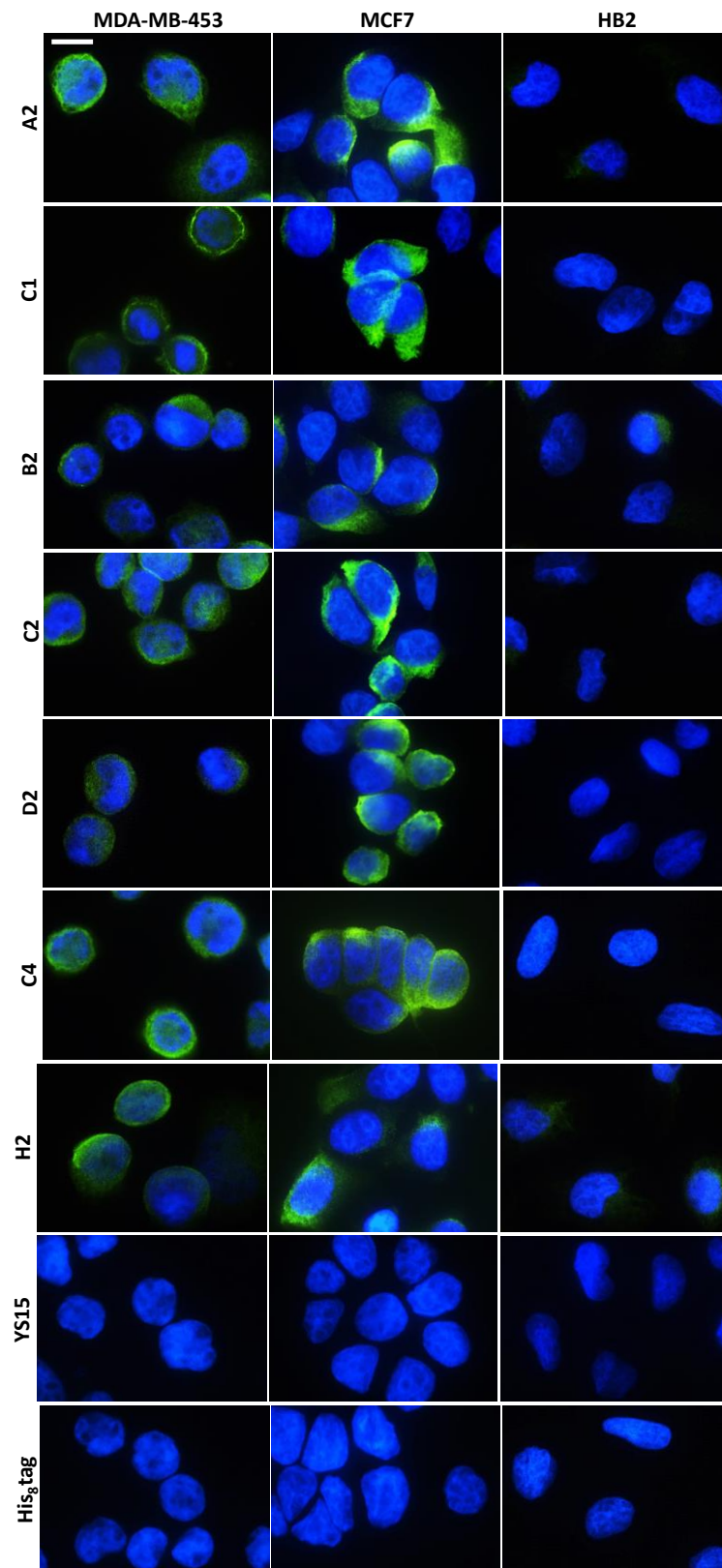


Figure 6.5 Immunofluorescence staining of cells using Affimer reagents. Cells were fixed with 4% PFA without permeabilisation. Affimers were incubated on cells at 4°C for overnight followed by detection and visualisation with his₈tag and anti-his Alexa488 conjugated antibodies (green). Negative controls, including the use of anti-his₈tag only and anti-YS15 Affimer reagents were included in the run. All images were merged with DAPI (blue). Scale bar: 10 μ m ($n = 3$).

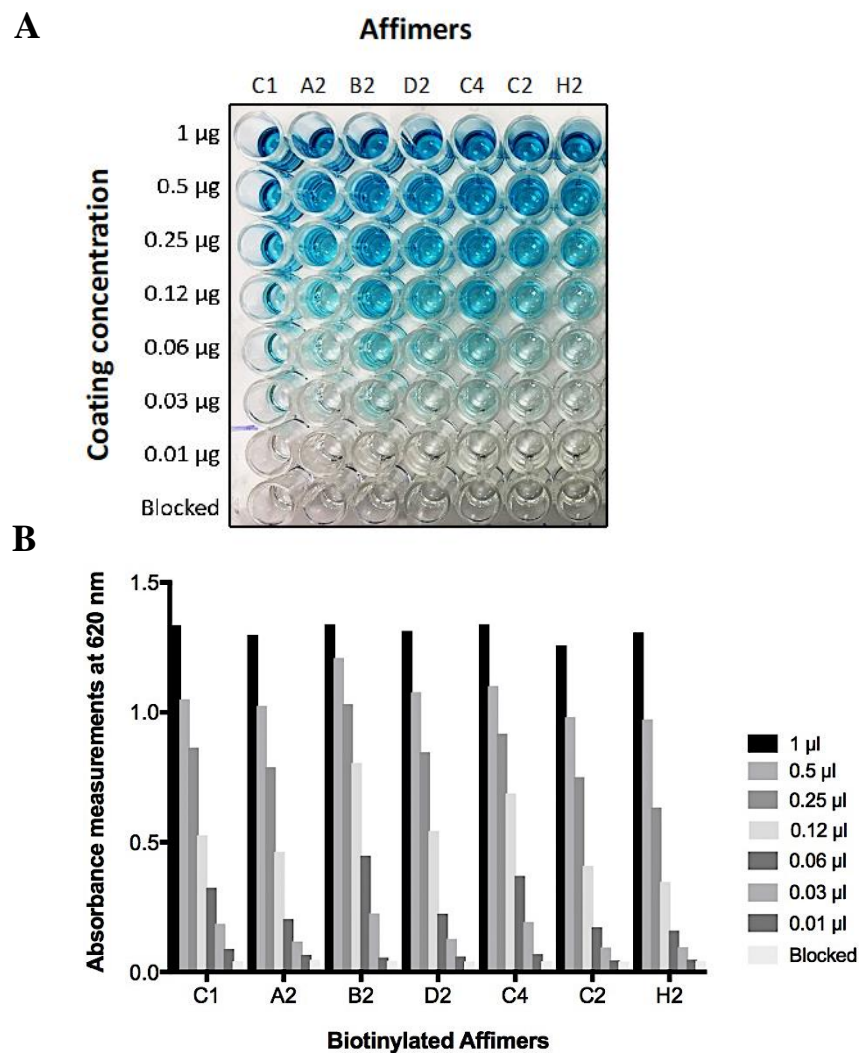


Figure 6.6 ELISA showing successful site-specific biotinylation of Affimers confirmed by ELISA assay. (A) Biotinylated Affimers were coated on wells at different concentration to enable the detection of biotin attached molecule by the streptavidin-HRP conjugated reagents. (B) Absorbance measurements were taken at 620 nm after the addition of TMB substrate. The plotted absorbance measurements represent the mean value of duplicated measurements from one experiment ($n = 5$).

cancerous cell lines. The staining pattern showed with **A2**, and **C1** Affimer may have indicated the heterogeneity of the protein expression to which they bound to, and at the same time it could have been a result of incomplete biotinylation of the Affimers as the percentage of the biotinylation was not evaluated prior to the staining. In future studies, it would be of advantage to adapt an approach to evaluate the biotinylation efficiency through quantitative approaches, such as mass spectrometry, before the use of the

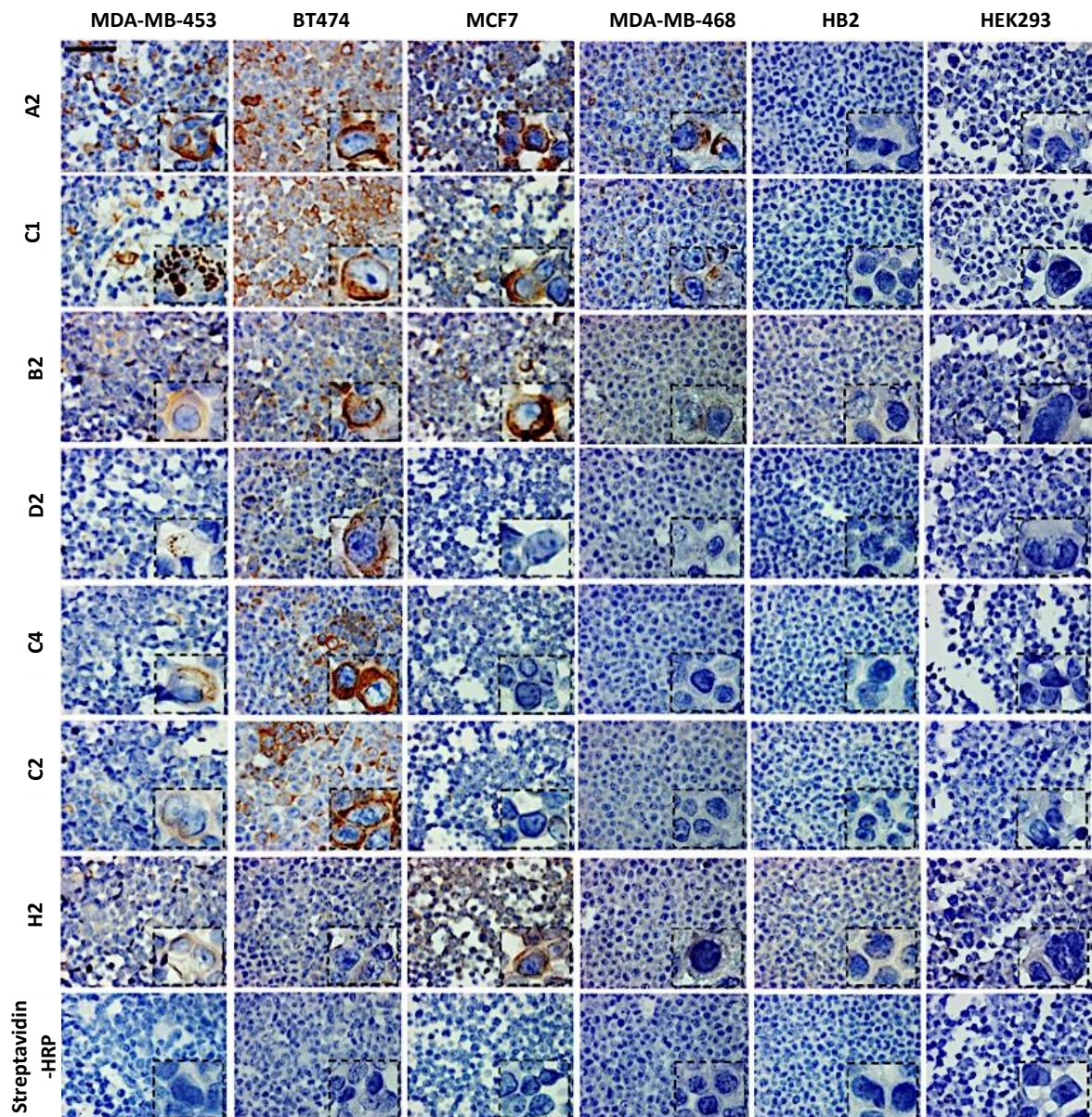


Figure 6.7 IHC-like staining on a panel of tumorigenic and non-tumorigenic cells confirming the binding selectivity of some soluble Affimers towards cancer cells. Affimers were added to formalin-fixed paraffin embedded cells for one hour at room temperature after retrieving the antigenicity of the proteins. Bound biotinylated Affimers were detected by streptavidin-HRP conjugated reagent and visualised by DAB substrate (brown). Scale bar: 50 μ m and magnification of 16X. Magnified cells are shown in the squares. ($n = 2$ per two different cell line blocks).

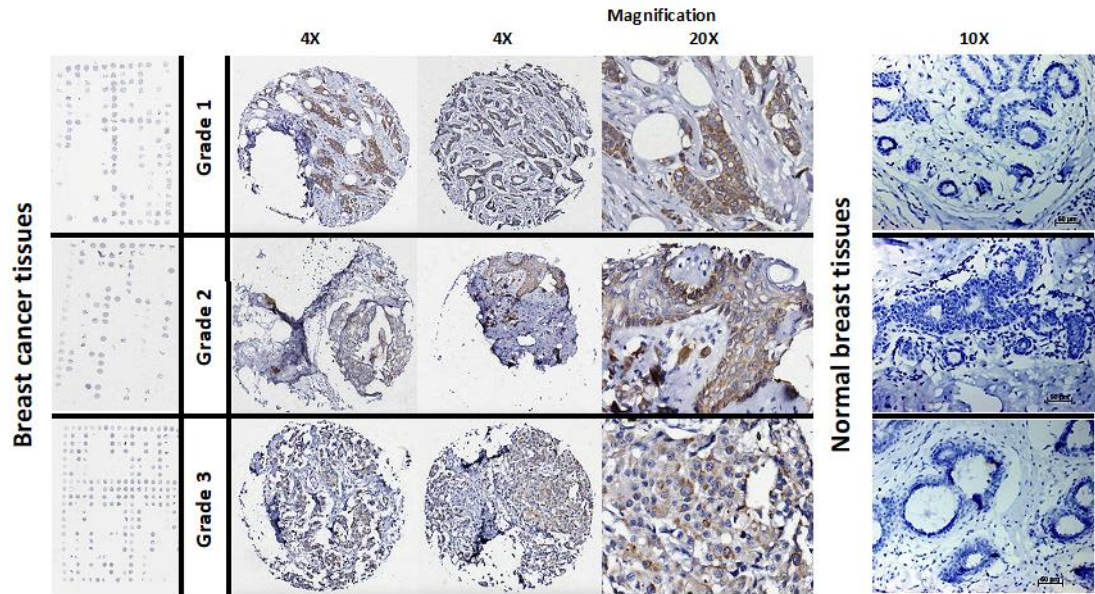
biotinylated Affimers in any molecular recognition application in order to verify the true explanation behind the heterogeneity of the staining results.

The staining pattern of **C4**, **D2**, **C2** towards MDA-MB-453 cells was weaker than expected compared to fluorescence microscopy (figure 6.7). This likely to be either caused by the difference in passage number of this cell line or the fixation process has altered binding ability and antigen presentation. Tissue or cell processing may also affect the localisation of the antigens as experienced by Dr. Sandra group (data obtained by personal communications). Consistent with the fluorescence imaging, both **H2** and **B2** Affimers showed staining on all cells (figure 6.7). The results of different microscopy staining assays confirmed selectivity of five Affimers towards cancer cells with **A2** and **C1** showing the most intense staining.

6.2.4 A2 and C1 Affimers staining is increased in breast cancer

Due to the binding selectivity of **A2** and **C1** Affimers exhibited, these were further characterised on tissue sections. Tissue microarrays (TMA) containing multiple cores of breast cancer tissue along with normal breast tissue, were used. All TMAs and whole tissue sections were obtained from Professor Speirs and purchased from USBiomax (see section 2.1.3 for more details). Both **A2** and **C1** Affimers showed strong heterogeneous staining pattern of tissue sections across different breast tumour cores (figure 6.8). Our preliminary showed an indirect correlation between the grade of cancer and staining intensity. In aggressive (grade III) tumours, the level of staining decreased when compared to low grade tumours (grade I) (figure 6.8). These results showed an downregulation of the cognate antigen to which Affimers bind in addition to the heterogeneity in its expression pattern among different grades of breast tumours. However, there is a need to study more tissue samples to confirm the existence of such an assumed correlation. Therefore, further histological scoring of the stained tissue cores coupled with correlation studies with different pathological parameters is currently work in progress.

Affimer A2



Affimer C1

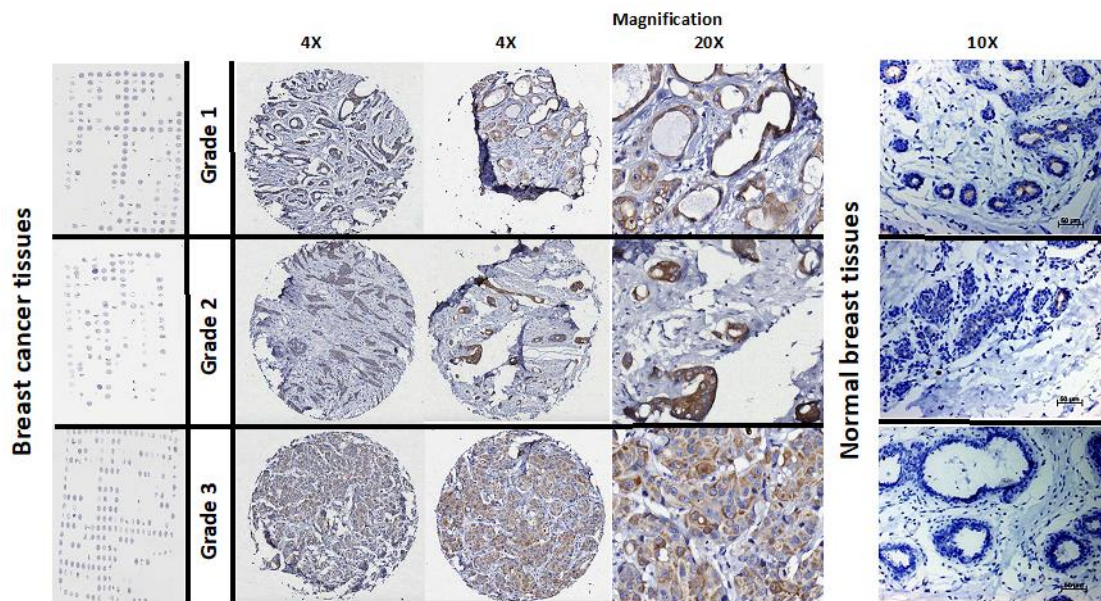


Figure 6.8 The cognate antigen to which both Affimer A2 and C1 bind is overexpressed in breast cancer. IHC staining using biotinylated Affimers on TMAs containing cancerous breast tissue cores of different tumour grades were performed. Whole tissue sections of normal breast samples were also stained ($n = 2$).

6.2.5 Both A2 and C1 Affimers bind to cytokeratin 19 and 18/8 proteins

Based on the fluorescence and IHC staining, MCF7 expresses the highest amount of the antigen recognized by the Affimer reagents. Cell lysates of MCF7 cells were prepared using non-denaturing lysing buffer to preserve membrane-associated proteins. Affimers were incubated with cancer cells and lysates prepared from HB2 cell line. Anti-yeast SUMO2 (YS15) Affimer reagent served as negative control. A pull-down assay was performed, as mentioned in chapter 2 (section 2.2.6.5), and Affimer-protein complexes were precipitated on a nickel-based agarose bead. The precipitated complexes were then eluted, separated on SDS-PAGE and Coomassie stained. Due to the variation of the amino acid sequence in the two variable loops of all 7 highly expressed Affimers in addition to the difference in their staining pattern on different cell lines, we aimed to identify the cognate antigen to which each of the 7 Affimers bind.

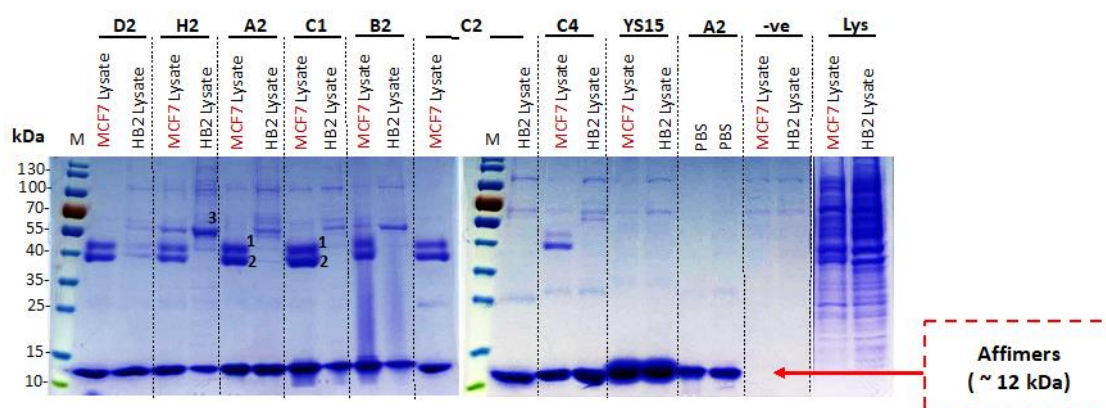


Figure 6.9 Isolated Affimers pulled down endogenous protein overexpressed in cancer cell lysates. Affimers were incubated with cell lysates prepared from MCF7 cells and HB2 cells for overnight at 4°C. The Affimer-protein complexes were precipitated and eluted. The eluates were then separated on SDS-PAGE gel. The gel was stained with Coomassie and the indicated protein bands were sequenced by mass spectrometry (MS) analysis by the MS facility service at University of Leeds, UK. ($n = 2$ for MS analysis and 3 for pull-down assays).

Coomassie staining of the gel loaded with pulled down complexes identified two bands of a size between 34 and 53 kDa. The complexes were observed in all lysates prepared from cancer cells. **H2** and **B2** were the only Affimers that pulled down a protein of an approximate 50 kDa in size from the HB2 cell lysate, correlating with the cross-reactivity observed in IHC staining (figure 6.7). The indicated protein bands (figure 6.9) were gel extracted, trypsin digested and identified by liquid chromatography tandem mass

spectroscopy (LC-MS, facility of MS analysis, Leeds University, UK). From both bands (indicated with number 1 and 2 in figure 6.9), we identified a total of 9 unique proteins. Within the identified proteins, 3 proteins yielded the highest percentage of peptide coverage (76 %, 74% and 60% of peptide coverage of CK18, CK19 and CK8 protein, respectively). and the same percentage was appeared in different mass spectroscopy analysis. Both **C1** and **A2** Affimers bound the same proteins that were identified as cytokeratin (CK) 19 and 18/8. As positive control, the anti-actin Affimer reagent demonstrated efficient pull down and sequencing of actin.

Interesting the Affimers appeared to only bind cytoskeletal proteins rather than extracellular proteins. This could reflect the biology of protein localisation during cancer development, as described by other researchers (Hung and Link, 2011; Wang and Li, 2014). For example, one study identified potential targets for breast-cancer diagnosis and treatment through the examination of plasma-membrane proteomics of different breast-cancer cell lines. In this study, a translocation of various proteins to the plasma membrane, such as the fatty acid synthetase protein, which is typically defined as an important cytoplasmic protein involved in lipogenesis to satisfy high-energy requirements, was observed (Ziegler et al., 2014).

6.2.6 Binding of A2 and C1 to cytokeratin 19 and 18 was confirmed by fluorescence microscopy and western blotting

The results of the mass spectrometry analysis were verified by microscopy to look for co-localisation. Different fixatives were used to assess the localisation of Affimer and cytokeratin antibodies as previous studies have demonstrated that fixatives can alter how well Affimers bind in IF (Lopata et al., 2018). Anti-yeast SUMO2 (YS15) Affimer and monoclonal his₈tag antibody alone were used as negative controls. Bound anti-his₈tag antibody in addition to other primary antibodies were then visualised by secondary anti-IgG specific alexa-488 conjugated antibodies. Both Affimers and anti-CKs antibodies were able to recognise CK19 and 18 proteins on both differentially fixed MCF7 cancerous cells. No staining was seen with the negative controls. Although all anti-CK19 and 18 affinity reagents worked with both fixatives, a high number of positively stained cells (green colour) showing detailed filamentous localisation of the cytokeratin proteins was observed in methanol fixed cells (figure 6.10). Therefore, methanol fixation is the preferred method to study the localisation of cytoskeletal proteins, such as cytokeratin.

Methanol fixation has also previously been shown to be better than PFA when staining other cytoskeletal proteins using Affimers (Lopata et al., 2018).

To further verify the specificity of **C1** and **A2** Affimers, the proteins precipitated from cell lysates by pull down were subjected to western blot analysis using the anti-CK 18 and CK19 antibodies (see section 2.2.6.5 for detailed protocol). CK18 and CK19 were detected in the affinity precipitate from both **C1** and **A2** (figure 6.11). The pull-down results verified that both of the cancer specific Affimers bind cyokeratin proteins (CK19 and 18) confirming the mass spectrometry results.

6.2.7 Cytokeratin 18 and 19 are expressed on the cell surface of cancer cells

Even though cyokeratin 19 and 18 are prominent type I filament proteins mainly expressed in the cytoplasm of cells (Karantza, 2011), our fluorescence and IHC results showed membrane and cytoplasmic localisation pattern in breast cancer cells. As such, we next explored whether the cyokeratin proteins are expressed on the cell surface by staining live cells with both Affimers and antibodies. In our experiment, Affimers (**C1** and **A2**) and anti-cyokeratin (CK18 and 19) antibodies were incubated with live MCF7 cancer cells for one hour prior to fixing with 4% PFA.

Affimers were detected with an anti- his₈tag antibody and visualised with a secondary Alexa488 conjugated antibody, while bound anti-CK18 and 19 antibodies were visualised with secondary Alexa488 conjugated antibody. Wheat germ agglutinin (WGA) Alexa594 conjugated was used as plasma membrane marker. As negative controls, anti-yeast SUMO2 (YS15) and anti-his₈tag antibody alone were used. All Affimers and antibodies showed granular staining around the plasma membrane of cells with little internalisation detected (figure 6.12). No staining was seen in the negative controls. At first, we reasoned our isolation of cyokeratin proteins for the possible internalisation of phage clones upon incubation at room temperature but our results here suggest findings that both cyokeratin 18 and 19 are expressed on the membrane of some cancer cells as demonstrated in recent study by Ju et al (Ju et al., 2015).

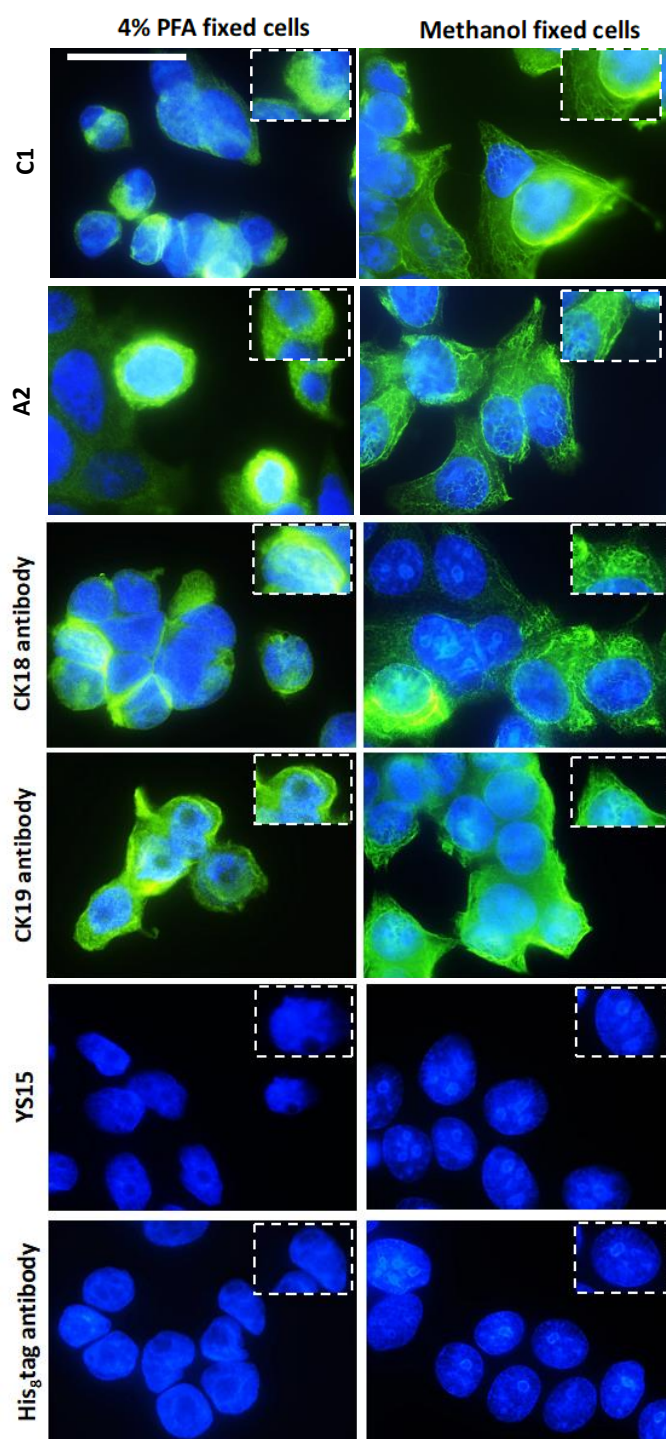


Figure 6.10 Immunofluorescence using Affimers and antibodies. Immunofluorescence staining was performed using Affimers and antibodies against CK19 and 18 proteins. Affimers were incubated for overnight at 4°C with MCF7 breast cancer cells fixed with either 4% PFA or methanol. Affimers were visualised using an anti-his₈tag and secondary Alexa488 conjugated antibody (green). Antibody binding was visualised with secondary Alexa488 conjugated antibody (green). Anti-YS15 Affimer and his₈tag antibody alone served as negative controls. All cells were counterstained with DAPI (blue). Scale bar: 20 μ m ($n = 3$ on different cells). Magnified part of cell is shown in the squares.

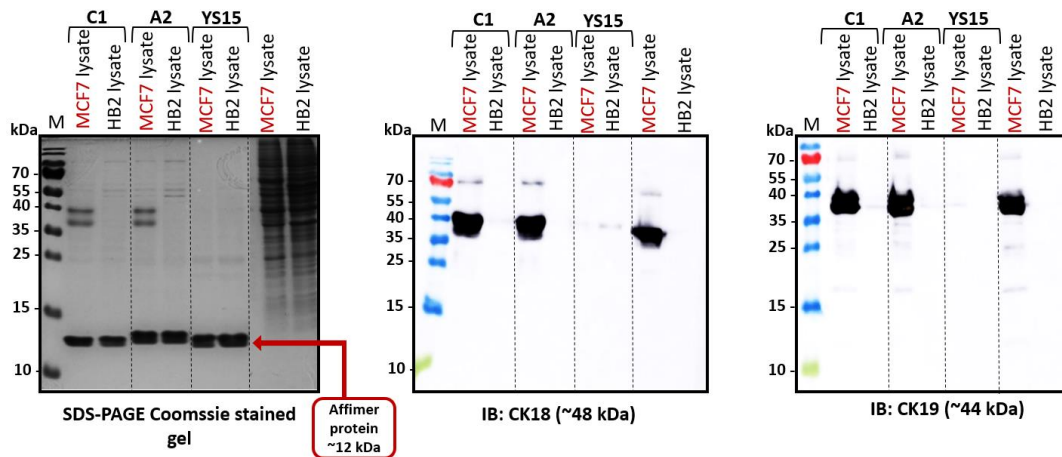


Figure 6.11 Affimer C1 and A2 pulled bind to cytokeratin in cancer cell lysates. Affimers were incubated with MCF7 or HB2 lysates, and the Affimer-protein complexes were precipitated on nickel agarose beads. Next, the complexes were eluted and separated SDS-PAGE gel and either stained with Coomassie blue or used in western blot analysis using CK18 and CK19 antibodies. Anti-YS15 Affimer and cell lysates were used as negative and positive controls, respectively (n = 3 for pull-down assays and 2 for western blot analysis).

6.2.8 Cytokeratin 19 expression upregulation is not solely dependent on HER2 overexpression in breast cancer

To confirm the previously suggested relationship between CK19 expression and the overexpression of HER2 in breast cancer (Ju et al., 2015), a panel of breast cancer cell lines were assessed for expression status of HER2, CK18, and CK19 using western blot analysis. Whole cell lysates were prepared under non-denaturing conditions. The lysates were ran on an SDS-PAGE gel followed by western blot analysis using CK18, CK19, HER2 and actin antibodies. Antibody against actin was used as loading control, while HB2 cells served as negative controls.

Our results showed increased CKs expression in all cell lines, which showed HER2 overexpression in addition to other HER2 deficient cells, such as MCF7 (figure 6.12). Other known triple negative breast cancer cell lines (ER-, PR-, and HER2-), including MDA-MB-468 and MDA-MB-231 showed weak expression of both CKs, while no protein was detected in the lysate of HB2 cells. Our data not only confirmed previous reports suggesting the association between HER2 expression status and CK19

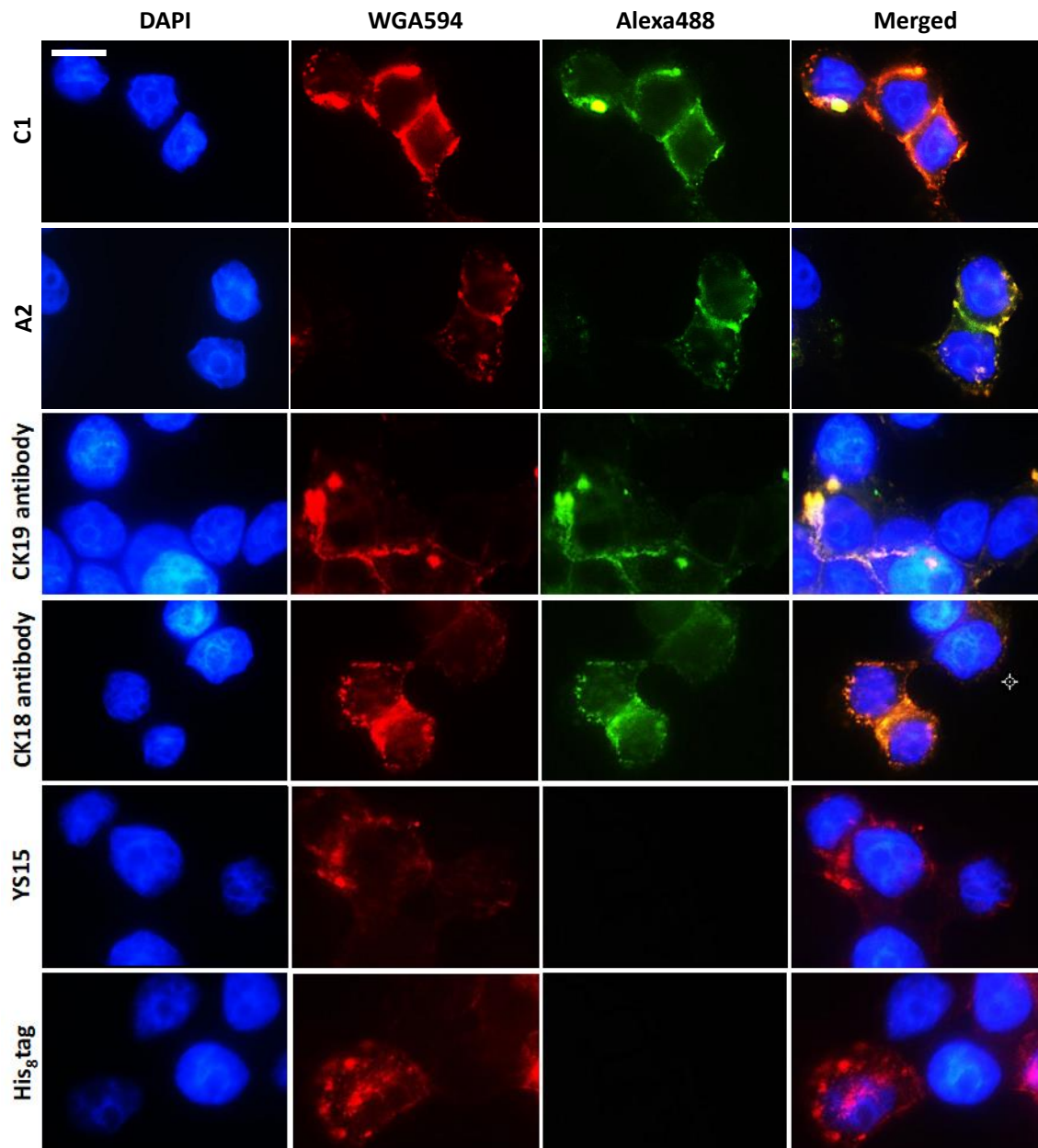


Figure 6.12 Cytokeratin proteins are expressed on cell surface. Affimer C1 and A2 in addition to antibodies against both CK18 and 19 proteins were incubated on MCF7 cells for one hour under physiological conditions prior to fixing. Membrane was stained with wheat germ agglutinin (WGA) conjugated to Alexa594. Anti-YS15 and anti-his₈tag were used as negative controls. Both Affimers and antibodies against CK18 and 19 were visualised by secondary conjugated Alexa488 antibody. Scale bar: 10 μ m ($n = 2$ per different cell line).

upregulation in breast cancer (Ju et al., 2015), but also supported other findings in which MCF7 cell line were found to highly express CK19 mRNA similar to the level detected in another HER2 overexpressing cell line (SKBR3) (Saha et al., 2017). The controversy about CK19 expression regulation in breast tumours can indicate its important tumorigenic role and further suggest the involvement of different cellular signalling mechanisms behind its upregulation in cancer.

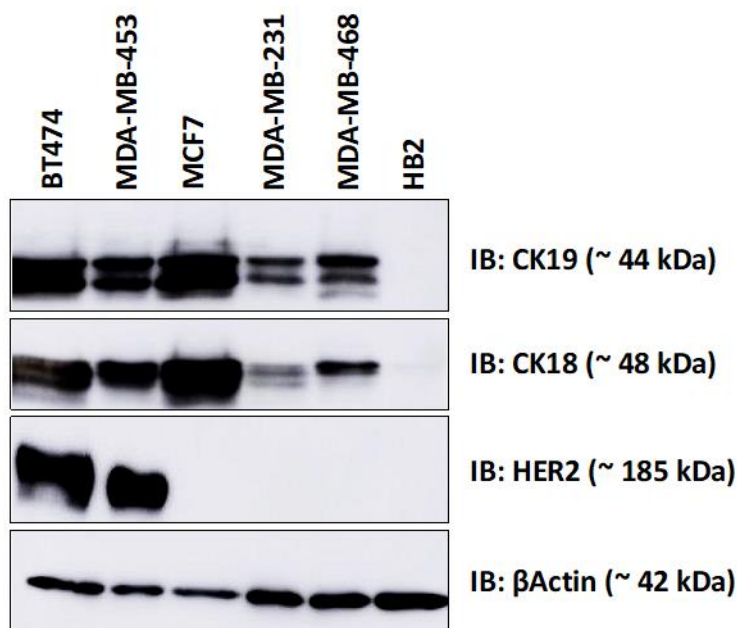


Figure 6.13 CK18 and 19 expression is not dependent on HER2 upregulation. Western blot analysis on whole cell lysates of cancerous and non-tumorigenic cell lines was performed using antibodies against CK18, 19 and HER2. Anti-actin antibody was used as a loading control. 5 μ l of lysates were loaded in each lane ($n = 2$).

Next, we stained a TMA containing 100 cores of breast tumours in addition to 10 cores of adjacent normal breast tissues to further investigate the staining pattern of CK in tumours in comparison to HER2 expression. The phenotype expression pattern of ER, PR and HER2 markers was known for all cases. IHC staining with biotinylated Affimer C1 was performed following the protocol reported in chapter 2 (section 2.2.6.4). The efficiency of endogenous biotin blocking was assessed by the addition of streptavidin-HRP conjugated reagent to FFPE cells (data not shown). In addition, a negative staining of the stromal cells within the tumour was considered as internal negative control. Our preliminary results demonstrated strong cytoplasmic and membranous staining of CKs in tumours with positive ER, PR and HER2 expression (figure 6.14). While tumours that

expressed low levels of ER, PR and HER2 showed low expression level of cytokeratins. In tumours with HER2 upregulation only, a distinctive membrane localisation was detected with the Affimer staining.

By examining normal breast tissues obtained from adjacent tumour tissue, basal expression level was observed in tissues where no ER and PR upregulation was reported. When the expression level of both hormonal receptors was altered, an increased CKs expression was seen. Although our results confirmed suggested association between CK19 and membrane translocation in HER2 overexpressing cells (Ju et al., 2015;Ohtsuka et al., 2016), we also revealed a potential relationship between altered expression of hormonal receptor (ER and PR) and CK 18 and 19 upregulation in breast cancer. Work is ongoing to score histologically and investigate the importance of CK19 and CK18 as prognostic biomarkers in breast cancer. This work involves a study of a large cohort of breast-cancer cases to investigate the relationship between the expression status of all ER, PR and HER2 markers and CKs.

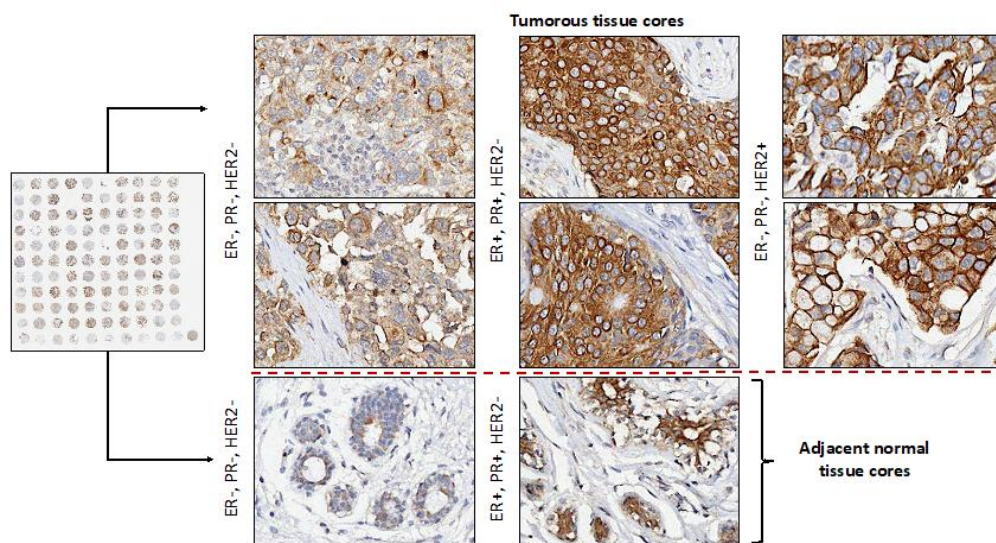


Figure 6.14 Affimer C1 confirms the heterogeneous localisation pattern of cytokeratins in the different molecular subtypes of breast cancer. Purchased TMA containing 110 cores of breast cancer tissues in addition to tumour adjacent normal tissues was used. All three common IHC-based biomarkers for breast cancer, including ER, PR, and HER2 were given. Affimer C1 was added to the tissue array for one hour at room temperature following the IHC staining protocol. TMA slide was scanned by Leeds Institute of biomedical and cellular studies (LIBAC). This figure represents some cases in the array as further detailed analysis will be conducted in the future studies ($n = 1$ per TMA). The magnification of the tissue cores is 20X as analysed by WebScope software.

6.3 Discussion

From the phage selection screen, the cognate antigen of two Affimers (**C1** and **A2**) was identified as cytokeratin 18 and 19 (figure 6.8) and confirmed by fluorescence microscopy (figure 6.10 and 6.12), pull-down assay coupled with western blot analysis (figure 6.111). Cytokeratin proteins are the largest and the most complex group of proteins among the superfamily of intermediate filaments (IF) (Karantza, 2011;Moll et al., 1982). In humans, 20 different cytokeratin isotypes have been identified (Takahashi et al., 1995;Schweizer et al., 2006). These isotypes have been further classified into two subfamilies.

Subfamily I of keratins includes 11 acidic CKs (CK 9 to 20), while type II keratins are more basic and include eight CKs (CK1 to 8) (Bragulla and Homberger, 2009). Pairs of acidic and basic cytokeratins are expressed differentially in different stages of cell development and differentiation (Moll et al., 2008). A recent interest in understanding the biological function of the most abundant cytokeratin proteins (CK 19, 18 and 8) in breast (Aiad et al., 2014;Saha et al., 2018;Alix-Panabieres et al., 2009), bladder (El-Salahy, 2002), lung (Nisman et al., 2008;Kosacka and Jankowska, 2007) and other cancer types (Turner and Milliken, 2000;Erkic and Kocer, 2005;Giovanella et al., 2017) have revealed a significant role of these CKs in modulating intracellular signalling by operating in conjunction with various related proteins. CK 19, 18 and 8 may affect carcinogenesis via several signalling pathways, such as PI3K/Akt (Ju et al., 2015), Wnt (Ikeda et al., 2006), NUMB-dependant NOTCH (Saha et al., 2017) and MAPK/ERK pathway (Ohtsuka et al., 2016). As such, these CKs can be used as predictive biomarkers in cancer.

The mammary gland is mainly composed of luminal epithelial cells expressing cytokeratin (CK) 19, 18 and 8, while other basal/myoepithelial cells express CK 5/6, 14 and 17 (Dairkee and Heid, 1993;Gusterson B. et al., 2005). Human breast cancer MDA-MB-453 cell line has been classified as molecular apocrine breast cancer cell line that expresses androgen receptor (AR) and HER2 with no ER or PR (Hall et al., 1994). Therefore, we did not expect to isolate cytokeratin proteins from this cell line. Interestingly, our microscope research using Affimers and antibodies against CK18 and 19, showed CKs upregulation in the MDA-MB-453 cell line. Our results further confirmed earlier findings in which luminal epithelial CK markers are also upregulated in non-luminal, HER2 positive classified breast cancer cell line, such as the SKBR3 (Ju et al., 2013).

By comparing the expression patterns of CKs in normal and cancerous cells (figure 6.5 and 6.7) and tissues (figure 6.8 and 6.14), we observed a distinctive membranous localisation of CKs in tissues with high HER2 expression, while other HER2 deficient tumours showed both cytoplasmic and membranous staining (figure 6.14). Even though HER2 positive tumours are an aggressive subtype of breast cancer (Arpino et al., 2015;Mitri et al., 2012), CK19 upregulation is not associated with the aggressiveness. A recent study also suggests a similar association between CK19 expression and ER status in different breast cancer subtypes (Saha et al., 2017). The study demonstrated that CK19 and ER expression is associated with the prognosis of breast cancer. The high expression of CK19 in ER positive tumours is associated with better prognosis compared to those with high level of expressed CK19 and negative ER expression. Similar to their findings, our preliminary data also suggest a correlation between CKs expression and the level of expressed ER, PR and HER2 proteins (figure 6.14). However, further statistical analysis correlating the clinico-pathological data of the patients and the expression levels of the different receptors in addition to CKs is needed.

In addition to the suggested correlation between CKs and other ER, PR and HER2 proteins, our preliminary results demonstrated a possible correlation between tumour grade and CKs expression levels in which low-graded breast cancers showed high expression levels of CK18 and 9 compared to the high-grade ones (figure 6.8). The observed results was in accordance to what have been reported recently by Aiad et al, (Aiad et al., 2014).

To understand the function of CKs in cancer, the underlying molecular mechanism of cytokeratin upregulation and translocation in different breast cell lines have been explored. It was previously demonstrated that active specificity protein-1/transcription factor 1 (Sp-1) binding to its specific site at CK19 gene promotor can affect the levels of the produced CK19 mRNA (Brembeck and Rustgi, 2000). SP-1 activity is further regulated by phosphorylation derives from active ERK protein. As such, it was reported that in HER2 overexpressing tumours (Ju et al., 2015), stimulation of ERK pathways can increase the expression level of CK19 through SP-1 phosphorylation (figure 6.15). The CK19 was then assembled in the cytoplasm where an active PI3K/Akt phosphorylates CK19 in its serine35 residue causing cytokeratin disassembly from filamentous to granulous shape (Ju et al., 2015). The granulous shape of CKs was observed in the IHC staining of some cancerous cell lines, particularly the MDA-MB-453 cell line, which overexpress HER2 (figure 6.7). The disassembled CK19 was then translocated to the cell

membrane to stabilise HER2 and inhibits its ubiquitination (Ju et al., 2015;Ohtsuka et al., 2016).

In conclusion, this chapter demonstrates the use of phage display as a tool for the discovery of proteins with altered expression in cancer. The identification of cytokeratin 19, 18 and 8 further revealed their important function in breast carcinogenesis in conjugation with other known biomarkers. Further investigations using a large cohort of breast cancer cases with known clinico-pathological features will clarify the role of epithelial CK19, 18 and 8 proteins as specific clinical biomarkers for breast cancer diagnosis, prognosis, and prediction of treatment response.

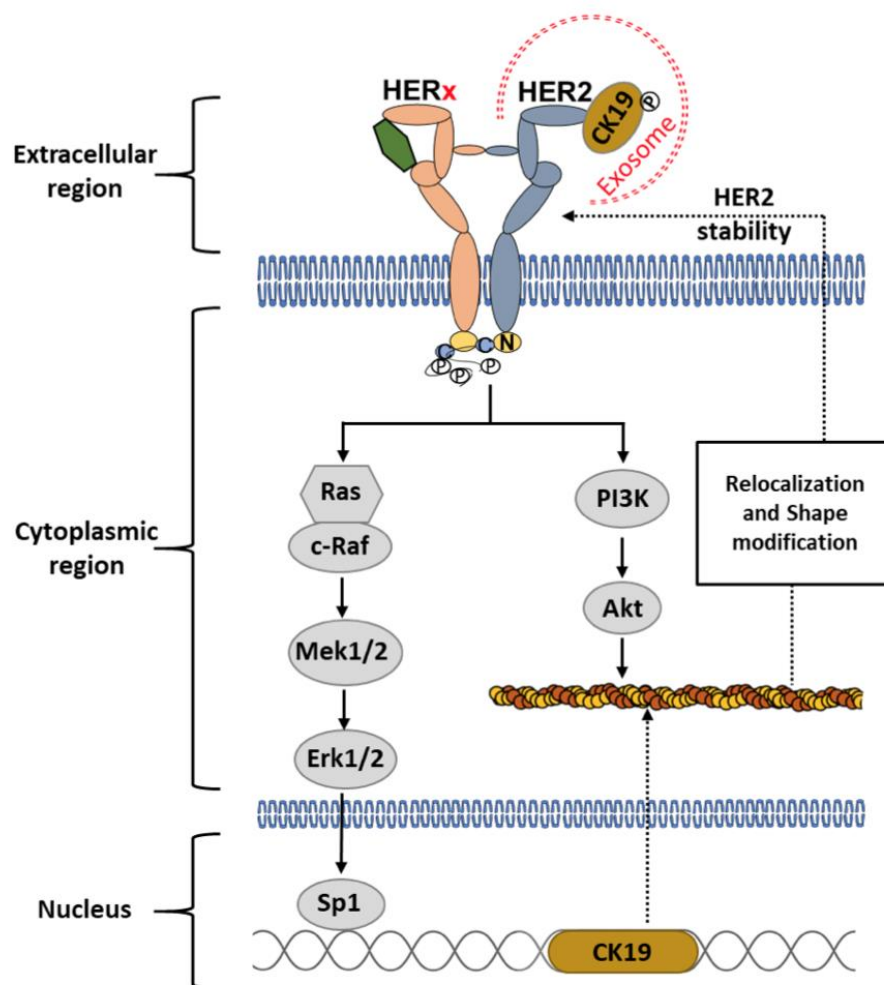


Figure 6.15 CK19 upregulation caused by HER2/ERK pathway is responsible for HER2 stability on cell membrane. Schematic model illustrating the stabilisation mechanism of HER2 on the membrane of cells, overexpressing HER2 protein, through CK19 upregulation. Activated-HER2 promote downstream signalling activation of MAPK/ERK pathway that cause more SP-1 protein to bind to the CK19 gene. The produced CK19 is phosphorylated at serine35 residue by Akt causing structural modification and translocation of the protein to the cell membrane (Ju et al., 2015).

CHAPTER 7

General discussion and future directions

The work presented in this PhD thesis sheds light on the potentials of Affimer technology as a versatile toolkit for cancer biomarker detection, discovery, and targeting. This chapter provides an overview of the fixed-cell phage display technology and its applicability in isolating Affimers with specific characteristics. The current status of Affimers as molecular recognition tools, with a focus on their functionalisation strategies and the possible ways to improve their detection sensitivity, is explored. Finally, their role in cancer biomarker targeting as a future direction of this research is reviewed, with emphasis on the possible engineering strategies that could be performed to expand their utilisation as cancer therapeutic agents.

7.1 Fixed-cells phage display as strategy for Affimers development

In 1985, Smith developed a phage display technology that led to the production of many phage libraries with the capability of screening for reagents that identify any class of target molecules with high specificity and binding affinity (Smith, 1985). This technology enabled the isolation of human monoclonal antibodies (McCafferty et al., 1990) and engineered-antibody derivatives (Holliger and Hudson, 2005), in addition to other protein scaffolds (Skrlec et al., 2015). Over 50 protein scaffolds have been developed and among them is the recently introduced Affimer scaffold (Tiede et al., 2014). The Affimer scaffold originated from the plant phytocystatin protein framework and was developed at the University of Leeds by the Bioscreening technology group (BSTG). Using this scaffold, we aim to develop phage selection strategies enabling the isolation of binding tools capable of detecting biomarkers in IHC-like applications, with a specificity comparable to that of antibodies.

More recently, whole-cell-based phage displays have been developed to obtain biomarker specific binders as well as to discover novel, cancer specific or cancer-associated markers (Stark et al., 2017; Jones et al., 2016). Using cancerous and immortalised (non-

tumorigenic) cells for the bio-panning process, specific antibodies (Kupsch et al., 1999), peptides (Zhou et al., 2015) and anti-CD55 ScFv (Ridgway et al., 1999) have been isolated. In these studies, known libraries were selected against live tumour cells to raise binders against either specific markers or new, un-identified potential biomarkers. The strategy of whole-cells based bio-panning may hold several advantages over the conventional-protein based selection, where immobilised-recombinant protein is used. These are the following advantages: (1) The protein, which is stably expressed on the surface of cells, sustains its native conformation, providing an indefinite supply of this particular protein; (2) Live or fixed-cell based panning can circumvent the omission of epitopes that might be hidden or denatured when the protein is adsorbed into the plastic. In the current research, we studied the amenability of fixed-cell phage selection, in which a monolayer of cells was fixed on a solid-phase to enable the selection of Affimers, which binds specifically to the fixed conformation of cell surface HERs proteins (HER1/EGFR, HER2, and HER3), allowing them to recognise the receptor on cells.

Despite the several advantages of using whole cells as the source of target protein, such selection strategies involving cells can be complex and challenging. This is mainly due to isolation of non-specific binders that bind to other non-target proteins, and thus, affect the overall enrichment of the desired binders, leading to unsuccessful phage screens (Alfaleh et al., 2017). To avoid this shortcoming of using whole cells, we adapted a negative selection approach (Tang et al., 2017), also known as a counter-selection, in which the Affimer library is depleted on a monolayer of fixed cells that do not express the receptor, prior to the selection of the corresponding target on cells overexpressing it. This approach helped in reducing the number of non-target binding Affimers, in addition to the decrease in the number of panning rounds required (total of 3 to 4 rounds) to observe the effective enrichment of specific binders. Hence, less effort was required to screen the isolated binders using the simple ELISA assay.

Using HER2 as the target protein, two cell-based selection strategies have been developed and assessed. In the first strategy, we selected a naïve Affimer phage library on HER2-transfected HB2 fixed cells (overexpressing HER2), after being depleted by the respective non-transfected cells. The resulting outcome of this selection approach was poorly enriched with HER2 specific binders. We reasoned it being so due to the type of cells used in the selection and the need for further optimisation to improve, both the negative selection and the washing steps, to remove the non-specific and non-binding phage. In the second approach, we utilised the previously developed selection strategies, which

emphasises on the advantage of using different target presentation formats in a single phage screen (Andersen et al., 1996). In the approach developed by Anderson et al., (1996), a Fab library was selected on cells expressing a specific antigen of the major histocompatibility complex (MHC) for three rounds, followed by an additional three round of selection on the peptide of the same MHC protein coated on beads. They declared that this strategy can replace the immunisation approach to generate highly specific MHC binders. As such, we exploited their strategy and decided to pre-enrich the naïve Affimer phage library against the HER2 recombinant protein before selecting it on cells. The reasons behind starting our selection approach with protein are as follows: (1) In our protein-based phage screens, the conformation of the protein is preserved through its presentation in the screen as biotinylated protein, immobilised on streptavidin coated wells; (2) It will be the pure source of the target, so that the proteins can better enrich the for the phage clones that specifically bind to HER2.

It appeared that the built selection cascade involved the use of a pre-enriched library to isolate binders from cell-based screens - the optimal approach to adapt for generating binders with specific characteristics, and thus, further reduce the efforts related to binder screening, generation and characterisation. To explore the robustness of the developed selection strategy, we evaluated its potential applicability to screen other targets, such as HER3. The screen output did not show a successful panning in which non-efficient enrichment of HER3 specific binders were observed. This confirmed the fact that there is no standard screen to apply to different antigens and thus a case-by-case optimisation is required.

7.1.1 Fixed-cell phage display for the discovery of new biomarkers

In a novel approach towards identifying cancer-specific biomarkers, we enriched a naïve Affimer library on breast cancerous cells that were fixed. Prior to target enrichment on cancerous cells, the library was depleted on immortalised (non-tumorigenic) breast cells to remove phage variants that bind to common antigens and thus directing the phage towards cancer biomarkers that either specifically expressed on or overexpressed by a cancer cell. A crucial step in this approach was the stringent washing of the non-binding phage that was applied in the second panning round. Due to the admixed environment of

cells, we speculate that stringent washing will not only reduce the number of non-specific binders but will also bias the selection towards binders with high binding affinity.

Once potent Affimers were selected, it could be readily expressed in high yields of up to several grams per litre in *E. coli* upon induction with IPTG, followed by their functionalisation and characterisation in several molecular techniques. In order to identify the biomarker to which some isolated Affimers bind, a pull-down assay was performed on cell lysate and the formed complexes were denatured, run in an SDS, and the desired protein bands were excised and analysed by mass-spectrometry (MS). The MS analysis revealed that the protein to which the Affimers bind is the cytokeratin 18/19 filamentous protein. Although cytokeratin was identified two decades ago (Powell et al., 1992), their role as important tumorigenic transformers has recently evolved (Saha et al., 2018;Ohtsuka et al., 2016;Giovanella et al., 2017). It has been revealed by Saha et al (2018) that cytokeratin 19 is crucial as a signalling component for cancer-stem cell reprogramming, and alteration of drug-sensitivity of cells (Saha et al., 2018). As a future direction of this thesis, with regards to revealing more potentials of the CK19 as a vital biomarker for cancer, exploring its biology in primary tumours and metastasised lesions that were either sensitive or resistant to drugs may give rise to new cancer therapeutic approaches.

In the future, various platforms can be tried to identify more novel biomarkers. Since drug-resistance tumours represent a major issue in cancer, selecting Affimers for drug-resistance cell lines can provide the opportunity to define some markers, enabling for a better understanding of the mechanism behind their treatment resistance, which may further lead to the development of novel treatment strategies. Furthermore, an understanding of the physiological role of the developed binding agent, in addition to the currently developed anti-CKs binding Affimers, can be then evaluated *in vitro* using either cell lines or other advanced developed platforms that offers mimetic carcinogenic microenvironments, as compared to that of the *in vivo* models. An example of these platforms is the organ-on-a chip platform (Ronaldson-Bouchard and Vunjak-Novakovic, 2018).

7.1.2 Cell-based vs protein-based phage selection strategies for the isolation of IHC-binding reagents

In addition to their ability of pulling down their target protein from a cellular lysate, most of the anti-EGFR, HER2, and HER3 binders, which were isolated from either a protein-based phage screen or screens that involved both protein and fixed cells, were able to bind to their target on fixed and live cells. However, none of them were able to work in IHC-like applications, despite the various staining optimisation strategies performed. In contrast, the cytokeratin 18/19 binding Affimers that were isolated from a pure cell-based screen were the only ones that showed binding in formalin-fixed paraffin embedded tissue. At this stage of research, it is not possible to conclude which approach of phage selection is the optimal for the isolation of IHC binding reagents. This mainly due to the fact that other Affimers, such as the anti-VEGFR2 and anti-TNC-C reagents (Tiede et al., 2017), that were isolated from a protein based-screen, have showed similar successful IHC applicability to that of the anti-CK18/19 ones. A comparison between the various strategies can be possible after examining the binding kinetics of the isolated Affimers. Such examination will highlight the ideal binding affinity required to enable the binders to work in IHC-like applications. In addition to their affinity characterisation, an optimal functionalisation strategy to generate Affimers as specific and sensitive detection reagents can also participate in the improvement of their detection ability in such IHC applications.

7.2 Efficient Affimers functionalisation and microscopic applications

We developed a toolset of Affimers against both the human epidermal growth factor receptors (HER1/EGFR, HER2 and HER3) and cytokeratin proteins (cytokeratin 18/19). Furthermore, we established strategies to use them as molecular recognition reagents in different microscopic studies, such as fluorescent and histochemistry staining (IF and IHC applications), by reliably labelling them with biotin or by genetically fusing them to other proteins, including the Fc-fragment of a rabbit and mouse IgG.

In this thesis, we introduce a method for a reliable biotin-labelling of Affimers, using surface cysteine and maleimide chemistry. Maleimide-biotin-labelled Affimers consistently recognised their targets better and produced less background, as compared to the corresponding NHS-randomly modified Affimers. The primary disadvantage of

NHS esters labelling reagents is that they react with amino groups randomly, causing a possible blocking of the binding sites of the Affimers and resulting in non-functional binding reagents. Using random labelling, it is difficult to adjust its density and a substantial molar excess of reagent is required to achieve an efficient labelling. In contrast to random labelling strategies, maleimide-site-specific labelling of proteins via their cysteine residues is quantitative, controllable, and can be efficiently achieved with stoichiometric amounts of reagents, making it far more economical. This site-specific labelling process also results in a homogenous population of efficiently labelled molecules compared to the random-labelling approach.

7.2.1 Affimers as primary reagents in IHC

In IHC application, all Affimers were initially used as primary biotin-conjugated reagents detected with streptavidin-HRP conjugated reagents, hence eliminating the need for secondary antibody ones. Comparable to antibodies, our biotinylated cytokeratin 18/19 and VEGFR2 binding Affimers did show specific staining, but with low signal intensity. Therefore, and as a proof-of principle, we introduced another cysteine residue in the Affimer scaffold of the VEGFR2 binders as a mean to amplify the signal by increasing the number of attached biotin-maleimide linkers to a single Affimer binder. This resulted in more streptavidin-HRP molecules to bind. This double cysteine containing VEGFR2 Affimer binders did demonstrate a successful amplification of the detection signal when compared to a single cysteine biotinylated binder. Another approach for biotinylation called Avitag, was recently developed by Kay et al., (Kay et al., 2009) and commercialised by GeneCopoeis, Inc (UK).

Avitag is a technology for protein biotinylation using the expressing vectors containing it where protein biotinylation occurs in bacteria with the aid of biotin ligase enzyme (BirA ligase) (Kay et al., 2009). Biotin ligase catalyses the amide linkage of a single biotin molecule to a specific lysine residue placed in Avitag. The only advantage of this system relies on the facility of site-specific biotinylation, without further modification of the protein scaffold. However, this system may produce a signal intensity similar to the single-cysteine biotinylated Affimers, as it presents one biotin molecule to the detection system. In order to see an amplification of the signal, a cysteine residue must be introduced to the Avitag-expressing vector, followed by a maleimide-biotinylation

process, resembling by that the double-cysteine amplification strategy we adapted with the Affimers.

Despite a successful signal amplification, using the biotin-streptavidin detection system is not preferable in clinical diagnostics due to its limited detection sensitivity, high costs, and time-consuming nature, since more reagents are required and more practical steps are involved (Vosse et al., 2007). Therefore, other signal amplification systems, such as the polymer-based detection kit, are frequently-used in routine IHC-diagnosis tests as they allow for signal amplification using a lower concentration of the primary binding reagents (Ramos-Vara and Miller, 2006). To gain such amplification, the VEGFR2-binding Affimers were engineered to contain an Fc-fragment of rabbit and mouse IgG. Upon evaluation, the Fc-Affimer fusion protein provided a comparable sensitivity to that which is observed in the anti-VEGFR2 antibody, when a polymer kit was used for the detection. As such, generating Affimers as Fc-fusions is the optimal solution to ease their introduction into the field of biomarker diagnosis without the need to change the current diagnostic protocols. We expect this Fc-conjugation strategy to be widely applicable to other Affimers, thus expanding the range of IHC Affimer reagents.

7.2.2 Affimers as primary reagents in fluorescence visualisation microscopy

Fluorescent labelling of proteins is one of the key tools for visualising and understanding cellular structures and various intracellular processes. The work presented in this research demonstrates a successful isolation of Affimers with promising potentials as detection reagents, using immunofluorescence (IF)-like applications to enable the visualisation of the protein targets in the cells. Most of the isolated reagents showed comparable staining patterns to that which was observed with the corresponding commercial antibody. In such applications, Affimers were detected by anti-his₆tag antibody and a secondary fluorescence-conjugated antibody. The use of anti-his₈tag antibody requires optimisation for diminishing the level of non-specific background staining, caused by the interaction of anti-his₈tag antibody with the endogenously expressed histidine-contained proteins in cells. Our optimised approach showed the specific detection of various membrane target proteins without non-specific background staining observed in cells. However, some Affimer binders did not give a specific staining pattern and we speculate that this non-specificity is a result of aggregation. All Affimers reagents were modified to contain a

cysteine residue for labelling, the presence of free-cysteine residues can cause Affimer molecules to aggregate. Although such aggregation can be solved by the addition of TCEP-HCL thiol reducing agents, it was not an option to use for microscopic studies. As such, this established protocol, involving anti-his₆tag antibody, is an option to use with unmodified-Affimers reagents. For modified cysteine contained Affimer binders it is better to use site-specific, fluorescent labelling approach. The use of fluorescently-labelled Affimers has already demonstrated its potential as ideal tools for visualising and monitoring proteins inside a living or fixed cells using an advanced super-resolution microscope (Lopata et al., 2018), or in *ex vivo* experiments using a conventional confocal microscope (Tiede et al., 2017). Even when there was one dye molecule per binding protein, all Affimer reagents showed specific staining of their target proteins with no background level.

Recently, two novel labelling techniques that hold promise for future Affimer labelling with organic dyes were reported. First, the researchers have exploited the use of a transpeptidase sortase A (SrtA) derived from *Staphylococcus aureus* to label a HER2 binding nanobody with a fluorescent dye Cy5 (Massa et al., 2016). To test the idea, anti-HER2 nanobody was provided with a C-terminal SrtA recognition motif (LPETG), also known as sortag, in addition to a Cy5 dye that was coupled with a pentapeptide (GGGYK), through the primary amine group of the lysine residue. Next, the SrtA catalysed the formation of a new peptide bond between the glycine of the pentapeptide and the threonine of the sortag, generating a stable bond between the fluorescent label and the nanobody. An excellent performance was achieved upon testing the labelled anti-HER2 nanobody for imaging the HER2 positive tumours in mice.

Second, researchers have also demonstrated the efficiency and the successful applicability of the furan cross-linking technology, by labelling thymosin β 4 peptides with different fluorescent dyes (Antonatou et al., 2016). In this technology, the photo-oxygenation of the furylalanine building block incorporated into the peptide results in the formation of a 4-oxo-enal moiety. Subsequently, the NH₂NH coupled-label is added to convert the furan-contained peptide into pyrrolidinone-based fluorescent probes. Beside the maleimide site-specific approach, and the two recently developed ones, more site-specific conjugation techniques will emerge, undoubtedly, to expand the incorporation of Affimers into different *in vivo* molecular recognition applications.

7.3 Future directions of Affimers as therapeutic agents

The identification of antigens specific to cancer cells (tumour-specific antigens) or overexpressed by cancer cells (tumour-associated antigens) has enabled researchers to develop personalised-treatments, including humanised monoclonal antibodies and small molecules and protein-inhibitors that precisely target these antigens (Attarwala, 2010). The progress of Affimers as targeting therapeutics is still in a very early stage. However, the development of a humanised version of the Affimer scaffold can facilitate such progress through the prevention of eliciting of immunogenic responses. Few promising works have already demonstrated the potentials of Affimers as protein-function modulators (Hughes et al., 2017) and as a signal transduction blockers (Tiede et al., 2017). In addition to the published work, our preliminary results also demonstrated a cellular effect of some of the developed anti-HER3 and anti-EGFR binders that caused inhibition of the downstream MAPK/ERK1/2 signalling pathways. It would be advantageous to confirm their inhibitory effect and to further explore the mechanism behind their inhibitory effect, by examining the effect of Affimers on the kinetics of both receptor degradation and cell proliferation.

However, the only disadvantage that can hold back Affimers from entering the therapeutic field is that they offer less avidity as compared to the full-length antibody. Although, the problem of reduced avidity can be circumvented by several strategies, including Affimer engineering, to generate a reagent with multivalent binding sites or the use of carriers, such as liposomes, to deliver many Affimer reagents to the target site (Holliger and Hudson, 2005). Focusing on genetic engineering techniques, different bivalent and multivalent versions of Affimers could be formed, and the avidity could be increased by constructing dimeric, trimeric, or even tetrameric conjugates, fused to a drug or toxin. In addition, to a bispecific construct can be fused to the human Fc-fragment of a humanised antibody, such as the FDA-approved Catumaxomab antibody, which is a bispecific (anti-EpCAM and anti-CD3) trifunctional antibody (Linke et al., 2010). The multivalence strategies have already been adapted by several protein scaffolds confirming that valency is a critical factor to gain the optimal inhibitory effect of the reagent and result in a better overall growth inhibitory rate of the tumour.

Boersma et al., designed a bispecific DARPIn reagent that targets EGFR receptor on the A431 cell line that is known to overexpress the receptor (Boersma et al., 2011). Their bispecific constructs showed effective inhibition of cell proliferation and receptor cycling

as compared to the non-inhibitory single anti-EGFR DARPIn reagent. In addition to that, a three-in-one nucleic acid aptamers-small interfering RNA (siRNA) chimera, that can inhibit the growth of the HER2 positive tumours, have been developed to target EGFR, HER2, and HER3 in those tumours (Yu et al., 2018). This chimera offers multiple targeting by one molecule reducing the cost and the cytotoxicity side effects resulting from using several reagents to target different antigens in a single tumour. The ease of Affimer engineering without the loss of functionality and stability, as we demonstrated in this research, can make the generation of such multivalent reagents achievable.

Owing to the small size and stability of the Affimers in the cytosol environment of the cells, made them great alternatives for the development of drug delivery systems. The internalisation ability of some anti-HER2, anti-HER3, and anti-EGFR Affimers can be used to develop an Affimer-drug conjugate that targets these receptors. Upon the binding of this conjugate to the receptor, its internalisation is mediated by endocytosis and the free drug is released in the intracellular compartment (Ritchie et al., 2013). The conjugation of the cytotoxic drugs or other protein toxins can be achieved through the chemical linking of killing agents to the cysteine residue in the Affimer.

7.4 Recommendation for future work

The research presented in this PhD thesis has raised several questions that lead to further research directions that should be pursued. The research results presented in Chapters 3, 4, 5 and 6 showed both the strength and the limitations of the Affimer phage library that was used (Ella2), the performed phage screens and the molecular applications that were employed to isolate, produce and partially characterise the generated Affimer reagents on recombinant proteins, whole cells or lysates. All observed limitations and strengths indicated the following areas as recommendations for future work.

7.4.1. Design and construction of a high-complexity library

In this research, only one Affimer phage-based library (Ella2), which was developed in 2014 at the University of Leeds (UK) and was based on the consensus sequence of the phytocystatin (Tiede et al., 2014), was employed in all phage screens. This was in order to isolate novel reagents towards various targets, including HER2, EGFR and HER3, and to identify new protein cancer-related biomarkers. However, two problems related to the

developed library should be addressed in order either to improve the current library or to construct a new one. One issue is that the library described by Tiede et al. (2014) does not enable the construction of trillion-member libraries as it includes bacterial transformation steps, and this limits the potential diversity and complexity of the library. To design a library with high complexity, the BSTG researchers have developed a new library in which only a small peptide of nine randomised amino acids was inserted into the second binding loop and the first binding loop was replaced with three residues of alanine (figure 7.1). Such modifications of the Affimer scaffold have resulted in smaller Affimer molecules with a less randomised site but better diversity (library size of $\sim 1 \times 10^{13}$). According to data obtained by verbal communication and other published work that presents the interaction between Affimers and the SUMO1/2 proteins (Hughes et al., 2017), the first randomised loop was deleted as it was not fully involved in the interaction with the target molecule or if it was involved, the binding affinity was very low compared with the interaction displayed by the second binding loop.

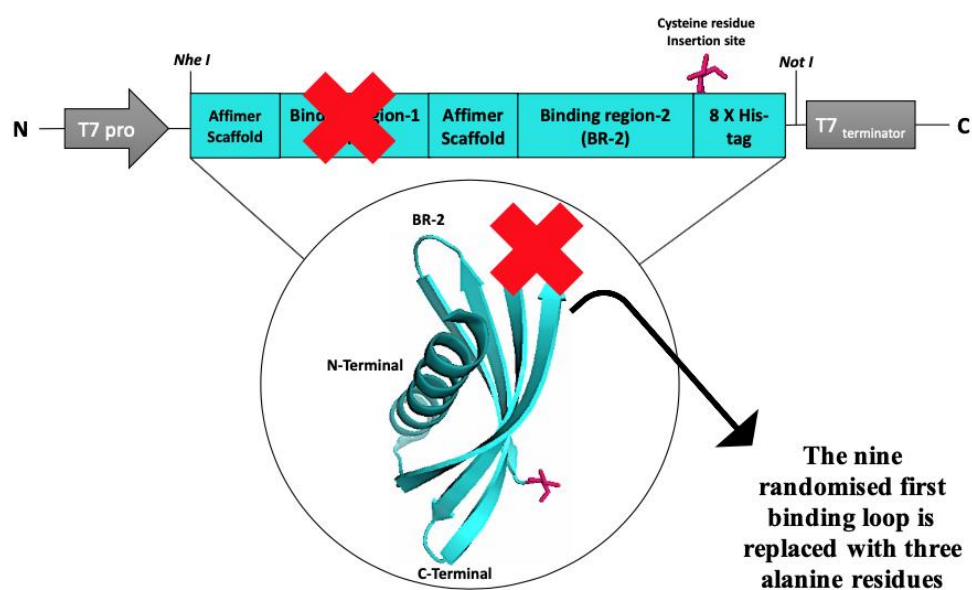


Figure 7.1 Schematic representation of the newly constructed and generated Affimer (single loop) library. Due to the limited diversity and complexity of the two-loop Affimer library (Ella2) employed in this research (Tiede et al., 2014), the BSTG researchers have constructed and produced a new library in which the binding loop 2 has been deleted and replaced with three alanine residues. The generated library shows better diversity and complexity with an actual size of 1×10^{13} . However, it requires further assessment and evaluation prior to use in different phage-selection approaches against multiple targets presented on different platforms.

The single loop library exhibits improved quality, but it is currently under further investigation and evaluation. Therefore, it would be of advantage to use this library to perform screens against the targets studied in this research (HER2, EGFR, HER3 and CK proteins) to explore the potential of generating binders with improved binding affinity and enhanced applicability compared with those generated for this study. The existence of another library would expand the diversity of the Affimer reagents, but it is necessary to assess and compare the biophysical properties of the single-loop scaffold (thermostability, production capacity in bacterial cells, ease of modification and storage stability after modification) and its binding quality (determined by the value of the dissociation constant). These findings should be compared with the properties of the double-loop scaffold before its use can be generalised to screen different targets presented on different platforms.

7.4.2. HER2-binding Affimers

Multiple phage-selection strategies were used to isolate binders to the HER2-ECD and eight isolated HER2-binding Affimers were characterised. The results suggest that D11 was the best binding variant as it was retrieved from different phage screens performed on the biotinylated HER2-ECD immobilised recombinant proteins and on both biotinylated proteins coupled with fixed cells that overexpressed the protein (Chapter 3). With more time and resources, we would pursue the characterisation of the D11 Affimer by, firstly, the determination of the binding kinetics of the Affimer using biosensor analysis (through use of the BLItz[®] or BIAcore[™] or both systems). This binding characterisation could be achieved using unlabelled HER2-ECD recombinant protein or other validated antibodies, such as trastuzumab or pertuzumab monoclonal antibodies.

These antibodies could be used as competitors to the isolated D11 Affimer. This experiment would offer an opportunity to identify the binding specificity of the D11 Affimer towards the ECD of HER2 and determine the domain to which the Affimer was bound, by referral to the crystal structure of HER2-antibody complexes. Furthermore, the binding interaction between Affimer-D11 and HER2 could be confirmed and elucidated through a crystallisation study that would involve the use of HER2-ECD protein expressed in mammalian cells (Chinese hamster ovary cells) as previously described (Ayoubi et al., 1996; Running Deer and Allison, 2004). Through the revelation of the crystal structure of the Affimer (D11)-HER2 complex, new libraries could be generated and different therapeutic targets could be developed.

After confirmation of the binding specificity of the D11 Affimer and assessment of its possible cross-reactive binding to other non-HER2 proteins, it would be of advantage to evaluate its cellular effect on the cell proliferation process in comparison with that of other therapeutic antibodies. From a diagnostic perspective, the generation of D11-Affimer-Fc-fragment fusion reagent would offer a research direction related to the production of HER2-binding detection reagents. The analytical sensitivity and stability of the developed Fc-fusion could then be compared with those properties of other available non-antibody HER2-binding reagents, such as the commercialised anti-HER2 affibody, by a panel of FFPE cells and tissue sections.

7.4.3. HER3-binding Affimers

Many alternative scaffolds have been described in the literature. However, to the author's knowledge, the only reported HER3-binding alternative scaffold that binds with subnanomolar affinity and cross-reactivity with the murine HER3 is the affibody scaffold (Gostring et al., 2012;Malm et al., 2016).The developed affibody reagents were generated from the combination of two display methods (conventional phage display and staphylococcal cell-surface display) followed by affinity maturation via semi-rational affinity maturation to generate the second generation of affibody molecules that bind HER3 with picomolar affinity.

In this research, 11 HER3-binding Affimers that were similar to affibodies were generated. Among these, only some Affimers seemed to bind to the receptor on cells (Affimers **G6**, **A5**, **A4** and **F3**) or in cellular lysate (Affimers **A1**, **D6**, **B6**, **H5** and **G6**) as presented in Chapter 4. Future research aims to repeat the phage screen against the biotinylated HER3-ECD recombinant protein using the newly developed single-loop library to isolate another set of Affimers against HER3 with better capability to work as detection reagents in IHC, as none of the 11 isolated reagents were found to do so. After isolating new reagents, the binding kinetics will be assessed and the cross-reactivity with other homologous HER proteins will be determined through use of cell lines that lack the expression of a specific HER protein, as illustrated by the human protein atlas (www.proteinatlas.org). The assessment in the current work of the specificity of the isolated binders was not complete due to a missing negative control cell line that did not express HER3. According to the RNA expression data presented in the human protein atlas, and the short tandem repeat (STR) profiling results illustrated on the website of the

American Type Culture Collection (ATCC), the B lymphoblast cell line Daudi does not express HER3. This can be purchased and used as a negative control in all assays that involve the assessment of -binding Affimers towards the receptor. Use of this cell line as a control would provide complete data regarding the binding specificity of the Affimers and thus confirm the novelty of the generated binders.

In accordance with the cellular effect presented by the specific HER3-binding affibodies (Gostring et al., 2012), five of the HER3-binding Affimers (**D6**, **C4**, **A1**, **F4** and **A5**) showed promising potential as therapeutic agents due to the antagonist effect they exerted upon binding to HER3. This effect caused partial inhibition of the downstream signalling pathway. However, due to limited time, this cellular study was performed only once, and our aim was to repeat the experiment at least two more times and then correlate the results obtained from this test with other results related to the evaluation of the Affimers' cytotoxicity on cell proliferation using one of the cell viability assays mentioned elsewhere (Riss et al., 2004;Stoddart, 2011).

7.4.4. EGFR-binding Affimers

Most of the binders that were isolated against the extracellular domain of EGFR and described in Chapter 4 showed improved IF staining and pulling down capability compared with the HER3-binding Affimers. However, their specificity could not be confirmed due to the absence of an appropriate negative control. Therefore, the next step to take these binders forward is to characterise fully their binding specificity by use of an appropriate cell line that does not express EGFR, such as the embryonal kidney cell line HEK-293 or the sarcoma cell line U-2-OS, according to the RNA expression data provided by the human protein atlas website. After characterisation of the binding specificity, the original research aim was to determine their binding kinetics and their ability to function in IHC applications in addition to the study of their cellular effect on cells. This aim could not be fulfilled, but some preliminary findings were made regarding their potential as inhibitors that block cellular proliferation by inactivation of the stimulatory effect of the EGFR receptor towards other downstream effector proteins.

A repeat of the performed cellular study would provide further details of the role of the EGFR-binding Affimers and take the research forward towards the creation of bispecific or trispecific Affimers in which two or three different EGFR-inhibitory Affimers, including the Affimers **G10**, **H9** and **H91**, would be linked through a flexible linker and

then tested on cells to be compared with their mono-specific counterparts. Furthermore, it would be useful to test the effect of these Affimers on cells that harboured the EGFRvIII mutation that occurs in up to 30 per cent of high-grade glioblastomas and which causes a constitutive activation of cell signalling, treatment resistance and poor prognosis (Chistiakov et al., 2017; Gan et al., 2013). There is a chance that the Affimers may block the mutated variant of the receptor by binding to it and causing it to internalise and degrade, if they bind only to the L2 or CR2 domain, as illustrated in Figure 7.2. If none of the isolated Affimers bound to the mutated variant, then the next step would be to perform a phage screen to isolate Affimers that could bind specifically to the EGFRvIII-mutated protein, through use of the two Affimer libraries.

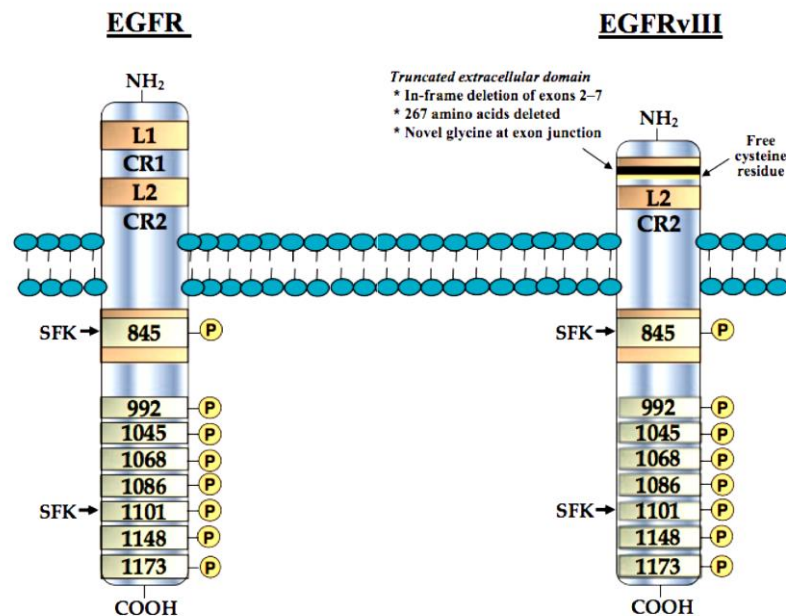


Figure 7.2 Schematic representation of the EGFR structure and its mutated variant. Compared with the wild-type EGFR, the mutated variant has a glycine residue inserted at the junction site and a shorter ECD because of the in-frame deletion of exons 2-7. The resultant mutated (truncated) variant is continuously active and cannot bind to any known EGF-ligand. The only conserved regions of the mutated EGFRvIII are the juxtamembrane and the intracellular regions. L1 and L2 are ligand-binding domains (also known as domains 1 and 3, respectively); CR1 and CR2 are cysteine-rich domains (known as domains 2 and 4, respectively); COOH: carboxy terminus; NH₂: amino terminus; SFK: Src family kinase. The figure is modified from (Gan et al., 2013).

For diagnostic applications, it is important to develop a novel reagent for use in different diagnostic applications which offers similar detection quality to that of the conventional full-length antibodies. Chapter 5 describes the evaluation of different modification strategies in order to generate optimal Affimer-based detection reagents that can be applied in the most commonly used diagnostic test, which is the IHC assay. We conclude that the best way to create such reagents is by the fusion of Affimers to the Fc-fragment, as this fusion provides the desired analytical sensitivity and signal amplification through the use of polymer-based commercial kits. However, during the research, this concept was examined with one Affimer only (anti-VEGFR2 Affimer). Therefore, the obtained results cannot be generalised to the Affimer scaffold prior to the development of different Fc-fusions and the examination of their applicability in the staining of different targets in IHC. As three anti-EGFR Affimers showed promising binding to the receptors on cells and in cell lysate according to the IF and pull-down assay results presented in Chapter 4, it would be advantageous to fuse the three EGFR-binding Affimers to the Fc-fragment and test them on IHC. These fusions would be the first non-antibody alternatives developed against the EGFR-ECD.

7.4.5. Application of Affimer technology to biomarker discovery

In this research, we examined the potential of Affimer-based phage technology to be used as a tool to enable the discovery of new cancer-related biomarkers and develop novel binding reagents against them. By selecting the Affimer library on fixed monolayers of MDA-MB-453 cells, we isolated novel reagents against CK19 and CK18/8 and we showed that, as with other cytoplasmic proteins, cytokeratin filamentous protein could translocate to the plasma membrane to stabilise the membrane receptors, such as HER2, and maintain the survival mechanism required for cancer-cell proliferation as previously described (Alix-Panabieres et al., 2009; Ju et al., 2015; Ju et al., 2013; Ohtsuka et al., 2016; Saha et al., 2017; Saha et al., 2018). All these studies showed the importance of CK19 or CK18 as diagnostic biomarkers that enabled improved stratification of cancer types to subtypes. However, their prognostic role remains controversial and requires further exploration. The next stage to follow the research explained in this thesis would be to use the developed CK binders as detection reagents and stain multiple TMAs in order to correlate the expression levels of the CKs in different histological subtypes of

breast tumours with the pathological, clinical and five-year survival data of patients and to compare the results with the matched normal samples.

Furthermore, other studies have suggested that targeting CK19 in HER2-resistant tumours may provide new therapeutic routes to treat tumours that overexpress HER2 and display resistance to both chemotherapeutic and personalised monoclonal antibodies (trastuzumab). To our knowledge, targeting CK19 remains a hypothesis and has not been tested with either antibodies or other non-antibody alternative scaffolds. Thus, performance of a cell proliferation assay by use of the novel CK-binding Affimers would clarify the suggested hypothesis and further explore the potential of the Affimers. However, prior to the start of performing a cell proliferation assay, we aimed to study the cellular behaviour of cells that showed both CK19 overexpression and CK19 knocked down to examine further the biological importance of these CK filamentous proteins in cancer proliferation and metastasis properties. These biological studies could be achieved *in vivo* and *in vitro*.

Production of an X-ray crystal structure of the CK19/18-Affimer complex would be the final step towards completion of research related to CK proteins, after the exploration of the biological significance of the CK protein and examination of the potential of the generated CK-binding Affimer. To date no crystal structure has been elucidated for CK19 or CK18 filaments. Revelation of the crystal structure of the filament could be challenging, but it would represent an important source for improved understanding of the protein biology. To achieve successful results in crystallisation of such a complex, the CK protein and the Affimer-CK complex could be prepared as described in the actin crystallisation study (Graceffa and Dominguez, 2003).

The cell-based screen on a fixed monolayer of MDA-MB-453 breast-cancer cell line through use of the naïve Affimer library (Ella2) resulted in the isolation of novel cytokeratin binding reagents. Therefore, we aimed to repeat the selection strategy by use of two different non-tumorigenic breast cell lines (such as HB2 and MCF-10A) and five different breast cancerous cell lines, such as SKBR3, MDA-MB-231, MCF7, MDA-MB-468 and BT474, which would represent the different subtypes of breast cancer in one screen. The reason for the incorporation of different cell lines in one screen is based on the heterogeneous nature of breast tumours, which result in different molecular profiles as reported previously (Ziegler et al., 2014). The reported data presented the differences in the expression profiles of plasma-membrane proteins, in which some cell lines showed

higher numbers of the total proteins expressed on the plasma membrane compared with other cells. This population increase could have represented a diverse profile in which some proteins were expressed in some cell lines but not in others, or an increase in expression of an individual protein (overexpression of a single protein, such as HER2 in SKBR3). The study also suggested that MCF-10A could be the optimal cell line to serve as a normal counterpart of the cancerous cell lines instead of the HB2 cell line we employed in our screen that involved the fixed monolayer of MDA-MB-453 cells. This was because MCF-10A expressed a comparable level of proteins in the plasma membrane, which could provide improved negative selection (depletion) of the shared antigens in both cancerous and normal tissues and thus increase the chance of identifying cancer-specific biomarkers.

In addition to studies related to breast cancer, we had the opportunity to collaborate with Dr. Sandra Bell who provided us with ovarian tissue sections (cancerous tissues of different histological grades and their matched normal tissues). The aim was to isolate cancer-specific Affimers against certain protein biomarkers expressed on cancer cells through use of the same cell-based phage-selection strategy applied to the MDA-MB-453 cell line and by following the previously described protocol in relation to specimen preparation for the phage screen (Wang et al., 2016). However, due to lack of time we were not able to pursue the aim of our collaboration. This collaboration could represent a new research line to help to generate novel reagents against specific cancer biomarkers in ovarian cancer. This cancer represents a gynaecological type of cancer with a high mortality rate and no known reliable biomarker that can aid in early diagnosis and the development of targeted therapy (Kozak et al., 2003; Terry et al., 2016). Therefore, the use of phage-selection technology with the Affimer library could provide a promising opportunity towards improved cancer diagnosis and progression towards drug development.

7.5 Conclusion

Affimers will add to the growing repertoire of next-generation's tools for detection, visualisation, and exploration of the function of antigens that are inaccessible to full-length antibodies. Due to their structural properties, high stability, and fast production, Affimers are seen as promising agents in basic research. In addition, their Fc-fusions and chemical functionalisation opens the way towards the generation of powerful reagents in

current diagnostic and future therapeutic applications. Furthermore, Affimer-phage display technology, coupled with pull-down assay, mass spectrometry analysis and other miniaturisation techniques, such as tissue microarrays validation studies can create a promising platform for biomarker discovery. Undoubtedly, in the upcoming years, new applications of Affimers, in disease diagnostics and therapeutics, will continue to surface.

References

- ACETO, N., DUSS, S., MACDONALD, G., MEYER, D. S., ROLOFF, T. C., HYNES, N. E. & BENTIRESLI, M. 2012. Co-expression of HER2 and HER3 receptor tyrosine kinases enhances invasion of breast cells via stimulation of interleukin-8 autocrine secretion. *Breast Cancer Res*, 14, R131.
- ADAM, P. J., BOYD, R., TYSON, K. L., FLETCHER, G. C., STAMPS, A., HUDSON, L., POYSER, H. R., REDPATH, N., GRIFFITHS, M., STEERS, G., HARRIS, A. L., PATEL, S., BERRY, J., LOADER, J. A., TOWNSEND, R. R., DAVIET, L., LEGRAIN, P., PAREKH, R. & TERRETT, J. A. 2003. Comprehensive proteomic analysis of breast cancer cell membranes reveals unique proteins with potential roles in clinical cancer. *J Biol Chem*, 278, 6482-9.
- ADAMS, G. P. & WEINER, L. M. 2005. Monoclonal antibody therapy of cancer. *Nat Biotechnol*, 23, 1147-57.
- AHN, S. G., YOON, C. I., LEE, J. H., LEE, H. S., PARK, S. E., CHA, Y. J., CHA, C., BAE, S. J., LEE, K. A. & JEONG, J. 2018. Low PR in ER(+)/HER2(-) breast cancer: high rates of TP53 mutation and high SUV. *Endocr Relat Cancer*.
- AHRAM, M. & PETRICOIN, E. F. 2008. Proteomics Discovery of Disease Biomarkers. *Biomark Insights*, 3, 325-333.
- AIAD, H. A., SAMAKA, R. M., ASAAD, N. Y., KANDIL, M. A., SHEHATA, M. A. & MILIGY, I. M. 2014. Relationship of CK8/18 expression pattern to breast cancer immunohistochemical subtyping in Egyptian patients. *Ecancermedicalscience*, 8, 404.
- AL-OGAIDI, I., GOU, H., AGUILAR, Z. P., GUO, S., MELCONIAN, A. K., AL-KAZAZ, A. K., MENG, F. & WU, N. 2014. Detection of the ovarian cancer biomarker CA-125 using chemiluminescence resonance energy transfer to graphene quantum dots. *Chem Commun (Camb)*, 50, 1344-6.
- ALBANELL, J., CODONY, J., ROVIRA, A., MELLADO, B. & GASCON, P. 2003. Mechanism of action of anti-HER2 monoclonal antibodies: scientific update on trastuzumab and 2C4. *Adv Exp Med Biol*, 532, 253-68.
- ALFALEH, M., JONES, M., HOWARD, C. & MAHLER, S. 2017. Strategies for Selecting Membrane Protein-Specific Antibodies using Phage Display with Cell-Based Panning. *Antibodies*, 6, 1-19.
- ALIX-PANABIÈRES, C. & PANTEL, K. 2014. Challenges in circulating tumour cell research. *Nat Rev Cancer*, 14, 623-31.
- ALIX-PANABIÈRES, C., VENDRELL, J. P., SLIJPER, M., PELLE, O., BARBOTTE, E., MERCIER, G., JACOT, W., FABBRO, M. & PANTEL, K. 2009. Full-length cytokeratin-19 is released by human tumor cells: a potential role in metastatic progression of breast cancer. *Breast Cancer Res*, 11, R39.
- ALLEGRA, A., INNAO, V., GERACE, D., VADDINELLI, D., ALLEGRA, A. G. & MUSOLINO, C. 2018. Nanobodies and Cancer: Current Status and New Perspectives. *Cancer Invest*, 36, 221-237.
- ALMENDRO, V., MARUSYK, A. & POLYAK, K. 2013. Cellular heterogeneity and molecular evolution in cancer. *Annu Rev Pathol*, 8, 277-302.
- ALT, K., PATERSON, B. M., WESTEIN, E., RUDD, S. E., PONIGER, S. S., JAGDALE, S., ARDIPRADJA, K., CONNELL, T. U., KRIPPNER, G. Y., NAIR, A. K., WANG, X., TOCHON-DANGUY, H. J., DONNELLY, P. S., PETER, K. & HAGEMEYER, C. E. 2015. A versatile approach for the site-specific modification of recombinant antibodies using a combination of enzyme-mediated bioconjugation and click chemistry. *Angew Chem Int Ed Engl*, 54, 7515-9.
- ANDERSEN, P. S., STRYHN, A., HANSEN, B. E., FUGGER, L., ENGBERG, J. & BUUS, S. 1996. A recombinant antibody with the antigen-specific, major histocompatibility complex-restricted specificity of T cells. *Proc Natl Acad Sci U S A*, 93, 1820-4.

- ANTONATOU, E., HOOGEWIJS, K., KALAITZAKIS, D., BAUDOT, A., VASSILIKOGIANNAKIS, G. & MADDER, A. 2016. Singlet Oxygen-Induced Furan Oxidation for Site-Specific and Chemoselective Peptide Ligation. *Chemistry*, 22, 8457-61.
- ARORA, A. & SCHOLAR, E. M. 2005. Role of tyrosine kinase inhibitors in cancer therapy. *J Pharmacol Exp Ther*, 315, 971-9.
- ARPINO, G., MILANO, M. & DE PLACIDO, S. 2015. Features of aggressive breast cancer. *Breast*, 24, 594-600.
- ARTEAGA, C. 2003. Targeting HER1/EGFR: a molecular approach to cancer therapy. *Semin Oncol*, 30, 3-14.
- ATTA, H. M. 1999. Edwin Smith Surgical Papyrus: the oldest known surgical treatise. *Am Surg*, 65, 1190-2.
- ATTARWALA, H. 2010. Role of antibodies in cancer targeting. *J Nat Sci Biol Med*, 1, 53-6.
- AYOUBI, T. A., MEULEMANS, S. M., ROEBROEK, A. J. & VAN DE VEN, W. J. 1996. Production of recombinant proteins in Chinese hamster ovary cells overexpressing the subtilisin-like proprotein converting enzyme furin. *Mol Biol Rep*, 23, 87-95.
- BADAWI, A. 2017. The Potential of Omics Technologies in Lyme Disease Biomarker Discovery and Early Detection. *Infect Dis Ther*, 6, 85-102.
- BADR, L. K., BOURDEANU, L., ALATRASH, M. & BEKARIAN, G. 2018. Breast Cancer Risk Factors: a Cross- Cultural Comparison between the West and the East. *Asian Pac J Cancer Prev*, 19, 2109-2116.
- BAKHSHINEJAD, B., ZADE, H. M., SHEKARABI, H. S. & NEMAN, S. 2016. Phage display biopanning and isolation of target-unrelated peptides: in search of nonspecific binders hidden in a combinatorial library. *Amino Acids*, 48, 2699-2716.
- BALBAS, P. 2001. Understanding the art of producing protein and nonprotein molecules in Escherichia coli. *Mol Biotechnol*, 19, 251-67.
- BAO, J., WOLPOWITZ, D., ROLE, L. W. & TALMAGE, D. A. 2003. Back signaling by the Nrg-1 intracellular domain. *J Cell Biol*, 161, 1133-41.
- BASELGA, J., ALBANELL, J., MOLINA, M. A. & ARRIBAS, J. 2001. Mechanism of action of trastuzumab and scientific update. *Semin Oncol*, 28, 4-11.
- BASELGA, J., CORTES, J., KIM, S. B., IM, S. A., HEGG, R., IM, Y. H., ROMAN, L., PEDRINI, J. L., PIENKOWSKI, T., KNOTT, A., CLARK, E., BENYUNES, M. C., ROSS, G., SWAIN, S. M. & GROUP, C. S. 2012. Pertuzumab plus trastuzumab plus docetaxel for metastatic breast cancer. *N Engl J Med*, 366, 109-19.
- BASELGA, J. & SWAIN, S. M. 2009. Novel anticancer targets: revisiting ERBB2 and discovering ERBB3. *Nat Rev Cancer*, 9, 463-75.
- BAST, R. C., JR. 2010. CA 125 and the detection of recurrent ovarian cancer: a reasonably accurate biomarker for a difficult disease. *Cancer*, 116, 2850-3.
- BAUM, R. P., PRASAD, V., MULLER, D., SCHUCHARDT, C., ORLOVA, A., WENNBORG, A., TOLMACHEV, V. & FELDWISCH, J. 2010. Molecular imaging of HER2-expressing malignant tumors in breast cancer patients using synthetic ¹¹¹In- or ⁶⁸Ga-labeled affibody molecules. *J Nucl Med*, 51, 892-7.
- BAYAT, P., NOSRATI, R., ALIBOLANDI, M., RAFATPANAHI, H., ABNOUS, K., KHEDRI, M. & RAMEZANI, M. 2018. SELEX methods on the road to protein targeting with nucleic acid aptamers. *Biochimie*, 154, 132-155.
- BAYELE, H. K., CHITI, A., COLINA, R., FERNANDES, O., KHAN, B., KRISHNAMOORTHY, R., OZDAG, H. & PADUA, R. A. 2010. Isotopic biomarker discovery and application in translational medicine. *Drug Discov Today*, 15, 127-36.
- BEBENEK, A. & ZIUZIA-GRACZYK, I. 2018. Fidelity of DNA replication-a matter of proofreading. *Curr Genet*, 64, 985-996.
- BEDFORD, R., TIEDE, C., HUGHES, R., CURD, A., MCPHERSON, M. J., PECKHAM, M. & TOMLINSON, D. C. 2017. Alternative reagents to antibodies in imaging applications. *Biophys Rev*.
- BENETKIEWICZ, M., PIOTROWSKI, A., DIAZ DE STAHL, T., JANKOWSKI, M., BALA, D., HOFFMAN, J., SRUTEK, E., LASKOWSKI, R., ZEGARSKI, W. & DUMANSKI, J. P. 2006. Chromosome 22

- array-CGH profiling of breast cancer delimited minimal common regions of genomic imbalances and revealed frequent intra-tumoral genetic heterogeneity. *Int J Oncol*, 29, 935-45.
- BEREZOVSKY, I. N. & BASTOLLA, U. 2017. Editorial overview: Proteins: bridging theory and experiment. *Curr Opin Struct Biol*, 42, viii-x.
- BESTE, G., SCHMIDT, F. S., STIBORA, T. & SKERRA, A. 1999. Small antibody-like proteins with prescribed ligand specificities derived from the lipocalin fold. *Proc Natl Acad Sci U S A*, 96, 1898-903.
- BINZ, H. K., AMSTUTZ, P., KOHL, A., STUMPP, M. T., BRIAND, C., FORRER, P., GRUTTER, M. G. & PLUCKTHUN, A. 2004. High-affinity binders selected from designed ankyrin repeat protein libraries. *Nat Biotechnol*, 22, 575-82.
- BINZ, H. K., STUMPP, M. T., FORRER, P., AMSTUTZ, P. & PLUCKTHUN, A. 2003. Designing repeat proteins: well-expressed, soluble and stable proteins from combinatorial libraries of consensus ankyrin repeat proteins. *J Mol Biol*, 332, 489-503.
- BOBKOV, V., ZARCA, A. M., VAN HOUT, A., ARIMONT, M., DOIJEN, J., BIALKOWSKA, M., TOFFOLI, E., KLARENBECK, A., VAN DER WONING, B., VAN DER VLIET, H. J., VAN LOY, T., DE HAARD, H., SCHOLS, D., HEUKERS, R. & SMIT, M. J. 2018. Nanobody-Fc constructs targeting chemokine receptor CXCR4 potently inhibit signaling and CXCR4-mediated HIV-entry and induce antibody effector functions. *Biochem Pharmacol*, 158, 413-424.
- BOERSMA, Y. L., CHAO, G., STEINER, D., WITTRUP, K. D. & PLUCKTHUN, A. 2011. Bispecific designed ankyrin repeat proteins (DARPin) targeting epidermal growth factor receptor inhibit A431 cell proliferation and receptor recycling. *J Biol Chem*, 286, 41273-85.
- BONNER, J. A., HARARI, P. M., GIRALT, J., COHEN, R. B., JONES, C. U., SUR, R. K., RABEN, D., BASELGA, J., SPENCER, S. A., ZHU, J., YOUSOUFIAN, H., ROWINSKY, E. K. & ANG, K. K. 2010. Radiotherapy plus cetuximab for locoregionally advanced head and neck cancer: 5-year survival data from a phase 3 randomised trial, and relation between cetuximab-induced rash and survival. *Lancet Oncol*, 11, 21-8.
- BOSRON, W. F., ANDERSON, R. A., FALK, M. C., KENNEDY, F. S. & VALLEE, B. L. 1977. Effect of magnesium on the properties of zinc alkaline phosphatase. *Biochemistry*, 16, 610-4.
- BOULANGER, R. R., JR. & KANTROWITZ, E. R. 2003. Characterization of a monomeric Escherichia coli alkaline phosphatase formed upon a single amino acid substitution. *J Biol Chem*, 278, 23497-501.
- BOUTUREIRA, O. & BERNARDES, G. J. 2015. Advances in chemical protein modification. *Chem Rev*, 115, 2174-95.
- BRADDOCK, M. 2007. 11th annual Inflammatory and Immune Diseases Drug Discovery and Development Summit 12-13 March 2007, San Francisco, USA. *Expert Opin Investig Drugs*, 16, 909-17.
- BRAGULLA, H. H. & HOMBERGER, D. G. 2009. Structure and functions of keratin proteins in simple, stratified, keratinized and cornified epithelia. *J Anat*, 214, 516-59.
- BRASHER, B. B., ROUMIANTSEV, S. & VAN ETTEN, R. A. 2001. Mutational analysis of the regulatory function of the c-Abl Src homology 3 domain. *Oncogene*, 20, 7744-52.
- BREMBECK, F. H. & RUSTGI, A. K. 2000. The tissue-dependent keratin 19 gene transcription is regulated by GKLf/KLF4 and Sp1. *J Biol Chem*, 275, 28230-9.
- BROWN, K. C. 2000. New approaches for cell-specific targeting: identification of cell-selective peptides from combinatorial libraries. *Curr Opin Chem Biol*, 4, 16-21.
- BROWNE, C. A. 1991. Epidermal growth factor and transforming growth factor alpha. *Baillieres Clin Endocrinol Metab*, 5, 553-69.
- BRUNO, J. G., CARRILLO, M. P. & PHILLIPS, T. 2008. Development of DNA aptamers to a foot-and-mouth disease peptide for competitive FRET-based detection. *J Biomol Tech*, 19, 109-15.
- BUICK, R. N., FILMUS, J. & CHURCH, J. 1990. Studies of EGF-mediated growth control and signal transduction using the MDA-MB-468 human breast cancer cell line. *Prog Clin Biol Res*, 354A, 179-91.

- BULLINGER, D., NEUBAUER, H., FEHM, T., LAUFER, S., GLEITER, C. H. & KAMMERER, B. 2007. Metabolic signature of breast cancer cell line MCF-7: profiling of modified nucleosides via LC-IT MS coupling. *BMC Biochem*, 8, 25.
- BUSSOLATI, G. & RADULESCU, R. T. 2011. Blocking endogenous peroxidases in immunohistochemistry: a mandatory, yet also subtle measure. *Appl Immunohistochem Mol Morphol*, 19, 484.
- BYLA, P., ANDERSEN, M. H., HOLTET, T. L., JACOBSEN, H., MUNCH, M., GAD, H. H., THOGERSEN, H. C. & HARTMANN, R. 2010. Selection of a novel and highly specific tumor necrosis factor alpha (TNFalpha) antagonist: insight from the crystal structure of the antagonist-TNFalpha complex. *J Biol Chem*, 285, 12096-100.
- CALMETTES, C., MOUKHTAR, M. S. & MILHAUD, G. 1979. [Tumours markers. Calcitonin and carcinoembryonic antigen in medullary carcinoma of the thyroid (author's transl)]. *Presse Med*, 8, 3947-50.
- CAMPOCHIARO, P. A., CHANNA, R., BERGER, B. B., HEIER, J. S., BROWN, D. M., FIEDLER, U., HEPP, J. & STUMPP, M. T. 2013. Treatment of diabetic macular edema with a designed ankyrin repeat protein that binds vascular endothelial growth factor: a phase I/II study. *Am J Ophthalmol*, 155, 697-704, 704 e1-2.
- CANCER GENOME ATLAS, N. 2012. Comprehensive molecular portraits of human breast tumours. *Nature*, 490, 61-70.
- CHAMES, P., VAN REGENMORTEL, M., WEISS, E. & BATY, D. 2009. Therapeutic antibodies: successes, limitations and hopes for the future. *Br J Pharmacol*, 157, 220-33.
- CHAN, C. E., LIM, A. P., MACARY, P. A. & HANSON, B. J. 2014. The role of phage display in therapeutic antibody discovery. *Int Immunol*, 26, 649-57.
- CHAN, P. P., WASINGER, V. C. & LEONG, R. W. 2016. Current application of proteomics in biomarker discovery for inflammatory bowel disease. *World J Gastrointest Pathophysiol*, 7, 27-37.
- CHEN, X., ZARO, J. L. & SHEN, W. C. 2013. Fusion protein linkers: property, design and functionality. *Adv Drug Deliv Rev*, 65, 1357-69.
- CHIARELLA, P. & FAZIO, V. M. 2008. Mouse monoclonal antibodies in biological research: strategies for high-throughput production. *Biotechnol Lett*, 30, 1303-10.
- CHIDA, K. 1993. Immunohistochemical detection of alkaline phosphatase in formalin-fixed and paraffin-embedded rat liver. *Okajimas Folia Anat Jpn*, 70, 151-5.
- CHIRCOP, M. & SPEIDEL, D. 2014. Cellular stress responses in cancer and cancer therapy. *Front Oncol*, 4, 304.
- CHISTIakov, D. A., CHEKHONIN, I. V. & CHEKHONIN, V. P. 2017. The EGFR variant III mutant as a target for immunotherapy of glioblastoma multiforme. *Eur J Pharmacol*, 810, 70-82.
- CITRI, A., SKARIA, K. B. & YARDEN, Y. 2003. The deaf and the dumb: the biology of ErbB-2 and ErbB-3. *Exp Cell Res*, 284, 54-65.
- CLAUS, J., PATEL, G., AUTORE, F., COLOMBA, A., WEITSMAN, G., SOLIMAN, T. N., ROBERTS, S., ZANETTI-DOMINGUES, L. C., HIRSCH, M., COLLU, F., GEORGE, R., ORTIZ-ZAPATER, E., BARBER, P. R., VOJNOVIC, B., YARDEN, Y., MARTIN-FERNANDEZ, M. L., CAMERON, A., FRATERNALI, F., NG, T. & PARKER, P. J. 2018. Inhibitor-induced HER2-HER3 heterodimerisation promotes proliferation through a novel dimer interface. *Elife*, 7.
- CLELAND, J. L., LAM, X., KENDRICK, B., YANG, J., YANG, T. H., OVERCASHIER, D., BROOKS, D., HSU, C. & CARPENTER, J. F. 2001. A specific molar ratio of stabilizer to protein is required for storage stability of a lyophilized monoclonal antibody. *J Pharm Sci*, 90, 310-21.
- COHEN, S., CARPENTER, G. & KING, L., JR. 1981. Epidermal growth factor-receptor-protein kinase interactions. *Prog Clin Biol Res*, 66 Pt A, 557-67.
- COLAS, P., COHEN, B., JESSEN, T., GRISHINA, I., MCCOY, J. & BRENT, R. 1996. Genetic selection of peptide aptamers that recognize and inhibit cyclin-dependent kinase 2. *Nature*, 380, 548-50.

- COLLINS, D. C., SUNDAR, R., LIM, J. S. J. & YAP, T. A. 2017. Towards Precision Medicine in the Clinic: From Biomarker Discovery to Novel Therapeutics. *Trends Pharmacol Sci*, 38, 25-40.
- CONSORTIUM, E. P. 2012. An integrated encyclopedia of DNA elements in the human genome. *Nature*, 489, 57-74.
- CORREA, C. R., BERTOLLO, C. M. & GOES, A. M. 2009. Establishment and characterization of MACL-1 and MGSO-3 cell lines derived from human primary breast cancer. *Oncol Res*, 17, 473-82.
- CREIGHTON, C. J., MASSARWEH, S., HUANG, S., TSIMELZON, A., HILSENBECK, S. G., OSBORNE, C. K., SHOU, J., MALORNI, L. & SCHIFF, R. 2008. Development of resistance to targeted therapies transforms the clinically associated molecular profile subtype of breast tumor xenografts. *Cancer Res*, 68, 7493-501.
- CREPIN, R., VEGGIANI, G., DJENDER, S., BEUGNET, A., PLANEIX, F., PICHON, C., MOUTEL, S., AMIGORENA, S., PEREZ, F., GHINEA, N. & DE MARCO, A. 2017. Whole-cell biopanning with a synthetic phage display library of nanobodies enabled the recovery of follicle-stimulating hormone receptor inhibitors. *Biochem Biophys Res Commun*, 493, 1567-1572.
- CROCE, C. M., ZHANG, K. & WEI, Y. Q. 2016. Announcing Signal Transduction and Targeted Therapy. *Signal Transduct Target Ther*, 1, 15006.
- CROSWELL, J. M., KRAMER, B. S., KREIMER, A. R., PROROK, P. C., XU, J. L., BAKER, S. G., FAGERSTROM, R., RILEY, T. L., CLAPP, J. D., BERG, C. D., GOHAGAN, J. K., ANDRIOLE, G. L., CHIA, D., CHURCH, T. R., CRAWFORD, E. D., FOUAD, M. N., GELMANN, E. P., LAMERATO, L., REDING, D. J. & SCHOEN, R. E. 2009. Cumulative incidence of false-positive results in repeated, multimodal cancer screening. *Ann Fam Med*, 7, 212-22.
- CUNNINGHAM, M. P., ESSAPEN, S., THOMAS, H., GREEN, M., LOVELL, D. P., TOPHAM, C., MARKS, C. & MODJTAHEDI, H. 2005. Coexpression, prognostic significance and predictive value of EGFR, EGFRvIII and phosphorylated EGFR in colorectal cancer. *Int J Oncol*, 27, 317-25.
- CURRAN, K. J., PEGRAM, H. J. & BRENTJENS, R. J. 2012. Chimeric antigen receptors for T cell immunotherapy: current understanding and future directions. *J Gene Med*, 14, 405-15.
- CURRID, C. A. & GALLAGHER, W. M. 2008. Selected highlights of the Third Annual Biomarkers Congress: from discovery to validation in the drug development arena. *Expert Opin Med Diagn*, 2, 1091-4.
- CYRANKA-CZAJA, A. & OTLEWSKI, J. 2012. A novel, stable, helical scaffold as an alternative binder - construction of phage display libraries. *Acta Biochim Pol*, 59, 383-90.
- CZAJKOWSKY, D. M., HU, J., SHAO, Z. & PLEASS, R. J. 2012. Fc-fusion proteins: new developments and future perspectives. *EMBO Mol Med*, 4, 1015-28.
- DAIRKEE, S. & HEID, H. W. 1993. Cytokeratin profile of immunomagnetically separated epithelial subsets of the human mammary gland. *In Vitro Cell Dev Biol Anim*, 29A, 427-32.
- DARMANIS, S., NONG, R. Y., HAMMOND, M., GU, J., ALDERBORN, A., VANELID, J., SIEGBAHN, A., GUSTAFSDOTTIR, S., ERICSSON, O., LANDEGREN, U. & KAMALI-MOGHADDAM, M. 2010. Sensitive plasma protein analysis by microparticle-based proximity ligation assays. *Mol Cell Proteomics*, 9, 327-35.
- DAUGHERTY, P. S. 2007. Protein engineering with bacterial display. *Curr Opin Struct Biol*, 17, 474-80.
- DE MELO GAGLIATO, D., JARDIM, D. L., MARCHESI, M. S. & HORTOBAGYI, G. N. 2016. Mechanisms of resistance and sensitivity to anti-HER2 therapies in HER2+ breast cancer. *Oncotarget*, 7, 64431-64446.
- DHAWAN, S. 2006. Signal amplification systems in immunoassays: implications for clinical diagnostics. *Expert Rev Mol Diagn*, 6, 749-60.
- DI FIORE, P. P. P. J. H. K. M. H. S. O. K. C. R., ; AND AARONSON S.A. 1987. erbB-2 is a potent oncogene when overexpressed in NIH/3T3 cells. *Science*, 10, 178-182.

- DIETEL, E., BROBEIL, A., TAG, C., GATTENLOEHNER, S. & WIMMER, M. 2018. Effectiveness of EGFR/HER2-targeted drugs is influenced by the downstream interaction shifts of PTPIP51 in HER2-amplified breast cancer cells. *Oncogenesis*, 7, 64.
- DINE, J., GORDON, R., SHAMES, Y., KASLER, M. K. & BARTON-BURKE, M. 2017. Immune Checkpoint Inhibitors: An Innovation in Immunotherapy for the Treatment and Management of Patients with Cancer. *Asia Pac J Oncol Nurs*, 4, 127-135.
- DIVGI, C. 1995. Radiolabelled Monoclonal Antibody Imaging in Cancer. *Clinical Immunotherapeutics*, 3, 218-226.
- DOWNWARD, J. 2004. PI 3-kinase, Akt and cell survival. *Semin Cell Dev Biol*, 15, 177-82.
- DREBIN, J. A., LINK, V. C., STERN, D. F., WEINBERG, R. A. & GREENE, M. I. 1985. Down-modulation of an oncogene protein product and reversion of the transformed phenotype by monoclonal antibodies. *Cell*, 41, 697-706.
- DRUCKER, E. & KRAPFENBAUER, K. 2013. Pitfalls and limitations in translation from biomarker discovery to clinical utility in predictive and personalised medicine. *EPMA J*, 4, 7.
- DUAN, Z. & SIEGUMFELDT, H. 2010. An efficient method for isolating antibody fragments against small peptides by antibody phage display. *Comb Chem High Throughput Screen*, 13, 818-28.
- DUFFY, M. J., O'DONOVAN, N. & CROWN, J. 2011. Use of molecular markers for predicting therapy response in cancer patients. *Cancer Treat Rev*, 37, 151-9.
- DUQUESNE, K., PRIMA, V. & STURGIS, J. N. 2016. Membrane Protein Solubilization and Composition of Protein Detergent Complexes. *Methods Mol Biol*, 1432, 243-60.
- DUQUESNE, K. & STURGIS, J. N. 2010. Membrane protein solubilization. *Methods Mol Biol*, 601, 205-17.
- DURAIYAN, J., GOVINDARAJAN, R., KALIYAPPAN, K. & PALANISAMY, M. 2012. Applications of immunohistochemistry. *J Pharm Bioallied Sci*, 4, S307-9.
- EBERSBACH, H., FIEDLER, E., SCHEUERMANN, T., FIEDLER, M., STUBBS, M. T., REIMANN, C., PROETZEL, G., RUDOLPH, R. & FIEDLER, U. 2007. Affilin-novel binding molecules based on human gamma-B-crystallin, an all beta-sheet protein. *J Mol Biol*, 372, 172-85.
- EGGENSTEIN, E., EICHINGER, A., KIM, H. J. & SKERRA, A. 2014. Structure-guided engineering of Anticalins with improved binding behavior and biochemical characteristics for application in radio-immuno imaging and/or therapy. *J Struct Biol*, 185, 203-14.
- EL-SALAHY, E. M. 2002. Evaluation of cytokeratin-19 & cytokeratin-20 and interleukin-6 in Egyptian bladder cancer patients. *Clin Biochem*, 35, 607-13.
- EMDE, B., HEINEN, A., GODECKE, A. & BOTTERMANN, K. 2014. Wheat germ agglutinin staining as a suitable method for detection and quantification of fibrosis in cardiac tissue after myocardial infarction. *Eur J Histochem*, 58, 2448.
- ENSINGER, C. & STERLACCI, W. 2008. Implications of EGFR PharmDx kit for cetuximab eligibility. *Expert Rev Mol Diagn*, 8, 141-8.
- ERKILIC, S. & KOCER, N. E. 2005. The role of cytokeratin 19 in the differential diagnosis of true papillary carcinoma of thyroid and papillary carcinoma-like changes in Graves' disease. *Endocr Pathol*, 16, 63-6.
- ERLER, J. T. & LINDING, R. 2010. Network-based drugs and biomarkers. *J Pathol*, 220, 290-6.
- FACCHINETTI, F., PROTO, C., MINARI, R., GARASSINO, M. & TISEO, M. 2018. Mechanisms of Resistance to Target Therapies in Non-small Cell Lung Cancer. *Handb Exp Pharmacol*, 249, 63-89.
- FAGET, L. & HNASKO, T. S. 2015. Tyramide Signal Amplification for Immunofluorescent Enhancement. *Methods Mol Biol*, 1318, 161-72.
- FALCHOOK, G. S., JANKU, F., TSAO, A. S., BASTIDA, C. C., STEWART, D. J. & KURZROCK, R. 2013. Non-small-cell lung cancer with HER2 exon 20 mutation: regression with dual HER2 inhibition and anti-VEGF combination treatment. *J Thorac Oncol*, 8, e19-20.
- FALLS, D. L. 2003. Neuregulins: functions, forms, and signaling strategies. *Exp Cell Res*, 284, 14-30.

- FARR, A. G. & NAKANE, P. K. 1981. Immunohistochemistry with enzyme labeled antibodies: a brief review. *J Immunol Methods*, 47, 129-44.
- FERGUSON, K. M., BERGER, M. B., MENDROLA, J. M., CHO, H. S., LEAHY, D. J. & LEMMON, M. A. 2003. EGF activates its receptor by removing interactions that autoinhibit ectodomain dimerization. *Mol Cell*, 11, 507-17.
- FERLAY, J., SHIN, H. R., BRAY, F., FORMAN, D., MATHERS, C. & PARKIN, D. M. 2010. Estimates of worldwide burden of cancer in 2008: GLOBOCAN 2008. *Int J Cancer*, 127, 2893-917.
- FERNANDEZ-CASTANE, A., VINE, C. E., CAMINAL, G. & LOPEZ-SANTIN, J. 2012. Evidencing the role of lactose permease in IPTG uptake by Escherichia coli in fed-batch high cell density cultures. *J Biotechnol*, 157, 391-8.
- FIGUEROA, J. A., VIGNESH, K. S., DEEPE, G. S., JR. & CARUSO, J. 2014. Selectivity and specificity of small molecule fluorescent dyes/probes used for the detection of Zn²⁺ and Ca²⁺ in cells. *Metallomics*, 6, 301-15.
- FINLAY, W. J., BLOOM, L., GRANT, J., FRANKLIN, E., SHUILLEABHAIN, D. N. & CUNNINGHAM, O. 2017. Phage Display: A Powerful Technology for the Generation of High-Specificity Affinity Reagents from Alternative Immune Sources. *Methods Mol Biol*, 1485, 85-99.
- FLEISCHMAN, M. L., CHUNG, J., PAUL, E. P. & LEWUS, R. A. 2017. Shipping-Induced Aggregation in Therapeutic Antibodies: Utilization of a Scale-Down Model to Assess Degradation in Monoclonal Antibodies. *J Pharm Sci*, 106, 994-1000.
- FRANKE, T. F., KAPLAN, D. R. & CANTLEY, L. C. 1997. PI3K: downstream AKTion blocks apoptosis. *Cell*, 88, 435-7.
- FRANKLIN, M. C., CAREY, K. D., VAJDOS, F. F., LEAHY, D. J., DE VOS, A. M. & SLIWKOWSKI, M. X. 2004. Insights into ErbB signaling from the structure of the ErbB2-pertuzumab complex. *Cancer Cell*, 5, 317-28.
- FREISE, A. C. & WU, A. M. 2015. In vivo imaging with antibodies and engineered fragments. *Mol Immunol*, 67, 142-52.
- FRENZEL, A., KUGLER, J., WILKE, S., SCHIRRMANN, T. & HUST, M. 2014. Construction of human antibody gene libraries and selection of antibodies by phage display. *Methods Mol Biol*, 1060, 215-43.
- FRIEDMAN, M., NORDBERG, E., HOIDEN-GUTHENBERG, I., BRISMAR, H., ADAMS, G. P., NILSSON, F. Y., CARLSSON, J. & STAHL, S. 2007. Phage display selection of Affibody molecules with specific binding to the extracellular domain of the epidermal growth factor receptor. *Protein Eng Des Sel*, 20, 189-99.
- FROGER, A. & HALL, J. E. 2007. Transformation of plasmid DNA into E. coli using the heat shock method. *J Vis Exp*, 253.
- FUTREAL, P. A., COIN, L., MARSHALL, M., DOWN, T., HUBBARD, T., WOOSTER, R., RAHMAN, N. & STRATTON, M. R. 2004. A census of human cancer genes. *Nat Rev Cancer*, 4, 177-83.
- GAI, S. A. & WITTRUP, K. D. 2007. Yeast surface display for protein engineering and characterization. *Curr Opin Struct Biol*, 17, 467-73.
- GAN, H. K., CVRLJEVIC, A. N. & JOHNS, T. G. 2013. The epidermal growth factor receptor variant III (EGFRvIII): where wild things are altered. *FEBS J*, 280, 5350-70.
- GAZDAR, A. F., SHIGEMATSU, H., HERZ, J. & MINNA, J. D. 2004. Mutations and addiction to EGFR: the Achilles 'heal' of lung cancers? *Trends Mol Med*, 10, 481-6.
- GEELEHER, P., COX, N. J. & HUANG, R. S. 2016. Cancer biomarker discovery is improved by accounting for variability in general levels of drug sensitivity in pre-clinical models. *Genome Biol*, 17, 190.
- GERARDUZZI, C., DE POLO, A., LIU, X. S., EL KHARBILI, M., LITTLE, J. B. & YUAN, Z. M. 2016. Human epidermal growth factor receptor 4 (Her4) Suppresses p53 Protein via Targeting the MDMX-MDM2 Protein Complex: IMPLICATION OF A NOVEL MDMX SER-314 PHOSPHOSITE. *J Biol Chem*, 291, 25937-25949.
- GETMANOVA, E. V., CHEN, Y., BLOOM, L., GOKEMEIJER, J., SHAMAH, S., WARIKOO, V., WANG, J., LING, V. & SUN, L. 2006. Antagonists to human and mouse vascular endothelial

- growth factor receptor 2 generated by directed protein evolution in vitro. *Chem Biol*, 13, 549-56.
- GETZ, E. B., XIAO, M., CHAKRABARTY, T., COOKE, R. & SELVIN, P. R. 1999. A comparison between the sulfhydryl reductants tris(2-carboxyethyl)phosphine and dithiothreitol for use in protein biochemistry. *Anal Biochem*, 273, 73-80.
- GEYER, C. R., MCCAFFERTY, J., DUBEL, S., BRADBURY, A. R. & SIDHU, S. S. 2012. Recombinant antibodies and in vitro selection technologies. *Methods Mol Biol*, 901, 11-32.
- GIJS, M., PENNER, G., BLACKLER, G. B., IMPENS, N. R., BAATOUT, S., LUXEN, A. & AERTS, A. M. 2016. Improved Aptamers for the Diagnosis and Potential Treatment of HER2-Positive Cancer. *Pharmaceuticals (Basel)*, 9.
- GILBERT, E. S. & MARKS, S. 1979. The nuclear worker and ionizing radiation. Bertell, Rosalie: (Am. Ind. Hyg. Assoc. J. 40:395 1979). *Am Ind Hyg Assoc J*, 40, 916-9.
- GILBRETH, R. N., ESAKI, K., KOIDE, A., SIDHU, S. S. & KOIDE, S. 2008. A dominant conformational role for amino acid diversity in minimalist protein-protein interfaces. *J Mol Biol*, 381, 407-18.
- GIOVANELLA, L., IMPERIALI, M. & TRIMBOLI, P. 2017. Role of serum cytokeratin 19 fragment (Cyfra 21.1) as a prognostic biomarker in patients with differentiated thyroid cancer. *Sci Rep*, 7, 7359.
- GLASSY, M. C. & GUPTA, R. 2014. Technical and ethical limitations in making human monoclonal antibodies (an overview). *Methods Mol Biol*, 1060, 9-36.
- GOLDSTEIN, R., SOSABOWSKI, J., LIVANOS, M., LEYTON, J., VIGOR, K., BHAVSAR, G., NAGY-DAVIDESCU, G., RASHID, M., MIRANDA, E., YEUNG, J., TOLNER, B., PLUCKTHUN, A., MATHER, S., MEYER, T. & CHESTER, K. 2015. Development of the designed ankyrin repeat protein (DARPin) G3 for HER2 molecular imaging. *Eur J Nucl Med Mol Imaging*, 42, 288-301.
- GONZALEZ, L. C. 2012. Protein microarrays, biosensors, and cell-based methods for secretome-wide extracellular protein-protein interaction mapping. *Methods*, 57, 448-58.
- GOOSSENS, N., NAKAGAWA, S., SUN, X. & HOSHIDA, Y. 2015. Cancer biomarker discovery and validation. *Transl Cancer Res*, 4, 256-269.
- GOSTRING, L., MALM, M., HOIDEN-GUTHENBERG, I., FREJD, F. Y., STAHL, S., LOFBLUM, J. & GEDDA, L. 2012. Cellular effects of HER3-specific affibody molecules. *PLoS One*, 7, e40023.
- GOWN, A. M. 2016. Diagnostic Immunohistochemistry: What Can Go Wrong and How to Prevent It. *Arch Pathol Lab Med*, 140, 893-8.
- GRACEFFA, P. & DOMINGUEZ, R. 2003. Crystal structure of monomeric actin in the ATP state. Structural basis of nucleotide-dependent actin dynamics. *J Biol Chem*, 278, 34172-80.
- GRAVALOS, C. & JIMENO, A. 2008. HER2 in gastric cancer: a new prognostic factor and a novel therapeutic target. *Ann Oncol*, 19, 1523-9.
- GRAVES, P. R., DIN, S. U., ASHAMALLA, M., ASHAMALLA, H., GILBERT, T. S. K. & GRAVES, L. M. 2017. Ionizing radiation induces EphA2 S897 phosphorylation in a MEK/ERK/RSK-dependent manner. *Int J Radiat Biol*, 93, 929-936.
- GUO, C., MANJILI, M. H., SUBJECK, J. R., SARKAR, D., FISHER, P. B. & WANG, X. Y. 2013. Therapeutic cancer vaccines: past, present, and future. *Adv Cancer Res*, 119, 421-75.
- GUO, S., CHEN, D., HUANG, X., CAI, J., WERY, J. P. & LI, Q. X. 2016. Cetuximab response in CRC patient-derived xenografts seems predicted by an expression based RAS pathway signature. *Oncotarget*, 7, 50575-50581.
- GUO, Y., DUAN, Z., JIA, Y., REN, C., LV, J., GUO, P., ZHAO, W., WANG, B., ZHANG, S., LI, Y. & LI, Z. 2018. HER4 isoform CYT2 and its ligand NRG1III are expressed at high levels in human colorectal cancer. *Oncol Lett*, 15, 6629-6635.
- GUREN, T. K., THOMSEN, M., KURE, E. H., SORBYE, H., GLIMELIUS, B., PFEIFFER, P., OSTERLUND, P., SIGURDSSON, F., LOTHE, I. M. B., DALSGAARD, A. M., SKOVLUND, E., CHRISTOFFERSEN, T. & TVEIT, K. M. 2017. Cetuximab in treatment of metastatic

- colorectal cancer: final survival analyses and extended RAS data from the NORDIC-VII study. *Br J Cancer*, 116, 1271-1278.
- GUSTERSON B., ROSS D., HEATH V. & STEINT. 2005. Basal cytokeratins and their relationship to the cellular origin and functional classification of breast cancer. *Breast Cancer Research*, 7, 143-148.
- GUTIERREZ-XICOTENCATL, L., PLETT-TORRES, T., MADRID-GONZALEZ, C. L. & MADRID-MARINA, V. 2009. Molecular diagnosis of human papillomavirus in the development of cervical cancer. *Salud Publica Mex*, 51 Suppl 3, S479-88.
- HA, J. H., KIM, J. E. & KIM, Y. S. 2016. Immunoglobulin Fc Heterodimer Platform Technology: From Design to Applications in Therapeutic Antibodies and Proteins. *Front Immunol*, 7, 394.
- HALFORD, S. E., LENNETTE, D. A. & SCHLESINGER, M. J. 1972. A mutationally altered alkaline phosphatase from *Escherichia coli*. II. Structural and catalytic properties of the activated enzyme. *J Biol Chem*, 247, 2095-101.
- HALL, A., HAKANSSON, K., MASON, R. W., GRUBB, A. & ABRAHAMSON, M. 1995. Structural basis for the biological specificity of cystatin C. Identification of leucine 9 in the N-terminal binding region as a selectivity-conferring residue in the inhibition of mammalian cysteine peptidases. *J Biol Chem*, 270, 5115-21.
- HALL, R. E., BIRRELL, S. N., TILLEY, W. D. & SUTHERLAND, R. L. 1994. MDA-MB-453, an androgen-responsive human breast carcinoma cell line with high level androgen receptor expression. *Eur J Cancer*, 30A, 484-90.
- HAMERS-CASTERMAN, C., ATARHOUCHE, T., MUYLDERMANS, S., ROBINSON, G., HAMERS, C., SONGA, E. B., BENDAHDAN, N. & HAMERS, R. 1993. Naturally occurring antibodies devoid of light chains. *Nature*, 363, 446-8.
- HAMMOND, G. W., AHLUWALIA, G. S., BARKER, F. G., HORSMAN, G. & HAZELTON, P. R. 1982. Comparison of direct and indirect enzyme immunoassays with direct ultracentrifugation before electron microscopy for detection of rotaviruses. *J Clin Microbiol*, 16, 53-9.
- HANAHAH, D. & WEINBERG, R. A. 2000. The hallmarks of cancer. *Cell*, 100, 57-70.
- HANAHAH, D. & WEINBERG, R. A. 2011. Hallmarks of cancer: the next generation. *Cell*, 144, 646-74.
- HANES, J., JERMUTUS, L., WEBER-BORNHAUSER, S., BOSSHARD, H. R. & PLUCKTHUN, A. 1998. Ribosome display efficiently selects and evolves high-affinity antibodies in vitro from immune libraries. *Proc Natl Acad Sci U S A*, 95, 14130-5.
- HANES, J., SCHAFFITZEL, C., KNAPPIK, A. & PLUCKTHUN, A. 2000. Picomolar affinity antibodies from a fully synthetic naive library selected and evolved by ribosome display. *Nat Biotechnol*, 18, 1287-92.
- HANNA, W., O'MALLEY F, P., BARNES, P., BERENDT, R., GABOURY, L., MAGLIOCCO, A., PETTIGREW, N., ROBERTSON, S., SENGUPTA, S., TETU, B. & THOMSON, T. 2007. Updated recommendations from the Canadian National Consensus Meeting on HER2/neu testing in breast cancer. *Curr Oncol*, 14, 149-53.
- HARLOW, E. & LANE, D. 2006. Labeling antibodies with biotin. *CSH Protoc*, 2006.
- HARPER, K., KERSCHBAUMER, R. J., ZIEGLER, A., MACINTOSH, S. M., COWAN, G. H., HIMMLER, G., MAYO, M. A. & TORRANCE, L. 1997. A scFv-alkaline phosphatase fusion protein which detects potato leafroll luteovirus in plant extracts by ELISA. *J Virol Methods*, 63, 237-42.
- HE, F., WOODS, C. E., TRILISKY, E., BOWER, K. M., LITOWSKI, J. R., KERWIN, B. A., BECKER, G. W., NARHI, L. O. & RAZINKOV, V. I. 2011. Screening of monoclonal antibody formulations based on high-throughput thermostability and viscosity measurements: design of experiment and statistical analysis. *J Pharm Sci*, 100, 1330-40.
- HEIDENREICH, A. & NITSCHMANN, S. 2010. [Impact of PSA screening on mortality. PLCO project team (prostate, lung, colorectal, ovarian cancer screening trial)]. *Internist (Berl)*, 51, 219-20.
- HENDRIKSEN, C. F. & DE LEEUW, W. 1998a. Production of monoclonal antibodies by the ascites method in laboratory animals. *Res Immunol*, 149, 535-42.

- HENDRIKSEN, C. F. & DE LEEUW, W. A. 1998b. In vivo and in vitro production of monoclonal antibodies: current possibilities and future perspectives. Discussion. *Res Immunol*, 149, 611-20.
- HENRIKSEN, L., GRANDAL, M. V., KNUDSEN, S. L., VAN DEURS, B. & GROVDAL, L. M. 2013. Internalization mechanisms of the epidermal growth factor receptor after activation with different ligands. *PLoS One*, 8, e58148.
- HENRY, N. L. & HAYES, D. F. 2012. Cancer biomarkers. *Mol Oncol*, 6, 140-6.
- HICKS, D. G. & KULKARNI, S. 2008. HER2+ breast cancer: review of biologic relevance and optimal use of diagnostic tools. *Am J Clin Pathol*, 129, 263-73.
- HIGASHI, H., SUGII, T. & KATO, S. 1988. Specific staining on thin-layer chromatograms of glycosphingolipids of neolacto series and gangliosides with a terminal N-acetylneuraminy residue by different procedures with wheat germ agglutinin. *Biochim Biophys Acta*, 963, 333-9.
- HOBOR, S., VAN EMBURGH, B. O., CROWLEY, E., MISALE, S., DI NICOLANTONIO, F. & BARDELLI, A. 2014. TGFalpha and amphiregulin paracrine network promotes resistance to EGFR blockade in colorectal cancer cells. *Clin Cancer Res*, 20, 6429-38.
- HOFFMANN, A., KOVERMANN, M., LILIE, H., FIEDLER, M., BALBACH, J., RUDOLPH, R. & PFEIFER, S. 2012. New binding mode to TNF-alpha revealed by ubiquitin-based artificial binding protein. *PLoS One*, 7, e31298.
- HOGBOM, M., EKLUND, M., NYGREN, P. A. & NORDLUND, P. 2003. Structural basis for recognition by an in vitro evolved affibody. *Proc Natl Acad Sci U S A*, 100, 3191-6.
- HOLBRO, T., BEERLI, R. R., MAURER, F., KOZICZAK, M., BARBAS, C. F., 3RD & HYNES, N. E. 2003. The ErbB2/ErbB3 heterodimer functions as an oncogenic unit: ErbB2 requires ErbB3 to drive breast tumor cell proliferation. *Proc Natl Acad Sci U S A*, 100, 8933-8.
- HOLLAND, R. L. 2016. What makes a good biomarker? *Advances in Precision Medicine*, 1, 4-11.
- HOLLIDAY, D. L. & SPEIRS, V. 2011. Choosing the right cell line for breast cancer research. *Breast Cancer Res*, 13, 215.
- HOLLIGER, P. & HUDSON, P. J. 2005. Engineered antibody fragments and the rise of single domains. *Nat Biotechnol*, 23, 1126-36.
- HONG, H., GOEL, S., ZHANG, Y. & CAI, W. 2011. Molecular imaging with nucleic acid aptamers. *Curr Med Chem*, 18, 4195-205.
- HOYER, W., GRONWALL, C., JONSSON, A., STAHL, S. & HARD, T. 2008. Stabilization of a beta-hairpin in monomeric Alzheimer's amyloid-beta peptide inhibits amyloid formation. *Proc Natl Acad Sci U S A*, 105, 5099-104.
- HUANG, G., ZHONG, Z., MIERSCH, S., SIDHU, S. S., HOU, S. C. & WU, D. 2018. Construction of Synthetic Phage Displayed Fab Library with Tailored Diversity. *J Vis Exp*.
- HUANG, R., KISS, M., BATONICK, M., WEINER, M. & KAY, B. 2016. Generating Recombinant Antibodies to Membrane Proteins through Phage Display. *Antibodies*, 5, 1-11.
- HUDELIST, G., PACHER-ZAVISIN, M., SINGER, C. F., HOLPER, T., KUBISTA, E., SCHREIBER, M., MANAVI, M., BILBAN, M. & CZERWENKA, K. 2004. Use of high-throughput protein array for profiling of differentially expressed proteins in normal and malignant breast tissue. *Breast Cancer Res Treat*, 86, 281-91.
- HUGHES, D. J., TIEDE, C., PENSWICK, N., TANG, A. A., TRINH, C. H., MANDAL, U., ZAJAC, K. Z., GAULE, T., HOWELL, G., EDWARDS, T. A., DUAN, J., FEYFANT, E., MCPHERSON, M. J., TOMLINSON, D. C. & WHITEHOUSE, A. 2017. Generation of specific inhibitors of SUMO-1- and SUMO-2/3-mediated protein-protein interactions using Affimer (Adhiron) technology. *Sci Signal*, 10.
- HUNG, M. C. & LINK, W. 2011. Protein localization in disease and therapy. *J Cell Sci*, 124, 3381-92.
- HUSAIN, B., PADUCHURI, S., RAMANI, S. R. & MARTINEZ-MARTIN, N. 2019. Extracellular Protein Microarray Technology for High Throughput Detection of Low Affinity Receptor-Ligand Interactions. *J Vis Exp*.

- HUSE, W. D., SASTRY, L., IVERSON, S. A., KANG, A. S., ALTING-MEES, M., BURTON, D. R., BENKOVIC, S. J. & LERNER, R. A. 1992. Generation of a large combinatorial library of the immunoglobulin repertoire in phage lambda. 1989. *Biotechnology*, 24, 517-23.
- HYATT, D. C. & CERESA, B. P. 2008. Cellular localization of the activated EGFR determines its effect on cell growth in MDA-MB-468 cells. *Exp Cell Res*, 314, 3415-25.
- HYNES, N. E. & MACDONALD, G. 2009. ErbB receptors and signaling pathways in cancer. *Curr Opin Cell Biol*, 21, 177-84.
- IKEDA, S., FUJIMORI, M., SHIBATA, S., OKAJIMA, M., ISHIZAKI, Y., KURIHARA, T., MIYATA, Y., ISEKI, M., SHIMIZU, Y., TOKUMOTO, N., OZAKI, S. & ASAHARA, T. 2006. Combined immunohistochemistry of beta-catenin, cytokeratin 7, and cytokeratin 20 is useful in discriminating primary lung adenocarcinomas from metastatic colorectal cancer. *BMC Cancer*, 6, 31.
- ILEANA DUMBRAVA, E., MERIC-BERNSTAM, F. & YAP, T. A. 2018. Challenges with biomarkers in cancer drug discovery and development. *Expert Opin Drug Discov*, 13, 685-690.
- INGVARSSON, J., WINGREN, C., CARLSSON, A., ELLMARK, P., WAHREN, B., ENGSTROM, G., HARMENBERG, U., KROGH, M., PETERSON, C. & BORREBAECK, C. A. 2008. Detection of pancreatic cancer using antibody microarray-based serum protein profiling. *Proteomics*, 8, 2211-9.
- ISAZA MEJIA, G., YEPES ZAPATA, G. & CASTANO, M. 1971. [Histological structure of the human placenta by phase contrast and clinical applications]. *Rev Colomb Obstet Ginecol*, 22, 19-24.
- IVELL, R., TEERDS, K. & HOFFMAN, G. E. 2014. Proper application of antibodies for immunohistochemical detection: antibody crimes and how to prevent them. *Endocrinology*, 155, 676-87.
- JACOB, W., JAMES, I., HASMANN, M. & WEISSER, M. 2018. Clinical development of HER3-targeting monoclonal antibodies: Perils and progress. *Cancer Treat Rev*, 68, 111-123.
- JACOBS, T. W., GOWN, A. M., YAZIJI, H., BARNES, M. J. & SCHNITT, S. J. 1999. Specificity of HercepTest in determining HER-2/neu status of breast cancers using the United States Food and Drug Administration-approved scoring system. *J Clin Oncol*, 17, 1983-7.
- JAIN, A., LIU, R., XIANG, Y. K. & HA, T. 2012. Single-molecule pull-down for studying protein interactions. *Nat Protoc*, 7, 445-52.
- JENISON, R. D., GILL, S. C., PARDI, A. & POLISKY, B. 1994. High-resolution molecular discrimination by RNA. *Science*, 263, 1425-9.
- JOHNSON, A., SONG, Q., KO FERRIGNO, P., BUENO, P. R. & DAVIS, J. J. 2012. Sensitive affimer and antibody based impedimetric label-free assays for C-reactive protein. *Anal Chem*, 84, 6553-60.
- JONES, F. E. 2008. HER4 intracellular domain (4ICD) activity in the developing mammary gland and breast cancer. *J Mammary Gland Biol Neoplasia*, 13, 247-58.
- JONES, M. L., ALFALEH, M. A., KUMBLE, S., ZHANG, S., OSBORNE, G. W., YEH, M., ARORA, N., HOU, J. J., HOWARD, C. B., CHIN, D. Y. & MAHLER, S. M. 2016. Targeting membrane proteins for antibody discovery using phage display. *Sci Rep*, 6, 26240.
- JOSEPHSON, K., RICARDO, A. & SZOSTAK, J. W. 2014. mRNA display: from basic principles to macrocycle drug discovery. *Drug Discov Today*, 19, 388-99.
- JU, J. H., OH, S., LEE, K. M., YANG, W., NAM, K. S., MOON, H. G., NOH, D. Y., KIM, C. G., PARK, G., PARK, J. B., LEE, T., ARTEAGA, C. L. & SHIN, I. 2015. Cytokeratin19 induced by HER2/ERK binds and stabilizes HER2 on cell membranes. *Cell Death Differ*, 22, 665-76.
- JU, J. H., YANG, W., LEE, K. M., OH, S., NAM, K., SHIM, S., SHIN, S. Y., GYE, M. C., CHU, I. S. & SHIN, I. 2013. Regulation of cell proliferation and migration by keratin19-induced nuclear import of early growth response-1 in breast cancer cells. *Clin Cancer Res*, 19, 4335-46.
- JUNGIC, S., TUBIC, B. & SKREPNIK, T. 2012. The role of biomarkers in the development of novel cancer therapies. *Drug Metabol Drug Interact*, 27, 89-99.
- JUNTILA, M. R. & DE SAUVAGE, F. J. 2013. Influence of tumour micro-environment heterogeneity on therapeutic response. *Nature*, 501, 346-54.

- KARANTZA, V. 2011. Keratins in health and cancer: more than mere epithelial cell markers. *Oncogene*, 30, 127-38.
- KASSIS, J., MOELLINGER, J., LO, H., GREENBERG, N. M., KIM, H. G. & WELLS, A. 1999. A role for phospholipase C-gamma-mediated signaling in tumor cell invasion. *Clin Cancer Res*, 5, 2251-60.
- KAUR, J., KUMAR, A. & KAUR, J. 2018. Strategies for optimization of heterologous protein expression in *E. coli*: Roadblocks and reinforcements. *Int J Biol Macromol*, 106, 803-822.
- KAVANAGH, D. O., CHAMBERS, G., O'GRADY, L., BARRY, K. M., WALDRON, R. P., BENNANI, F., EUSTACE, P. W. & TOBBIA, I. 2009. Is overexpression of HER-2 a predictor of prognosis in colorectal cancer? *BMC Cancer*, 9, 1.
- KAY, B. K., THAI, S. & VOLGINA, V. V. 2009. High-throughput biotinylation of proteins. *Methods Mol Biol*, 498, 185-96.
- KEEFE, A. D., PAI, S. & ELLINGTON, A. 2010. Aptamers as therapeutics. *Nat Rev Drug Discov*, 9, 537-50.
- KHAN, G. N., KIM, E. J., SHIN, T. S. & LEE, S. H. 2017. Heterogeneous Cell Types in Single-cell-derived Clones of MCF7 and MDA-MB-231 Cells. *Anticancer Res*, 37, 2343-2354.
- KIM, J. S., KIM, J. E., KIM, K., LEE, J., PARK, J. O., LIM, H. Y., PARK, Y. S., KANG, W. K. & KIM, S. T. 2017. The Impact of Cetuximab Plus AKT- or mTOR- Inhibitor in a Patient-Derived Colon Cancer Cell Model with Wild-Type RAS and PIK3CA Mutation. *J Cancer*, 8, 2713-2719.
- KIM, S. W., ROH, J. & PARK, C. S. 2016. Immunohistochemistry for Pathologists: Protocols, Pitfalls, and Tips. *J Pathol Transl Med*, 50, 411-418.
- KIM, T. K. & EBERWINE, J. H. 2010. Mammalian cell transfection: the present and the future. *Anal Bioanal Chem*, 397, 3173-8.
- KING, C. R., KRAUS, M. H. & AARONSON, S. A. 1985. Amplification of a novel v-erbB-related gene in a human mammary carcinoma. *Science*, 229, 974-6.
- KIPRIYANOV, S. M. & LE GALL, F. 2004. Generation and production of engineered antibodies. *Mol Biotechnol*, 26, 39-60.
- KNOWLES, H. J. & HARRIS, A. L. 2001. Hypoxia and oxidative stress in breast cancer. Hypoxia and tumorigenesis. *Breast Cancer Res*, 3, 318-22.
- KOHLER, A., LAURITZEN, B. & VAN NOORDEN, C. J. 2000. Signal amplification in immunohistochemistry at the light microscopic level using biotinylated tyramide and nanogold-silver staining. *J Histochem Cytochem*, 48, 933-41.
- KOHLER, G. & MILSTEIN, C. 2005. Continuous cultures of fused cells secreting antibody of predefined specificity. 1975. *J Immunol*, 174, 2453-5.
- KOHLER, H., SMYK, S. & KLUSKENS, L. 1975. Specific suppression by anti-binding site antibody. *Cell Immunol*, 17, 295-9.
- KOHN, K. W., JACKMAN, J. & O'CONNOR, P. M. 1994. Cell cycle control and cancer chemotherapy. *J Cell Biochem*, 54, 440-52.
- KOIDE, A., BAILEY, C. W., HUANG, X. & KOIDE, S. 1998. The fibronectin type III domain as a scaffold for novel binding proteins. *J Mol Biol*, 284, 1141-51.
- KOIDE, A., GILBRETH, R. N., ESAKI, K., TERESHKO, V. & KOIDE, S. 2007. High-affinity single-domain binding proteins with a binary-code interface. *Proc Natl Acad Sci U S A*, 104, 6632-7.
- KOIDE, A., WOJCIK, J., GILBRETH, R. N., HOEY, R. J. & KOIDE, S. 2012. Teaching an old scaffold new tricks: monobodies constructed using alternative surfaces of the FN3 scaffold. *J Mol Biol*, 415, 393-405.
- KOMATSU, M., YOSHIMARU, T., MATSUO, T., KIYOTANI, K., MIYOSHI, Y., TANAHASHI, T., ROKUTAN, K., YAMAGUCHI, R., SAITO, A., IMOTO, S., MIYANO, S., NAKAMURA, Y., SASA, M., SHIMADA, M. & KATAGIRI, T. 2013. Molecular features of triple negative breast cancer cells by genome-wide gene expression profiling analysis. *Int J Oncol*, 42, 478-506.
- KOOPMAN, T., VAN DER VEGT, B., DIJKSTRA, M., BART, J., DUIKER, E., WISMAN, G. B. A., DE BOCK, G. H. & HOLLEMA, H. 2018. HER2 immunohistochemistry in endometrial and ovarian clear cell carcinoma: discordance between antibodies and with in-situ hybridisation. *Histopathology*, 73, 852-863.

- KOSACKA, M. & JANKOWSKA, R. 2007. [The prognostic value of cytokeratin 19 expression in non-small cell lung cancer]. *Pneumonol Alergol Pol*, 75, 317-23.
- KOUTRAS, A. K., FOUNTZILAS, G., KALOGERAS, K. T., STARAKIS, I., ICONOMOU, G. & KALOFONOS, H. P. 2010. The upgraded role of HER3 and HER4 receptors in breast cancer. *Crit Rev Oncol Hematol*, 74, 73-8.
- KOZAK, K. R., AMNEUS, M. W., PUSEY, S. M., SU, F., LUONG, M. N., LUONG, S. A., REDDY, S. T. & FARIAS-EISNER, R. 2003. Identification of biomarkers for ovarian cancer using strong anion-exchange ProteinChips: potential use in diagnosis and prognosis. *Proc Natl Acad Sci U S A*, 100, 12343-8.
- KRAUS, V. B. 2018. Biomarkers as drug development tools: discovery, validation, qualification and use. *Nat Rev Rheumatol*, 14, 354-362.
- KRAUSE, D. S. & VAN ETEN, R. A. 2005. Tyrosine kinases as targets for cancer therapy. *N Engl J Med*, 353, 172-87.
- KRUSER, T. J. & WHEELER, D. L. 2010. Mechanisms of resistance to HER family targeting antibodies. *Exp Cell Res*, 316, 1083-100.
- KUAN, C. T., WIKSTRAND, C. J. & BIGNER, D. D. 2000. EGFRvIII as a promising target for antibody-based brain tumor therapy. *Brain Tumor Pathol*, 17, 71-8.
- KUBOTA, K. 2011. Recent advances and limitations of surgical treatment for pancreatic cancer. *World J Clin Oncol*, 2, 225-8.
- KULASINGAM, V. & DIAMANDIS, E. P. 2007. Proteomics analysis of conditioned media from three breast cancer cell lines: a mine for biomarkers and therapeutic targets. *Mol Cell Proteomics*, 6, 1997-2011.
- KUMAR, P. & AGGARWAL, R. 2016. An overview of triple-negative breast cancer. *Arch Gynecol Obstet*, 293, 247-69.
- KUPSCH, J. M., TIDMAN, N. H., KANG, N. V., TRUMAN, H., HAMILTON, S., PATEL, N., NEWTON BISHOP, J. A., LEIGH, I. M. & CROWE, J. S. 1999. Isolation of human tumor-specific antibodies by selection of an antibody phage library on melanoma cells. *Clin Cancer Res*, 5, 925-31.
- KYLE, H. F., WICKSON, K. F., STOTT, J., BURSLEM, G. M., BREEZE, A. L., TIEDE, C., TOMLINSON, D. C., WARRINER, S. L., NELSON, A., WILSON, A. J. & EDWARDS, T. A. 2015. Exploration of the HIF-1 α /p300 interface using peptide and Adhiron phage display technologies. *Mol Biosyst*, 11, 2738-49.
- KYLE, S. 2018. Affimer Proteins: Theranostics of the Future? *Trends Biochem Sci*, 43, 230-232.
- LAFKY, J. M., WILKEN, J. A., BARON, A. T. & MAIHLE, N. J. 2008. Clinical implications of the ErbB/epidermal growth factor (EGF) receptor family and its ligands in ovarian cancer. *Biochim Biophys Acta*, 1785, 232-65.
- LAKHIN, A. V., TARANTUL, V. Z. & GENING, L. V. 2013. Aptamers: problems, solutions and prospects. *Acta Naturae*, 5, 34-43.
- LAKSHMIPRIYA, T., GOPINATH, S. C. & TANG, T. H. 2016. Biotin-Streptavidin Competition Mediates Sensitive Detection of Biomolecules in Enzyme Linked Immunosorbent Assay. *PLoS One*, 11, e0151153.
- LAKZAEI, M., RASAEI, M. J., FAZAEI, A. A. & AMINIAN, M. 2018. A comparison of three strategies for biopanning of phage-scFv library against diphtheria toxin. *J Cell Physiol*.
- LALLI, E., SARTI, G. & BOI, C. 2018. Effect of the spacer arm on non-specific binding in membrane affinity chromatography. *Materials research society*, 8, 65-70.
- LANDER, E. S., LINTON, L. M., BIRREN, B., NUSBAUM, C., ZODY, M. C., BALDWIN, J., DEVON, K., DEWAR, K., DOYLE, M., FITZHUGH, W., FUNKE, R., GAGE, D., HARRIS, K., HEAFORD, A., HOWLAND, J., KANN, L., LEHOCZKY, J., LEVINE, R., MCEWAN, P., MCKERNAN, K., MELDRIM, J., MESIROV, J. P., MIRANDA, C., MORRIS, W., NAYLOR, J., RAYMOND, C., ROSETTI, M., SANTOS, R., SHERIDAN, A., SOUGNEZ, C., STANGE-THOMANN, Y., STOJANOVIC, N., SUBRAMANIAN, A., WYMAN, D., ROGERS, J., SULSTON, J., AINSCOUGH, R., BECK, S., BENTLEY, D., BURTON, J., CLEE, C., CARTER, N., COULSON, A., DEADMAN, R., DELOUKAS, P., DUNHAM, A., DUNHAM, I., DURBIN, R., FRENCH, L., GRAFHAM, D.,

- GREGORY, S., HUBBARD, T., HUMPHRAY, S., HUNT, A., JONES, M., LLOYD, C., MCMURRAY, A., MATTHEWS, L., MERCER, S., MILNE, S., MULLIKIN, J. C., MUNGALL, A., PLUMB, R., ROSS, M., SHOWNKEEN, R., SIMS, S., WATERSTON, R. H., WILSON, R. K., HILLIER, L. W., MCPHERSON, J. D., MARRA, M. A., MARDIS, E. R., FULTON, L. A., CHINWALLA, A. T., PEPIN, K. H., GISH, W. R., CHISSOE, S. L., WENDL, M. C., DELEHAUNTY, K. D., MINER, T. L., DELEHAUNTY, A., KRAMER, J. B., COOK, L. L., FULTON, R. S., JOHNSON, D. L., MINX, P. J., CLIFTON, S. W., HAWKINS, T., BRANSCOMB, E., PREDKI, P., RICHARDSON, P., WENNING, S., SLEZAK, T., DOGGETT, N., CHENG, J. F., OLSEN, A., LUCAS, S., ELKIN, C., UBERBACHER, E., FRAZIER, M., et al. 2001. Initial sequencing and analysis of the human genome. *Nature*, 409, 860-921.
- LASSERE, M. N. 2008. The Biomarker-Surrogacy Evaluation Schema: a review of the biomarker-surrogate literature and a proposal for a criterion-based, quantitative, multidimensional hierarchical levels of evidence schema for evaluating the status of biomarkers as surrogate endpoints. *Stat Methods Med Res*, 17, 303-40.
- LEBERT, J. M., LESTER, R., POWELL, E., SEAL, M. & MCCARTHY, J. 2018. Advances in the systemic treatment of triple-negative breast cancer. *Curr Oncol*, 25, S142-S150.
- LEDSCGAARD, L., KILSTRUP, M., KARATT-VELLATT, A., MCCAFFERTY, J. & LAUSTSEN, A. H. 2018. Basics of Antibody Phage Display Technology. *Toxins (Basel)*, 10.
- LEE, J. M., LEDERMANN, J. A. & KOHN, E. C. 2014. PARP Inhibitors for BRCA1/2 mutation-associated and BRCA-like malignancies. *Ann Oncol*, 25, 32-40.
- LEE, S. B., HASSAN, M., FISHER, R., CHERTOV, O., CHERNOMORDIK, V., KRAMER-MAREK, G., GANDJBAKHCHÉ, A. & CAPALA, J. 2008. Affibody molecules for in vivo characterization of HER2-positive tumors by near-infrared imaging. *Clin Cancer Res*, 14, 3840-9.
- LEE-HOEFELICH, S. T., CROCKER, L., YAO, E., PHAM, T., MUNROE, X., HOEFELICH, K. P., SLIWKOWSKI, M. X. & STERN, H. M. 2008. A central role for HER3 in HER2-amplified breast cancer: implications for targeted therapy. *Cancer Res*, 68, 5878-87.
- LEENAARS, M. & HENDRIKSEN, C. F. 2005. Critical steps in the production of polyclonal and monoclonal antibodies: evaluation and recommendations. *ILAR J*, 46, 269-79.
- LENDEL, C., DOGAN, J. & HARD, T. 2006. Structural basis for molecular recognition in an affibody:affibody complex. *J Mol Biol*, 359, 1293-304.
- LI, L. & ROSS, A. H. 2007. Why is PTEN an important tumor suppressor? *J Cell Biochem*, 102, 1368-74.
- LI, N., NGUYEN, H. H., BYROM, M. & ELLINGTON, A. D. 2011. Inhibition of cell proliferation by an anti-EGFR aptamer. *PLoS One*, 6, e20299.
- LI, Y., ALMASSALHA, L. M., CHANDLER, J. E., ZHOU, X., STYPULA-CYRUS, Y. E., HUJSAK, K. A., ROTH, E. W., BLEHER, R., SUBRAMANIAN, H., SZLEIFER, I., DRAVID, V. P. & BACKMAN, V. 2017. The effects of chemical fixation on the cellular nanostructure. *Exp Cell Res*, 358, 253-259.
- LINGGI, B. & CARPENTER, G. 2006. ErbB receptors: new insights on mechanisms and biology. *Trends Cell Biol*, 16, 649-56.
- LINKE, R., KLEIN, A. & SEIMETZ, D. 2010. Catumaxomab: clinical development and future directions. *MAbs*, 2, 129-36.
- LIPES, B. D., CHEN, Y. H., MA, H., STAATS, H. F., KENAN, D. J. & GUNN, M. D. 2008. An entirely cell-based system to generate single-chain antibodies against cell surface receptors. *J Mol Biol*, 379, 261-72.
- LIPMAN, N. S., JACKSON, L. R., TRUDEL, L. J. & WEIS-GARCIA, F. 2005. Monoclonal versus polyclonal antibodies: distinguishing characteristics, applications, and information resources. *ILAR J*, 46, 258-68.
- LIU, P., O'MARA, B. W., WARRACK, B. M., WU, W., HUANG, Y., ZHANG, Y., ZHAO, R., LIN, M., ACKERMAN, M. S., HOCKNELL, P. K., CHEN, G., TAO, L., RIEBLE, S., WANG, J., WANG-IVERSON, D. B., TYMIAK, A. A., GRACE, M. J. & RUSSELL, R. J. 2010. A tris (2-carboxyethyl) phosphine (TCEP) related cleavage on cysteine-containing proteins. *J Am Soc Mass Spectrom*, 21, 837-44.

- LIU, X., XU, Y., WAN, D. B., XIONG, Y. H., HE, Z. Y., WANG, X. X., GEE, S. J., RYU, D. & HAMMOCK, B. D. 2015. Development of a nanobody-alkaline phosphatase fusion protein and its application in a highly sensitive direct competitive fluorescence enzyme immunoassay for detection of ochratoxin A in cereal. *Anal Chem*, 87, 1387-94.
- LOCKWOOD, C. M., ROBERTS, M. D., DALBO, V. J., SMITH-RYAN, A. E., KENDALL, K. L., MOON, J. R. & STOUT, J. R. 2017. Effects of Hydrolyzed Whey versus Other Whey Protein Supplements on the Physiological Response to 8 Weeks of Resistance Exercise in College-Aged Males. *J Am Coll Nutr*, 36, 16-27.
- LOPATA, A., HUGHES, R., TIEDE, C., HEISSLER, S. M., SELLERS, J. R., KNIGHT, P. J., TOMLINSON, D. & PECKHAM, M. 2018. Affimer proteins for F-actin: novel affinity reagents that label F-actin in live and fixed cells. *Sci Rep*, 8, 6572.
- LOREY, S., FIEDLER, E., KUNERT, A., NERKAMP, J., LANGE, C., FIEDLER, M., BOSSE-DOENECKE, E., MEYSING, M., GLOSER, M., RUNDFELDT, C., RAUCHHAUS, U., HANSSGEN, I., GOTTLER, T., STEUERNAGEL, A., FIEDLER, U. & HAUPTS, U. 2014. Novel ubiquitin-derived high affinity binding proteins with tumor targeting properties. *J Biol Chem*, 289, 8493-507.
- LOSET, G. A., ROOS, N., BOGEN, B. & SANDLIE, I. 2011. Expanding the versatility of phage display II: improved affinity selection of folded domains on protein VII and IX of the filamentous phage. *PLoS One*, 6, e17433.
- LOVE, J. C. 2010. Making antibodies from scratch. *Nat Biotechnol*, 28, 1176-8.
- LOWE, D., DUDGEON, K., ROUET, R., SCHOFIELD, P., JERMUTUS, L. & CHRIST, D. 2011. Aggregation, stability, and formulation of human antibody therapeutics. *Adv Protein Chem Struct Biol*, 84, 41-61.
- LU, B. Y. & CHANG, J. Y. 2010. Rapid and irreversible reduction of protein disulfide bonds. *Anal Biochem*, 405, 67-72.
- LU, C., LIU, X., ZHANG, C. S., GONG, H., WU, J. W. & WANG, Z. X. 2017. Structural and Dynamic Insights into the Mechanism of Allosteric Signal Transmission in ERK2-Mediated MKP3 Activation. *Biochemistry*, 56, 6165-6175.
- LYONS, T. J. & BASU, A. 2012. Biomarkers in diabetes: hemoglobin A1c, vascular and tissue markers. *Transl Res*, 159, 303-12.
- LYU, H., HAN, A., POLSDOFER, E., LIU, S. & LIU, B. 2018. Understanding the biology of HER3 receptor as a therapeutic target in human cancer. *Acta Pharm Sin B*, 8, 503-510.
- MA, C. X., LUO, J. & ELLIS, M. J. 2010. Molecular profiling of triple negative breast cancer. *Breast Dis*, 32, 73-84.
- MACHLEIDT, A., BUCHHOLZ, S., DIERMEIER-DAUCHER, S., ZEMAN, F., ORTMANN, O. & BROCKHOFF, G. 2013. The prognostic value of Her4 receptor isoform expression in triple-negative and Her2 positive breast cancer patients. *BMC Cancer*, 13, 437.
- MADDAMS, J., UTLEY, M. & MOLLER, H. 2012. Projections of cancer prevalence in the United Kingdom, 2010-2040. *Br J Cancer*, 107, 1195-202.
- MAIRAL, T., OZALP, V. C., LOZANO SANCHEZ, P., MIR, M., KATAKIS, I. & O'SULLIVAN, C. K. 2008. Aptamers: molecular tools for analytical applications. *Anal Bioanal Chem*, 390, 989-1007.
- MALM, M., FREJD, F. Y., STAHL, S. & LOFBLUM, J. 2016. Targeting HER3 using mono- and bispecific antibodies or alternative scaffolds. *MAbs*, 8, 1195-1209.
- MANN, D., REINEMANN, C., STOLTENBURG, R. & STREHLITZ, B. 2005. In vitro selection of DNA aptamers binding ethanolamine. *Biochem Biophys Res Commun*, 338, 1928-34.
- MARKLAND, W., LEY, A. C. & LADNER, R. C. 1996a. Iterative optimization of high-affinity protease inhibitors using phage display. 2. Plasma kallikrein and thrombin. *Biochemistry*, 35, 8058-67.
- MARKLAND, W., LEY, A. C., LEE, S. W. & LADNER, R. C. 1996b. Iterative optimization of high-affinity proteases inhibitors using phage display. 1. Plasmin. *Biochemistry*, 35, 8045-57.
- MARMOR, M. D., SKARIA, K. B. & YARDEN, Y. 2004. Signal transduction and oncogenesis by ErbB/HER receptors. *Int J Radiat Oncol Biol Phys*, 58, 903-13.

- MARTINCORENA, I. & CAMPBELL, P. J. 2015. Somatic mutation in cancer and normal cells. *Science*, 349, 1483-9.
- MARUSYK, A., ALMENDRO, V. & POLYAK, K. 2012. Intra-tumour heterogeneity: a looking glass for cancer? *Nat Rev Cancer*, 12, 323-34.
- MARUSYK, A. & POLYAK, K. 2010. Tumor heterogeneity: causes and consequences. *Biochim Biophys Acta*, 1805, 105-17.
- MASSA, S., VIKANI, N., BETTI, C., BALLE, S., VANDERHAEGEN, S., STEYAERT, J., DESCAMPS, B., VANHOVE, C., BUNSCHOTEN, A., VAN LEEUWEN, F. W., HERNOT, S., CAVELIERS, V., LAHOUTTE, T., MUYLDERMANS, S., XAVIER, C. & DEVOOGDT, N. 2016. Sortase A-mediated site-specific labeling of camelid single-domain antibody-fragments: a versatile strategy for multiple molecular imaging modalities. *Contrast Media Mol Imaging*, 11, 328-339.
- MATOS, L. L., TRUFELLI, D. C., DE MATOS, M. G. & DA SILVA PINHAL, M. A. 2010. Immunohistochemistry as an important tool in biomarkers detection and clinical practice. *Biomark Insights*, 5, 9-20.
- MAYER, G. 2009. The chemical biology of aptamers. *Angew Chem Int Ed Engl*, 48, 2672-89.
- MCCAFFERTY, J., GRIFFITHS, A. D., WINTER, G. & CHISWELL, D. J. 1990. Phage antibodies: filamentous phage displaying antibody variable domains. *Nature*, 348, 552-4.
- MCDERMOTT, J. E., WANG, J., MITCHELL, H., WEBB-ROBERTSON, B. J., HAFEN, R., RAMEY, J. & RODLAND, K. D. 2013. Challenges in Biomarker Discovery: Combining Expert Insights with Statistical Analysis of Complex Omics Data. *Expert Opin Med Diagn*, 7, 37-51.
- MEDINTZ, I. L., MATTOUSSI, H. & CLAPP, A. R. 2008. Potential clinical applications of quantum dots. *Int J Nanomedicine*, 3, 151-67.
- MENG, Q., SHAO, L., LUO, X., MU, Y., XU, W., GAO, L., XU, H. & CUI, Y. 2016. Expressions of VEGF-A and VEGFR-2 in placentae from GDM pregnancies. *Reprod Biol Endocrinol*, 14, 61.
- MERMIN, J., EKWARU, J. P., WERE, W., DEGERMAN, R., BUNNELL, R., KAHARUZA, F., DOWNING, R., COUTINHO, A., SOLBERG, P., ALEXANDER, L. N., TAPPERO, J., CAMPBELL, J. & MOORE, D. M. 2011. Utility of routine viral load, CD4 cell count, and clinical monitoring among adults with HIV receiving antiretroviral therapy in Uganda: randomised trial. *BMJ*, 343, d6792.
- MEULEMANS, E. V., NIELAND, L. J., DEBIE, W. H., RAMAEKERS, F. C. & VAN EYS, G. J. 1995. Phage displayed antibodies specific for a cytoskeletal antigen. Selection by competitive elution with a monoclonal antibody. *Hum Antibodies Hybridomas*, 6, 113-8.
- MEULEMANS, E. V., SLOBBE, R., WASTERVAL, P., RAMAEKERS, F. C. & VAN EYS, G. J. 1994. Selection of phage-displayed antibodies specific for a cytoskeletal antigen by competitive elution with a monoclonal antibody. *J Mol Biol*, 244, 353-60.
- MIETTINEN, M., RIKALA, M. S., RYS, J., LASOTA, J. & WANG, Z. F. 2012. Vascular endothelial growth factor receptor 2 as a marker for malignant vascular tumors and mesothelioma: an immunohistochemical study of 262 vascular endothelial and 1640 nonvascular tumors. *Am J Surg Pathol*, 36, 629-39.
- MITRI, Z., CONSTANTINE, T. & O'REGAN, R. 2012. The HER2 Receptor in Breast Cancer: Pathophysiology, Clinical Use, and New Advances in Therapy. *Chemother Res Pract*, 2012, 743193.
- MOFFATT, B. A. & STUDIER, F. W. 1987. T7 lysozyme inhibits transcription by T7 RNA polymerase. *Cell*, 49, 221-7.
- MOHAMMED, A., BIEGERT, G., ADAMEC, J. & HELIKAR, T. 2017. Identification of potential tissue-specific cancer biomarkers and development of cancer versus normal genomic classifiers. *Oncotarget*, 8, 85692-85715.
- MOLL, R., DIVO, M. & LANGBEIN, L. 2008. The human keratins: biology and pathology. *Histochem Cell Biol*, 129, 705-33.
- MOLL, R., FRANKE, W. W., SCHILLER, D. L., GEIGER, B. & KREPLER, R. 1982. The catalog of human cytokeratins: patterns of expression in normal epithelia, tumors and cultured cells. *Cell*, 31, 11-24.

- MROSS, K., RICHLI, H., FISCHER, R., SCHARR, D., BUCHERT, M., STERN, A., GILLE, H., AUDOLY, L. P. & SCHEULEN, M. E. 2013. First-in-human phase I study of PRS-050 (Angiocal), an Anticalin targeting and antagonizing VEGF-A, in patients with advanced solid tumors. *PLoS One*, 8, e83232.
- MULLER, B. H., LAMOURE, C., LE DU, M. H., CATTOLICO, L., LAJEUNESSE, E., LEMAITRE, F., PEARSON, A., DUCANCEL, F., MENEZ, A. & BOULAIN, J. C. 2001. Improving Escherichia coli alkaline phosphatase efficacy by additional mutations inside and outside the catalytic pocket. *Chembiochem*, 2, 517-23.
- MURRAY, G. I. & EWEN, S. W. 1992. A new fluorescence method for alkaline phosphatase histochemistry. *J Histochem Cytochem*, 40, 1971-4.
- NAGARIA, T. S., SHI, C., LEDUC, C., HOSKIN, V., SIKDAR, S., SANGRAR, W. & GREER, P. A. 2017. Combined targeting of Raf and Mek synergistically inhibits tumorigenesis in triple negative breast cancer model systems. *Oncotarget*, 8, 80804-80819.
- NEFF, R. T., SENTER, L. & SALANI, R. 2017. BRCA mutation in ovarian cancer: testing, implications and treatment considerations. *Ther Adv Med Oncol*, 9, 519-531.
- NELSON, A. L., DHIMOLEA, E. & REICHERT, J. M. 2010. Development trends for human monoclonal antibody therapeutics. *Nat Rev Drug Discov*, 9, 767-74.
- NICHOLSON, R. I., GEE, J. M. & HARPER, M. E. 2001. EGFR and cancer prognosis. *Eur J Cancer*, 37 Suppl 4, S9-15.
- NIELSEN, B. B., KASTRUP, J. S., RASMUSSEN, H., HOLTET, T. L., GRAVERSEN, J. H., ETZERODT, M., THOGERSEN, H. C. & LARSEN, I. K. 1997. Crystal structure of tetranectin, a trimeric plasminogen-binding protein with an alpha-helical coiled coil. *FEBS Lett*, 412, 388-96.
- NIMSE, S. B., SONAWANE, M. D., SONG, K. S. & KIM, T. 2016. Biomarker detection technologies and future directions. *Analyst*, 141, 740-55.
- NISMAN, B., BIRAN, H., HECHING, N., BARAK, V., RAMU, N., NEMIROVSKY, I. & PERETZ, T. 2008. Prognostic role of serum cytokeratin 19 fragments in advanced non-small-cell lung cancer: association of marker changes after two chemotherapy cycles with different measures of clinical response and survival. *Br J Cancer*, 98, 77-9.
- NISSIM, A. & CHERNAJOVSKY, Y. 2008. Historical development of monoclonal antibody therapeutics. *Handb Exp Pharmacol*, 3-18.
- NOBORI, T., TOSAKA, K., KAWAMURA, A., JOICHI, T., KAMINO, K., KISHIMURA, A., BABA, E., MORI, T. & KATAYAMA, Y. 2018. Alkaline Phosphatase-Catalyzed Amplification of a Fluorescence Signal for Flow Cytometry. *Anal Chem*, 90, 1059-1062.
- ODES, E., RANDOLPH-QUINNEY, P., STEYN, M., ZACH THROCKMORTON, Z., SMILG, J., ZIPFEL, B., AUGUSTINE, T., BEER, F., HOFFMAN, J., FRANKLIN, R. & BERGER, L. 2016. Earliest hominin cancer: 1.7-million-year-old osteosarcoma from Swartkrans Cave, South Africa. *South African Journal of Science*, 112, 1-5.
- OGISO, H., ISHITANI, R., NUREKI, O., FUKAI, S., YAMANAKA, M., KIM, J. H., SAITO, K., SAKAMOTO, A., INOUE, M., SHIROUZU, M. & YOKOYAMA, S. 2002. Crystal structure of the complex of human epidermal growth factor and receptor extracellular domains. *Cell*, 110, 775-87.
- OHTSUKA, T., SAKAGUCHI, M., YAMAMOTO, H., TOMIDA, S., TAKATA, K., SHIEN, K., HASHIDA, S., MIYATA-TAKATA, T., WATANABE, M., SUZAWA, K., SOH, J., YOUYI, C., SATO, H., NAMBA, K., TORIGOE, H., TSUKUDA, K., YOSHINO, T., MIYOSHI, S. & TOYOOKA, S. 2016. Interaction of cytokeratin 19 head domain and HER2 in the cytoplasm leads to activation of HER2-Erk pathway. *Sci Rep*, 6, 39557.
- OLADIPUPO, S. S., KABIR, A. U., SMITH, C., CHOI, K. & ORNITZ, D. M. 2018. Impaired tumor growth and angiogenesis in mice heterozygous for Vegfr2 (Flk1). *Sci Rep*, 8, 14724.
- OLSEN, J. R. & MICHALSKI, J. M. 2013. PSA screening for colorectal cancer patients: proceeding with caution. *Oncology (Williston Park)*, 27, 1041-2.
- ONITILLO, A. A., ENGEL, J. M., GREENLEE, R. T. & MUKESH, B. N. 2009. Breast cancer subtypes based on ER/PR and Her2 expression: comparison of clinicopathologic features and survival. *Clin Med Res*, 7, 4-13.

- ORLOVA, A., MAGNUSSON, M., ERIKSSON, T. L., NILSSON, M., LARSSON, B., HOIDEN-GUTHENBERG, I., WIDSTROM, C., CARLSSON, J., TOLMACHEV, V., STAHL, S. & NILSSON, F. Y. 2006. Tumor imaging using a picomolar affinity HER2 binding affibody molecule. *Cancer Res*, 66, 4339-48.
- PABLA, B., BISSONNETTE, M. & KONDA, V. J. 2015. Colon cancer and the epidermal growth factor receptor: Current treatment paradigms, the importance of diet, and the role of chemoprevention. *World J Clin Oncol*, 6, 133-41.
- PAIK, S., KIM, C. & WOLMARK, N. 2008. HER2 status and benefit from adjuvant trastuzumab in breast cancer. *N Engl J Med*, 358, 1409-11.
- PANDE, J., SZEWCZYK, M. M. & GROVER, A. K. 2010. Phage display: concept, innovations, applications and future. *Biotechnol Adv*, 28, 849-58.
- PARK, C. C., BISSELL, M. J. & BARCELLOS-HOFF, M. H. 2000. The influence of the microenvironment on the malignant phenotype. *Mol Med Today*, 6, 324-9.
- PARK, S. H., PARK, S., KIM, D. Y., PYO, A., KIMURA, R. H., SATHIRACHINDA, A., CHOY, H. E., MIN, J. J., GAMBHIR, S. S. & HONG, Y. 2015. Isolation and Characterization of a Monobody with a Fibronectin Domain III Scaffold That Specifically Binds EphA2. *PLoS One*, 10, e0132976.
- PASCHKE, M. 2006. Phage display systems and their applications. *Appl Microbiol Biotechnol*, 70, 2-11.
- PASTORE, J., CLAMPETT, C., MILLER, J., PORTER, K. & MILLER, D. 1995. A Rapid Immunoenzyme Double Labeling Technique Using EPOS Reagents. *Journal of Histotechnology*, 18, 35-39.
- PENTO, J. T. 2017. Monoclonal Antibodies for the Treatment of Cancer. *Anticancer Res*, 37, 5935-5939.
- PEREZ, E. A., CORTES, J., GONZALEZ-ANGULO, A. M. & BARTLETT, J. M. 2014a. HER2 testing: current status and future directions. *Cancer Treat Rev*, 40, 276-84.
- PEREZ, E. A., ROMOND, E. H., SUMAN, V. J., JEONG, J. H., SLEDGE, G., GEYER, C. E., JR., MARTINO, S., RASTOGI, P., GRALOW, J., SWAIN, S. M., WINER, E. P., COLON-OTERO, G., DAVIDSON, N. E., MAMOUNAS, E., ZUJEWSKI, J. A. & WOLMARK, N. 2014b. Trastuzumab plus adjuvant chemotherapy for human epidermal growth factor receptor 2-positive breast cancer: planned joint analysis of overall survival from NSABP B-31 and NCCTG N9831. *J Clin Oncol*, 32, 3744-52.
- PERICO, N., PURTELL, J., DILLON, T. M. & RICCI, M. S. 2009. Conformational implications of an inversed pH-dependent antibody aggregation. *J Pharm Sci*, 98, 3031-42.
- PERLIS, R. H. 2011. Translating biomarkers to clinical practice. *Mol Psychiatry*, 16, 1076-87.
- PETERSON, N. C. 2000. Behavioral, clinical, and physiologic analysis of mice used for ascites monoclonal antibody production. *Comp Med*, 50, 516-26.
- PIETRAS, K. & OSTMAN, A. 2010. Hallmarks of cancer: interactions with the tumor stroma. *Exp Cell Res*, 316, 1324-31.
- PILLAI, R. N., BEHERA, M., BERRY, L. D., ROSSI, M. R., KRIS, M. G., JOHNSON, B. E., BUNN, P. A., RAMALINGAM, S. S. & KHURI, F. R. 2017. HER2 mutations in lung adenocarcinomas: A report from the Lung Cancer Mutation Consortium. *Cancer*, 123, 4099-4105.
- PINKAS-KRAMARSKI, R., SOUSSAN, L., WATERMAN, H., LEVKOWITZ, G., ALROY, I., KLAPPER, L., LAVI, S., SEGER, R., RATZKIN, B. J., SELA, M. & YARDEN, Y. 1996. Diversification of Neu differentiation factor and epidermal growth factor signaling by combinatorial receptor interactions. *EMBO J*, 15, 2452-67.
- POLYAK, K. 2011. Heterogeneity in breast cancer. *J Clin Invest*, 121, 3786-8.
- POPANDA, O., ZHENG, C., MAGDEBURG, J. R., BUTTNER, J., FLOHR, T., HAGMULLER, E. & THIELMANN, H. W. 2000. Mutation analysis of replicative genes encoding the large subunits of DNA polymerase alpha and replication factors A and C in human sporadic colorectal cancers. *Int J Cancer*, 86, 318-24.
- POTTHOFF, K., HOFHEINZ, R., HASSEL, J. C., VOLKENANDT, M., LORDICK, F., HARTMANN, J. T., KARTHAUS, M., RIESS, H., LIPP, H. P., HAUSCHILD, A., TRARBACH, T. & WOLLENBERG, A.

2011. Interdisciplinary management of EGFR-inhibitor-induced skin reactions: a German expert opinion. *Ann Oncol*, 22, 524-35.
- POWELL, B., CROCKER, L. & ROGERS, G. 1992. Hair follicle differentiation: expression, structure and evolutionary conservation of the hair type II keratin intermediate filament gene family. *Development*, 114, 417-33.
- POWERS, A. D. & PALECEK, S. P. 2012. Protein analytical assays for diagnosing, monitoring, and choosing treatment for cancer patients. *J Healthc Eng*, 3, 503-534.
- PRAT, A., CAREY, L. A., ADAMO, B., VIDAL, M., TABERNERO, J., CORTES, J., PARKER, J. S., PEROU, C. M. & BASELGA, J. 2014. Molecular features and survival outcomes of the intrinsic subtypes within HER2-positive breast cancer. *J Natl Cancer Inst*, 106.
- PRAT, A., PASCUAL, T. & ADAMO, B. 2017. Intrinsic molecular subtypes of HER2+ breast cancer. *Oncotarget*, 8, 73362-73363.
- PRESS, M. F., SAUTER, G., BERNSTEIN, L., VILLALOBOS, I. E., MIRLACHER, M., ZHOU, J. Y., WARDEH, R., LI, Y. T., GUZMAN, R., MA, Y., SULLIVAN-HALLEY, J., SANTIAGO, A., PARK, J. M., RIVA, A. & SLAMON, D. J. 2005. Diagnostic evaluation of HER-2 as a molecular target: an assessment of accuracy and reproducibility of laboratory testing in large, prospective, randomized clinical trials. *Clin Cancer Res*, 11, 6598-607.
- RADER, C. 2009. Overview on concepts and applications of Fab antibody fragments. *Curr Protoc Protein Sci*, Chapter 6, Unit 6 9.
- RADULESCU, R. T. & BOENISCH, T. 2007. Blocking endogenous peroxidases: a cautionary note for immunohistochemistry. *J Cell Mol Med*, 11, 1419.
- RAMOS-VARA, J. A. 2011. Principles and methods of immunohistochemistry. *Methods Mol Biol*, 691, 83-96.
- RAMOS-VARA, J. A., FRANK, C. B., DUSOLD, D. & MILLER, M. A. 2016. Immunohistochemical Detection of Pax8 and Napsin A in Canine Thyroid Tumours: Comparison with Thyroglobulin, Calcitonin and Thyroid Transcription Factor 1. *J Comp Pathol*, 155, 286-298.
- RAMOS-VARA, J. A. & MILLER, M. A. 2006. Comparison of two polymer-based immunohistochemical detection systems: ENVISION+ and ImmPRESS. *J Microsc*, 224, 135-9.
- REGGI, E. & DIVIANI, D. 2017. The role of A-kinase anchoring proteins in cancer development. *Cell Signal*, 40, 143-155.
- REICHERT, J. M. 2008. Monoclonal antibodies as innovative therapeutics. *Curr Pharm Biotechnol*, 9, 423-30.
- REICHERT, J. M. 2017. Antibodies to watch in 2017. *MAbs*, 9, 167-181.
- REW, D. A. & WILSON, G. D. 2000. Cell production rates in human tissues and tumours and their significance. Part II: clinical data. *Eur J Surg Oncol*, 26, 405-17.
- REYNOLDS, N. A. & WAGSTAFF, A. J. 2004. Cetuximab: in the treatment of metastatic colorectal cancer. *Drugs*, 64, 109-18; discussion 119-121.
- RIDGWAY, J. B., NG, E., KERN, J. A., LEE, J., BRUSH, J., GODDARD, A. & CARTER, P. 1999. Identification of a human anti-CD55 single-chain Fv by subtractive panning of a phage library using tumor and nontumor cell lines. *Cancer Res*, 59, 2718-23.
- RIESE, D. J., 2ND & STERN, D. F. 1998. Specificity within the EGF family/ErbB receptor family signaling network. *Bioessays*, 20, 41-8.
- RISS, T. L., MORAVEC, R. A., NILES, A. L., DUELLMAN, S., BENINK, H. A., WORZELLA, T. J. & MINOR, L. 2004. Cell Viability Assays. In: SITTAMPALAM, G. S., COUSSENS, N. P., BRIMACOMBE, K., GROSSMAN, A., ARKIN, M., AULD, D., AUSTIN, C., BAELL, J., BEJCEK, B., CAAVEIRO, J. M. M., CHUNG, T. D. Y., DAHLIN, J. L., DEVANARYAN, V., FOLEY, T. L., GLICKSMAN, M., HALL, M. D., HAAS, J. V., INGLESE, J., IVERSEN, P. W., KAHL, S. D., KALES, S. C., LAL-NAG, M., LI, Z., MCGEE, J., MCMANUS, O., RISS, T., TRASK, O. J., JR., WEIDNER, J. R., WILDEY, M. J., XIA, M. & XU, X. (eds.) *Assay Guidance Manual*. Bethesda (MD).

- RITCHIE, M., TCHISTIAKOVA, L. & SCOTT, N. 2013. Implications of receptor-mediated endocytosis and intracellular trafficking dynamics in the development of antibody drug conjugates. *MAbs*, 5, 13-21.
- ROBERTS, J. D. & KUNKEL, T. A. 1988. Fidelity of a human cell DNA replication complex. *Proc Natl Acad Sci U S A*, 85, 7064-8.
- ROBERTS, P. J. & DER, C. J. 2007. Targeting the Raf-MEK-ERK mitogen-activated protein kinase cascade for the treatment of cancer. *Oncogene*, 26, 3291-310.
- ROBINSON, J. I., BAXTER, E. W., OWEN, R. L., THOMSEN, M., TOMLINSON, D. C., WATERHOUSE, M. P., WIN, S. J., NETTLESHIP, J. E., TIEDE, C., FOSTER, R. J., OWENS, R. J., FISHWICK, C. W. G., HARRIS, S. A., GOLDMAN, A., MCPHERSON, M. J. & MORGAN, A. W. 2018. Affimer proteins inhibit immune complex binding to FcγRIIIa with high specificity through competitive and allosteric modes of action. *Proc Natl Acad Sci U S A*, 115, E72-E81.
- ROCKBERG, J., SCHWENK, J. M. & UHLEN, M. 2009. Discovery of epitopes for targeting the human epidermal growth factor receptor 2 (HER2) with antibodies. *Mol Oncol*, 3, 238-47.
- ROMOND, E. H., PEREZ, E. A., BRYANT, J., SUMAN, V. J., GEYER, C. E., JR., DAVIDSON, N. E., TANCHIU, E., MARTINO, S., PAIK, S., KAUFMAN, P. A., SWAIN, S. M., PISANSKY, T. M., FEHRENBACHER, L., KUTTEH, L. A., VOGEL, V. G., VISSCHER, D. W., YOTHERS, G., JENKINS, R. B., BROWN, A. M., DAKHIL, S. R., MAMOUNAS, E. P., LINGLE, W. L., KLEIN, P. M., INGLE, J. N. & WOLMARK, N. 2005. Trastuzumab plus adjuvant chemotherapy for operable HER2-positive breast cancer. *N Engl J Med*, 353, 1673-84.
- RONALDSON-BOUCHARD, K. & VUNJAK-NOVAKOVIC, G. 2018. Organs-on-a-Chip: A Fast Track for Engineered Human Tissues in Drug Development. *Cell Stem Cell*, 22, 310-324.
- RONNMARK, J., HANSSON, M., NGUYEN, T., UHLEN, M., ROBERT, A., STAHL, S. & NYGREN, P. A. 2002. Construction and characterization of affibody-Fc chimeras produced in *Escherichia coli*. *J Immunol Methods*, 261, 199-211.
- ROSANO, G. L. & CECCARELLI, E. A. 2014. Recombinant protein expression in *Escherichia coli*: advances and challenges. *Front Microbiol*, 5, 172.
- ROSKOSKI, R., JR. 2014. The ErbB/HER family of protein-tyrosine kinases and cancer. *Pharmacol Res*, 79, 34-74.
- RUBIN, I. & YARDEN, Y. 2001. The basic biology of HER2. *Ann Oncol*, 12 Suppl 1, S3-8.
- RUDLOFF, U. & SAMUELS, Y. 2010. A growing family: adding mutated *ErbB4* as a novel cancer target. *Cell Cycle*, 9, 1487-503.
- RUIGROK, V. J., LEVISSON, M., EPPINK, M. H., SMIDT, H. & VAN DER OOST, J. 2011. Alternative affinity tools: more attractive than antibodies? *Biochem J*, 436, 1-13.
- RUNNING DEER, J. & ALLISON, D. S. 2004. High-level expression of proteins in mammalian cells using transcription regulatory sequences from the Chinese hamster EF-1α gene. *Biotechnol Prog*, 20, 880-9.
- RUSSO, D., AMBROSINO, A., VITTORIA, A. & CECIO, A. 2003. Signal amplification by combining two advanced immunohistochemical techniques. *Eur J Histochem*, 47, 379-84.
- SABATINO, M., KIM-SCHULZE, S., PANELLI, M. C., STRONCEK, D., WANG, E., TABACK, B., KIM, D. W., DERAFFELE, G., POS, Z., MARINCOLA, F. M. & KAUFMAN, H. L. 2009. Serum vascular endothelial growth factor and fibronectin predict clinical response to high-dose interleukin-2 therapy. *J Clin Oncol*, 27, 2645-52.
- SAHA, S. K., CHOI, H. Y., KIM, B. W., DAYEM, A. A., YANG, G. M., KIM, K. S., YIN, Y. F. & CHO, S. G. 2017. KRT19 directly interacts with beta-catenin/RAC1 complex to regulate NUMB-dependent NOTCH signaling pathway and breast cancer properties. *Oncogene*, 36, 332-349.
- SAHA, S. K., KIM, K., YANG, G. M., CHOI, H. Y. & CHO, S. G. 2018. Cytokeratin 19 (KRT19) has a Role in the Reprogramming of Cancer Stem Cell-Like Cells to Less Aggressive and More Drug-Sensitive Cells. *Int J Mol Sci*, 19.
- SAKAMOTO, G. & MITSUYAMA, S. 2000. New molecule-targeting therapy with herceptin (trastuzumab), an anti-HER2 (c-erbB-2) monoclonal antibody. *Breast Cancer*, 7, 350-7.

- SALAMANCA, S. A., SORRENTINO, E. E., NOSANCHUK, J. D. & MARTINEZ, L. R. 2014. Impact of methamphetamine on infection and immunity. *Front Neurosci*, 8, 445.
- SALLAM, R. M. 2015. Proteomics in cancer biomarkers discovery: challenges and applications. *Dis Markers*, 2015, 321370.
- SAMPATH, L., KWON, S., KE, S., WANG, W., SCHIFF, R., MAWAD, M. E. & SEVICK-MURACA, E. M. 2007. Dual-labeled trastuzumab-based imaging agent for the detection of human epidermal growth factor receptor 2 overexpression in breast cancer. *J Nucl Med*, 48, 1501-10.
- SANCHEZ-MARTIN, D., SORENSEN, M. D., LYKKEMARK, S., SANZ, L., KRISTENSEN, P., RUOSLAHTI, E. & ALVAREZ-VALLINA, L. 2015. Selection strategies for anticancer antibody discovery: searching off the beaten path. *Trends Biotechnol*, 33, 292-301.
- SANDOW, J. J., RAINCZUK, A., INFUSINI, G., MAKANJI, M., BILANDZIC, M., WILSON, A. L., FAIRWEATHER, N., STANTON, P. G., GARAMA, D., GOUGH, D., JOBLING, T. W., WEBB, A. I. & STEPHENS, A. N. 2018. Discovery and Validation of Novel Protein Biomarkers in Ovarian Cancer Patient Urine. *Proteomics Clin Appl*, 12, e1700135.
- SARODE, V. R., XIANG, Q. D., CHRISTIE, A., COLLINS, R., RAO, R., LEITCH, A. M., EUHUS, D. & HALEY, B. 2015. Evaluation of HER2/neu Status by Immunohistochemistry Using Computer-Based Image Analysis and Correlation With Gene Amplification by Fluorescence In Situ Hybridization Assay: A 10-Year Experience and Impact of Test Standardization on Concordance Rate. *Arch Pathol Lab Med*, 139, 922-8.
- SCHLATTER, D., BRACK, S., BANNER, D. W., BATEY, S., BENZ, J., BERTSCHINGER, J., HUBER, W., JOSEPH, C., RUFER, A., VAN DER KLOOSTER, A., WEBER, M., GRABULOVSKI, D. & HENNIG, M. 2012. Generation, characterization and structural data of chymase binding proteins based on the human Fyn kinase SH3 domain. *MAbs*, 4, 497-508.
- SCHLEHUBER, S. & SKERRA, A. 2002. Tuning ligand affinity, specificity, and folding stability of an engineered lipocalin variant -- a so-called 'anticalin' -- using a molecular random approach. *Biophys Chem*, 96, 213-28.
- SCHMADEKA, R., HARMON, B. E. & SINGH, M. 2014. Triple-negative breast carcinoma: current and emerging concepts. *Am J Clin Pathol*, 141, 462-77.
- SCHNEIDER, L., LUMRY, W., VEGH, A., WILLIAMS, A. H. & SCHMALBACH, T. 2007. Critical role of kallikrein in hereditary angioedema pathogenesis: a clinical trial of ecallantide, a novel kallikrein inhibitor. *J Allergy Clin Immunol*, 120, 416-22.
- SCHNEIDER, S., BUCHERT, M., GEORGIEV, O., CATIMEL, B., HALFORD, M., STACKER, S. A., BAECHI, T., MOELLING, K. & HOVENS, C. M. 1999. Mutagenesis and selection of PDZ domains that bind new protein targets. *Nat Biotechnol*, 17, 170-5.
- SCHREVEL, M., OSSE, E. M., PRINS, F. A., TRIMBOS, J., FLEUREN, G. J., GORTER, A. & JORDANOVA, E. S. 2017. Autocrine expression of the epidermal growth factor receptor ligand heparin-binding EGF-like growth factor in cervical cancer. *Int J Oncol*, 50, 1947-1954.
- SCHUMACHER, D., HELMA, J., SCHNEIDER, A. F. L., LEONHARDT, H. & HACKENBERGER, C. P. R. 2018. Nanobodies: Chemical Functionalization Strategies and Intracellular Applications. *Angew Chem Int Ed Engl*, 57, 2314-2333.
- SCHUTZE, T., WILHELM, B., GREINER, N., BRAUN, H., PETER, F., MORL, M., ERDMANN, V. A., LEHRACH, H., KONTHUR, Z., MENGER, M., ARNDT, P. F. & GLOKLER, J. 2011. Probing the SELEX process with next-generation sequencing. *PLoS One*, 6, e29604.
- SCHWEIZER, J., BOWDEN, P. E., COULOMBE, P. A., LANGBEIN, L., LANE, E. B., MAGIN, T. M., MALTAIS, L., OMARY, M. B., PARRY, D. A., ROGERS, M. A. & WRIGHT, M. W. 2006. New consensus nomenclature for mammalian keratins. *J Cell Biol*, 174, 169-74.
- SEEMAYER, T. A. & CAVENEE, W. K. 1989. Molecular mechanisms of oncogenesis. *Lab Invest*, 60, 585-99.
- SELLECK, M. J., SENTHIL, M. & WALL, N. R. 2017. Making Meaningful Clinical Use of Biomarkers. *Biomark Insights*, 12, 1177271917715236.

- SEO, H. D., LEE, J. J., KIM, Y. J., HANTSCH, O., LEE, S. G. & KIM, H. S. 2017. Alkaline phosphatase-fused rebody as a new format of immuno-reagent for an immunoassay. *Anal Chim Acta*, 950, 184-191.
- SESHACHARYULU, P., PONNUSAMY, M. P., HARIDAS, D., JAIN, M., GANTI, A. K. & BATRA, S. K. 2012. Targeting the EGFR signaling pathway in cancer therapy. *Expert Opin Ther Targets*, 16, 15-31.
- SEYHAN, A. 2010. Biomarkers in drug discovery and development. *European pharmaceutical reviews*, 19-25.
- SHAFIEE, F., RABBANI, M. & JAHANIAN-NAJAFABADI, A. 2017. Optimization of the Expression of DT386-BR2 Fusion Protein in Escherichia coli using Response Surface Methodology. *Adv Biomed Res*, 6, 22.
- SHEN, Y., FUJII, T., UENO, N. T., TRIPATHY, D., FU, N., ZHOU, H., NING, J. & XIAO, L. 2019. Comparative efficacy of adjuvant trastuzumab-containing chemotherapies for patients with early HER2-positive primary breast cancer: a network meta-analysis. *Breast Cancer Res Treat*, 173, 1-9.
- SHI, Q., JUVONEN, M., HOU, Y., KAJALA, I., NYSSOLA, A., MAINA, N. H., MAAHEIMO, H., VIRKKI, L. & TENKANEN, M. 2016. Lactose- and cellobiose-derived branched trisaccharides and a sucrose-containing trisaccharide produced by acceptor reactions of Weissella confusa dextransucrase. *Food Chem*, 190, 226-236.
- SHI, S. R., SHI, Y. & TAYLOR, C. R. 2011. Antigen retrieval immunohistochemistry: review and future prospects in research and diagnosis over two decades. *J Histochem Cytochem*, 59, 13-32.
- SHUKLA, A. A., SORGE, L., BOLDMAN, J. & WAUGH, S. 2001. Process characterization for metal-affinity chromatography of an Fc fusion protein: a design-of-experiments approach. *Biotechnol Appl Biochem*, 34, 71-80.
- SHUKLA, G. S. & KRAG, D. N. 2005. Phage display selection for cell-specific ligands: development of a screening procedure suitable for small tumor specimens. *J Drug Target*, 13, 7-18.
- SIDHU, S. S. 2001. Engineering M13 for phage display. *Biomol Eng*, 18, 57-63.
- SIERKE, S. L., CHENG, K., KIM, H. H. & KOLAND, J. G. 1997. Biochemical characterization of the protein tyrosine kinase homology domain of the ErbB3 (HER3) receptor protein. *Biochem J*, 322 (Pt 3), 757-63.
- SILACCI, M., BAENZIGER-TOBLER, N., LEMBKE, W., ZHA, W., BATEY, S., BERTSCHINGER, J. & GRABULOVSKI, D. 2014. Linker length matters, fynomer-Fc fusion with an optimized linker displaying picomolar IL-17A inhibition potency. *J Biol Chem*, 289, 14392-8.
- SILVER, G. A. 1987. Virchow, the heroic model in medicine: health policy by accolade. *Am J Public Health*, 77, 82-8.
- SILVERMAN, J., LIU, Q., BAKKER, A., TO, W., DUGUAY, A., ALBA, B. M., SMITH, R., RIVAS, A., LI, P., LE, H., WHITEHORN, E., MOORE, K. W., SWIMMER, C., PERLROTH, V., VOGT, M., KOLKMAN, J. & STEMMER, W. P. 2005. Multivalent avimer proteins evolved by exon shuffling of a family of human receptor domains. *Nat Biotechnol*, 23, 1556-61.
- SIMEON, R. & CHEN, Z. 2018. In vitro-engineered non-antibody protein therapeutics. *Protein Cell*, 9, 3-14.
- SINGH, B., CARPENTER, G. & COFFEY, R. J. 2016. EGF receptor ligands: recent advances. *F1000Res*, 5.
- SINGH, I. & ROSE, N. 2009. Biomarkers in psychiatry. *Nature*, 460, 202-7.
- SINGH, P. & SOOD, N. 2017. A Combination of Antigen Retrieval Methods Significantly Enhances the Unmasking of Tedious Antigens of Lymphangiogenesis and Angiogenesis in Canine Mammary Tumour. *Journal of Biosciences and Medicines*, 5, 44-55.
- SINGH, S., KUMAR, N. K., DWIWEDI, P., CHARAN, J., KAUR, R., SIDHU, P. & CHUGH, V. K. 2018. Monoclonal Antibodies: A Review. *Curr Clin Pharmacol*, 13, 85-99.
- SIONTOROU, C. G. 2013. Nanobodies as novel agents for disease diagnosis and therapy. *Int J Nanomedicine*, 8, 4215-27.

- SKERRA, A. 2000. Engineered protein scaffolds for molecular recognition. *J Mol Recognit*, 13, 167-87.
- SKERRA, A. 2007. Alternative non-antibody scaffolds for molecular recognition. *Curr Opin Biotechnol*, 18, 295-304.
- SKRLEC, K., STRUKELJ, B. & BERLEC, A. 2015. Non-immunoglobulin scaffolds: a focus on their targets. *Trends Biotechnol*.
- SLAMON, D. J., CLARK, G. M., WONG, S. G., LEVIN, W. J., ULLRICH, A. & MCGUIRE, W. L. 1987. Human breast cancer: correlation of relapse and survival with amplification of the HER-2/neu oncogene. *Science*, 235, 177-82.
- SLEDGE, G. W., MAMOUNAS, E. P., HORTOBAGYI, G. N., BURSTEIN, H. J., GOODWIN, P. J. & WOLFF, A. C. 2014. Past, present, and future challenges in breast cancer treatment. *J Clin Oncol*, 32, 1979-86.
- SMITH, G. P. 1985. Filamentous fusion phage: novel expression vectors that display cloned antigens on the virion surface. *Science*, 228, 1315-7.
- SMITH, G. P. & SCOTT, J. K. 1993. Libraries of peptides and proteins displayed on filamentous phage. *Methods Enzymol*, 217, 228-57.
- SMITH, K. L. & ISAACS, C. 2011. BRCA mutation testing in determining breast cancer therapy. *Cancer J*, 17, 492-9.
- SMITH, R. A., ANDREWS, K. S., BROOKS, D., FEDEWA, S. A., MANASSARAM-BAPTISTE, D., SASLOW, D., BRAWLEY, O. W. & WENDER, R. C. 2018. Cancer screening in the United States, 2018: A review of current American Cancer Society guidelines and current issues in cancer screening. *CA Cancer J Clin*, 68, 297-316.
- SOLTOFF, S. P., CARRAWAY, K. L., 3RD, PRIGENT, S. A., GULLICK, W. G. & CANTLEY, L. C. 1994. ErbB3 is involved in activation of phosphatidylinositol 3-kinase by epidermal growth factor. *Mol Cell Biol*, 14, 3550-8.
- SOMERVILLE, G. & PROCTOR, R. 2013. Cultivation conditions and the diffusion of oxygen into culture media: The rationale for the flask-to-medium ratio in microbiology. *BioMed Central Microbiology*, 13, 1471-2180.
- SORENSEN, H. P. & MORTENSEN, K. K. 2005. Soluble expression of recombinant proteins in the cytoplasm of Escherichia coli. *Microb Cell Fact*, 4, 1.
- SORENSEN, M. D., MELCHJORSEN, C. J., MANDRUP, O. A. & KRISTENSEN, P. 2013. Raising antibodies against circulating foetal cells from maternal peripheral blood. *Prenat Diagn*, 33, 284-91.
- SPICER, C. D. & DAVIS, B. G. 2014. Selective chemical protein modification. *Nat Commun*, 5, 4740.
- STADLER, L. K., HOFFMANN, T., TOMLINSON, D. C., SONG, Q., LEE, T., BUSBY, M., NYATHI, Y., GENDRA, E., TIEDE, C., FLANAGAN, K., COCKELL, S. J., WIPAT, A., HARWOOD, C., WAGNER, S. D., KNOWLES, M. A., DAVIS, J. J., KEEGAN, N. & FERRIGNO, P. K. 2011. Structure-function studies of an engineered scaffold protein derived from Stefin A. II: Development and applications of the SQT variant. *Protein Eng Des Sel*, 24, 751-63.
- STAHL, P. L., SALMEN, F., VICKOVIC, S., LUNDMARK, A., NAVARRO, J. F., MAGNUSSON, J., GIACOMELLO, S., ASP, M., WESTHOLM, J. O., HUSS, M., MOLLBRINK, A., LINNARSSON, S., CODELUPPI, S., BORG, A., PONTEN, F., COSTEA, P. I., SAHLEN, P., MULDER, J., BERGMANN, O., LUNDEBERG, J. & FRISEN, J. 2016. Visualization and analysis of gene expression in tissue sections by spatial transcriptomics. *Science*, 353, 78-82.
- STANFIELD, R. L., DOOLEY, H., FLAJNIK, M. F. & WILSON, I. A. 2004. Crystal structure of a shark single-domain antibody V region in complex with lysozyme. *Science*, 305, 1770-3.
- STANO, N. M. & PATEL, S. S. 2004. T7 lysozyme represses T7 RNA polymerase transcription by destabilizing the open complex during initiation. *J Biol Chem*, 279, 16136-43.
- STARK, Y., VENET, S. & SCHMID, A. 2017. Whole Cell Panning with Phage Display. *Methods Mol Biol*, 1575, 67-91.
- STEELAND, S., VANDENBROUCKE, R. E. & LIBERT, C. 2016. Nanobodies as therapeutics: big opportunities for small antibodies. *Drug Discov Today*, 21, 1076-113.

- STEMMSON, J. D., BAAKE, M., RAKONJAC, J., ARCUS, V. L. & LIDDAMENT, M. T. 2014. Tracking molecular recognition at the atomic level with a new protein scaffold based on the OB-fold. *PLoS One*, 9, e86050.
- STEGEMAN, J. H. & TREFFERS, P. E. 1980. Histological appearances of the human placenta observed by electron microscopy after hypertonic saline abortion. *Acta Obstet Gynecol Scand*, 59, 45-53.
- STEVENSON, R. P., VELTMAN, D. & MACHESKY, L. M. 2012. Actin-bundling proteins in cancer progression at a glance. *J Cell Sci*, 125, 1073-9.
- STODDART, M. J. 2011. Cell viability assays: introduction. *Methods Mol Biol*, 740, 1-6.
- STUDIER, F. W. & MOFFATT, B. A. 1986. Use of bacteriophage T7 RNA polymerase to direct selective high-level expression of cloned genes. *J Mol Biol*, 189, 113-30.
- SUBIK, K., LEE, J. F., BAXTER, L., STRZEPEK, T., COSTELLO, D., CROWLEY, P., XING, L., HUNG, M. C., BONFIGLIO, T., HICKS, D. G. & TANG, P. 2010. The Expression Patterns of ER, PR, HER2, CK5/6, EGFR, Ki-67 and AR by Immunohistochemical Analysis in Breast Cancer Cell Lines. *Breast Cancer (Auckl)*, 4, 35-41.
- SUN, Y., SHUKLA, G. S., KENNEDY, G. G., WARSHAW, D. M., WEAVER, D. L., PERO, S. C., FLOYD, L. & KRAG, D. N. 2009. Biopanning Phage-Display Libraries on Small Tissue Sections Captured by Laser Capture Microdissection. *J Biotech Res*, 1, 55-63.
- TAKAGI, S., BANNO, H., HAYASHI, A., TAMURA, T., ISHIKAWA, T. & OHTA, Y. 2014. HER2 and HER3 cooperatively regulate cancer cell growth and determine sensitivity to the novel investigational EGFR/HER2 kinase inhibitor TAK-285. *Oncoscience*, 1, 196-204.
- TAKAHASHI, K., PALADINI, R. D. & COULOMBE, P. A. 1995. Cloning and characterization of multiple human genes and cDNAs encoding highly related type II keratin 6 isoforms. *J Biol Chem*, 270, 18581-92.
- TANG, A. A., TIEDE, C., HUGHES, D. J., MCPHERSON, M. J. & TOMLINSON, D. C. 2017. Isolation of isoform-specific binding proteins (Affimers) by phage display using negative selection. *Sci Signal*, 10.
- TANG, Z., SHANGGUAN, D., WANG, K., SHI, H., SEFAH, K., MALLIKRATCHY, P., CHEN, H. W., LI, Y. & TAN, W. 2007. Selection of aptamers for molecular recognition and characterization of cancer cells. *Anal Chem*, 79, 4900-7.
- TAVARE, R., MCCRACKEN, M. N., ZETTLITZ, K. A., KNOWLES, S. M., SALAZAR, F. B., OLAFSEN, T., WITTE, O. N. & WU, A. M. 2014. Engineered antibody fragments for immuno-PET imaging of endogenous CD8+ T cells in vivo. *Proc Natl Acad Sci U S A*, 111, 1108-13.
- TERNYNCK, T. & AVRAMEAS, S. 1990. Avidin-biotin system in enzyme immunoassays. *Methods Enzymol*, 184, 469-81.
- TERRY, K. L., SCHOCK, H., FORTNER, R. T., HUSING, A., FICHOROVA, R. N., YAMAMOTO, H. S., VITONIS, A. F., JOHNSON, T., OVERVAD, K., TJONNELAND, A., BOUTRON-RUAULT, M. C., MESRINE, S., SEVERI, G., DOSSUS, L., RINALDI, S., BOEING, H., BENETOU, V., LAGIOU, P., TRICHOPOULOU, A., KROGH, V., KUHN, E., PANICO, S., BUENO-DE-MESQUITA, H. B., ONLAND-MORET, N. C., PEETERS, P. H., GRAM, I. T., WEIDERPASS, E., DUELL, E. J., SANCHEZ, M. J., ARDANAZ, E., ETXEZARRETA, N., NAVARRO, C., IDAHL, A., LUNDIN, E., JIRSTROM, K., MANJER, J., WAREHAM, N. J., KHAW, K. T., BYRNE, K. S., TRAVIS, R. C., GUNTER, M. J., MERRITT, M. A., RIBOLI, E., CRAMER, D. W. & KAKS, R. 2016. A Prospective Evaluation of Early Detection Biomarkers for Ovarian Cancer in the European EPIC Cohort. *Clin Cancer Res*, 22, 4664-75.
- THEODORESCU, D., WITTKE, S., ROSS, M. M., WALDEN, M., CONAWAY, M., JUST, I., MISCHAK, H. & FRIERSON, H. F. 2006. Discovery and validation of new protein biomarkers for urothelial cancer: a prospective analysis. *Lancet Oncol*, 7, 230-40.
- TIEDE, C., BEDFORD, R., HESELTINE, S. J., SMITH, G., WIJETUNGA, I., ROSS, R., ALQALLAF, D., ROBERTS, A. P., BALLS, A., CURD, A., HUGHES, R. E., MARTIN, H., NEEDHAM, S. R., ZANETTI-DOMINGUES, L. C., SADIGH, Y., PEACOCK, T. P., TANG, A. A., GIBSON, N., KYLE, H., PLATT, G. W., INGRAM, N., TAYLOR, T., COLETTA, L. P., MANFIELD, I., KNOWLES, M., BELL, S., ESTEVES, F., MAQBOOL, A., PRASAD, R. K., DRINKHILL, M., BON, R. S., PATEL, V.,

- GOODCHILD, S. A., MARTIN-FERNANDEZ, M., OWENS, R. J., NETTLESHIP, J. E., WEBB, M. E., HARRISON, M., LIPPIAT, J. D., PONNAMBALAM, S., PECKHAM, M., SMITH, A., FERRIGNO, P. K., JOHNSON, M., MCPHERSON, M. J. & TOMLINSON, D. C. 2017. Affimer proteins are versatile and renewable affinity reagents. *Elife*, 6.
- TIEDE, C., TANG, A. A., DEACON, S. E., MANDAL, U., NETTLESHIP, J. E., OWEN, R. L., GEORGE, S. E., HARRISON, D. J., OWENS, R. J., TOMLINSON, D. C. & MCPHERSON, M. J. 2014. Adhiron: a stable and versatile peptide display scaffold for molecular recognition applications. *Protein Eng Des Sel*, 27, 145-55.
- TLSTY, T. D. & COUSSENS, L. M. 2006. Tumor stroma and regulation of cancer development. *Annu Rev Pathol*, 1, 119-50.
- TOLCHER, A. W., SWEENEY, C. J., PAPADOPOULOS, K., PATNAIK, A., CHIOREAN, E. G., MITA, A. C., SANKHALA, K., FURFINE, E., GOKEMEIJER, J., IACONO, L., EATON, C., SILVER, B. A. & MITA, M. 2011. Phase I and pharmacokinetic study of CT-322 (BMS-844203), a targeted Adnectin inhibitor of VEGFR-2 based on a domain of human fibronectin. *Clin Cancer Res*, 17, 363-71.
- TORISU, T., MARUNO, T., HAMAJI, Y., OHKUBO, T. & UCHIYAMA, S. 2017. Synergistic Effect of Cavitation and Agitation on Protein Aggregation. *J Pharm Sci*, 106, 521-529.
- TUBBS, R. R., PETTAY, J. D., ROCHE, P. C., STOLER, M. H., JENKINS, R. B. & GROGAN, T. M. 2001. Discrepancies in clinical laboratory testing of eligibility for trastuzumab therapy: apparent immunohistochemical false-positives do not get the message. *J Clin Oncol*, 19, 2714-21.
- TUEFFERD, M., COUTURIER, J., PENAULT-LLORCA, F., VINCENT-SALOMON, A., BROET, P., GUASTALLA, J. P., ALLOUACHE, D., COMBE, M., WEBER, B., PUJADE-LAURAIN, E. & CAMILLERI-BROET, S. 2007. HER2 status in ovarian carcinomas: a multicenter GINECO study of 320 patients. *PLoS One*, 2, e1138.
- TURNER, J. J. & MILLIKEN, S. 2000. A case of keratin-positive acute myeloid leukemia: a possible role for cytokeratin 19 as a specific epithelial marker. *Pathology*, 32, 98-101.
- UNTCH, M. & LUCK, H. J. 2010. Lapatinib - Member of a New Generation of ErbB-Targeting Drugs. *Breast Care (Basel)*, 5, 8-12.
- VAN AUDENHOVE, I. & GETTEMANS, J. 2016. Nanobodies as Versatile Tools to Understand, Diagnose, Visualize and Treat Cancer. *EBioMedicine*, 8, 40-48.
- VAN MEER, L., MOERLAND, M., COHEN, A. F. & BURGGRAAF, J. 2014. Urinary kidney biomarkers for early detection of nephrotoxicity in clinical drug development. *Br J Clin Pharmacol*, 77, 947-57.
- VARGA, Z. & NOSKE, A. 2015. Impact of Modified 2013 ASCO/CAP Guidelines on HER2 Testing in Breast Cancer. One Year Experience. *PLoS One*, 10, e0140652.
- VAUGHT, J. D., BOCK, C., CARTER, J., FITZWATER, T., OTIS, M., SCHNEIDER, D., ROLANDO, J., WAUGH, S., WILCOX, S. K. & EATON, B. E. 2010. Expanding the chemistry of DNA for in vitro selection. *J Am Chem Soc*, 132, 4141-51.
- VAZQUEZ-LOMBARDI, R., PHAN, T. G., ZIMMERMANN, C., LOWE, D., JERMUTUS, L. & CHRIST, D. 2015. Challenges and opportunities for non-antibody scaffold drugs. *Drug Discov Today*, 20, 1271-83.
- VERRI, E., GUGLIELMINI, P., PUNTONI, M., PERDELLI, L., PAPADIA, A., LORENZI, P., RUBAGOTTI, A., RAGNI, N. & BOCCARDO, F. 2005. HER2/neu oncoprotein overexpression in epithelial ovarian cancer: evaluation of its prevalence and prognostic significance. Clinical study. *Oncology*, 68, 154-61.
- VISINTIN, I., FENG, Z., LONGTON, G., WARD, D. C., ALVERO, A. B., LAI, Y., TENTHOREY, J., LEISER, A., FLORES-SAAIB, R., YU, H., AZORI, M., RUTHERFORD, T., SCHWARTZ, P. E. & MOR, G. 2008. Diagnostic markers for early detection of ovarian cancer. *Clin Cancer Res*, 14, 1065-72.
- VOGEL, C. L., COBLEIGH, M. A., TRIPATHY, D., GUTHEIL, J. C., HARRIS, L. N., FEHRENBACHER, L., SLAMON, D. J., MURPHY, M., NOVOTNY, W. F., BURCHMORE, M., SHAK, S., STEWART, S.

- J. & PRESS, M. 2002. Efficacy and safety of trastuzumab as a single agent in first-line treatment of HER2-overexpressing metastatic breast cancer. *J Clin Oncol*, 20, 719-26.
- VON MINCKWITZ, G., PROCTER, M., DE AZAMBUJA, E., ZARDAVAS, D., BENYUNES, M., VIALE, G., SUTER, T., ARAHMANI, A., ROUCHET, N., CLARK, E., KNOTT, A., LANG, I., LEVY, C., YARDLEY, D. A., BINES, J., GELBER, R. D., PICCART, M., BASELGA, J., COMMITTEE, A. S. & INVESTIGATORS 2017. Adjuvant Pertuzumab and Trastuzumab in Early HER2-Positive Breast Cancer. *N Engl J Med*, 377, 122-131.
- VOPEL, S., MUHLBACH, H. & SKERRA, A. 2005. Rational engineering of a fluorescein-binding anticalin for improved ligand affinity. *Biol Chem*, 386, 1097-104.
- VOSSE, B. A., SEELENTAG, W., BACHMANN, A., BOSMAN, F. T. & YAN, P. 2007. Background staining of visualization systems in immunohistochemistry: comparison of the Avidin-Biotin Complex system and the EnVision+ system. *Appl Immunohistochem Mol Morphol*, 15, 103-7.
- WAHLBERG, E., LENDEL, C., HELGSTRAND, M., ALLARD, P., DINCIBAS-RENQVIST, V., HEDQVIST, A., BERGLUND, H., NYGREN, P. A. & HARD, T. 2003. An affibody in complex with a target protein: structure and coupled folding. *Proc Natl Acad Sci U S A*, 100, 3185-90.
- WANG, L., HU, Y., LI, W., WANG, F., LU, X., HAN, X., LV, J. & CHEN, J. 2016. Identification of a peptide specifically targeting ovarian cancer by the screening of a phage display peptide library. *Oncol Lett*, 11, 4022-4026.
- WANG, S. E., SHIN, I., WU, F. Y., FRIEDMAN, D. B. & ARTEAGA, C. L. 2006a. HER2/Neu (ErbB2) signaling to Rac1-Pak1 is temporally and spatially modulated by transforming growth factor beta. *Cancer Res*, 66, 9591-600.
- WANG, S. H., ZHANG, J. B., ZHANG, Z. P., ZHOU, Y. F., YANG, R. F., CHEN, J., GUO, Y. C., YOU, F. & ZHANG, X. E. 2006b. Construction of single chain variable fragment (ScFv) and BiscFv-alkaline phosphatase fusion protein for detection of Bacillus anthracis. *Anal Chem*, 78, 997-1004.
- WANG, T., CHEN, C., LARCHER, L. M., BARRERO, R. A. & VEEDU, R. N. 2018. Three decades of nucleic acid aptamer technologies: Lessons learned, progress and opportunities on aptamer development. *Biotechnol Adv*.
- WANG, X. & LI, S. 2014. Protein mislocalization: mechanisms, functions and clinical applications in cancer. *Biochim Biophys Acta*, 1846, 13-25.
- WARRAM, J. M., DE BOER, E., SORACE, A. G., CHUNG, T. K., KIM, H., PLEIJHUIS, R. G., VAN DAM, G. M. & ROSENTHAL, E. L. 2014. Antibody-based imaging strategies for cancer. *Cancer Metastasis Rev*, 33, 809-22.
- WEBSTER, J. D., MILLER, M. A., DUSOLD, D. & RAMOS-VARA, J. 2010. Effects of prolonged formalin fixation on the immunohistochemical detection of infectious agents in formalin-fixed, paraffin-embedded tissues. *Vet Pathol*, 47, 529-35.
- WEIDLE, U. H., AUER, J., BRINKMANN, U., GEORGES, G. & TIEFENTHALER, G. 2013. The emerging role of new protein scaffold-based agents for treatment of cancer. *Cancer Genomics Proteomics*, 10, 155-68.
- WEIGEL, M. T. & DOWSETT, M. 2010. Current and emerging biomarkers in breast cancer: prognosis and prediction. *Endocr Relat Cancer*, 17, R245-62.
- WEIGELT, B., PETERSE, J. L. & VAN 'T VEER, L. J. 2005. Breast cancer metastasis: markers and models. *Nat Rev Cancer*, 5, 591-602.
- WEINER, G. J. 2015. Building better monoclonal antibody-based therapeutics. *Nat Rev Cancer*, 15, 361-70.
- WEINER, L. M. 2007. Building better magic bullets--improving unconjugated monoclonal antibody therapy for cancer. *Nat Rev Cancer*, 7, 701-6.
- WELLS, A. & GRANDIS, J. R. 2003. Phospholipase C-gamma1 in tumor progression. *Clin Exp Metastasis*, 20, 285-90.
- WESSELING, J., TINTERRI, C., SAPINO, A., ZANCONATI, F., LUTKE-HOLZIK, M., NGUYEN, B., DECK, K. B., QUERZOLI, P., PERIN, T., GIARDINA, C., SEITZ, G., GUINEBRETIERE, J. M., BARONE, J., DEKKER, L., DE SNOO, F., STORK-SLOOTS, L., ROEPMAN, P., WATANABE, T. &

- CUSUMANO, P. 2016. An international study comparing conventional versus mRNA level testing (TargetPrint) for ER, PR, and HER2 status of breast cancer. *Virchows Arch*, 469, 297-304.
- WHALEY, S. R., ENGLISH, D. S., HU, E. L., BARBARA, P. F. & BELCHER, A. M. 2000. Selection of peptides with semiconductor binding specificity for directed nanocrystal assembly. *Nature*, 405, 665-8.
- WHO 2001. Biomarkers in risk assessment: Validity and validation. *WHO*.
- WHO 2013. European Health Report 2012: Charting the way to Well Being. WHO - Regional Office for Europe.
- WHO 2018. Latest global cancer data: Cancer burden rises to 18.1 million new cases and 9.6 million cancer deaths in 2018. *The International Agency for Research on Cancer*.
- WIEDORN, K. H., GOLDMANN, T., HENNE, C., KUHL, H. & VOLLMER, E. 2001. EnVision+, a new dextran polymer-based signal enhancement technique for in situ hybridization (ISH). *J Histochem Cytochem*, 49, 1067-71.
- WIEDUWILT, M. J. & MOASSER, M. M. 2008. The epidermal growth factor receptor family: biology driving targeted therapeutics. *Cell Mol Life Sci*, 65, 1566-84.
- WIKMAN, M., STEFFEN, A. C., GUNNERIUSSON, E., TOLMACHEV, V., ADAMS, G. P., CARLSSON, J. & STAHL, S. 2004. Selection and characterization of HER2/neu-binding affibody ligands. *Protein Eng Des Sel*, 17, 455-62.
- WOLCKE, J. & WEINHOLD, E. 2001. A DNA-binding peptide from a phage display library. *Nucleosides Nucleotides Nucleic Acids*, 20, 1239-41.
- WONG, A., SYKORA, C., ROGERS, L., HIGGINBOTHAM, J. & WANG, J. 2018. Modified Nanoantibodies Increase Sensitivity in Avidin-Biotin Immunohistochemistry. *Appl Immunohistochem Mol Morphol*, 26, 682-688.
- WOODMAN, R., YEH, J. T., LAURENSEN, S. & KO FERRIGNO, P. 2005. Design and validation of a neutral protein scaffold for the presentation of peptide aptamers. *J Mol Biol*, 352, 1118-33.
- XIE, C., TIEDE, C., ZHANG, X., WANG, C., LI, Z., XU, X., MCPHERSON, M. J., TOMLINSON, D. C. & XU, W. 2017. Development of an Affimer-antibody combined immunological diagnosis kit for glypican-3. *Sci Rep*, 7, 9608.
- YANG, C., GAO, X. & GONG, R. 2017. Engineering of Fc Fragments with Optimized Physicochemical Properties Implying Improvement of Clinical Potentials for Fc-Based Therapeutics. *Front Immunol*, 8, 1860.
- YANG, J. M., VASSIL, A. D. & HAIT, W. N. 2001. Activation of phospholipase C induces the expression of the multidrug resistance (MDR1) gene through the Raf-MAPK pathway. *Mol Pharmacol*, 60, 674-80.
- YARDEN, Y. 2001. The EGFR family and its ligands in human cancer. signalling mechanisms and therapeutic opportunities. *Eur J Cancer*, 37 Suppl 4, S3-8.
- YARDEN, Y. & PINES, G. 2012. The ERBB network: at last, cancer therapy meets systems biology. *Nat Rev Cancer*, 12, 553-63.
- YARDEN, Y. & SLIWKOWSKI, M. X. 2001. Untangling the ErbB signalling network. *Nat Rev Mol Cell Biol*, 2, 127-37.
- YAZIJI, H., TAYLOR, C. R., GOLDSTEIN, N. S., DABBS, D. J., HAMMOND, E. H., HEWLETT, B., FLOYD, A. D., BARRY, T. S., MARTIN, A. W., BADVE, S., BAEHNER, F., CARTUN, R. W., EISEN, R. N., SWANSON, P. E., HEWITT, S. M., VYBERG, M., HICKS, D. G. & MEMBERS OF THE STANDARDIZATION AD-HOC CONSENSUS, C. 2008. Consensus recommendations on estrogen receptor testing in breast cancer by immunohistochemistry. *Appl Immunohistochem Mol Morphol*, 16, 513-20.
- YOON, H., SONG, J. M., RYU, C. J., KIM, Y. G., LEE, E. K., KANG, S. & KIM, S. J. 2012. An efficient strategy for cell-based antibody library selection using an integrated vector system. *BMC Biotechnol*, 12, 62.
- YU, X., GHAMANDE, S., LIU, H., XUE, L., ZHAO, S., TAN, W., ZHAO, L., TANG, S. C., WU, D., KORKAYA, H., MAIHLE, N. J. & LIU, H. Y. 2018. Targeting EGFR/HER2/HER3 with a Three-


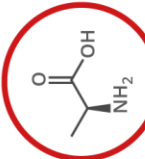
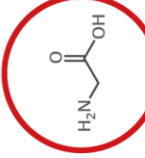
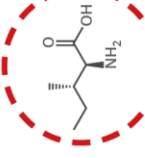
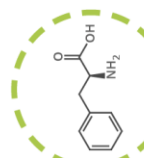
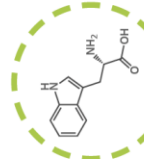
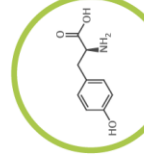
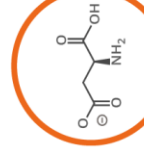
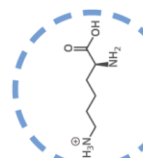
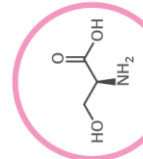
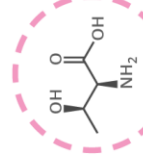
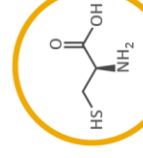







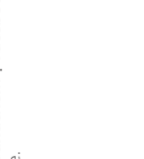
- in-One Aptamer-siRNA Chimera Confers Superior Activity against HER2(+) Breast Cancer. *Mol Ther Nucleic Acids*, 10, 317-330.
- YU, X., YANG, Y. P., DIKICI, E., DEO, S. K. & DAUNERT, S. 2017. Beyond Antibodies as Binding Partners: The Role of Antibody Mimetics in Bioanalysis. *Annu Rev Anal Chem (Palo Alto Calif)*, 10, 293-320.
- YUAN, L., XU, L. & LIU, S. 2012. Integrated tyramide and polymerization-assisted signal amplification for a highly-sensitive immunoassay. *Anal Chem*, 84, 10737-44.
- YUAN, Q. A., ROBINSON, M. K., SIMMONS, H. H., RUSSEVA, M. & ADAMS, G. P. 2008. Isolation of anti-MISIIR scFv molecules from a phage display library by cell sorter biopanning. *Cancer Immunol Immunother*, 57, 367-78.
- ZAHAVY, E., BER, R., GUR, D., ABRAMOVICH, H., FREEMAN, E., MAOZ, S. & YITZHAKI, S. 2012. Application of nanoparticles for the detection and sorting of pathogenic bacteria by flow-cytometry. *Adv Exp Med Biol*, 733, 23-36.
- ZAHND, C., AMSTUTZ, P. & PLUCKTHUN, A. 2007. Ribosome display: selecting and evolving proteins in vitro that specifically bind to a target. *Nat Methods*, 4, 269-79.
- ZAHND, C., PECORARI, F., STRAUMANN, N., WYLER, E. & PLUCKTHUN, A. 2006. Selection and characterization of Her2 binding-designed ankyrin repeat proteins. *J Biol Chem*, 281, 35167-75.
- ZAHNOW, C. A. 2006. ErbB receptors and their ligands in the breast. *Expert Rev Mol Med*, 8, 1-21.
- ZAIDI, A. U., ENOMOTO, H., MILBRANDT, J. & ROTH, K. A. 2000. Dual fluorescent in situ hybridization and immunohistochemical detection with tyramide signal amplification. *J Histochem Cytochem*, 48, 1369-75.
- ZHANG, A., SINGH, S. K., SHIRTS, M. R., KUMAR, S. & FERNANDEZ, E. J. 2012. Distinct aggregation mechanisms of monoclonal antibody under thermal and freeze-thaw stresses revealed by hydrogen exchange. *Pharm Res*, 29, 236-50.
- ZHANG, L., CONEJO-GARCIA, J. R., KATSAROS, D., GIMOTTY, P. A., MASSOBRIO, M., REGNANI, G., MAKRIGIANNAKIS, A., GRAY, H., SCHLIENGER, K., LIEBMAN, M. N., RUBIN, S. C. & COUKOS, G. 2003. Intratumoral T cells, recurrence, and survival in epithelial ovarian cancer. *N Engl J Med*, 348, 203-13.
- ZHANG, W. & LIU, H. T. 2002. MAPK signal pathways in the regulation of cell proliferation in mammalian cells. *Cell Res*, 12, 9-18.
- ZHANG, X., GUREASKO, J., SHEN, K., COLE, P. A. & KURIYAN, J. 2006. An allosteric mechanism for activation of the kinase domain of epidermal growth factor receptor. *Cell*, 125, 1137-49.
- ZHOU, C., KANG, J., WANG, X., WEI, W. & JIANG, W. 2015. Phage display screening identifies a novel peptide to suppress ovarian cancer cells in vitro and in vivo in mouse models. *BMC Cancer*, 15, 889.
- ZHURAUSKI, P., ARYA, S. K., JOLLY, P., TIEDE, C., TOMLINSON, D. C., KO FERRIGNO, P. & ESTRELA, P. 2018. Sensitive and selective Affimer-functionalised interdigitated electrode-based capacitive biosensor for Her4 protein tumour biomarker detection. *Biosens Bioelectron*, 108, 1-8.
- ZIEGLER, Y. S., MORESCO, J. J., TU, P. G., YATES, J. R., 3RD & NARDULLI, A. M. 2014. Plasma membrane proteomics of human breast cancer cell lines identifies potential targets for breast cancer diagnosis and treatment. *PLoS One*, 9, e102341.

Appendix A

A GUIDE TO THE TWENTY COMMON AMINO ACIDS

AMINO ACIDS ARE THE BUILDING BLOCKS OF PROTEINS IN LIVING ORGANISMS. THERE ARE OVER 500 AMINO ACIDS FOUND IN NATURE - HOWEVER, THE HUMAN GENETIC CODE ONLY DIRECTLY ENCODES 20. 'ESSENTIAL' AMINO ACIDS MUST BE OBTAINED FROM THE DIET, WHILST NON-ESSENTIAL AMINO ACIDS CAN BE SYNTHESISED IN THE BODY.

Chart Key: ● ALIPHATIC ● AROMATIC ● ACIDIC ● BASIC ● HYDROXYLIC ● SULFUR-CONTAINING ● AMIDIC ○ NON-ESSENTIAL ○ ESSENTIAL

Chemical Structure single letter code	NAME three letter code DNA codons	CLASSIFICATION	Chemical Structure	NAME three letter code DNA codons	CLASSIFICATION	Chemical Structure	NAME three letter code DNA codons	CLASSIFICATION	Chemical Structure	NAME three letter code DNA codons	CLASSIFICATION
	ALANINE Ala GCT, GCC, GCA, GCG	Aliphatic, Acidic		GLYCINE Gly GGT, GGC, GGA, GGG	Aliphatic, Acidic		ISOLEUCINE Ile ATT, ATC, ATA	Aliphatic, Hydroxylic, Essential		LEUCINE Leu CTT, CTC, CTA, CTG, TTA, TTG	Aliphatic, Hydroxylic, Essential
	TRYPTOPHAN Trp TGG	Aromatic, Acidic, Essential		TYROSINE Tyr TAT, TAC	Aliphatic, Aromatic, Hydroxylic, Acidic, Essential		ASPARTIC ACID Asp GAT, GAC	Aliphatic, Hydroxylic, Acidic, Essential		GLUTAMIC ACID Glu GAA, GAG	Aliphatic, Hydroxylic, Acidic, Essential
	PHENYLALANINE Phe TTT, TTC	Aromatic, Acidic, Essential		THREONINE Thr ACT, ACC, ACA, ACG	Aliphatic, Hydroxylic, Acidic, Essential		CYSTEINE Cys TGT, TGC	Aliphatic, Hydroxylic, Sulfur-containing, Essential		METHIONINE Met ATG	Aliphatic, Sulfur-containing, Essential
	LYSINE Lys AAA, AAG	Aliphatic, Acidic, Essential		ASPARAGINE Asn AAT, AAC	Aliphatic, Amidic, Essential		ARGININE Arg CGT, CGC, CGA, CCG, AGA, AGG	Aliphatic, Amidic, Essential		HISTIDINE His CAT, CAC	Aliphatic, Aromatic, Amidic, Essential
	VALINE Val GTT, GTC, GTA, GTG	Aliphatic, Acidic, Essential		GLUTAMINE Gln CAA, CAG	Aliphatic, Amidic, Essential		GLUTAMINE Gln CAA, CAG	Aliphatic, Amidic, Essential		GLUTAMINE Gln CAA, CAG	Aliphatic, Amidic, Essential

Note: This chart only shows those amino acids for which the human genetic code directly codes for. Selenocysteine is often referred to as the 21st amino acid, but is encoded in a special manner. In some cases, distinguishing between asparagine/aspartic acid and glutamine/glutamic acid is difficult. In these cases, the codes asx (B) and gx (Z) are respectively used.

Appendix B

Publications & conference proceeding

B.1. Accepted Manuscripts

TIEDE, C., BEDFORD, R., HESELTINE, S. J., SMITH, G., WIJETUNGA, I., ROSS, R., **ALQALLAF, D.**, ROBERTS, A. P., BALLS, A., CURD, A., HUGHES, R. E., MARTIN, H., NEEDHAM, S. R., ZANETTI-DOMINGUES, L. C., SADIGH, Y., PEACOCK, T. P., TANG, A. A., GIBSON, N., KYLE, H., PLATT, G. W., INGRAM, N., TAYLOR, T., COLETTA, L. P., MANFIELD, I., KNOWLES, M., BELL, S., ESTEVES, F., MAQBOOL, A., PRASAD, R. K., DRINKHILL, M., BON, R. S., PATEL, V., GOODCHILD, S. A., MARTIN-FERNANDEZ, M., OWENS, R. J., NETTLESHIP, J. E., WEBB, M. E., HARRISON, M., LIPPIAT, J. D., PONNAMBALAM, S., PECKHAM, M., SMITH, A., FERRIGNO, P. K., JOHNSON, M., MCPHERSON, M. J. & TOMLINSON, D. C. 2017. Affimer proteins are versatile and renewable affinity reagents. *Elife*, 6.

B.2. Poster presentations

ALQallaf D. Bell S, Mcpherson M, and Tomlinson D (March 2015) Development of Adhirons as antibody replacements in biomarker detection. *Postgraduate Symposium*, Leeds, UK.

ALQallaf D. Bell S, Esteves S, Tiede C, Mcpherson M, and Tomlinson D (March 2016) Affimers for biomarker detection and discovery in cancer. *Postgraduate Symposium*, Leeds, UK. – **Joint 1st place poster prize.**

ALQallaf D. Mcpherson M, Bell S, and Tomlinson D (May 2016) Developing Adhirons as tools to detect novel biomarkers in cancer. *21st Health Science Centre Poster Conference*, Kuwait.

ALQallaf D. Bell S, Esteves S, Tiede C, Mcpherson M, and Tomlinson D (September 2016) Affimers for biomarker detection and discovery in cancer. *7th International Conference and Expo on Molecular and Cancer biomarker*, Berlin, Germany. – **Best scientific poster prize.**

B.3 Oral presentations

ALQallaf D. Bell S, Esteves S, Tiede C, Mcpherson M, and Tomlinson D (March 2018) Development of Affimers for biomarker detection and discovery in cancer. *Postgraduate Symposium*, Leeds, UK.

Chair session: Plant Science talks, Postgraduate Symposium, Leeds.UK (March 2018).